Electrolytic coloration of the alkali halides with a special reference to the alkali fluorides

by

Khalil Ibrahim Jawad

A thesis submitted for the degree of Ph.D.

Department of Chemistry

City University

March 1992

Contents

List of Tables

List of Figures

Figure N0

Follows Page

Acknowledgements

Gratitude is especially due to Professor R.S Davidson.Head of Chemistry Department for permission to carry out this work as part time internal student in the Department.

I am indebted to Dr. P.J. Baldry for his keen interest in this work and for his detailed, constructive remarks at the early stage of this work.

I wish to thank Dr. M. Koussa for his supervision and guidance at all stages of the work and in preparation of the manuscript in the stimulating atmosphere of Physics Department, Damascus University.

The co-operation of the staff of the mechanical, electronics and glass-blowing workshops is gratefully acknowledged.

I am grateful for the great assistance given to me by Dr. K.C.Bass. His continuous correspondence and advice were very valuable throughout the period I spent on this work.

Finally, I wish to thank Dr. B. Shaaban for her assistance during the preparation of the manuscript. Her moral support during this work has been much appreciated.

Declaration

This is to grant powers of discretion to the City University Librarian to allow the thesis to be copied in whole or in part without further reference to the author. This permission covers only single copies made for study purposes, subject to normal conditions of acknowledgement.

Abstract

The kinetics of electrolytic coloration of the alkali halides is investigated. The first stage of the process takes place prior to the onset of coloration. It involves cation vacancy migration and creates conditions for the injection of electrons from an alkali metal cathode formed on the original pointed cathode. The injection of electrons into the alkali halides initiates a second stage (the electron-injection stage) which is characterised by the emergence of F coloration with a high concentration of F-centres near to the cathode. The concentration of F-centres is found to decrease linearly towards the anode. Electron injection takes place at the coloration starting temperature T_c which is found to be a characteristic of the particular alkali halide. Towards the start of the third or steady-current stage, a constant current density is established in the specimen and the concentration of F-centres is distributed homogeneously throughout the bulk of the specimen.

The diffusion of F-centres in electrolytically coloured alkali halides is also studied. It is found that this process is governed by two mechanisms. The first, which dominates in the extrinsic range of temperature, is consistent with a diffusion process involving cation vacancy migration. At high temperatures (intrinsic range) the mechanism is thought to involve the self-diffusion of alkali ions.

The successful application of the electrolytic technique to the production of homogeneous distribution of F and other colour centres in alkali fluorides containing mercury is also reported. It is shown, by means of ionic conductivity measurements corroborated with optical and other experimental data, that it is the divalent mercury cations which play the essential part in promoting electrolytic coloration.

The effect of plastic deformation on electrolytic coloration is also investigated. It is suggested that dislocations present in the bulk of the specimens act as the principal source of excess anion vacancies. This suggestion is supported by optical as well as thermodynamic data.

The influence of OH^- ions on electrolytic coloration is found to reduce the colourability of mercury-doped alkali halides due to the formation of Hg^{2+} -OH^- complexes.

The optical properties of various electron and hole excess centres are reported for nine alkali halides. The effect of both thermal and optical treatment in the evolution of these

centres is studied. It is deduced that electrolytic coloration is capable of a reproducible production of most of the known colour centres.

The optical properties of uncoloured and electrolytically coloured alkali halides containing mercury are studied. The absorption spectra correlate with the ionic conductivity and thermal treatment results and indicate the formation of divalent, monovalent and neutral atomic centres. Two other centres, identified as $(Hg - Hg)^{2+}$ and $(Hg\text{-}Hg)^{o}$, are also formed following thermal treatment and electrolytic coloration/ de-coloration respectively. Electrolytic coloration is found to change the valence of the mercury centres. An argument is presented for the formation of Hg^{-} centres.

The sectioning technique is used to study the diffusion of mercury in alkali halides. The diffusion coefficient of Hg^{2+} cations in KF in the temperature range 540° C to 800° C can be expressed as $D = 2.68 \times 10^{-3} \exp\left(-\frac{0.993}{kT}\right)$ cm^2 sec^{-} where 0.993 eV is the activation energy for the diffusion of Hg^{2+} cations. The Hg^{2+} cations mobility at 665° C is 2.5×10^{-9} cm^2 sec^{-1} V^{-1}.

Colour Centres: Outline

Centre	Type	Method of Production	Description
F	Electro Excess Centre (EEC)	Irradiation, Electrolytic, Additive (Irr, Ele, Add)	Intrinsic defect consists of an anion vacancy which has trapped an electron/F-absorption is a function of lattice spacing
K	EEC	Irr, Ele	Excited states of F-centre
L_1, L_2, L_3, ...	EEC	Irr	Excited states of F-centre
F'	EEC	Irr	F-centre plus a second weakly bound electron
F_A	Impurity Association	Irr, Ele, Add	F-centre with one of the nearest neighbour positive ion replaced by a different impurity alkali ion with smaller size
Z	Impurity Association	Irr, Ele, Add	F-centre next to a divalent ion
U	Impurity Association	Irr	F-centre plus a hydrogen atom at a halogen site
C	Impurity Association	Irr, Ele, Add Thermal Treatment	Colloid of small spherical metal inclusions which show optical absorption but not Tyndall effect
Impurity Centres	Impurity Association	Doping, Irr, Ele, Photothermal	Centres of monovalent, divalent, ...ions which may be substitutional or interstitial or of a more complex nature and which show absorption band
$M(F_2)$	EEC	Irr, Ele, Add	Two nearest neighbour F-centres with optical absorption which satisfy Ivey's Relation
M_2, M_2'-M_7	EEC	Optical Treatment (OT)	Variants of the M-centre with less intense transition
$R(F_3)$	EEC	Irr, Ele, Add	Three nearest neighbour F-centres arranged in an equilateral triangle in a (III) anion plane
R_1, R_2, R_M, R_N	EEC	OT	Excited states of the R-centre
R'_1, R'_2	EEC	Irr, OT	Variants of the R-centre with extra electron
$N(F_4)$	EEC	Irr, Ele, OT, Thermal	Four F-centres arranged tetrahedrally on adjacent sites with two associated absorption bands - N_1 and N_2
I	Interstitial	Irr	Interstitial anion
U_1	Interstitial	Irr	Interstitial hydrogen ion
U_2	Interstitial	Irr	Interstitial hydrogen atom

Colour Centres: Outline

Centre	Type	Method of Production	Description
V_1 - V_8	Hole Excess Centres (HEC)	Irr, Add, Ele	Variants of HEC which appear at energies higher than that of the F-band
V_K	HEC		Self-trapped hole shared by two adjacent habgenions
H	Interstitial	Irr	Interstitial anion atom
$V_1(H_A)$	HEC	Irr	H-centre associated with an alkali impurity
V_F	HEC	Irr, Ele	The antimorph of the F-centre
α	Vacancy	Irr, Ele	F-centre from which the electron is missing
ß	Vacancy	Irr, Ele	Anion excitation near to the F-centre
γ	Vacancy	Irr, Ele	Higher excited state of the α-centre

CHAPTER ONE

Colour Centres

1. Introduction

1.1 Constitution of colour centre

The term 'colour centre' was originally applied to any point defect in a crystal which produced a characteristic absorption band in the visible region of the spectrum, thereby literally colouring the crystal. Such centres were first observed in the early nineteenth century and were studied in detail by Pohl and co-workers (see Prizbram,1986) The prototype centres were labelled F-centres by Pohl from the German 'Farbzentren.'(Pohl,1937)

The basic model for the F-centre first proposed by de Boer (1937) seems to be established beyond any reasonable doubt. It consists of an anion vacancy (lattice site where the negative ion is missing) which has trapped an electron, the electron being shared by the six neighbouring alkali ions. The F-absorption corresponds to an electron transition from the ground state to an excited state close to the bottom of the conduction band. Electron paramagnetic resonance (EPR) has provided the most convincing evidence in favour of this model (for details and literature references see Fowler, 1984).

An extension of the de Boor model, due to Stockmann (1952), considers the F-centre as an electron trapped in a potential box. The energy levels are given by

$$E_k = \frac{h^2 k^2}{m^* a^2} \qquad (1.1)$$

where k is the principl quantum number, a is the lattice constant and m* is the effective mass of the electron. The frequency of the optical transition between the ground state and the first excited state is then

$$\nu = \frac{3}{8} \frac{h}{m^* a^2} \qquad (1.2)$$

Equation (1.2) leads to the following simple relation

$$va^2 = \text{constant} \qquad (1.3)$$

This relation is well verified and a better empirical value for the exponent is 1.84 (Ivey, 1947). More detailed models have been given by Pekar (1946), Gourary and Adrian (1960) and others. The proposed models agree, at least qualitatively, with the experimental observation that the F band depends systematically on the lattice constant a of the alkali halide crystals, as shown in figure 1.1

The F-band and other trapped-electron centres are observed after a variety of different treatments which bring together electrons and anion vacancies. The methods of producing colour centres in alkali halide crystals are discussed in section 5 of this chapter. Similar treatments are required to produce analogous trapped-electron centres in alkaline halides and oxides (see Henderson and Wertz, 1968 for oxides and Fong, 1967 for fluorite lattices).

The wavelength at which the peak of the bell-shaped F band occurs is a function of the crystal temperature as shown in figure 1.2. The F band, which is almost Gaussian, has a further temperature dependent parameter; namely the bandwidth (Flynn, 1982). Figure 1.3 shows the satisfactory agreement between the theoretical and experimental results for the case of the F-centre bandwidth in NaCl (Markham and Konitzer, 1961).

A perusal of the reviews on colour centre phenomena which have appeared over the past fifty five years since the original contributions of Pohl (1937), makes it clear that the F-centre has been the focal point of colour centre research. This can be said to be due

to the fact that it is the F-centre which gives rise to the most prominent optical absorption band in a large number of the alkali halide crystals, and indeed in other crystals. The second reason is the relative simplicity of the F-centre which makes it a particularly attractive defect to study from an experimental as well as a theoretical point of view (Mott and Gurney, 1948; Seitz, 1954; Schulman and Compton, 1962. Kittel, 1985). However, the number of different centres has increased to a current total of about thirty (Compton and Rabin, 1964.; Prizbram,1986) Most prominent of these are the family of M-, R- and N- centres (figure 1.4) known as F-aggregate centres which give rise to optical absorption bands on the long-wavelength side of the F band.

It is not the purpose of this chapter to review all the different colour centres, but to mention the most prominent centres and those of concern to the subject of the present investigation. Hence, it is worthwhile mentioning the well-studied colloid centres consisting of particles of alkali metal in alkali halide crystals. The nature of these centres and their corresponding optical absorption band has been well established theoretically (Doyle, 1965; Karlsson and Beckman, 1967; Radchenko, 1968; Harrison 1982) and experimentally through studies of their optical, electrical and magnetic properties (Scott et al, 1953; Doyle, 1960; Jain

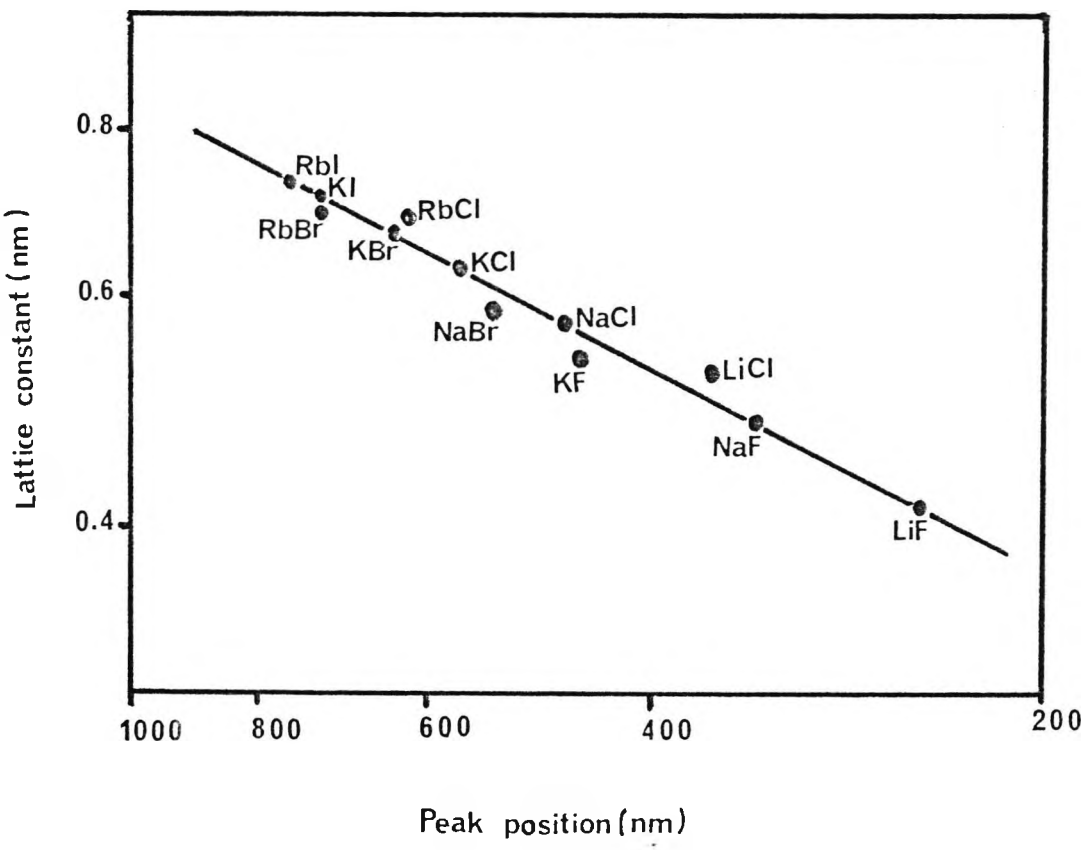

Figure 1.1 Dependence of the F band peak position on the lattice constant of the host crystal. After Pick (1958)

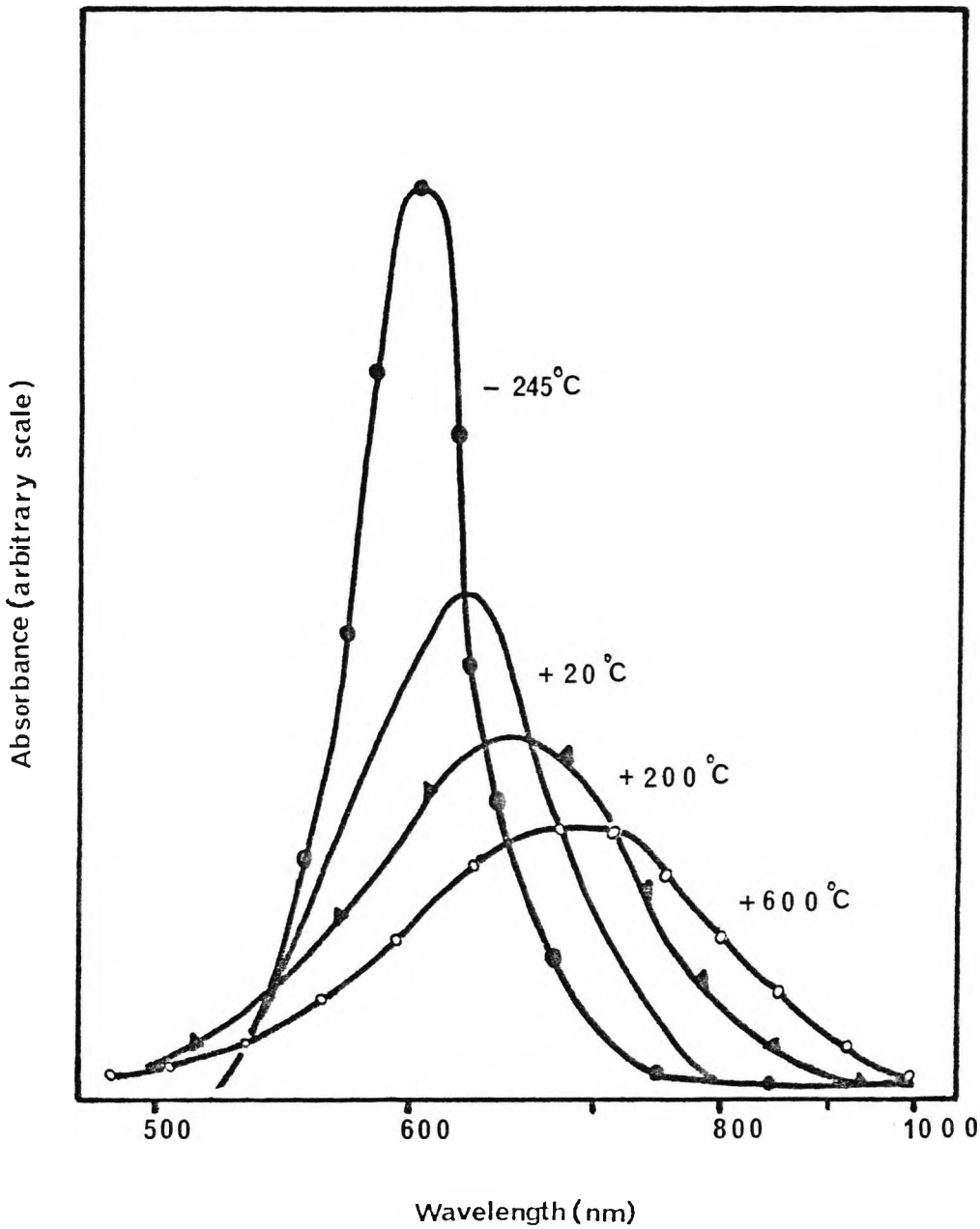

Figure 1.2 The absorption spectrum of the F band in KBr at several temperatures. After Pohl (1937)

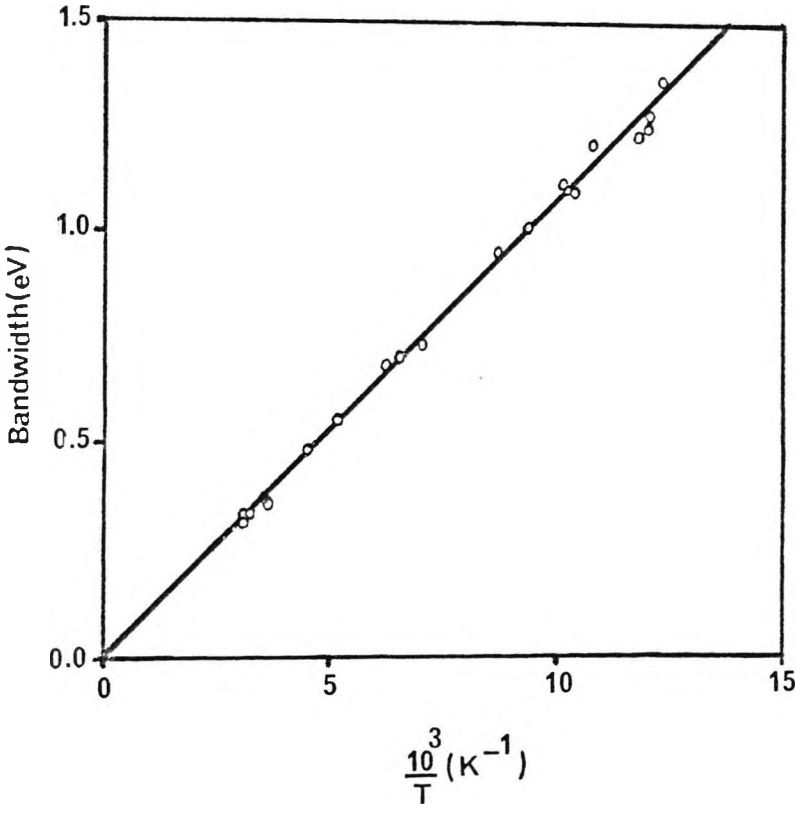

Figure 1.3 Temperature dependence of F-centre bandwidths in NaCl. After Flynn (1972)

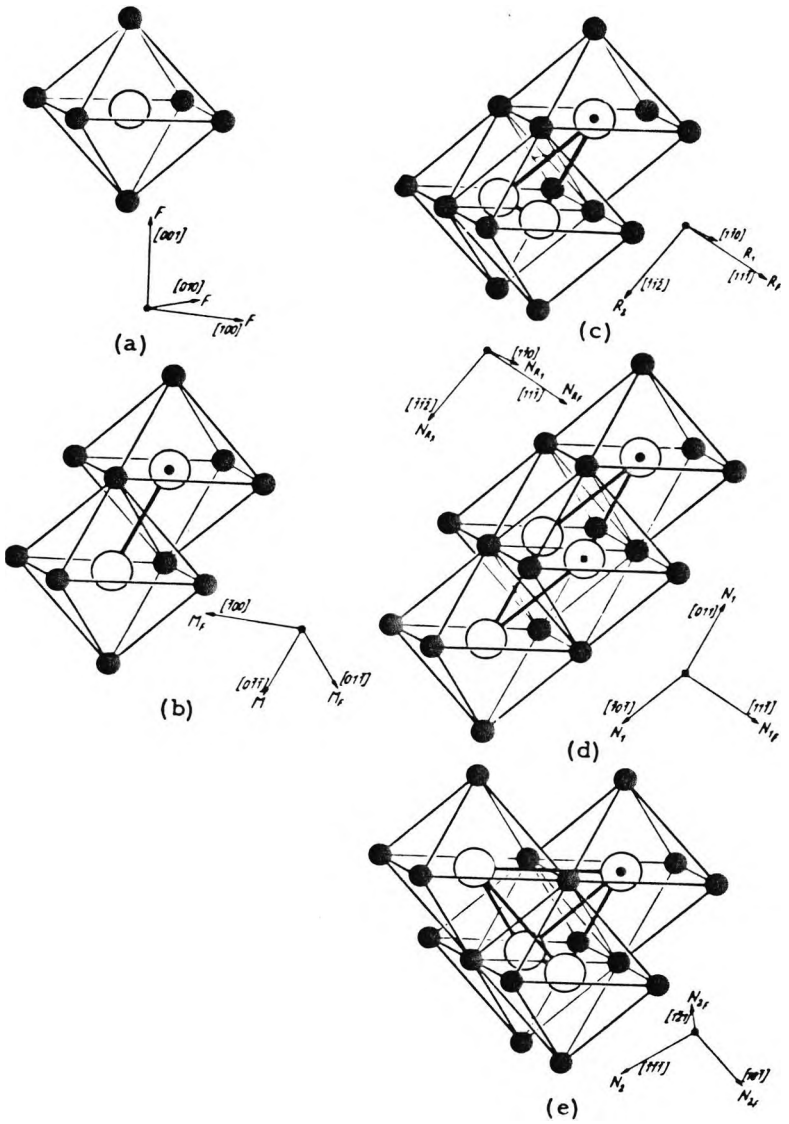

Figure 1.4 Models of the (a) F-centre (b) M-centre (c) R-centre (d) N_1-centre and (e) N_2-centre After Pick (1960)

and Sootha, 1968; Jain and Radhakrishnal, 1969; Kalal et al, 1983; Maiti and Goswami, 1983; Jaque, 1985).

There are other colour centres, such as the F-impurity complexes which are referred to in the literature as F_A -centres. The F_A -centre is produced when one nearest-neighbour cation of the F-centre is replaced by an alkali ion of smaller size (Petroff, 1950; Kojima et al, 1961; Luty, 1961). Similarly Z-centres are formed by association between divalent cation impurities and F-centres. However, other types of imperfections can also cause colour in certain crystals (Weller, 1973). Coloration is often caused in insulators by the introduction of foreign atom impurities. Transition metals, for example, are prime candidates for impurities that cause colour in normally colourless solids (pure aluminium oxide compared to ruby, $Al_2O_3:Cr^{3+}$, is an example).

There is, in fact, another important group of colour centres, other than the electron-excess centres, which give rise to optical absorption bands in the ultra-violet region of the spectrum in a large number of alkali halide crystals (Mollow, 1937; Nakai, 1958; Delbecq et al, 1961; Seitz, 1963; Orton, 1986). These centres,named V-centres, are thought to be hole-excess centres (Barr and Dawson, 1965 ; Markham, 1966; Townsend and Kelly, 1973). The structures of several species of V-centres have been elucidated mainly by EPR (Castner and Kanzig, 1957; Orton, 1986) and optical measurements (Delbecq et al, 1958; Greenwood, 1984), but a number of known optical centres remain incompletely understood due in part to the complicated overlapping of V band spectra (Flynn, 1982;Prizbram,1986) The experimental investigation first confirmed the V-centre structure shown in figure 1.5. A typical absorption spectrum of the V bands produced in KCl is shown in figure 1.6. In each case a halogen molecular ion forms the basis of the V_K -and V_F-centres).

1.2 Principal investigation method

In the early days of colour centre research, all colour centre structures had to be deduced by a careful study of the methods by which they were formed and the kinetics of their formation. Some additional information about the symmetry of a centre was obtained by studies using polarised light (Fowler, 1984). A correlation between thermoluminescence, which measures the binding energy of the defect, and bleaching of the absorption bands also gave valuable data (Compton and Rabin, 1964). But the most powerful technique for paramagnetic defects is often EPR (Seidel and Wolf, 1965; Orton, 1986). The method depends on the interaction of electronic spins with magnetic fields. The energy levels of an unpaired electron in an applied field B are split by $\beta B g$ where β is the Bohr magneton and g the

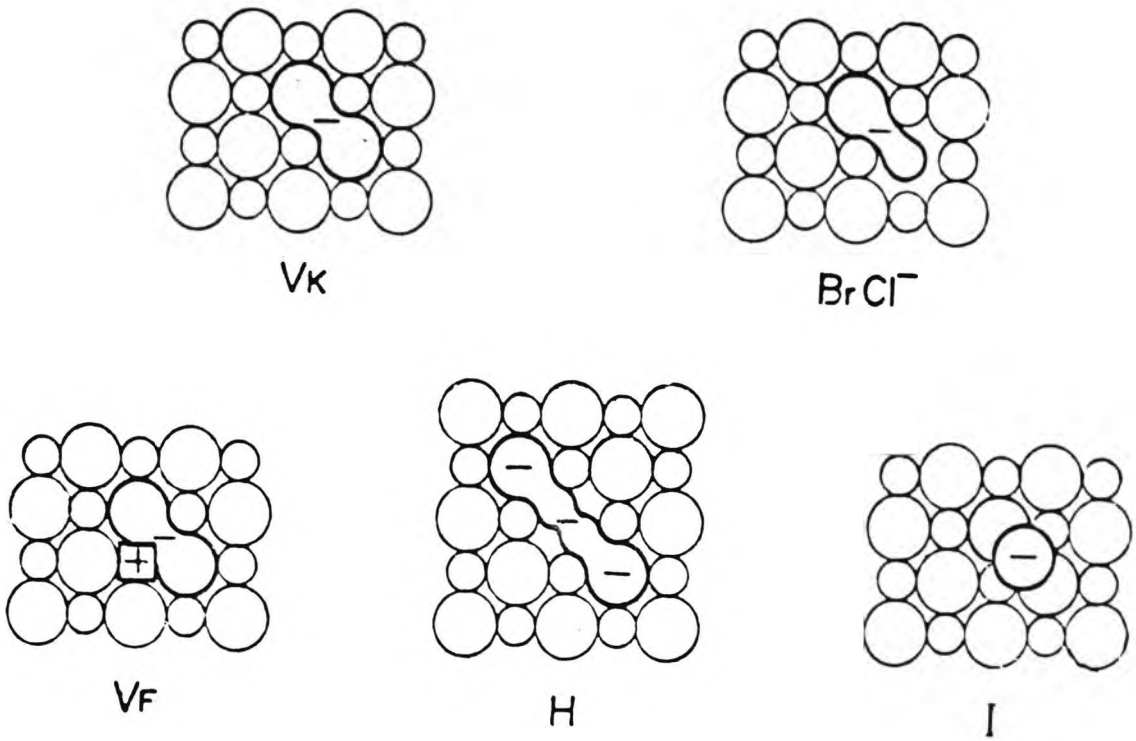

Figure 1.5 Models of interstitial centres in KCl and KBr. After Itoh (1972)

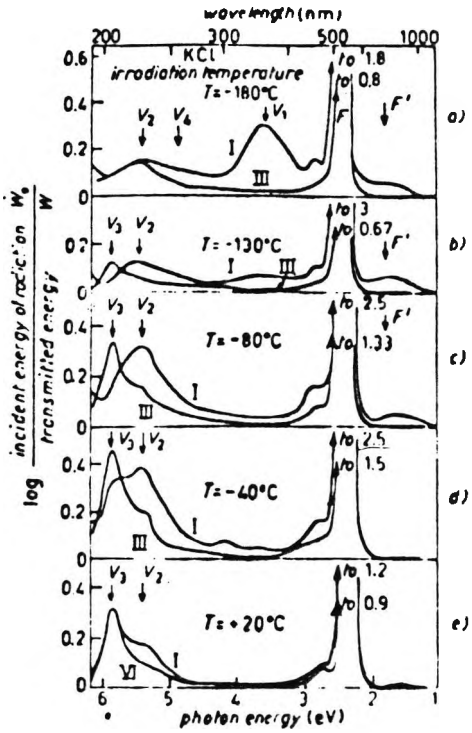

Figure 1.6 The *V*-bands produced in KCl when irradiated with X-rays at various temperatures. The curve I in each panel shows the absorption spectrum immediately after irradiation, whereas curve III shows the spectrum after the specimen was raised to room temperature. All measurements were made at liquid-nitrogen temperature to achieve maximum resolution. In this material the V_3-band grows on warming, whereas the other bands decrease. From Seitz (1954).

spectroscopic splitting factor. Application of microwaves to the crystal results in a resonant absorption at a frequency

$$\nu = g\,\beta\frac{B}{h} \qquad (1.4)$$

The value of g, which is strictly a tensor, provides information about the symmetry of the centre. In many cases, particularly where EPR for paramagnetic impurity ions is being studied, the observed spectrum is considerably more complex than equation (1.4) suggests and may be described by an effective spin Hamiltonian which links the symmetry of the spectrum with that of the crystal field at the paramagnetic centre (Orton, 1986). If there are ions which have non-zero nuclear spins in the neighbourhood of the defects the resonance due to the interaction of the electron spin with the nuclear spins may be resolved. This hyperfine interaction can give two important additional pieces of information; the identity of the neighbours and the unpaired electron density at the neighbours. If the EPR and optical absorptions measurements can be correlated, an almost complete characterisation of the centre is possible. Electron nuclear double resonance (ENDOR) gives even greater detail about the weaker interactions (coupling strengths and symmetry) by analysing the overlapping components of each of the EPR lines (Fowler and Kunz, 1970). The sensitivity of the ENDOR measurements is such that it is possible to detect interaction with at least seventh shell neighbours where the electron density of the F-centre electron is decreased by 10^6 from the central density (Seidel and Wolf, 1968).

As well as the EPR measurements, the optical properties of colour centres yield useful data. Due to the large energy gap of the alkali halides, optical absorption has historically been used to detect and characterise the colour centres and to study their nature. The absorption bands are generally broad and bell-shaped. With increasing temperature, the near-Gaussian F band tends to broaden and shift to lower energy. The oscillator strength of the transition remains close to unity, the maximum for a one-electron centre (Fowler, 1984). There is also an F-emission band with similar features, but there is a large separation in energy between the absorption and emission peaks (Stokers shift, Harrison, 1982). Other important parameters of colour centres are the luminescence efficiency and radioactive lifetime of the excited state (Delbecq, 1963), and the pressure and uniaxial stress dependencies of transition energies (Knof and Maisch, 1963). In some cases a splitting of the excited level due to spin-orbit effects is observed. The width, Stokes shift and temperature dependence of the bands are lattice-dynamical effects and will not be considered in this thesis

Petrescu (1963) has shown that photoemission from some alkali halide crystals coloured by electron bombardment exhibits, as a function of the wavelength of the incident radiation, well established maxima which correspond to the energy levels of the electrons

trapped in the lattice. The results reported by Petrescu (1965, 1971) give a general view of the information which may be obtained using this new experimental technique, which he named "Electron Emission Spectroscopy (EES)", including its accuracy in measurement of energy levels of the trapped electrons and the location of colour centres. Hence, EES means the emergence of a new characteristic for a given alkali halide crystal. In spite of the serious experimental difficulties which face this technique, the use of the EES has many advantages. It is sensitive compared to optical spectroscopy, particularly in the study of electron kinetics where irradiations of the order of minutes are sufficient to produce a marked modification of the ratio of level populations, while much longer periods are necessary to give the same effect by the conventional optical absorption method.

In this chapter the F-centre is emphasised as it is the best-known centre from both experimental and theoretical aspects and is important in the present investigation. However, the range of colour centres is, as mentioned above, large and, though section three of this chapter discusses some aspects of their properties, a more comprehensive review is given by Sonder and Sibley in Crawford and Slifkin (1982) and by Fowler (1984).

2. Theoretical models of F-centre

2.1. Theoretical methods

The structure of the F-center has been established to be an electron trapped at an anion vacancy. The first question which has to be asked before formulating a theoretical model concerns the depth of the trap. In other words, is the defect strongly localised or is the wavefunction of the trapped electron spread out over large distances in the lattice. Some evidence for a localised model comes from the Ivey relation (Mollwo, 1931; 1937, refined by Ivey, 1947) which quite accurately relates the energy E of the F band peak in various alkali halides to the nearest-neighbour distant, a (a in nm and E in eV)

$$E = 0.2558a^{-1.84} \qquad (1.5)$$

Even a rudimentary localised model gives approximately the right dependence on lattice parameters (see equations 1.2 and 1.3). However most models which include the concept of a square well give an absorption energy in the right region so that they should be judged on the finer details of their predictions.

Stoneham (1972)has classed colour centres calculations as :

(a) continuum calculations, based on variants of effective -mass theory;

(b) variational calculations, including pseudopotential theories;

(c) molecular methods, including the method of localised orbitals, and
various semi-empirical schemes;
(d) Green's function methods.

Stoneham (1972) goes on to discuss the strengths and weaknesses of these theories. Extensive reviews are to be found in Markham (1959); Crawford and Slifkin (1982) and Fowler (1984). Only the main features of three models, based on the continuum, semi-continuum, and Hartree-Fock theories are discussed here.

2.2. Continuum model

The basic assumption in the continuum model is that the electron state is diffuse, contrary to the general conclusion above. The electron is loosely bound to the net positive charge of the anion vacancy and moves in this coulomb field with an effective mass m* in a medium of effective permittivity ε Then the absorption energy is $\frac{3}{8}\frac{m^*}{\varepsilon^2}$, which does not show the required variation with lattice constant. Thus local effects are not included, but long-range effects of polarisation and distortion are. It is possible to deal with the coupling between the centre and the lattice vibration, but the model does not allow for the presence of a local mode.

The continuum method is, however, successful in predicting the energy of the radiation emitted by the F-centre with a realistic adjustment of the parameter m* to fit the absorption energy. This leads to another topic, that of the nature of the excited state of the F-centre. Although a detailed discussion is not relevant here, it may be mentioned that there is evidence that the wavefuntion of the excited state is quite diffuse, and may be treated appropriately by continuum theory. The diffuse character is suggested by the EPR work of Mollenauer and Baldacchini (1972) and by the work on radioactive lifetimes of Swank and Brown (1963; cited by Fowler, 1964).

Continuum theory gives the right temperature dependence of the width of the absorption band (Huang and Rhys, 1950; Pekar, 1953). The neglect of short range interactions, however, is a serious defect. The treatment of polarisation as long-range is surely not correct as a negligible field is expected far from the defect. Furthermore, the effective mass obtained by fitting to the absorption energies are very large. They are about twice the free electron mass, as compared to about one-half as determined by cyclotron resonance. But despite their drawbacks, continuum theories have some special uses (see, for example, Stoneham, 1972). The review of Eshelby (1956) about the continuum theory of lattice defects refers to the fact that this theory perhaps suffers from the disadvantage that its

limitations are more immediately obvious than are those of other approximate methods which have to be used in dealing with the solid state defects; for it sometimes gives good results even in what appear to be extreme cases.

2.3 Semi-continuum model

The first semi-continuum model was introduced by Tibbs (1939), but in the form in which it is used today is largely due to Simpson (1949). A fuller treatment is given by Krumhansl and Schwartz (1953) and their method is discussed in detail by Gourary and Adrian (1960). The method is to divide the crystal into two regions. The first region lies within a radius r_{ML}, called the Mott-Littleton radius (Mott and Littleton 1938; sometimes the nearest neighbour distance is used), where the Hamiltonian is that of a free electron in a square well of depth V_o. Beyond r_{ML} the effective mass approximation is used. V_o is made up of the Madelung potential and a polarisation correction. The method is thus suited to calculations which include polarisation and it is also possible to include the coupling of the F-centre to longitudinal optical phonons.

However, the model is, for practical purposes, only a spherically symmetrical one. Thus it cannot deal with defects of low symmetry. Also it is difficult to include lattice distortion in the model. The theory also has to be fitted to experiment by adjusting the effective mass of the electron, the Mott-Littleton radius and the effective permittivity. These drawbacks are absent in theories based on the Hartree-Fock approximation.

2.4. Hartree-Fock theory

The following outline of the Hartree-Fock theory is presented. A detailed discussion is given by Fowler (1984). The essential features of the theory are the separation of electronic and nuclear coordinates, the assumption of a static lattice in some equilibrium configuration, and the correct treatment of the Pauli exclusion principle. Thus, although the defect electrons move slowly outside the potential well and the resultant polarisation of the valence electrons of the ions should follow them, this is beyond Hartree-Fock theory. In this approximation, each electron responds only to the average position of the others. The Hartree-Fock theory of colour centres has been approximated in various ways. The simplest was introduced by Gourary and Adrian (1957). They studied only the wavefunction of the F-centre electron and assumed that the valence electrons are localised near the ion cores. The effective Hamiltonian treats the lattice as an array of point ions and, as the Hamiltonian represents an observable, it is Hermitian, so that the variational theorem applies. Gourary and Adrian (1957) predict

absorption energies to within 15%. They find that the wavefunctions are well localised, and so distortion and polarisation effects are small.

The shortcomings of the point-ion approximation are that the computed wavefunctions are not orthogonal to the valence and core states of the ions so that the Pauli exclusion principle is not satisfied. Furthermore, ionic potentials and polarisation effects have been ignored. The next problem is to investigate the corrections to the point-ion model.

The first improvement is the inclusion of the finite sizes of the ions. This requires a correct treatment of the Coulomb and exchange interactions, as well as the orthogonalisation of the defect wavefunction to the ionic wavefunctions. These can be included in two equivalent ways, the extended-ion method (Kojima, 1957 a, b; Wood and Joy, 1964; Wood and Opik, 1969) or the approximate pseudopotential methods (Kubler and Friauf, 1965; Bartram et al, 1968). Both the extended-ion and pseudopotential methods give improved agreement with experiment, although the pseudopotential calculations contain approximations to the integrals. The extended-ion model has been studied well and in considerable detail by Wood and Opik (1969). They include polarisation corrections, but this requires the introduction of a cut-off radius similar to that in the semi-continuum model. One important point which they do not treat exactly is the requirement that the wavefunctions of the ion cores should be orthogonal, although they mention that an approximate orthogonalisation procedure yields improved F band energies. They also discuss distortion effects, but here additional problems concerning the interionic potentials are encountered.

The advantage of the Hartree-Fock approach is that it treats the lattice on a microscopic scale. Although the calculations are lengthy, they are well suited to the localised character of the F-centre and allow the region near to the defect to be treated in an exact manner. There are still difficulties with polarisation and distortion effect, but these can be added as extensions to the Hartree-Fock theory. In particular, by representing the local structure of the lattice, defects of low symmetry can be treated and both hyperfine and spin-orbit interactions can be calculated in a consistent manner.

3. Classification of colour centres

3.1 The F-centre and its aggregates

The F-centre in alkali halides and other materials is one of the best known defects in solids . It has received extensive investigation both theoretically and experimentally and by now many review articles and books can be found devoted to the study of its properties, or to its use as a prototype in the study of the other types of colour centres (Markham, 1966;

Petrashen et al, 1970; Townsend and Kelly, 1973; Renn, 1974; Harker, 1976; Imanaka et al, 1977; Fowler, 1984).

From a theoretical viewpoint the F-centre is a sufficiently simple defect to enable the energy levels and the lattice interactions of both the ground and excited states to be calculated and checked against experimental observations. An important aspect of the F-centres is that it can be produced as a dominant absorption band in all the alkali halide crystals and by all types of treatments including irradiation, electrolytic or additive coloration. As this centre can be considered as a simple intrinsic defect with an absorption which is a simple function of the lattice spacing only, it may be used as a successful model for all defect studies.

Consequently, a considerable amount of experimental work started with this centre in order to study the different phenomena related to lattice defects, including the effect of pressure on band shifts (Maisch and Drickamer, 1958) and studies relating to fluorescence (Van. Doorn and Haven, 1956), field ionisation (Luty, 1956)EPR (Seidel and Wolf, 1968; Mollenauer et al, 1971), ENDOR (Fowler and Kunz, 1970; Wolbarst, 1973) and mixed crystals (Gnaedinger, 1953), Logatchov et al, 1970).

There are many colour centres related closely to the F-centre in the sense that they are all electron-excess centres which have been studied with differing degrees of interest. They include the excited states (K, L_1 , L_2 , L_3 ...) of the F-centre (Chiarotti and Grassano, 1966; Dawber and Parker, 1970; Kayanuma and Kondo, 1977) and the F'-centre (Pick, 1968; Delbecq , 1963; Bennett, 1970) which consists of an F - centre plus a second weakly bound electron. The effects of impurity association have been studied in the form of the F_A -centre which is an F-centre with one of the nearest-neighbour positive ions replaced by a different (impurity) alkali ion (Luty, 1968; Alig, 1970), the Z-centre, which is again an F-centre next to a divalent ion (Camagni et al, 1960; Logatchov, 1967), and the U-centre which is an F-centre plus a hydrogen atom (H^- ion) at a halogen site (Gourary, 1958; Gota et al, 1963).

Changes in peak position and defect stability can also occur if the F-centre experiences an electric field (Stark effect; Grassano, 1977) in, for example, the vicinity of dislocations (Arsenovici and Townsend, 1972). All these possible forms of F-centre have different thermal stabilities and, even if the broad F band disguises their presence, they can be detected as a series of annealing stages of nominally the same peak (Jain and Mehendru, 1965).

There are other anion vacancy defects which are associated with F-centres. They include the α -centre which is an anion vacancy or an F-centre from which the electron is missing (Onaka and Fujita, 1960), the β -centre which is an anion excitation near to the F-centre (Delbecq et al, 1951), the γ -centre which is thought to involve a higher excited state of the α -centre (Klick and Patterson, 1963) and the F-aggregate centres.

The general features of the F-aggregate centres and their phenomenology have been well established in the past few years but many related problems remain to be solved. The

absorption bands due to electronic transitions within these aggregate centres are known as M, R and N bands for historical reasons. However, a more logical set of labels has been suggested by Sonder and Sibley (1970) in which the charge state of the defect, compared with the neutral lattice, is indicated by a superscript and the number of associated F-centres by a subscript.

The M-centre (F_2 -centre) is so called after Molnar (1940) who made the first systematic study of the centre, though Ottmar (1928) was the first to notice it. It consists of two nearest neighbour F-centres and many models have been proposed (Seitz, 1954; Herman et al, 1956; Knox, 1959; Eva Restov, 1964) based on the result of a considerable amount of experimental work (Van Dorn, 1960; Compton and Rabin 1964; Hirai and Hashizume, 1967). A summary of the latest assignment, due to Englstrom (1975), names the optical transitions of this centre as M_1 which is the primary and most intense transition as well as being the one which satisfies the Ivey relation (1947). The other transitions are M_2 , M_2' , M_3 , M_3' and M_4 . However, Susman (1963) observed several other absorptions which are believed to arise from variants of the M-centre making a total of six (M_2 to M_7).

It is well known that the R-centre (F_3 -centre)is composed of three nearest -neighbour F-centres arranged in an equilateral triangle in a (111) anion plane (see figure 1.4). The most intense and well known absorption bands of this centre are the R_1 and R_2 bands. Two other absorption bands lie towards longer wavelengths, the R_M band, which overlaps the M_1 band, and the R_N band. The results obtained by Silsbee (1965) strongly suggest that the first excited state of the R-centre could account for the virtual absorption in the N band region (Von Der Lugt and Kim, 1966).

In accordance with the reported literature so far, the N-centre is the F_4 -centre and consists of four F-centres arranged tetrahedrally on adjacent sites as suggested by Pick (1960) (figure 1.4). There are two associated absorption bands (N_1 and N_2) though Hattori (1960) suggests that these two bands arise from different centres.

Considerable interest has been shown in the variants of F-aggregate centres, such as the F_2^+ , F_3^+ , M' (Chandra, 1969; Chandra and Holcomb, 1969), R_1' , R_2' (Hirai et al, 1962; Hughes, 1966; Naham, 1967), N_{1A} , N_{1B} (Schneider, 1966)and the N_{2A} , N_{2B} (Kikuchi and Ozawa, 1973)centres. More work, both experimental and theoretical, is needed in the field of F-aggregate studies to justify the proposed models. The review paper by Rolfe and Morrison (1977) and the reviews of Compton and Rabin (1964) and of Fowler (1984) provide further insight into the field.

The colloid centres are metal inclusions usually formed in additively (Doyle, 1958) and electrolytically coloured (Radchenko and Udod, 1971)alkali halide crystals as a result of F-centre aggregation due to thermal or photochemical treatment (Jain and Radhakrishna, 1969). The presence of these colloidal particles of alkali metal in alkali halide crystals has been well established by the studies of their optical, electrical and magnetic properties (Shatalov, 1956;

Compton, 1957; Doyle, 1960; Kaplan and Bray, 1963; Jain and Sootha, 1968). The position of the absorption bands due to these centres can be calculated theoretically on the basis of Mie's theory (Mie, 1908; Doyle, 1965; Radchenko, 1968) and the expected position of the colloid band for small spherical particles ($\leq$20 nm) can be calculated using the expression (Doyle, 1958):

$$\lambda_0 = (1 + 2n_0^2)^{\frac{1}{2}} \lambda_c \qquad (1.6)$$

where n_0 is the refractive index of the alkali halide crystal and λ_c is the Wood-Zener wavelength of the alkali metal (Wood, 1933).

Irradiated coloured crystals of alkali halides show these centres too, under certain conditions (Pappu and McCarthy, 1971). However, there are the c-centres, which arise from very small colloid formations consisting of dispersed metallic centres which do not exhibit the Tyndall effect but show only optical absorption (Udod, 1968).

The literature is extensive on these centres, but it appears from the existing proposed tentative mechanism for colloid formation (Sastry, 1969) that there is a need for further systematic investigations of the different factors involved in the thermal transformation of F-centres into colloids and vice-versa.

3.2 Hole-excess and other centres

Colour centres can be of other types than the electron-excess F-centre and its aggregate. Impurity centres and hole-excess centres (commonly known V-centres) are two important examples which may be produced by thermal, photothermal and doping processes similar to those used for producing F-centres. Despite their importance in defect studies of alkali halides and the extensive amount of investigative effort devoted to them, they are still in many respects not adequately understood. This is particularly true with regard to previous theoretical work and is illustrated by the number of tentative and speculative models and production mechanisms which have been suggested so far for these centres.

When impurity centres (for example Tl^+ , In^{2+} , Sn^{2+} , Pb^{2+}, Ag^+, Cu^+) are present in alkali halide crystals, a number of new absorption bands appear on the low -energy side of the fundamental bands. Typical absorption bands of such centres are reported for Ag^+ -doped alkali halide crystals by Fussganger et al (1965) and for Hg^{2+} in alkali halide crystals (Baranov, 1977). These centres may be substitutional (the above mentioned centres)or intestitial or may be of a more complex nature (Klick and Schulman, 1957; Fowler, 1984). The identification of these centres is usually achieved by using chemical, optical and EPR techniques.

The interstitial centres which have been identified most clearly are the H-centre which is essentially an interstitial anion atom (Kanzig and Woodruff, 1958), the I-centre which is the interstitial anion (Thermalingham, 1964) (figure 1.5), the U_1 -centre which is the interstitial hydrogen ion H^- (Klein, 1968) and the U_2 -centre which is interstitial hydrogen atom H^o (Delbecq et al, 1956).

The list of the already recognised substitutional and interstitial impurity centres is long but a good review of the subject, which places the emphasis on the already well understood V_k -, H- and I-centres, is given by Itoh (1972).

The hole-excess centres colour some of the alkali halide crystals when produced additively (Mollow, 1937; Nakai, 1958) and electrolytically (Uchida and Nakai, 1953). However, temperature determines the type of V bands which are formed by ionizing radiation (figure 1.6) (Dorendorf and Pick, 1950; Dorendorf, 1951). For example, at room temperature only V_2 and V_3 bands are produced (Alexander and Schneider, 1949)while at liquid nitrogen temperature the V_1 band is seen (Ruchardt, 1956; Hersch, 1957). For historical reasons the absorption bands arising from the hole-excess centres, which appear at energies higher than that of the F-band, are labelled V_1 , V_2 ... , V_7 , V_8 .

The electrical, optical and other properties of V-centres have been studied extensively (Dutton and Maurer, 1953; Ishii and Rolfe, 1966; Hoshino and Shimoji, 1971; Gorbenko and Kovtun, 1972; Flynn, 1982). But, despite the amount of experimental information which has been gathered, only a few of these centres, namely the V_k - , V_1 -and V_F -centres, are well understood. Many models have been suggested since the original proposals of Seitz (1954) (Schulman and Compton, 1962; Itoh, 1972). Using EPR and optical methods there is now strong evidence about the nature of the three centres. The V_k -centre is thought to be a self-trapped hole shared by two adjacent halogen ions (Delbecq et al, 1961), the V_1 -centre is assigned to an H-centre associated with an alkali impurity ($V_1 \equiv H_A$) (Yuster et al, 1967)and the V_F -centre is the antimorph of the F-centre (figure1.5), that is, it is a positive hole trapped by a cation vacancy (Kanxig, 1960; Schoemaker, 1968; Lobanov, 1975). The identification of the V-centre has changed since the first optical bands were attributed to hole excess-centres. For example, Schulman and Compton (1962) have summarised some of the early models proposed for the V_1 -centre which include a model assigning the V_1 - centre to be the antimorph of the F-centre.

4. The host lattice

4.1. Ionic solids

The structure of the host lattice is clearly an important factor in determining the properties of colour centres. Even the simplest square-well model of the F-centre includes the nearest neighbour distance as a parameter. In general the more detailed the model is, the more information about the structure of the host crystal must be included. Modifications and corrections must also be added to models based on perfect crystals by, for example, adding information on the positions of ions to the point-ion model, and by including the average permittivity and ionic polarisabilities (Dexter, 1958; Greenwood, 1984).

The crystals which are dealt with in this work are ionic and both static lattice effects, such as the symmetry of the colour centre, and dynamic effects, such as the influence of lattice vibrations of the surrounding medium on the colour centre, are clearly important.

In a perfectly ionic solid there is complete charge transfer to form positive and negative ions which are then held together by electrostatic forces. The ionicity (Weller, 1973) of any of these crystals determines the degree of electron density localisation around the ions. The formation of an ionic solid can be described in the following way.

The atoms are assumed initially to be separated by a large distance so that they do not interact. An electron is then removed from each electropositive atom, requiring an energy equal to the ionization potential I, and is placed on an electronegative atom regaining an energy E equal to the electron affinity. Finally the ions are brought together to a separation r, thereby gaining the Madelung energy. Thus the total energy Δ per molecule due to the charge transfer is

$$\Delta = I - E - \frac{\eta e^2}{4 \pi e_0 r} \qquad (1.7)$$

where $\frac{e^2}{4 \pi e_0 r}$ is the coulomb potential and η is the Madelung constant.If Δ becomes negative for some spacing r_0 , the solid will be stable with a cohesive energy of Δ . The crystal is prevented from collapsing completely by the overlapping of ions. The overlap of the charge clouds results in a smaller coulomb energy gain than with zero overlap, but also introduces exchange effects. The net result is that, at the equilibrium separation, the cohesive energy deviates only by 10% to 20% from the Madelung energy. Detailed calculations of the cohesive energies of ionic solids can be found in the literature (see, for example, Lowdin, 1962). It is interesting to see that the cohesive energy may be split into various terms

$$E_{coh} = E_{mad} + E_{corr} + E_{exch} + E_{ov} \qquad (1.8)$$

where E_{mad} is the Madelung energy, E_{corr} is the difference between E_{mad} and the coulomb interactions of atoms treated as classical charge distributions, E_{exch} is the sum of two-centre

exchange interactions and E_{ov} is the energy contribution explicitly dependent on overlap between ion-core orbitals.

These quantities have been evaluated by Howland (1958) for KC1 using free ion core orbitals but including the overlap between the outer shell orbitals of a Cl^- and its nearest-neighbour K^+ and second neighbour $C1^-$ ion. His values are given in table 1.1.

Two types of lattice defects can exist in ionic crystals. Schottky defects are formed as dissociated pairs of anion and cation vacancies. The thermal production and motion of these vacancies is crucial in the present work as they play a fundamental role in electrolytic coloration (Suptit z and Teltow, 1967; Nadler and Rossel. 1973; Seitz, 1980).

Two kinds of Frenkel defects are possible in ionic crystals. Either the cations or the anions may move into interstitial positions (figure 1.7) leaving equal concentrations of the respective vacancies. The work of Jost (1933)helped to establish the plausibility of the early models of intrinsic lattice defects due to Frenkel (1926)and to Schottky and Wagner (1930) by showing that, despite the large cohesive energies of ionic crystals, reasonable values for defect formation energies could be obtained as a result of the large gain in energy due to the polarization of the lattice by the net charge of the defects. A major step forward was made by Mott and Littleton (1938) who presented a reasonable approximation for describing the polarization and displacement fields around the defects within a discrete lattice model. A number of workers (Brauer, 1952; Tosi and Fumi, 1957; Jurosawa, 1958; Scholz, 1964; Simpson, 1965; Tosi and Dyama, 1966) have subsequently worked on this line and, in general, the published results of their calculations show fairly good agreement with experiment (table 1.2).

4.2 Alkali halides

The purpose of this section is to give a general understanding of the main characteristic features of alkali halide crystals, especially those which are related to the formation of point defects. This is important since, in any study of colour centres, defect formation is the more challenging problem than its identification because of its dynamic nature and its relations with many variables.

In alkali halide crystals the lattice defects which cause conductivity and diffusion are the Schottky defects (Rolfe, 1964). The concentration of Schottky defect pairs which are in thermal equilibrium at a given temperature is

$$N_s = N \exp\left[-\frac{g_s}{2kT} \right] \qquad (1.9)$$

Table 1.1. Theoretical energies involved in the calculation of cohesive energy for KCl (Howland 1958).

	eV
E_{mad}	- 8.18
E_{corr}	- 0.89
E_{exch}	- 2.64
E_{ov}	-4.69
E_{coh}	7.02
$E_{coh\ (exp.)}$	7.1

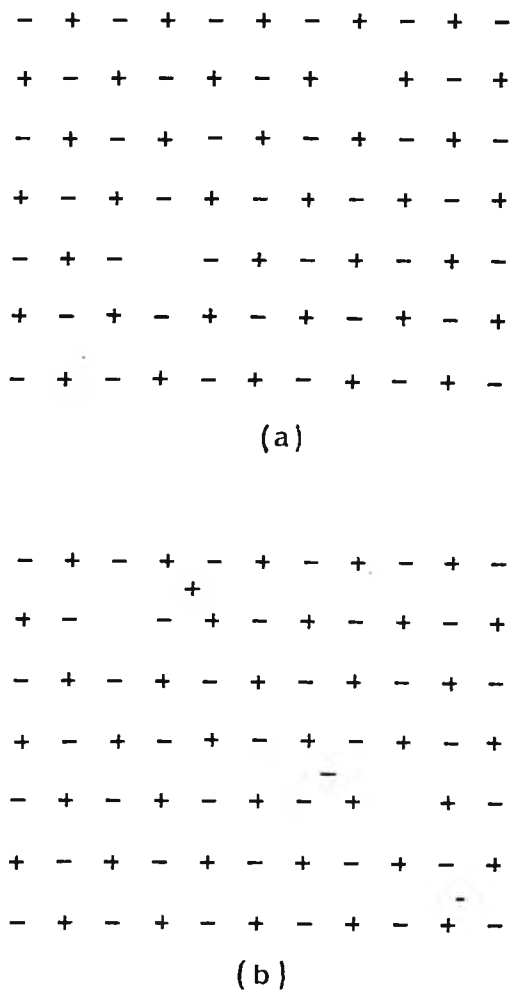

Figure 1.7 (a) The Schottky defect and (b) the Frenkel defects

Table 1.2 Values of the Schottky formation energy E_s (eV) and the cohesive energy (eV) of alkali halides. The theoretical values of E_s are calculated as described in the work of Boswarva (1972). The theoretical values of cohesive energy are those given by Tosi (1964).

	E_{coh}	E_S	E_S (expt)	References
LiF	10.7	2.71	2.68	Haven (1950)
NaF	9.5	3.23	2.56	Bauer and Whitmore (1970)
NaCl	7.9	2.27	2.12	Dreyfus and Nowick (1962)
NaBr	7.5	2.23	1.72	Hoshino and Shimoji (1967)
NaI	6.8	1.84	2.27	Hoodless et al (1971)
KCl	7.1	2.50	2.49	Fuller et al (1968)
KBr	6.8	2.42	2.53	Chandra and Rolfe (1971)
KI	6.3	2.29	2.21	Chandra and Rolfe (1970a)

where g_s is the free energy of formation of a pair of vacancies of opposite sign and N is the total concentration of ion pairs. Charge neutrality requires that, in ideally pure crystals, the concentrations of cation and anion vacancies are equal. In practice, however, aliovalent impurities introduce an excess of vacancies of a given sign, which become predominant at low temperature where the number of defects given by equation (1.9) is small. The divalent cations are a very common impurity which go substitutionally into the crystal lattice (Pick and Weber , 1950), thus giving rise to an excess of cation vacancies.(Harrison 1982)

A typical conductivity against temperature plot is, therefore, made up of two distinct and clearly identifiable regions. In the high temperature intrinsic range, the concentration of vacancies is given by equation (1.9) whereas in the low temperature impurity range the concentration of vacancies is essentially constant and the activation energy obtained from the conductivity plot is often the activation energy for the migration of the excess mobile defects (Kerkhoff 1951) provided by the impurities.

Comparison between diffusion and conductivity (drift) is illuminating as to the nature of defects in certain crystals. If both forms of transport are due to the same mechanism, the ratio between the diffusion coefficient D and the electrical conductivity σ should be governed by the familiar Nernst-Einstein equation

$$\frac{D}{\sigma} = \frac{kT}{Ne^2} \qquad (1.10)$$

Extensive investigations in ionic crystals, with alkali crystals as prototypes, have established that mass transport takes place by the exchange of ions with vacant lattice sites (Barr and Lidiard, 1970). Lidiard (1957) has developed the theory of diffusion by the vacancy mechanism. According to his theory extra vacancies are created by polyvalent impurity ions and the vacancies form associated pairs with the impurity ions (table 1.3). This association takes the form of a vacancy-impurity complex at temperatures about room temperature and below. The activation energy of this association can be obtained from the third region of the conductivity against temperature plot. The diffusion coefficient depends on the degree of association, which is a function of impurity concentration and temperature. Various aspects of this theory find excellent quantitative agreement with the results of diffusion work in alkali halide crystals (Flynn, 1982).

The association of vacancies into pairs (neutral pairs of cation and anion vacancies which are commonly known as vacancy pairs (Tosi and Fumi, 1958)) has been studied extensively, giving the fractional concentration of these pairs m as (Tosi and Airoldi, 1958)

$$\frac{m}{N} = 6 \exp\left[\frac{E_p}{kT}\right] \qquad (1.11)$$

Table 1.3 Association energies (eV) for the divalent cation-cation vacancy complex in alkali halides. Values in parenthesis are for ionic radii from Pauling (1960) in nm.

	KI	KBr	KCl	NaCl
Ca^{2+} (0.099)	0.38(1)	0.46 (2)	0.52 (3)	0.67 (2)
Sr^{2+} (0.113)	0.26 (4)	-	0.42 (5)	0.52 (4)

(1) Lawson (1962)

(2) Süptitz and Teltow (1967)

(3) Barr and LeClaire (1964)

(4) Nadler and Rossel (1973)

(5) Manning (1964).

where $N = N+ = N-$ (intrinsic range) and E_p is the binding energy of a pair in its fundamental state.

The importance of vacancy pairs, especially in the electrolytic coloration method, lies in the fact that their fractional concentration increases with temperature, and it reaches a high value only just below the melting point. However, while these pairs do not play any part in the conductivity process, they contribute to the diffusion and related mass transport processes because of their high mobility (Roy et al, 1947; Dienes, 1948; Lawrence, 1960). The association of a divalent cation impurity and a cation vacancy into a pair has the same importance, since they have their marked influence on the mass transport processes and the Z-centre (Seitz, 1951; West and Compton 1957; Remaut and Dekeyser, 1958; Ishiguro et al, 1960; Crawford and Slifkin, 1982). The success of the Born model of cohesion (Tosi, 1964; Kittel, 1985) has encouraged atomistic calculations of the characteristic energies of point defects giving formation and migration activation energies.

Alkali halide crystals have a well defined lattice (figure 1.8) and many phenomena are well documented. The electrical, optical and physical properties of these crystals have received extensive investigation (see, for example, Seitz, 1950; Ahrenkil and Brown, 1964; Fumi and Tosi, 1964; Peterescu, 1965; Pooley, 1966; Komnik, 1968; Torrens and Chadderton, 1968; Marat-Mendes and Comins, 1977; Lamb, 1986). In the present work the principal properties of the alkali halides which are of interest are the vacancy mechanism of matter transport, the role of ionic conductivity in electrolytic coloration and the influence of divalent impurities.

4.3. Alkali fluorides

The physical properties of LiF (Eisenstadt, 1963), and to a lesser extent of NaF (Bauer and Whitemore, 1970) and KF (Pitchie and Lew, 1964), have been studied for many years. A detailed study of their ionic conductivity and diffusion parameters is still lacking, though some work has been done in this field (Pantanelli and Whitemore, 1974). As the lattice disorder in these three materials is known to be of the Schottky type, the predominant defects are cation and anion vacancies and matter transport is controlled by the concentration and mobility of these vacancies. Since, in the alkali halide crystals which have been studied so far, the anion vacancies are less mobile than the cation vacancies, the mobility of the latter will be dominant in the ionic conductivity (Stoebe and Huggins, 1966; Jain and Sootha, 1967; Greenwood, 1984).

The data given by studies of fluorine diffusion in NaF and LiF (Matzde, 1971; Lamb, 1986) shows that the contribution of the vacancy pair mechanism to anion mobility at high temperature is more important in alkali fluoride crystals than in alkali chloride, bromide and iodide crystals. This is an important point to note since it is always the cation vacancies

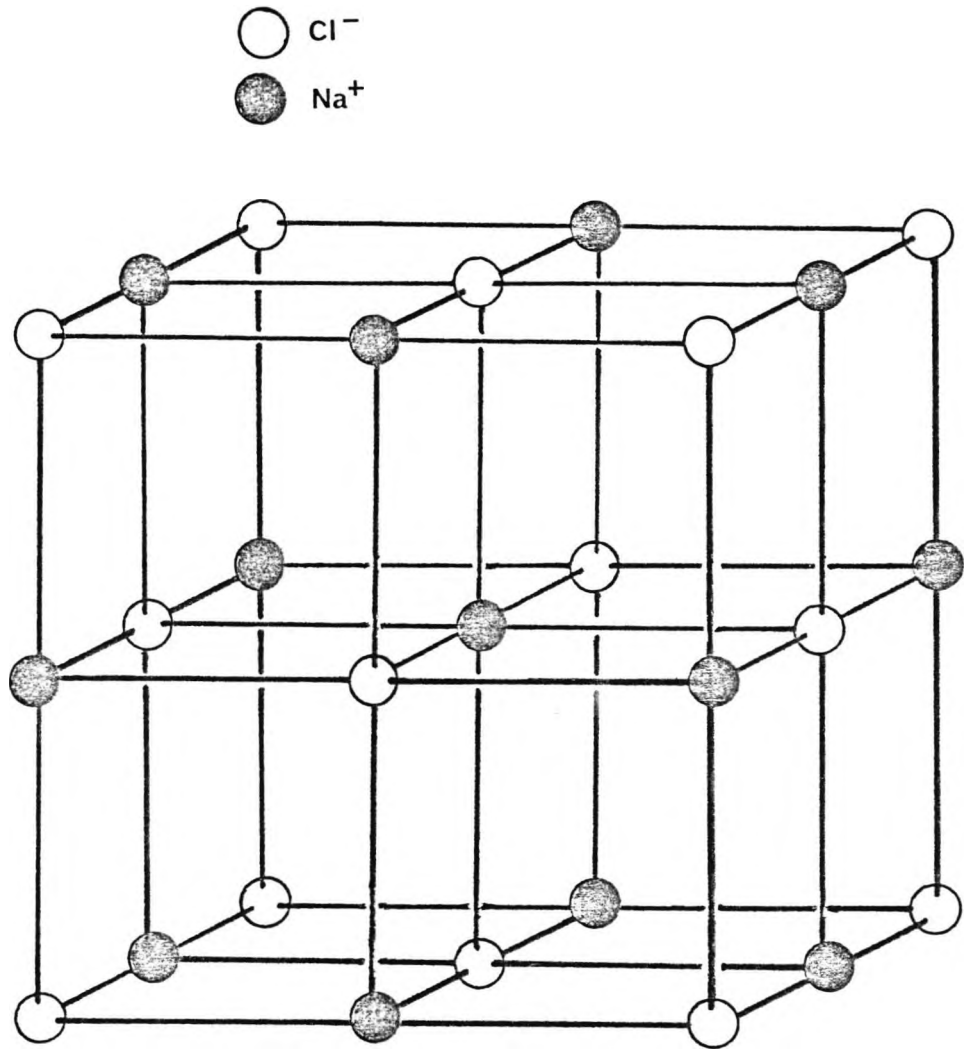

Figure 1.8 The fcc unit cell of NaCl

which dominate the ionic conductivity through their high concentration and mobility. The role of divalent cation impurities is also important because of the cation vacancies which they contribute.

The interionic distances in the alkali fluorides are the smallest of the alkali halide crystals so that they provide the most stable electron traps or electronic colour centres. It is necessary, therefore, to look for special phenomena, such as the reported impossibility of introducing well-characterized colour centres into these crystals by the additive and electrolytic coloration methods (Gorlich et al, 1963; Podini, 1965; Jirgal et al, 1968; Meistrick, 1968; Ozawa, 1973; Lampert and Mark 1985). The reasons which have been given for this phenomenon are many and include, in addition to the small interionic distances, the low vapour pressure of lithium metal and the high OH^- (> 1ppm) content of the crystals (Collins et al, 1974). Thus, the irradiation technique has been used so far in the coloration of alkali fluorides (Kubo, 1974; Przibram 1986) and the reported properties of the F-centre and its aggregate centres in these crystals refer to irradiated crystals.

Clearly, much more work has yet to be done on these crystals. Although the F-centre and its aggregate centres have been identified by their absorption bands or zero-phonon lines, the absorption bands appearing on the low-energy side of the M band are relatively untouched and their characteristic properties and correlations are uncertain at present despite much empirical data (Knorad and Neubert, 1967). Many of the colour centres produced by the irradiation technique followed by various chemical, thermal and optical treatments have disputed identification (Kubo, 1969, Kituchi and Ozawa, 1973; Przibram, 1986).

There are many advantages in studying the coloration of alkali fluoride crystals electrolytically since this method provides relatively stable colour centres which can be easily identified using Ivey's relations. The coloration process itself and the subsequent thermal and optical treatments of the coloured crystals can provide more information on the mechanism of electrolytic coloration and on the colourability of the alkali fluoride crystals. These and other aspects of alkali fluoride crystals are discussed later on, in chapters 3 and 6.

5. Methods of colour centre production

5.1. Requirements for coloration and available methods

The two factors which control the production of F-centres are the supply of negative ion vacancies and the availability of electrons which can be trapped at these vacancies. Referring back to section 4.2, a perfect alkali halide crystal is an insulator with a filled valence band, an empty conduction band and no ion vacancies. But, because of thermal equilibrium, the as-grown alkali halide crystal contains a finite concentration of cation and anion vacancies.

Since the ground state energy level of the F-centre lies in the forbidden energy gap between the valence and conduction bands (Schulman and Compton, 1962) it cannot normally be occupied by an electron.

F-centres can be introduced into an alkali halide crystal by three principal methods (Markham, 1966). The first method is by irradiation, the second by additive coloration and the third by electron injection or electrolytic coloration. Another method of colour centre production is that of chemical coloration and has been a great help in establishing models for these colour centres. Chandra (1969) and Chandra and Hocomb (1969) have used a chemical doping method to control the concentration of colour centres in NaF resulting from X-irradiation and to assist in their identification.

Each of the three methods mentioned above has its own features and its own practical use and advantages. Ionising irradiation, for example, applied to an alkali halide crystal provides enough electrons and anion vacancies to produce F-centres at room or lower temperatures. On the other hand, the apparatus used in additive coloration and particularly in electrolytic coloration is much less expensive than the sources of ionising irradiation. The next three sections of this chapter give a short review of the main features of each of the three principal methods of colour centre production including the most likely mechanism by which each method produces F-centres. The F-centres produced by any of the above methods have been shown to be identical (Markham, 1966; Kittel, 1985).

Other colour centres can also be produced by these methods provided that the correct conditions of temperature, pressure, energy dose, wavelength, current flow etc. are chosen. Optical, chemical, thermal and other treatments of the F-coloured crystals can produce other colour centres such as F-aggregate centres, F_A - , Z- and V-centres. Some of the colour centres are transitional (for example, the M-, R-centres) while others overlap with the absorption band of other more prominent colour centres. The V-centres are usually produced in the irradiated alkali halide while it is possible to introduce these centres into KI and KBr crystals only by using the additive or electrolytic coloration methods.

5.2. Irradiation method

All of the known colour centres can be produced in the alkali halide crystals when these crystals are exposed to short-wavelength photons (X - rays, γ - rays, ultra-violet radiation) or bombarded by particles (neutron, proton, electron) of sufficient energy. The phenomenon was first described by Goldstein in 1891 (cited by Pick, 1958) in connection with cathode rays, and has been explored systematically several decades later by Pohl et al (1938).

A typical absorption spectrum resulting from the irradiation of KCl with X-rays is shown in figure 1.6. In the main, three bands are distinguished. The first is a strong peak in

the visible (F band), the second consists of one or more peaks in the ultra-violet (V bands or an α band)whilst the third is a weak absorption in the red or near infrared (M band).

A number of phenomena are associated with this method of colouring. For example, optical bleaching of the F-band by irradiation with light within the F band region not only reduces the colour density but also creates new absorption bands in the red (R and N bands). Bleaching can occur spontaneously, unlike the F band produced by other methods which are more durable.

On studying the quantitative aspects of radiation damage in alkali halide crystals, it is found that the energy required to create an ion vacancy is considerably lower than might be expected from the mechanical properties of the material or from the interionic binding energies involved (Seitz and Koehler, 1956). Historically the Seitz model (Seitz, 1954) was the first which attempted to show how vacancies could be formed in alkali halide crystals by X-rays assisted by the motion of edge dislocations and the formation of an exciton. A pair of vacancies is created in the crystal when this exciton interacts with the dislocations. Varley (1954) proposed a multiple ionisation of a halogen ion as a mechanism by which halogen vacancy-interstital pair might be generated. Much work has been carried out on the original Varley mechanism in order to modify its shortcomings (Dexter, 1960; Varley, 1962; Williams, 1962). The Varley model does not describe the subsequent fate of the interstitial or suggest how far the components of the pair are separated at low temperatures. Klick (1960) proposed a mechanism based on the suggestion of pairing of the neutral atoms to form a molecule which could diffuse away from the defect site by hole migration along the line of halogens. However, measurements of luminescence and defect formation rates as a function of temperature led both Pooley (1965) and Hersh (1966) to propose basically the same model for the formation of F- and H-centres in the alkali halide crystals during irradiation with either X-rays or low-energy photons. The observation that there is an anti-correlation between the rates suggests that the incident radiation is passed to the lattice in either of two ways, one of which gives luminescence and the other produces displacements. It is proposed that the essential entity in this energy conversion is a molecular halide ion which undergoes excitation from a bound electron-hole pair. The self-trapping of the hole part of the pair and the return of the electron to the ground state leads to the formation of H-and F-centres. Pooley's model is supported by many experiments, like that of Goldstein (1967) and that of Pooley and Runciman (1970) on the anti-correlation between the rates of defect production and luminescence during irradiation. Furthermore, the pulse experiments of Still and Pooley (1969) and those of Ueta et al (1969) on mixed crystals showed that Frenkel defects are the product of irradiation and, therefore, provided results which are consistent with this model but not with others.

The growth of colour centre concentration with irradiation is a complex function of the concentration and nature of defects, impurities and dislocations and of the temperature and

irradiation conditions (Etzel, 1955; Nowick, 1958; Govinda, 1974; Harrison, 1982). Coloration by photon irradiation tends to produce a non-uniform distribution of centres and coloration by X-rays seems to be a linear function of the time of exposure (Duerig and Markham, 1952; Martienssen, 1952). The effect of divalent impurities on coloration depends on the temperature of irradiation. At low temperature Ca^{2+} increases the colourability of the crystal (Etzel, 1952; Rabin, 1959) but the effects are more complicated for irradiation performed near to room temperature (Hesketh, 1959, Harrison, 1962, Herrmann and Pinard, 1972).

In general, however, the coloration curve of alkali crystals can be divided into three stages. The early or rapidly growing initial stage (Stage1) is characterised by the relatively easy production of F-centres and the easy destruction of these centres by optical bleaching (Bron, 1963). This stage is followed by an essentially flat region (StageII). The saturation shown by this region depends on the divalent impurity content (Sibley et al, 1964), the plastic strain (Prizbram, 1986) and the radiation intensity (Mitchell et al, 1961, Agullo-Lopez and Jaque, 1972; Kittel, 1985). The region progressively bends upwards to reach once again a relatively high F-centres production rate (Stage III). The primary process of the colouring in this stage is the creation of Frenkel pairs (Crawford, 1968; Durand, 1969; Pauling 1980).

5.3. Additive coloration

F-centres can be produced additively by heating the alkali halide crystals in alkali metal vapour and then rapidly cooling them to room temperature. The crystal acquires a visible coloration which depends on the particular alkali halide crystal. This method shows that F-centres are due to a stoichiometric excess of metal (Kleinschrod, 1936) and, when considered together with theories of the intrinsic Frenkel and Schottky defects, suggests that the centres consist either of an interstitial neutral atom or an electron replacing an anion at a lattice site. Another suggestion which has been made considers the F-centres as a self-trapped electron on the basis that, if an electron were to remain on a particular alkali atom for a time long compared with a vibrational period ($\sim 10^{12}$ .s.), the surrounding ions could become displaced in a stable manner from their equilibrium positions as a result of polarisation. This displacement then creates potential well in which the electron is bound. The suggestion can be ruled out by the physicochemical argument that the concentration of F-centres is proportional to the concentration of alkali vapour in which the alkali halide crystal is heated (Rogener, 1937). If the self-trapping model were correct, each alkali atom would dissociate into two defects, an interstitial alkali ion and an electron, and the concentration of F-centres would then be proportional to the square root of the vapour concentration. More work by Gilbert (cited in Fowler, 1984) shows that the self-trapped electron is not, in fact, stable.

At temperatures near to the melting point of the alkali halide crystals, the anion vacancies are very mobile. This mobility implies a similar mobility of the anions. At the surface a metal atom is ionized by giving off an electron, which migrates into the crystal. The metal ion then combines with a halide ion at the surface and the process eventually leads to the formation of new layers of material on the surface of the crystal, while an anion vacancy migrates inwards. In this way both the vacancies and electrons are produced at the surface. On cooling, an electron may be attracted towards a positively charged anion vacancy thereby forming an F-centre. In practice the vacancy may be a pre-existing vacancy, a vacancy formed by the additive coloration process, or even an anion vacancy which was part of a neutral pair. The picture given above implies that, on additive coloration, the density of the crystal decreases linearly with the concentration of F-centres formed. Witt(1952) (cited by Dekker, 1984) has studied the density changes and has found that the linearity is satisfied.

In princip , additive coloration experiments may be carried out using various combinations of metals and alkali halide crystals. However, alkali fluorides have always been difficult to colour using this method and the reasons given for this are the slow rates of diffusion or, in the case of lithium, the low vapour pressure. The various aspects of this method and its F-centre production mechanism have been investigated by many workers (for example, Van Doorn, 1961; Tsal and Pshkovskii, 1964; Ben-Dor et al, 1966; Kalnin and Itskovich, 1975).

However, by analogy with the introduction of electron-excess centres in alkali halide crystals by a stoichiometric excess of the alkali metal, it is possible to colour some of these crystals by annealing them in the corresponding halogen vapour at high temperature and high vapour pressure, followed by quenching. This was done by Moll wo (1937) for KI and KBr. The resultant absorption bands were called V bands by Seitz (1946). It should be noted that the production of V-centres by the additive method is considerably more difficult than the production of F-centre using the same method. In fact, it is not possible to incorporate excess chlorine into the alkali chloride crystals even at the highest possible temperature and pressure.

5.4. Electrolytic coloration

Electrolytic coloration is the least studied method of the three colour centre production methods. Unlike the irradiation method not all the alkali halide crystals can be coloured electrolytically but not all the colour centres can be produced using this method. The problem of the colourability of the alkali fluorides and the reported difficulty of introducing V-centres into alkali halide specimens by electrolytic coloration, except in the case of KI and KBr, are now well known (Schulman and Compton, 1962; Harrison, 1982).

The procedure of an electrolytic coloration experiment is normally to clamp the specimen between two electrodes in a furnace enclosure and then to apply an electric field along the length of the specimen at an elevated temperature. The electrodes are usually a flat anode and a short cathode in the form of a pointed rod. The electric field is applied when the specimen has come to thermal equilibrium. Within a few seconds of applying the field, coloration emerges from the pointed cathode and a few seconds later the coloration spreads out until it reaches the flat anode.

Pisarenko (1962)suggested that, at the initial period of applying an electric field, the specimen is polarised. Subsequently, a redistribution of the field occurs in such a way that, in the areas adjacent to the electrodes, fields of high intensity are created. The high intensity field created near the cathode promotes the injection of electron into the interior of the specimen. This is probably aided by a lowering of the electron emission work function due to the deposition of alkali metal on to the cathode. A proportion of the electric field in the region of the anode. This field attracts halogen ions to the anode, while alkali ions are neutralised by the electrons now present in excess and precipitate in the form of colloid. A further proportion of the remaining electrons recombine with trapping centres, including anion vacancies.

Pohl (1932) used the pointed cathode technique for the first time. Hadley (1968) has proposed that the use of a pointed cathode in the electrolytic coloration experiments facilitates the electron injection due to the high current density at the point. Therefore, the injected electrons are the result of the high accumulation rate of alkali metal and not to the high electric field around the cathode. Paramo and Sanchez (1971) and Lampert and Mark (1985) have investigated the plausibility of this hypothesis and have given experimental evidence that the formation of an alkali metal cathode and the thermionic emission from this new electrode are due to ionic conductivity mechanisms which take place in the specimen prior to electrolytic coloration. However, Uchida and Nakai (1953) and Kittel (1985) found that positive holes can be injected into alkali halide specimens and eventually V-centres can be formed when they reversed the polarity of the pointed electrode so that it becomes the anode.

Gorlich et al (1963) reported unsuccessful attempts to introduce F-centres into specimens of lithium fluoride using the electrolytic coloration method. Gritsenko (1971), whilst studying this problem, suggested that their failure was due to the high work function for the emission of elctrons from the metal into the LiF specimen compared with that from metal into KI or other alkali halides. However, Paramo and Sanchez (1971) have investigated the role of ionic processes in the electrolytic coloration of KBr and KI and have concluded that the cation vacancy migration plays the main role in the electron injection process at the outset of the electrolytic coloration. Tyagi et al (1970) used the continuity equation given by Smith (1959) to deduce from experimental data that the diffusion of F-centres in electrolytically coloured specimens is governed by the self diffusion of K^+ ions.

According to the generally accepted point of view (Pick, 1958; Amsel, 1982; Lamb, 1986) migration processes play an important part in F-centre formation, and therefore, in vacancy concentration changes in specimens during electrolytic coloration. The density of the alkali halide decreases during electrolytic coloration as has been reported by Hackskaylo and Groetzinger (1952). Heiland (1950) has also observed that electrolytic coloration is affected by the surrounding atmosphere.

Although relatively few studies of ionic conductivity have been devoted to electrolytically coloured alkali halide specimens doped with divalent cations (Ignateva et al, 1964 , Pershits and Ilin, 1968) have found that ionic conductivity in KC1:Pb^{2+} , KCl :Zn^{2+} and KC1: Cd^{2+} is considerably reduced by electrolytic coloration. The ionic conductivity of specimens doped with other divalent cations like Ca^{2+} , Sr^{2+} , Ba^{2+} and Ni^{2+} are not changed by electrolytic coloration and neither is the valence of the cations. These results led Topa and Yuste (1970) to suggest the existence of a correlation between the possibility of a change in the valence of the cations and their electronegativity. The change of valence by electrolytic coloration takes place for the more electronegative elements such as Ge, Sn, Zn, Cd and Mn (according to Pauling's scale see Gordy and Thomas, 1956) and not for the least electronegative elements such as Ca, Sr and Ba. On this basis it is possible to explain the formation of Z-centres in electrolytically coloured specimens doped with the second group of elements but not in the Pb^{2+}, Sn^{2+}, Zn^{2+} and Mn^{2+} -doped specimens.

The electrolytic coloration of alkali halide specimens doped with Pb^{2+} , Sn^{2+} and Ge^{2+} led to the formation of new stable centres called by Velicescu and Topa (1973) T-centres. They studied the optical, electrical and magnetic properties of these centres and showed that they are due to the reduction of the valence of the divalent cations and the creation of Pb^{-} , Sn^{-} and Ge^{-} ions. The work on Ag^{+} -doped alkali halide specimens showed similar effects (Kleeman, 1968; Topa, 1968).

The formation of colloid colour centres in KI, KBr and KC1 using electrolytic coloration have been studied by Radchenko and Udod (1971). Doyle and Agarwal (1965) have calculated the absorption band maximum of these centres in the electrolytically coloured alkali halides.

6. References.

Ahullo-Lopez F and Jaque F 1972 J. Phys. Chem. Solids 32 2009

Ahrenkiel R K and Brown F M 1964 Phys. Rev. 136 A223

Alexander J and Schneider E E 1949 Nature 164 653

Alig R C 1970 Phys. Rev. B2 2108

Allnatt A R, Pantelis P and Sime S J 1971 J. Phys. C: Solid St. Phys. 4 1978

Amsel G 1982 Physics of Solid Electrolytes, Academic Press, London

Arsenovici L C and Townsend P D 1972 Phil. Mag. 25 381

Baranov P.G., Zhitnikov R, A. and Khramtsov V.A. 1977 Sov. Phys-Solid St. 19 12.

Barr L W and Dawson D K 1965 Proc. Br. Ceram. Soc. 5 77

1971 Proc. Br..Cerm. Soc. 19 151

Barr L W and LeClaire A D 1964 Proc.Br.Ceram. Soc.1 109

Barr L W and Lidiard A B 1970 Phys. Chem. An Advanced Treatise Vol 10 Academic Press, London

Bartram R H , Stoneham A Mand Gush P W 1968 Phys.Rev.176 1014

Bassani F and Fumi F G 1954 Nuovo Cimento 11 274

Bauer G F and Whitmore D H 1970 Phys. ST.Solid. 37 585

Ben-dor L, Glasner A and Zolotov S 1966 Phys.St.Solid.18 593

Beniere F, Beniere M and Chemla M 1971 Z.Mat. 26A 915

Bennett H S 1970 Phys.Rev.B1 1702

Bereznyakii E N 1971 Sov. Phys.-Sol. St. 12 2970

Blum H 1962 Phys. Rev. 128 627

Bogan L D and Fitchen D B 1970 Phys. Rev. B1 4122

Boswarva I M and Lidiard A B 1967 Phil. Mag. 16 805

Boswarva I M 1973 J.Phys. C: Solid St. Phys. 5 L5

Brauer P 1952 Z. Naturf. A7 372

Bron W E 1963 Phys. Rev. 119 1578

Camagne P Ceresara S and Chiarotti C 1960 Phys.Rev. 118 1226

Capelletti R 1968 Nuovo Cimento 45B 233

Castner T C and Kanzig W 1957 J.Phys. Chem. Solids 3 178

Caulfield H J 1964 J. App. Phys. 35 2862

Chandra A 1969 J.Chem. Phys. 51 1499

Chandra A and Holcomb D F 1969 J.Chem.Phys. 51 1509

Chandra S and Rolfe J 1970 Ca. J. Phys. 48 397 and 412

1971 Can.J. Phys. 49 2098

Chaudhuri S, Roy D and Ghosh A K 1976 Ind. J. Phys. 49 928

Cochrane G and Fletcher N H 1971 J. Phys. Chem. Solids 32 2557

Collins W C, Schneider I, Klein P H and Johnson L R 1974 App. Phys. Lett. 24 403

Compton W D 1957 Phys. Rev. 107 1271

Compton W D and Rabin H 1964 Solid St. Phys. 16 121

Corish J and Jacobs P W M 1972 J. Phys. Chem. Solids 33 1799

Crawford J H Jnr 1968 Adv. Phys. 17 93

Crawford J H Jnr and Slifkin L M 1982 Point Defects in Solids: General and Ionic Crystals Vol. 1. Plenum Press

Dalal M L, Sivaraman S and Murti Y V 1983 J Pure App Phys. 21 6

Dannerfaer S 1975 J.Phys. E 8 97

Dawber P G and Parker I M 1970 J.Phys. C : Solid St. Phys. 3 2186

De Boer J H 1937 Rec. Trav. Chim. Pays-Bas. 56 301 Cited by Seitz 1963

Dekker A J 1984 Solid State Physics-macmillan & Co.-London

Delbecq C J 1973 Z.Phys. 171 560

Delbecq C J , Hayes W and yuster P H 1961 Phys. Rev. 121 1043

Delbecq C J , Pringsheim P and Yuster P H 1951 J.Chem.Phys.Solids 19 574

1952 J.Chem. Phys. Solids 20 746

Delbecq C J , Smaller B and Yuster P. H 1956 Phys. Rev. 104 599

1958 Phys. Rev.111 1235

Dexter D L 1958 Solid St. Phys. 6 353

1960 Phys. Rev. 118 934

Dienes G J 1948 J.Chem. Phys. 16 620

Dorendorf H Z 1951 Z. Phys. 129 317

Dorendorf H Z and Pick H 1950 Z.Phys.128 166

Doyle W T 1958 Phys. Rev.11 1067

1958 Phys. Rev. 111 1072

1960 Proc. Phys. Soc. 75 649

Doyle W T and Agarwal A 1965 J.Opt. Coc. Am. 55 305

Dreyfus R W and Laibowitz R B 1964 Phys. Rev. 135 A1413

Dreyfus R W and Nowick A S 1962 J.Appl.Phys. Suppl. 33 473 and

Phys Rev. 126 1367

Duering W and Markham J J 1952 Phys. Rev. 88 1043

Durand P, Farge Y and Lambert M 1969 J.Phys.Chem.Solids 30 1353

Dutton D and Maurer R J 1953 Phys. Rev.90 126

Eisenstakt M 1963 Phys. Rev. 132 630

Engstrom H 1975 Phys. Rev. B11 1689

Es helby J D 1956 Solid St. Phys. 3 79

Etzel H W 1952 Phys. Rev. 87 906

1955 Phys. Rev. 100 1643

Evarestov R A 1964 Opt. Spectry. U.S.S.R. 16 198

Flynn C P 1982 Point Defects and Diffusion-Clarendon Press

Fong F K 1967 Solid State Chemistry Vol.3-ed.H.Reiss-Pergamon Press

Fowler W B 1964 Phys. Rev. 135 A1725

Fowler E B 1984 Physics of Color Centres-Ed.W.B.Fowler-Academic Press, London

Fowler W B and Kunz A B 1970 Phys. St.Solid 40 249

Frenkel J 1926 Z.Phys. 35 652 Cited by Flynn 1972

Frohlich F, Hensel G and Ziller J 1971 Phys. St. Solids (a) 6 165

Fuller R G , Marguardt C L , Reilly M H and Wells Jr J C 1968

Phys. Rev. 176 1036 and

Phys. Rev. Lett. 20 662

Fumi F G and Tosi M P 1964 J.Phys. Chem.Solids 25 31 (I)

J.Phys. Chem. Solids 25 45 (II)

Gilman J J and Johnston W G 1962 Solid St.Phys. 13 147

Gnaedinger R J 1953 J.Chem. Phys. 21 323

Coldstein E 1896 Z.Instrumentenk 16 211 Cited by Pick, 1958

Goldstein F T 1967 Phys.St. Solid.20 379

Gorbenko P K and Kovtun A A 1972 Sov.Phys-Solid St. 13 2312

Gordy W and Thomas W J O 1956 J.Chem.Phys. 24 439

Gorlich P, Karras H and Kolitz G 1963 Phys.St.Solid 3 1929

Goto T, Ishii T and Ueta M 1963 J.Phys.Soc.Japan 18 1422

Gourary B S 1958 Phys. Rev. 112 337

Gourary B S and Adrian F J 1957 Phys. Rev. 105 1180

1960 Solid St. Phys. 10 128

Govinda S 1974 J. Phys. C : Solid St. Phys. 7 L374

Grassano U M 1977 Nuovo Cimento 39B 368

Greenwood N N 1984 Ionic Crystals, lattice Defects and Nonstoichiometry-

Butterworths

Gritsenko Yu I 1971 Phys. St. Solid (a) 7 113

Hackskaylo M and Groetzinger G 1952 Phys. Rev. 87 789

Hadley W B 1968 Intern.Symp. on Colour Centres in Alkali Halides Rome

Harker A H 1976 J.Phys.C :Solid St. Phys. 9 2273

Harrison P G 1962 J.Chem. Phys. 37 388

Harrison W A 1982 Solid St. Theory-McGraw-Hill

Hartmanova M 1971 Phys. St. Solid A 7 303

Hattori S 1960 J.Phys. Soc. Japan 15 2117 , also see
1962 J.Phys. Soc. Japan 17 1454

Haven Y 1950 Recl. Trav. Chim. Pays -Bas 69 1365

Hayce W 1962 J. App. Phys. 33 329

Heiland G 1950 Z.Phys. 128 144

Henderson B and Wertz J E 1968 Adv. Phys. 17 749

Herman R, Wallis M C and Wallis R F 1956 Phys. Rev. 103 87

Hermann F and Pinard P 1970 J.Phys. C :Solid St. Phys. 3 1037
1972 J.Phys. Chem.Solids 32 2649

Hersh H N 1957 Phys.Rev. 105 1158, also see
1957 J.Chem. Phys. 27 1330
1966 Phys. Rev. 148 928

Hesketh R V 1959 Phil. Mag. 4 114

Hirai M and Hashizume K 1967 J.Phys.Soc.Japan 1505

Hirai M, Ikezawa M and ueta M 1962 J. Phys.Soc. Japan 17 1483

Honda S and Tomura M 1970 J. Phys. Soc. Japan 29 522

Hoodless I M, Starge J H and Wylde L E 1971 J.Phys. C: Solid St. Phys. 4 2737

Hoshino H and Shimoji M 1967 J.Phys.Chem.Solids 32 385
1971 J.Phys. Chem.Solids 28 1169

Howard R E and Lidiard A B 1964 Rep.Prog.Phys. 27 161

Howland L P 1958 Phys. Rev. 109 1927

Huang K and Rhys A 1950 Proc. Roy.Soc.A204 406

Hughes A 1966 Solid St. Commun. 4 337

Ignateva M I, Zavadovskaya E K and m Lik-Gaikazgay I Ya 1964
Sov. Phys .-Solid St.5. 2031

Imanaka K, Lida T and Ohkura H 1977 J.Phys.Soc.Japan 43 519

Ishiguro M, Sugioka E and Takeuchi N 1960 J.Phys. Soc.Japan 15 1302

Ishii T and Rolfe J 1966 Phys. Rev. 141 758

Itoh N 1972 Crystal Lattice Defect 3 115

Ivey H F 1947 Phys.Rev. 72 341

Jackson B J H and Young D Y 1969 J.Phys. Chem. Solids 30 1973

Jacobs P W M and Pantelis P 1971 Phys. Rev. B 4 3757

Jain S C and Jain V K 1968 J. Phys. C: Solid St. Phys. 1 895

Jain S C and Radhakrish 1969 Phys. Rev. 181 1312
Jain S C and Mehendru P C 1965 Phys. Rev. 140 957
Jain S C and Mehendru P C 1965 Phys. Rev. 140 957
Jain S C and Sootha G D 1967 Phys. St. Solid 22 505
1968 Phys. Rev. 171 1075 and 1083
Jaque V 1985 J F Phys. 45 971
Jirgal C H Jr, Shaw M D and Noble G A 1969 Am.J.Phys. 37 963
Jost W 1933 J.Chem. Phys. 1 466
Kalnin Yu Kh and Hskovich Z S 1975 Soc. Phys.-Solid St. 16 1986
Kanzig W 1960 Phys. Rev. Lett. 4 117
Kanzig W and Woodruff T O 1958 J.Phys. Chem. Solid 9 70
Kaplan R and Bray P J 1963 Phys. Rev. 129 1919
Karlsson A V and Beckman O 1967 Solid St.Commun. 5 795
Karo A M and Hardy J R 1971 Phys. Rev. B3 3418
Kayanuma Y and Kondo Y 1977 Solid St. Commun. 24 447
Kerdhoff F 1951 Z. Phys. 130 449
Kikuchi A and Ozawa K 1968 Phys. Lett. 27 A443
Kikuchi A and Ozawak 1973 Phys.St. Solid (a) 18 567
Kittel C 1985 Introduction to Solid State Physics-Welley Publisher-New York
Kleeman W 1968 Z.Phys. 214 285
Klein M V 1968 see Fowler 1984 Ch.7
Kleinschrod F 1936 Ann.Phys. 27 97
Klick C C 1960 Phys. Rev. 120 670
Klick C C and Patterson D A 1963 Phys.Rev. 130 2169
Klick C C and Schulman J H 1957 Solid St. Phys. 5 97
Knof H and Maisch W G 1963 J.Phys.Chem. Solids 24 1625
Knox K S 1959 Phys. Rev. Lett. 2 87
Kojima T 1957a J.Phys. Soc. Japan 12 908
1957b J.Phys.Soc. Japan 12 918
Kojima K, Nishimaki N and Kojima T 1961 J.Phys.Soc.Japan 16 2033
Komnik S N 1986 Soc. Phys. -Solid St. 10 118
Konrad K and Neubert T J 1967 J. Chem.Phys. 47 4946
Kostopoubos D, Varotsos P and Mourikis S 1975 Can.J.Phys. 53 1318
Krumhanansl J A and Schwartz N 1953 Phys. Rev. 89 1154
Kubler J K and Friaud R J 1965 Phys. Rev.140 A 1742
Kubo K 1969 J.Phys. Soc. Japan 26 143
1974 J.Phys. Soc. Japan 37 1469
Kurosawa T 1958 J.Phys. Soc. Japan 13 153

Lamb D R 1986 Electrical Conduction Mechanisms in Insulators, Methuen Ltd, London

Lampert M A and mark P 1985 Current Injection in Solids, Academic Press Inc;, New Yor-London

Lardo E and Dartyge E 1969 Solid St. Commun. 7 1225

Lawrance n 1960 Phys. Rev. 120 57

Lawson A W 1962 J.Appl. Phys. 33 466

Lidiard A B 1957 Hanbuch der Phys. Vol.20 Cited by Howard and Lidiard 1964

Libanove B D, Alekseev P D and Parfianovich I A 1975 Sov.Phys.-Solid St 17 1435

Logatchov Yu A 1967 Phys.St.Solid. 19 K35

Logatchov Yu A and Evarestov R A 1970 Phys.St. Solid 40 493

Lowdin P O 1962 J.Appl. Phys.Suppl. 33 251

Luty F 1956 Colour Centre Symp. at Arogonne Nat. Lab. Nov. 1

1961 Z.Phys. 165 17

1968 see Fowler 1984 Ch. 3

Maiti A K , Goswami K, Chouduri S and Choudhury A 1981 J Electrochem Soc 128 1995

Maiti A K , Goswami K 1983 Solid St. Comm 48 519

Maisch W G and Drickamer H G 1958 J.Phys.Chem.Solids 5 328

Manning J R 1964 Phys.Rev. 136 A 1758

Marat-Mendses J N and Comins J D 1977 J.Phys.Chem.Solids 38 1003

Markham J J 1959 F-Centres In Alkali Halides-Academic Press

1966 Solid St. Phys. Suppl. 8

Martienssen W 1952 Z.Phys. 131 488

Matzke Hj 1971 J.Phys. Chem.Solids 32 437

Meistrich M L 1968 J.Phys.Chem.Solids 29 1119

Mie G 1908 Ann. der Phys. 25 377

Mitchell P V , Wiegand D A and Smoluchowski R 1961 Phys.Rev. 121 484

Mollenauer L F and Baldacchini G 1972 Phys. Rev. Lett. 29 465

Mollenauer L F , Pan S and Winnacker A 1971 Phys. Re .Lett. 26 1643

Mollenauer L F , Hatch B A , Olson D H and Guggenheim H J 1975 Phys. Rev. B 12 731

Mollwo E 1931 Nachr. Ges.Wiss .Cottingen Math-Phys. Ki 97

1937 Ann. Phys. 29 394

Molner J P 1940 Ph.D. Thesis M.I.T.-Cambridge Massachusetts U.S.A. Unpublished. Cited by Compton and Rabin 1964, also see

1941 Phys. Rev. 59 944 Abstr. No. 157

Mott N F and Gurney R W 1984 Electronic Processes in Ionic Crystals-Dover

Mott N F and Littleton M J 1938 Trans. Faraday Soc. 34 485

Nadler C and Rossel J 1973 Phys. St. Solid (a) 18 711

Nahum J 1967 Phys. Rev. 158 814

Nakai Y 1958 J.Phys. Soc. Japan 13 1424

Nowick A S 1958 Phys. Rev. 111 16

O'brien M F and Plovnick R H 1969 Mat. Res. Bull. 4 671

Onaka R and Jujita I 1960 Phys.Rev. 119 1597

Orton J W 1986 Electron Paramagnetic Resonance-Iliffe

Ottmer R 1928 Z. Phys. 46 798 Cited by Compton and Rabin 1984

Pantanelli G P and Whitmore D H 1974 J.Phys.Chem.Solids 55 445

Pappn S V and McCarthy K A 1971 J.Phys.Chem.Solids 32 1287

Paramo N and Sanchez C J 1971 J.Phys.Soc. Japan 30 1106

Parashar D C 1970 J.Phys.Chem. Solids 31 2795

Pauling L 1980 The Nature of the Chemical Bond. Cornell Uni. Press

Pekar S I 1953 Uzp. Fiz. Nauk 50 197

Pershits Ya N and Andrusich V A 1971 Sov. Phys.-Solid St. 13 221

Pershits Ya N and Ilin A N 1968 Sov. Phys.-Solid St. 10 719

Peterescu P 1963 Phys.St. Solid 3 950

1965 Phys. St. Solid 9 539

1971 Phys. St. Solid (a) 4 K3

Petrashen M I Abarenkov I.V.Berezin A A and Evarestov R A 1970

Phys. St.Solid. 40 9, and

Phys. St. Solid 40 433

Petroff S 1950 Z.Phys. 127 443

Pick H 1958 Suppl. Nuovo Cimento 7 498

1960 Z. Phys. 159 69

Pick H and Weber H 1950 Z.Phys. 128 409

Pikher F, Schinke D and Friauf R J 1963 J. Phys.Chem. Solids 24 1684

Pisarenko V F 1962 Sov. Phys.-Solid St. 3 2184

Pitchie R K and Lew H 1964 Can. J.Phys. 42 43

Podini P 1965 Phys. St. Solid. 9 737

Pohl R W 1932 Naturwiss. 20 932 Cited by Pohl, 1937

1937 Proc. Phys. Soc. 49 3, and

1938 Z. Phys. 39 36

Poole R T, Liesegang J, Leckey R C G and Jenkin J G 1973 Chem.

Phys. Lett. 23 194

Pooley D 1965 Solid St. Commun. 3 241

1966 Proc. Phys. Soc. 87 245, and

1966 Proc. Phys. Soc. 87 257

1966 proc. Phys. Coc. 89 723

Pooley D and Runciman W A 1970 J.Phys. C :Solid St. Phys. 1815

Przibram K 1986 Irradiation Colours and Luminescence-pergamon

Rabin H 1959 Phys. Rev. 116 1381

Radchenko I S 1968 Opt. Spectrosk. 25 500

Radchenko I S and Udod V V 1971 Sov. Phys.-Solid St. 12 1186

Remaut G and Dekeyser W 1958 Physica 24 20

Renn W 1974 Phys. Cond. Matter 17 233

Rogener H 1937 Ann. Phys. 29 386

Rolfe J 1964 Can. J. Phys. 42 2195

Rose S I 1983 Space Charge Effects in Ionic Crystals, University Press, New York

Rolfe J and Morrison S R 1977 Phys. Rev. 815 3211

Roy D, Sen S K and Manna A 1974 Phys. St. Solid (b) 61 723

Ruchardt H 1956 Phys. Rev. 103 873

Sastry P V 1969 J.Phys. Soc. Japan 26 73

Schneider I 1966 Solid St.Commun. 4 91

Schoemaker D 1968 Phys. Rev. 174 1060

Scholz A 1964 Phys. St. Solid 7 973

Schottky W and Wagner C 1930 Z. Phys. Chem. B11 163 Cited by Boswarva and Lidiard 1967

Schulman J H and Compton W D 1962 Color Centers in solids-Pergamon Press

Scott A B , Smith W A and Thompson M A 1953 J.Phys.Chem.57 757

Seevers R E and Scott A B 1970 J. Phys. Chem. Solids 31 729

Seidel H and Wolf H C 1965 Phys. St. Solid 11 3

1968 see Fowler, 1984 Ch. 8

Seitz F 1946 Rev. Mod.Phys. 18 384

Seitz F 1950 Phys. Rev. 80 239

1951 Phys. Rev. 83 134

1954 Rev. Mod. Phys. 26 7

1963 Proceedings of the International Summer School on Solid St.Phys held Aug. 12-31 at Mol Belgium Ed. Strumane R, Nihoul J, Gevers R and Amelinckx S. North-Holland Pun. Company Amsterdam

1980 The Modern Theory of Solids -McGraw Hill

Seitz F and Koehler J S 1956 Solid St. Phys. 2 305

Shatalov A A 1956 Sov.Phys.-JETP 2 725

Shing M CJ and MacGrove R K 1968 Phys. Rev. 176 1076

Siblely W A , Sonder E and Butler C T 1964 Phys. Rev. 136 A537

Silsbee R H 1965 Phys. Rev. 138 A180

Simpson J H 1949 Proc. Roy. Soc. A197 269

1965 Paper No. 176 Conference on Colour Centres in Alkali Halides Urbana Illinois U.S.A.

1970 Bull. Rad. and Elec Eng. Div., Nat. Rest.Coun.Can 20 8

Smith R A 1959 Semiconductors-Cambridge University Press

Sonder E and Sibley W A 1970 Cited by Townsend and Kelly 1973

Still P B and Pooley D 1969 Phys. St.Solid 32 K147

Stockman F 1952 Naturwiss, 39 230

Stoebe T G 1967 J. Phys. Chem. Solids 28 1375

Stoebe T G and Huggins R A 1966 J.Mat. Sci. 1 117

Stoneham A M 1972 Phys. St. Solid (b) 52 9

Suptitz P and Teltow J 1967 Phys. St. Solid 23 9

Susman S 1963 Cited by Compton and Rabin 1964

Swand R K and Brown F C 1963 Phys.Rev. 130 34

Tharmalingham K 1964 J.Phys. Chem. Solids 25 255

Tharmalingham K and Lidiard A B 1961 Phil. Mag. 6 1157

Tibbs S R 1939 Trans. Faraday Soc. 35 1471

Topa V 1968 Intern.Symp. on Colour Centres Rome

Topa V and Yuster M 1970 Phys. St. Solid (a) 3 131

Torrens I McC and Chadderton L T 1968 Can.J.Phys. 46 1303

Tosi M P 1964 Solid St.Phys. 16 1

Tosi M P and Fumi F. G 1957 Discuss. Faraday Soc. 23 92

Tosi M P and AIroldiG 1958 Nuovo Cimento 8 584

Tosi M P and Fumi F G 1958 Nuovo Cimento 7 95

Tosi M P and Doyama M 1966 Phys. Rev. 151 642

Townend P D and Kelly J C 1973 Colour Centres and Imperfections in Insulators and Semiconductors-Chatto and Windus for Sussex University Press.

Tsal N A and Pashkovskii M V 1964 Sov. Phys. -Solid St. 6 607

Tyagi R C , Singh R and Gupta A K 1970 J.Phys.C:Solid St. Phys.3 769

Tyapunin N A and Kolomutsev 1973 Sov. Phys.Crystal. 17 1102

Uchida Y and Nakai Y 1953 J.Phys.Coc. Japan 8 795

Udod V V 1968 Sov.Phys.-Solid St. 10 136

Ueta M , Kondo Y, Hirai M and Yoshinary T 1969 J Phys.Soc.Japan 26 1000

Van Der Lugt K L and Kim Y W 1966 Phys.Lett. 22 50

Van Doorn C Z 1960 Phys.Rev. Lett. 3 236

1961 Rev. Sci. Instrum. 32 755

Van Doorn C Z and Haven y 1956 Philops Res. Rep. 11 479

Varley J H O 1954 Nature 174 886 and

1954 J.Nuclear Energy 1 130

1962 J.Phys. Chem. Solids 23 985

Velicescu B and Topa V 1973 Phys. St. Solid (b) 55 793

Weller P F 1973 Solid St. Chem. and Phys. Ed. by Paul F Weller-Marcel

Dekker NC

West E J and Compton W D 1957 Phys.Rev. 108 576

Williams F E 1962 Phys. Rev. 126 70

Witt H 1952 Nachr. Akad. Wiss. Gottingern math-Phys. 4 17

Wolbarst A B 1973 Phys. St. Solid (b) 55 299

Wood R F and Joy H W 1964 Phys. Rev. 179 783

Wood R W 1933 Phys. Rev. 44 353

Yuster et al 1967 cited by Fowler, 1984 P. 133

CHAPTER TWO

Experimental Methods and Apparatus

1. Introduction

The purpose of this chapter is to describe the various experimental procedures which have been adopted in order to investigate the problem of electrolytically colouring crystals of the alkali fluorides. At the outset of this work various workers had reported that these crystals cannot be coloured electrolytically or additively (Gorlich et al, 1963; Pokini, 1965; Meistrich, 1968; Jirgal et al, 1969; Gritsenko 1971; Flynn, 1982) and it was decided to investigate as many of the conditions as possible which have a direct or an indirect influence on the electrolytic coloration process and which may, therefore, prevent their coloration.

The bulk of the experimental work on electrolytic coloration reported here was carried out using the constant current technique in contrast to all the previously reported literature which utilised constant voltage. The diffusion technique used in this work for doping the alkali halides with divalent mercury also differs from the techniques in general use elsewhere.

The alkali halide specimens used in this work were the potassium halides, the sodium halides and lithium fluoride. The main materials of interest among these were the alkali fluorides and the chief material in this category was potassium fluoride. The specimen preparation and electrolytic coloration procedures were standardised to take account of the fact that potassium fluoride is highly deliquescent.

2. Specimen sources and cleavage

With one exception, all specimens were supplied by the Harshaw Chemical Co., Cleveland, U.S.A. in the form of single crystals of size 3 cm x 2.5 cm x 1 cm which had been cleaved from large boules. One boule of KF grown by the Bridgman-Stockbarger method in a graphite crucible was supplied by Dr. D.A.Jones, Department of Natural Philosophy, University of Aberdeen. His furnace was contained in a sealed chamber and the material was grown in an atmosphere of oxygen-free dry nitrogen at a pressure just sufficient to prevent evaporation of the KF.

All the specimens of alkali halides were cleaved in air using stainless steel razor blades except for KF, NaI and NaBr. Since these crystals are highly deliquescent, it was not possible to cleave a specimen in air and to mount it in the coloration assembly without the surface becoming wet. Surface moisture influences the required good contact between the electrodes

and the specimen and, in the case of NaI, has a marked influence on its colourability (chapter 4). Special precautions were, therefore, necessary when preparing specimens of these materials. They were delivered in encapsulated containers and were stored in a desiccator at all times before being cleaved in a glovebox containing dry air or nitrogen.

Not all the alkali halide specimens behave identically when they are cleaved. Damage may be caused during cleavage when the material either shatters or cracks are introduced. For example, the as-received crystals of LiF were very difficult to cleave, while mercury-doped LiF could be cleaved without difficulty (Gilman and Johnston 1962). NaF was also difficult to cleave. The other alkali halide specimens were easy to cleave with the potassium halides being the easiest.

3. Electrolytic coloration

3.1. Introduction

Normally, an electrolytic coloration experiment is performed by heating the specimen to a fixed temperature and passing a constant current of 1 mA through it. It takes few seconds for the coloration cloud to move from its starting point at the pointed cathode to the other end of the specimen where it comes into contact with the flat anode. The apparatus described in this section also allowed the use of constant voltage as well as a variable temperature. Specimen size was generally of the order of 0.4 cm x 0.4 cm x 0.6 cm.

The technique of constant current was used in this work to colour alkali halide specimens electrolytically for the first time. In contrast to the constant voltage technique the new technique has the advantage of producing a homogeneously coloured specimen with pure F-centres. The other advantage is that the electrolytic coloration experiment is reproducible. Furthermore, the precise measurement of the coloration current, time and other factors provides an accurate estimation of the colour centre concentration. The various aspects of this technique are discussed in chapter 4.

3.2 The furnace

The specimens of alkali halide crystals were heated and coloured electrolytically in a furnace which was designed and constructed specifically for the purpose. The principal components of the furnace are shown in figure 2.1. The major design criteria are illustrated by the following constructional details.

The main heating chamber of the furnace consisted of a silica tube of internal diameter 3.8 cm, length 38 cm and wall thickness 0.3 cm. Two silica side tubes, each of internal diameter 2.2 cm, length 17 cm, and wall thickness 0.2 cm, were attached to the centre of the

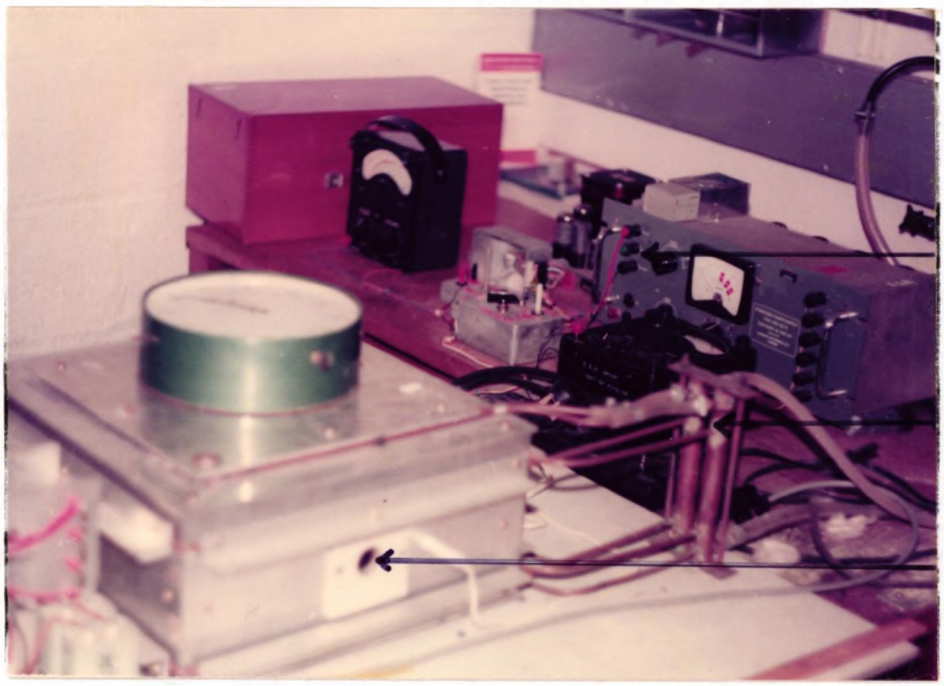

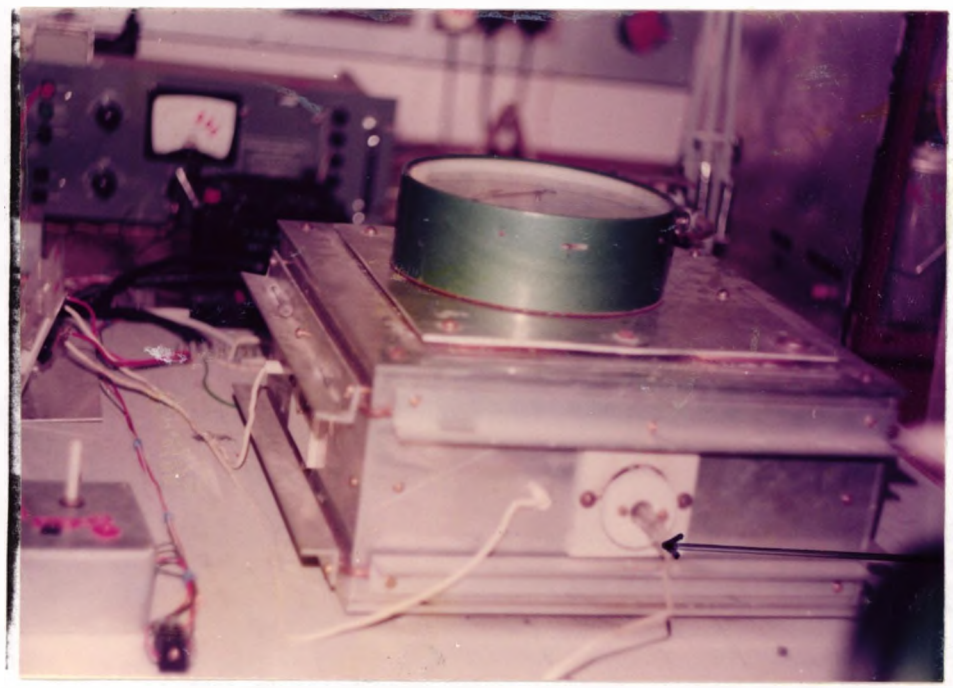

Figure 2.1 The furnace

main tube to form a cross shape. Silica windows were sealed to the ends of the side tubes. The specimen was located within its electrolytic coloration assembly at the intersection of the tubes so that it could be heated to the highest design temperature (about 1000 C) whilst the whole coloration process was observed through the side windows.

The furnace windings consisted of nichrome wire wound on thin asbestos paper which covered almost the whole length of both the main and side tubes. A layer of woven asbestos tape was bound around the windings to provide mechanical support. Heating the system to about 450° C produced a partial decomposition of the asbestos which entered the spaces between the windings and provided additional mechanical support. Four silica tubes placed tightly over the windings acted as retaining tubes for the windings.

A system of transformers and variacs (figure 2.2) was used to control independently the heating power to the main and side tubes. A temperature of 1000° C could be obtained at the centre of the furnace for a total power input of about 280 W. Temperatures as high as 700° C could be achieved in about 10 minutes starting from room temperature.

A thermocouple was attached to the outside of the main heating tube near to the centre point. The thermocouple wires were led through insulating seals and were connected to an automatic temperature controller [Ether 'Mini' Type 17-90B] which was connected in turn to the transformer-variac system for the main tube. As the temperature controller had a limited temperature range (up to 600° C), it was necessary to construct a d.c. back-off unit in series with the thermocouple leads to extend the range to 950° C

The furnace was contained in a dural box of dimensions 37 cm x 35 cm x 17 cm equipped with a water cooling system. The box provided a uniform temperature gradient around the heating tubes. The whole furnace, together with the heating and coloration current meters, was fixed on to a hard asbestos base.

3.3. The electrical arrangement

A schematic diagram of the electrical arrangement used to provide a constant current for the electrolytic coloration experiments is shown in figure 2.3. The arrangement is based on a modified constant voltage supply (power supply 1) and provided a constant current which could be varied from its usual value of 1 mA down to approximately 10 μA using S, P_1 and P_2 . Throughout any electrolytic coloration experiment the values of specimen current and voltage were either measured by a number of 'Avo' meters or were recorded on chart recorders as convenient.A potentio meter was used to measure the exact values as required during the experiments

The construction of this arrangement fulfilled the requirement for rapidly connecting the electrical circuit in accordance with the standardised procedure of electrolytic coloration for

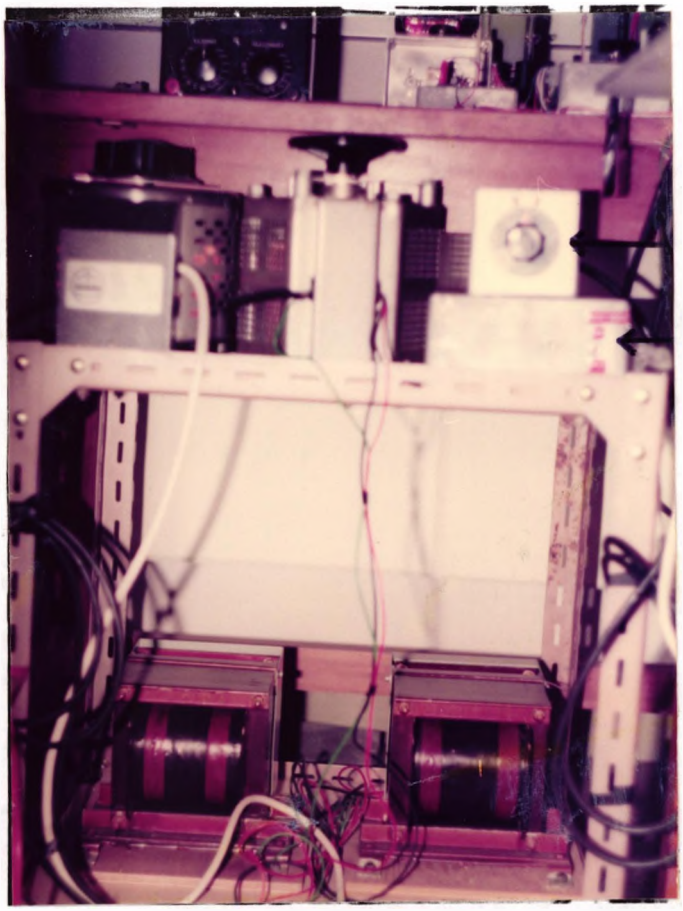

Figure 2.2 The heating system

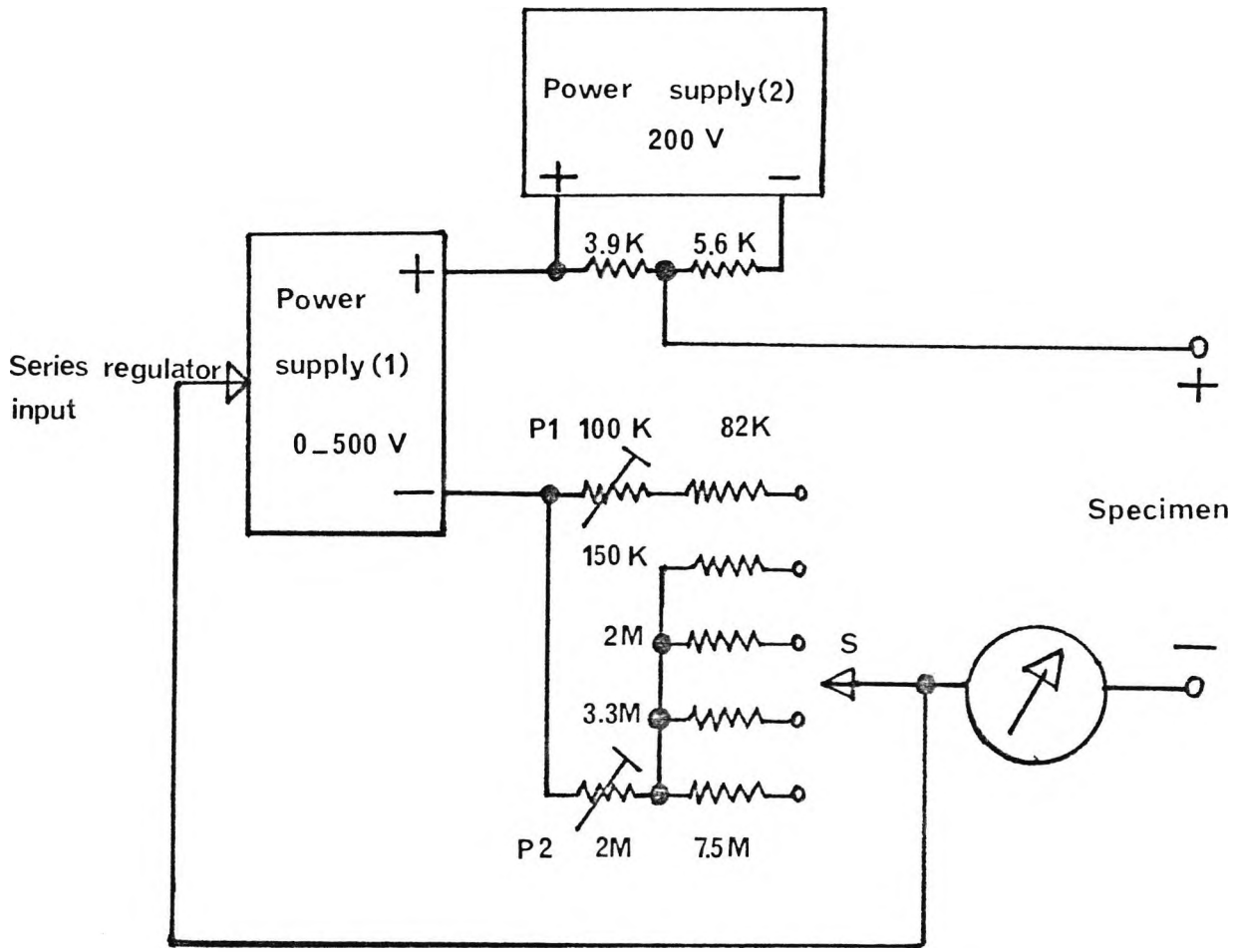

Figure 2.3 Schematic diagram of the constant current supply

potassium fluoride and other deliquescent specimens. Parts of the electrical arrangement can be seen in figure 2.1.

An ordinary constant voltage power supply was used in the electrolytic coloration experiments designed to test the previously reported experiments based on this technique.

3.4. The specimen holder

The electrolytic coloration process took place inside an assembly of three silica tubes which were fixed together using a joint, and two springs with four hooks to maintain the required good contact between the specimen and the electrodes (figure 2.4.). The first (outer) tube (length 38.0 cm and internal diameter 1.5 cm), which is labelled A in figure 2.4, had two silica hooks and a water jacket (length 7.0 cm) located near to the open end. A side tube is located at this end for the purpose of allowing electrolytic coloration to take place in a vacuum or in a nitrogen atmosphere. The other end is narrowed in order to provide a firm seat for the second silica tube (length 3.0 cm and internal diameter 1.1 cm) which is the pointed-electrode holder (labelled B in the figure).

The pointed electrode, which was usually used as the cathode, was made from a platinum wire or more often from a sharpened tungsten rod coated with platinum (Johnson-Matthey bright platinum). It was designed to be easily removable. The flat anode was made from platinum sheet and was also removable. Cleaning or replacing these parts after each experiment was an important experimental requirement. Other experimental points of importance are related to the special nature of the pointed electrode and include the sharpness of its point, the angle of contact with the specimen, the depth of its penetration and the uniformity of the platinum coating.

The actual specimen holder is the third silica tube (length 34.0 cm and internal diameter 0.9 cm), which is labelled C in figure 2.4, and has most of its length inside the first tube. The specimen is seated at the last half centimetre of the inside end of the third tube. Two hooks are located at the outer end of this tube which also has three arms to provide access for the electrode leads, the thermocouple (chromel-alumel) leads and for the nitrogen gas flow. The junction of the specimen thermocouple was embedded into a dummy specimen placed against the actual specimen but separated from it by a thin mica sheet (figure 2.5).

The advantage of this assembly is that it could be set up in the very short time available when dealing with the deliquescent KF, NaI and NaBr specimens. It also protected these specimens from atmospheric moisture during the experiment and, because of its ease of removal, provided rapid quenching for the specimens after the electrolytic coloration was completed.

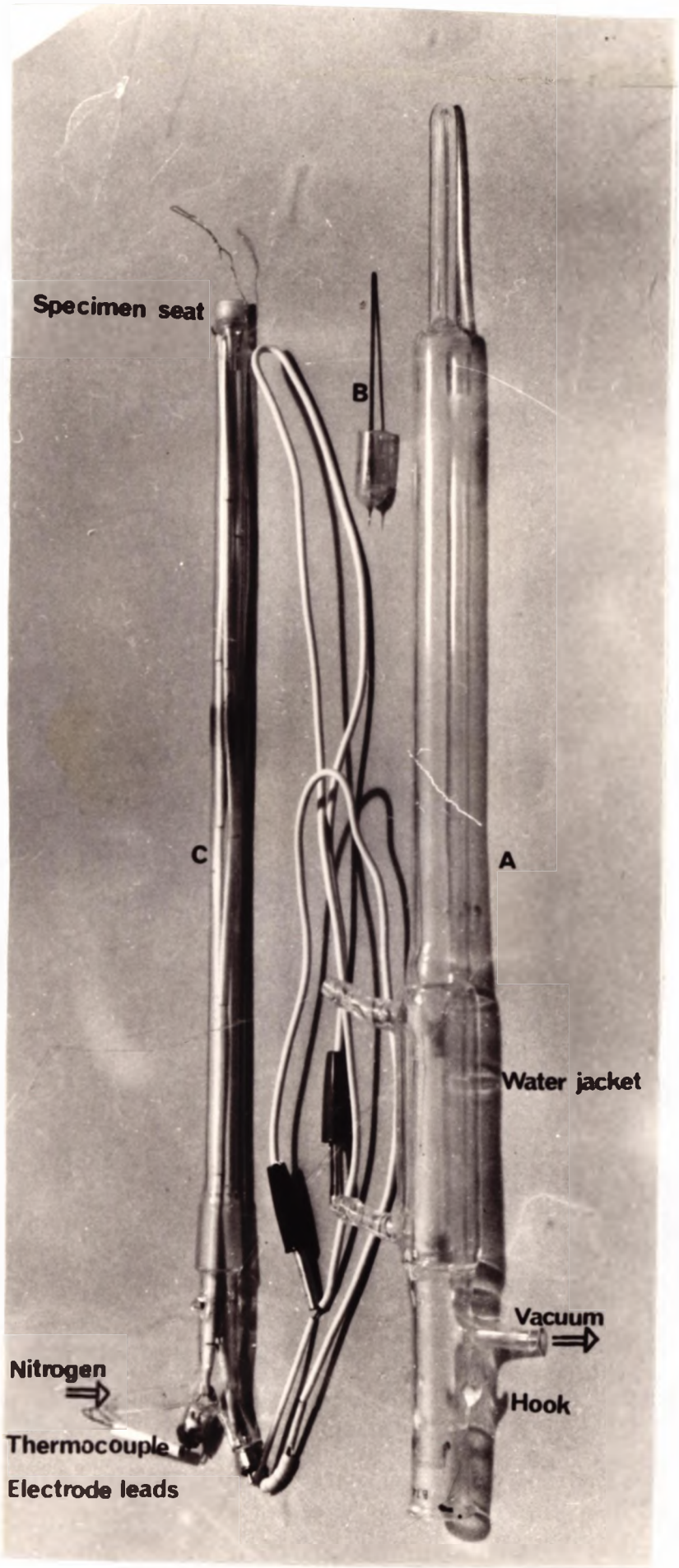

Figure 2.4 Apparatus used in electrolytic coloration

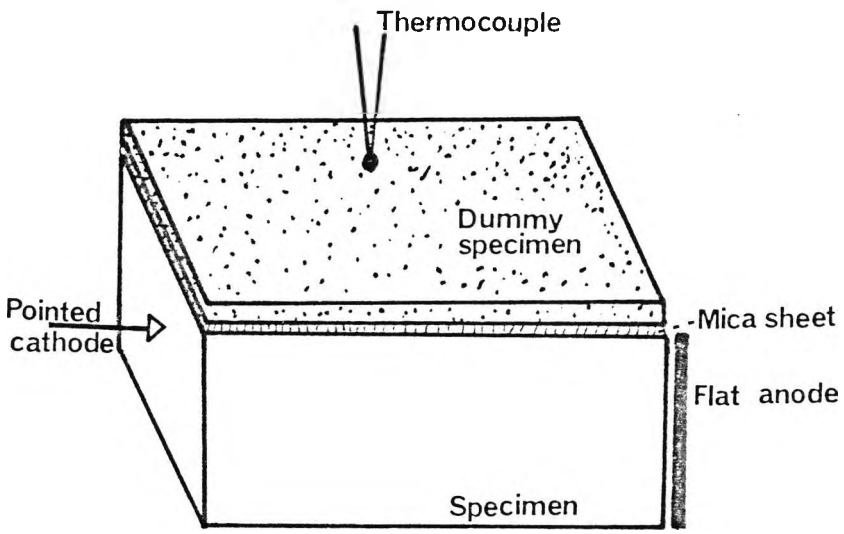

Figure 2.5 Specimen–electrodes–thermocouple contact

4. Optical measurements

4.1. Spectrophotometer

All the optical absorption measurements were made using a Perkin-Elmer 450 Spectrophotometer which is a double-beam recording instrument covering the far ultra-violet, ultra-violet, visible and near infrared wavelength ranges (165 nm to 2700 nm). The double-beam measurement provides the ratio of the radiant energy intensity transmitted by the specimen beam to that transmitted by the reference beam. In this work only three ranges (far ultra-violet is excluded) of wavelength were needed. The wavelength accuracy of the instrument in these ranges depends on the dial accuracy of the monochrometer which has a value falling between 0.02 nm and 2.0 nm, and on the chart accuracy, which is between 0.04 nm and 7.0 nm. The recorded ratio is usually plotted as a logarithmic function (absorbance A) on a linear scale against the wavelength on a non-linear scale. The absorbance is defined as

$$A = \log_{10} \frac{1}{T} \qquad (2.1)$$

where T is the transmittance (fraction of the incident intensity transmitted). The Perkin-Elmer 450 presents the absorbance directly on the assumption that Beer's law is adequate. Beer's law of absorption for low reflectivity materials like alkali halides is (Garbury 1965)

$$I_t = I_o e^{-\mu d} \qquad (2.2)$$

where I_t and I_o are the transmitted and incident light intensities, d is the thickens of the specimen and μ is the absorption coefficient which represents the fraction of light absorbed per unit length of the specimen. The absorbance is related to the absorption coefficient by

$$A = \frac{\mu d}{2.3} \qquad (2.3)$$

For all the quantitative measurements (concentration and oscillator strength) which are reported in this work, Smakula's equation was used. The expression which Dexter (1956) presented for a Gaussian band is

$$Nf = 0.87 \times 10^{17} \frac{n}{(n^2 + 2)^2} \mu_{max} W \qquad (2.4)$$

where N is the concentration in cm^{-3} , f is the oscillator strength, n is the refractive index of the specimen and W is the bandwidth at half maximum absorption in eV (halfwidth). The absorption coefficient μ_{max} is in cm^{-1} when N is in cm^{-3}

Before using the spectrophotometer the absorbance and wavelength scales were calibrated using reference specimens. The absorbance scale was usually calibrated using a Chance ON10 filter. The accuracy of the absorbance values is normally within the quoted 1.75% limit. Holmium oxide glass was used to calibrate the wavelength scale by comparing the test run spectrum with that provided by the instrument.

In determining the absorption coefficient, it was necessary to take into account the losses due to scattering at the surface and in the volume of the specimens as well as specular reflection losses at the surface. Kobayashi and Tomiki (1960) have shown that the scattering correction is negligible in the alkali halides and that the absorption coefficient can be measured adequately from the observed absorbance. As a first order correction to the reflection it is common practice to use a dummy specimen in the reference beam compartment of the spectrophotometer (Townsend and Kelly 1973).

4.2 Sources of F-light

F-light is the light produced by a certain source with a wavelength comparable to that of the F band of a particular alkali halide specimen. M-light and R-light can be similarly defined. A 30 mW helium-neon laser (Scientifica and Cook Electronics, England) was used to provide a wavelength of 633.8 nm. Also, an argon-krypton ion laser (Model 52G, Coherent Radiation, Palo Alto, California, U.S.A.) was used to provide a wide range of selection of wavelength. A mercury vapour lamp was also used to provide a source of ultra-violet light.

In all the optical irradiation experiments (F-light bleaching) an optical system of condensing lenses was arranged along with a light splitter in order that the incident beam irradiated both sides of the specimen equally.

4.3 Optical cell for low temperature measurements

The low temperature cryostat (figure 2.6) was made from a cylindrical liquid nitrogen container placed inside a second cylindrical container made of brass. The specimen holder was screwed to the copper bottom of the liquid nitrogen container and the space between the cylinders was evacuated. The cooling method is by conduction and the lowest temperature which could be obtained with this cryostat was 82 K compared with 77 K for the temperature of liquid nitrogen.

The liquid nitrogen container was screwed to the top of the brass container in such a way that the specimen was in line with the two quartz windows at the bottom of the brass container. The specimen could, therefore, be exposed perpendicularly to either F-light and /or to light from the spectrophotometer as required. The whole cryostat was mounted on a square metal base which was made to fit accurately in the spectrophotometer.

Specimen temperatures were measured with a chromel -alumel thermocouple calibrated at the boiling point of liquid nitrogen and at dry ice temperature. The thermocouple was fixed to a dummy specimen with a metal clip and this dummy specimen was pressed against the copper specimen holder near to the specimen.

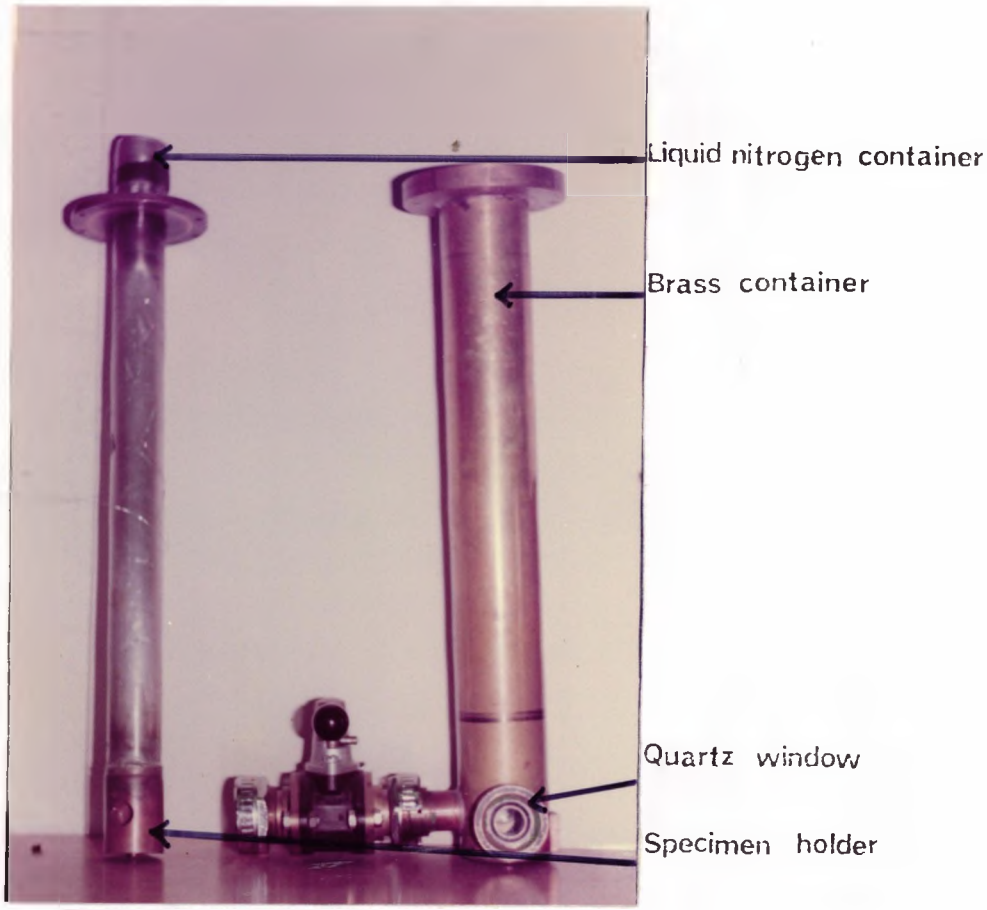

Figure 2.6 Liquid nitrogen temperature optical cell

The cryostat was evacuated using a standard pumping system which ensured a vacuum of at least 10^{-5} torr. The cryostat was also used at room temperature for the optical irradiation experiments on KF, NaI and NaBr specimens so that they could be kept under vacuum to prevent contact with moisture.

5. Mercury diffusion

5.1 Introduction

As a metal, mercury has a melting point of -39° C and a boiling point of 357° C. From a practical point of view, mercury has many advantages as a rich source of divalent cations. It has a high vapour pressure which can be calculated using the formula given by Weast (1970)

$$\mathrm{Log}_{10}p = \left(-0.2185\ \frac{A}{T}\right) + B \qquad (2.5)$$

where p is the pressure in torr at temperature T and A and B are constants. Mercury belongs to the sub-group of the periodic table which includes Zn and Cd. Pershits and Ilin (1968) have found that electrolytic coloration reduced the ionic conductivity of Zn^{2+} - and Cd^{2+}- doped KCl while Topa and Yuste (1970) have noticed that this phenomenon is also connected with a change in the valence of these ions and others like Pb^{2+} and Mn^{2+} but not ions like Ca^{2+}. It was expected that mercury with its high electronegativity, which is a common factor among the former elements (see table 2.1), would have an impact wider than the observed change of valence on the electrolytic coloration of alkali fluorides. Also, the maintenance of the experimental diffusion equipment is less of a problem compared with calcium or cadmium.

5.2 Diffusion apparatus

The main components of the mercury diffusion apparatus (figures 2.7 to 2.10) are the diffusion ampoule, the furnace, the pumping system and the safety system. The diffusion ampoule (figure 2.8) was made from stainless steel and consisted of two principal parts. The mercury container (length 27 cm and internal diameter 2.5 cm), which formed the first part, was equipped with a water jacket and an access point for the pumping system near to the open end of the ampoule. The second part is the specimen holder which was also used as a plug for the ampoule. It could be adjusted to occupy a variable length within the container and had a stainless steel disc at the top with lead-through connections for the specimen thermocouple. The two parts were fixed together using a system of metal clips and an O-ring. The specimen was usually held at the bottom of the specimen holder in a specially made box which shielded all the faces of the specimen but one.

Table 2.1. Electronegativity of divalent cations characterised by high values of electronegativity (taken from Gordy and Thomas (1956).

	Atomic number	Ionic radii (nm) (1)	Electronegativity (2)
Mn^{2+}	25	0.080	1.40
Zn^{2+}	30	0.074	1.50
Cd^{2+}	48	0.097	1.50
Sn^{2+}	50	0.112	1.65
Hg^{2+}	80	0.110	1.90
Pb^{2+}	82	0.120	1.60

(1) The values of ionic radii (nm) were given by Greenwood (1984). These values are based on Pauling's (1980) work.

(2) Pauling (1932) defined electronegativity as 'the power of an atom in a molecule to attract electrons to itself.'

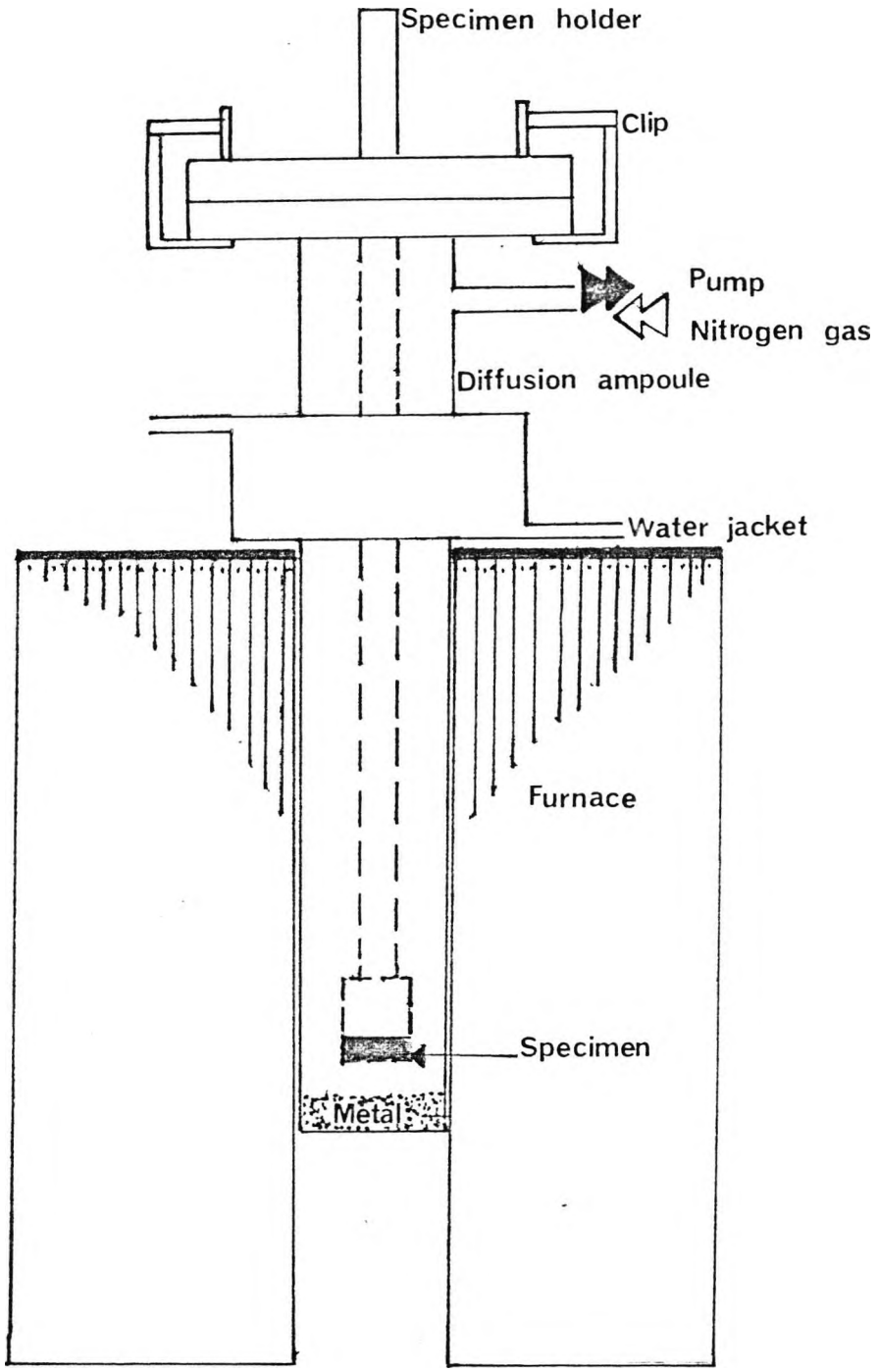

Figure 2.7 Diffusion apparatus

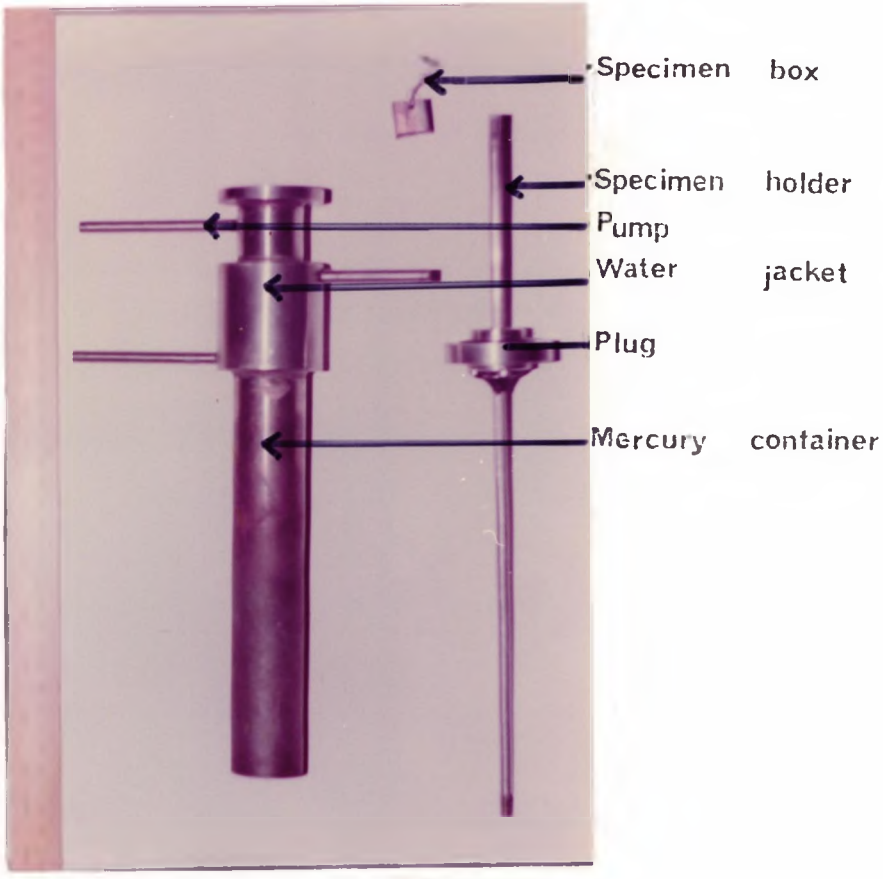

Figure 2.8 Mercury diffusion ampoule

The furnace incorporated a temperature controller which could hold the temperature of the specimen during the experiments to within ± 3°C. This furnace, like the electrolytic coloration furnace described in section 3.2 of this chapter, had a temperature range up to 1000°C. The specimen, which was separated from the mercury droplet, was kept at a temperature about 10°C higher than that of the mercury in order to prevent mercury condensation on to the specimen at low temperatures.

The pumping system, which was equipped with the appropriate pressure meters, was used to distil the mercury and thereby to remove any volatile impurities before the start of the diffusion. A nitrogen or argon gas container was linked to the pumping system for use in flushing the ampoule or to keep the internal ampoule pressure within safe limits.

Since mercury is a very volatile and toxic element, dangerous levels are readily attained in the laboratory atmosphere. The safety measures adopted are illustrated in figure 2.9 and involved enclosing the diffusion apparatus in a ventilated glovebox .The glovebox could be flushed by nitrogen and the ventilated air was pumped through three mercury traps (length 18 cm and diameter 4.5 cm) of a type shown in figure 2.10 before being removed from the laboratory. As an additional precaution, sulphur powder was kept inside the glovebox and also in the laboratory.

Usually a weighed amount of mercury and the specimens were sealed in the diffusion ampoule and were kept at the required temperature and pressure throughout the diffusion time of a few weeks. The ampoule was plunged into a liquid nitrogen container within the glovebox after each experiment had finished.

5.3 Optical measurement of Hg^{2+} concentration

Schulman et al (1950) and Sibley et al (1964) have shown that the concentration of lead in the alkali halides is proportional to the height of the lead absorption band over a wide range of concentrations. In this work the suitability of the optical absorption spectra as a method of measuring mercury concentration in alkali halide specimens was tested over the range of concentrations under investigation. Two methods were used in these measurements. The first method, which was developed in this work, was based on using known concentrations of divalent mercury in aqueous solutions of alkali halide since there is a close correspondence between the optical absorption bands of Hg^{2+} cations found in these solutions and those found in solid crystals (Papazian 1973). The measurements using this method were aimed at obtaining an absorption coefficient-Hg^{2+} concentration relation. It was possible then to measure optically the doping levels of Hg^{2+} in the specimen using this relation which was plotted as a graph. The distribution of Hg^{2+} within a specimen could then be determined by a sectioning technique.

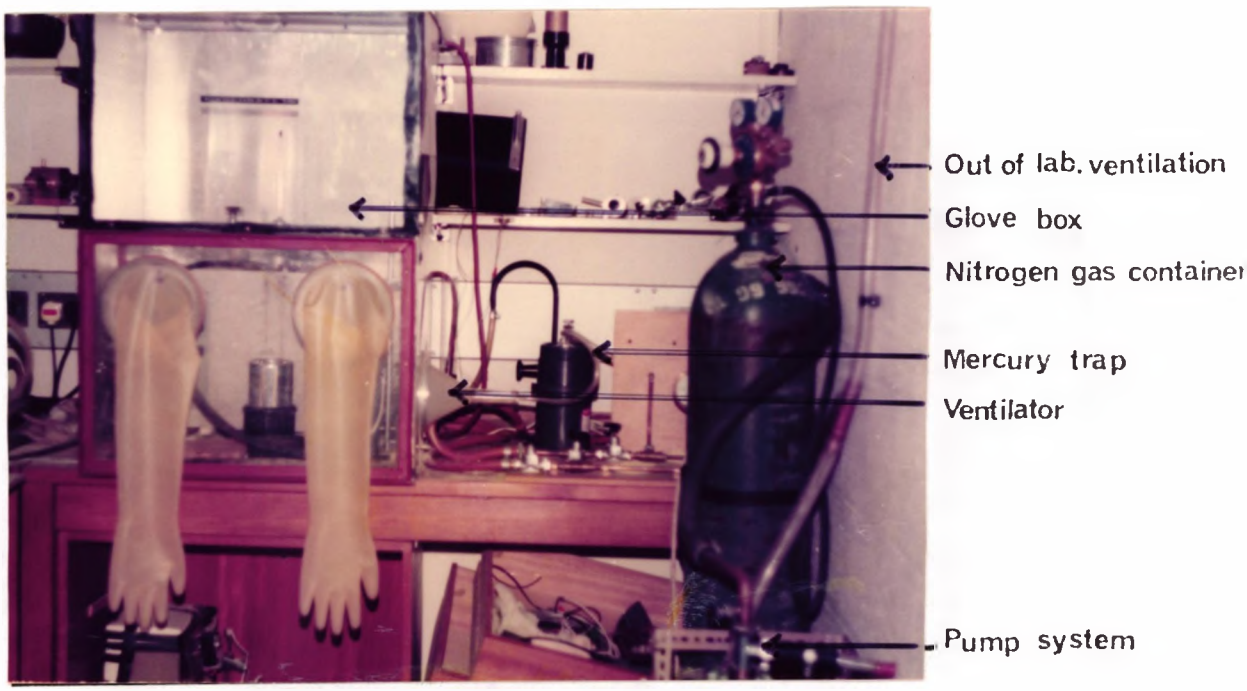

Figure 2.9 Mercury diffusion equipment

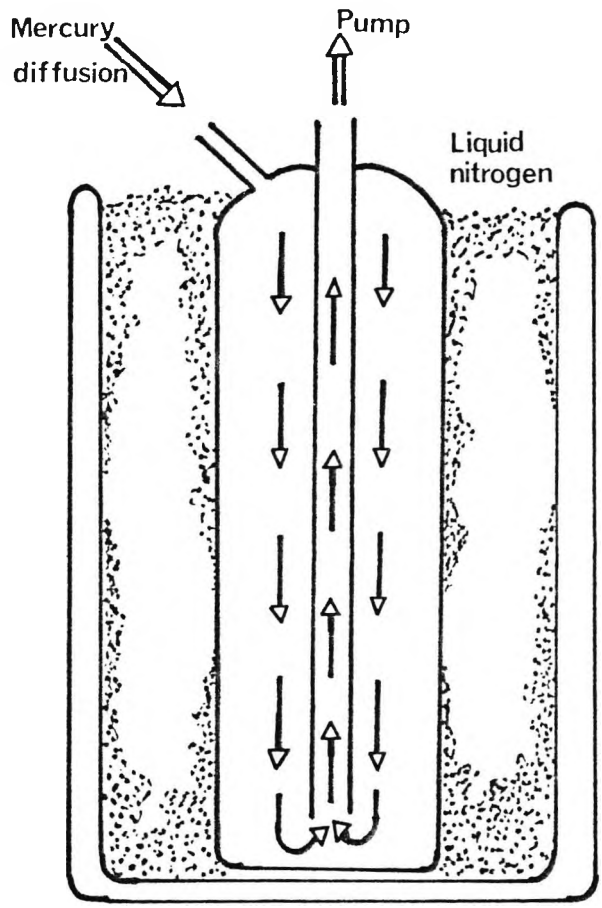

Figure 2.10 Mercury trap

This method of measuring Hg^{2+} concentration involved some corrections which are accurate within a limit of concentrations. The proportionality between the absorbance A or the absorption coefficient μ of the Hg^{2+} absorption band and the concentration N of Hg^{2+} cations was missing for concentrations below 10^{16} cm^{-3} , and it was not possible for concentrations above $10^{19}cm^{-3}$ since the mercury-doped specimen becomes non-transparent. The factors which preclude the accurate measurement of concentration beyond these limits were not investigated.

Since the concentration of Hg^{2+} in alkali halide specimens doped with mercury were approximately $10^{18}cm^{-3}$, the Hg^{2+} cations are expected to be distributed randomly in the lattice (Burstein et al 1951) and the interaction between divalent mercury cations may be assumed to be negligible. Subsequent experiments using the sectioning technique have confirmed that the distribution of Hg^{2+} cations is also uniform for sufficiently long diffusion times. So the observed absorbance of the Hg^{2+} optical absorption band is due to isolated Hg^{2+} cations which are treated as non-associative centres occupying cation lattice sites in all the optical measurements described in this work. It should be noted that not all the mercury added to the specimen necessarily enters the lattice as free Hg^{2+} cations.

Considerable differences were observed in the positions of the long-wavelength edge of the fundamental absorption and also between mercury-doped alkali halide specimens with different thicknesses. Figure 2.11 shows that the absorption coefficients increase as the thickness of the KF specimen decreases ((a) =0.05 cm, (b) =0.16 cm, (c) =0.20 cm and (d) = 0.26 cm). Any change in wavelength of the Hg^{2+} absorption band causes a change in the absorption coefficient . This fact required the preparation of a series of specimens covering a wide range of thicknesses and the measured absorption coefficient were corrected using the method of Moser and Urbach (1956). The points on the dashed line in figure 2.12 represent the absorption coefficient free from errors where the condition $\mu d = 1$ is satisfied (Kobayashi and Tomiki 1961). Moser and Urbach (1956) used the Urbach (1953) empirical equation.

$$\mu = \mu_0 \exp\left[- \frac{\sigma (h\nu_0 - h\nu)}{kT} \right] \qquad (2.6)$$

where μ_0 , ν_0 and σ are constants chosen by curve fitting and $h\nu$ is the photon energy at μ and T. Equation (2.6) has been found to be particularly valid in alkali halide specimens (Martienssen 1957, Haupt 1959) at doping levels above about $10^{16}cm^{-3}$. At lower concentrations, the Urbach equation does not hold (Klicik et al, 1964) and the absorbance is not proportional to the concentration changes. Figure 2.13 shows the relationship between the Hg^{2+} absorption band and the concentration of divalent mercury cations in the KF specimen over the range $2.x10^{16}cm^{-3} \leq N \leq 8 \times 10^{18}$ cm^{-3}.Each point on the line

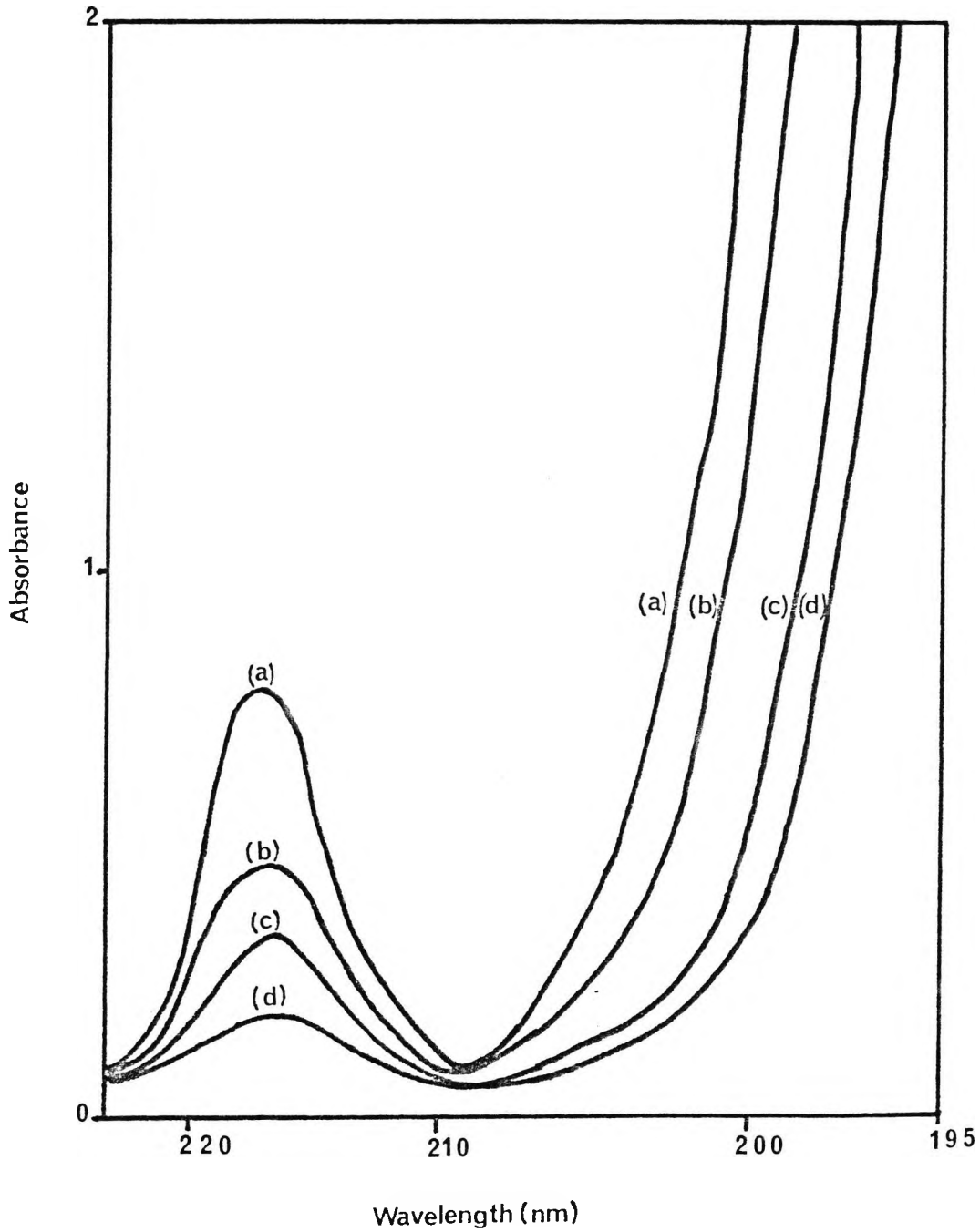

Figure 2.11 Spectra of mercury-doped specimens of different thicknesses

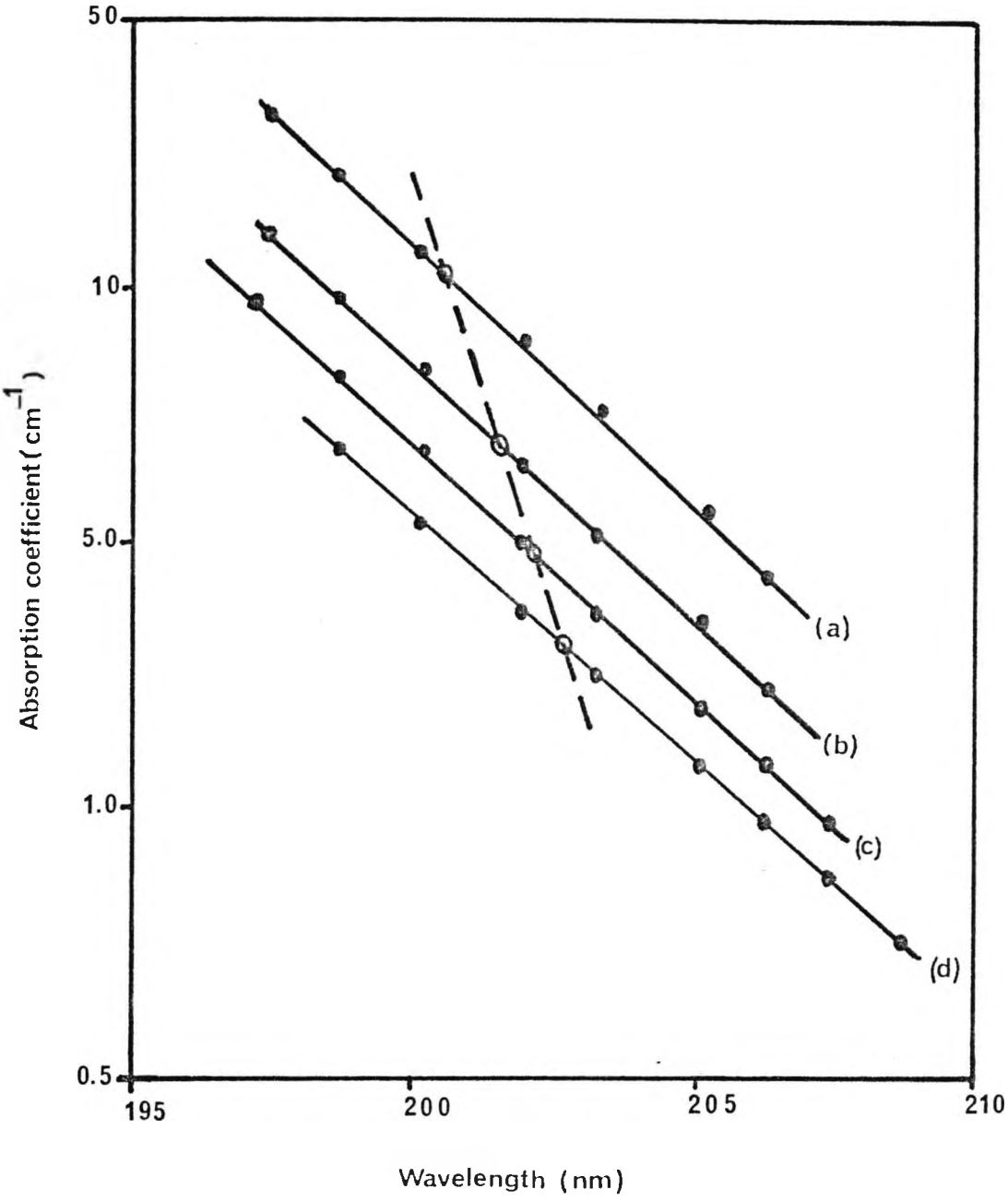

Figure 2.12 Correction of error due to different thicknesses

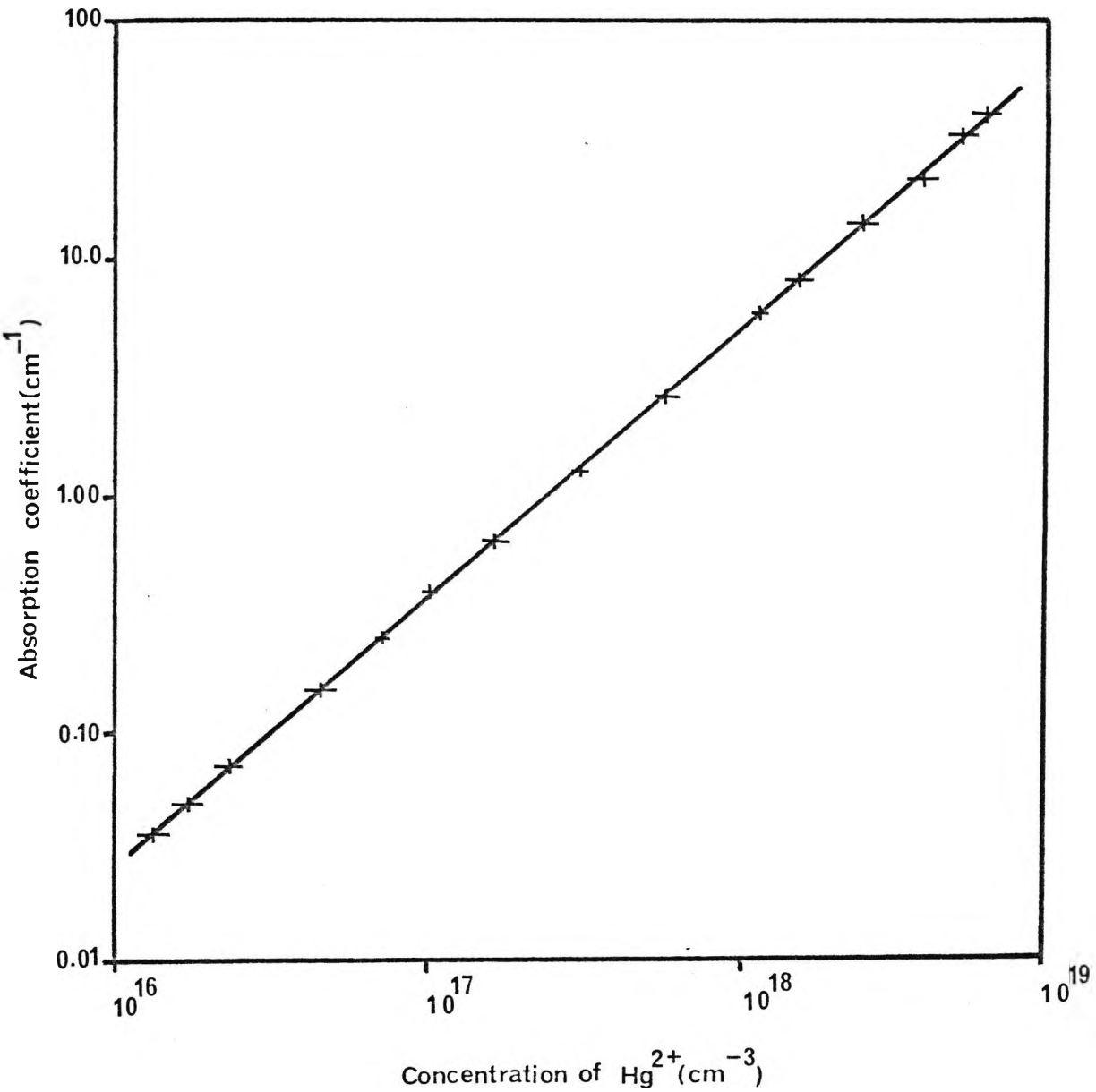

Figure 2.13 Relation between the Hg^{2+} absorption band and the concentration of divalent mercury cations

represents a range of measurements with the corrections taken into account. The uncertainties are shown on each point. Non-linear concentration dependencies were identified as deviations.

The optical determination of Hg^{2+} concentration was also carried out using another method provided by Wagner (1964). This method is based on a rather laborious procedure to eliminate the measurement errors caused by scattering from scratches and cloudings (caused by air humidity during the course of measurement) on the unequal surfaces of the specimen and a control specimen. The later specimen is an undoped specimen which was used in the reference beam of the spectrophotometer to eliminate errors due to reflections of the two solid-vacuum interfaces. If $\mu'_c(E)$ is the absorption curve of the control specimen and $\mu'(E)$ is the measured absorption curve, then the error-free absorption curve $\mu(E)$ is given by the transformation

$$\mu(E) = \mu'(E) - [\, a - b\mu'_c(E) \,] \qquad (2.7)$$

where a and b are constants determined by extrapolation to points where $\mu(E) = 0$ .From this procedure the effective absorption average of an Hg^{2+} centre per cm^3 Δ, which is the constant of proportionality between the absorption band and concentration, becomes equal for all concentrations over the range of doping levels under investigation. Hence,

$$\Delta(E) = \frac{\mu}{N} \text{ or } \Delta(E) = \frac{2.3}{N.d} A \qquad (2.8)$$

To measure the divalent mercury cation concentration in any mercury-doped alkali halide specimen it was necessary to determine Δ_{max} for the Hg^{2+} optical absorption band. Figure 2.14 shows Δ for KF plotted against λ (nm) and E (eV). At this stage the measurement of Hg^{2+} concentration presented no difficulty since the Hg^{2+} optical absorption band occurred in an optically available wavelength spectrum in all the mercury-doped alkali halide specimens. Errors due to extrapolation and to the optical measurements may be generally ignored. In addition the error arising in the measurement of thickness was considered and it was found to be very small with sufficient precautions. Hence, if the absorption coefficient at the peak of the Hg^{2+} absorption band μ_{max} is quoted in cm^{-1}, the constant Δ_{max} in cm^2 and the concentration of Hg^{2+} cations N in cm^{-3} , it follows that

$$N = \frac{\mu_{max}}{\Delta_{max}} \quad \text{or} \quad N = \frac{2.3}{\Delta_{max} d} A_{max} \qquad (2.9)$$

From figure 2.14 Δ_{max} for mercury-doped KF specimen is

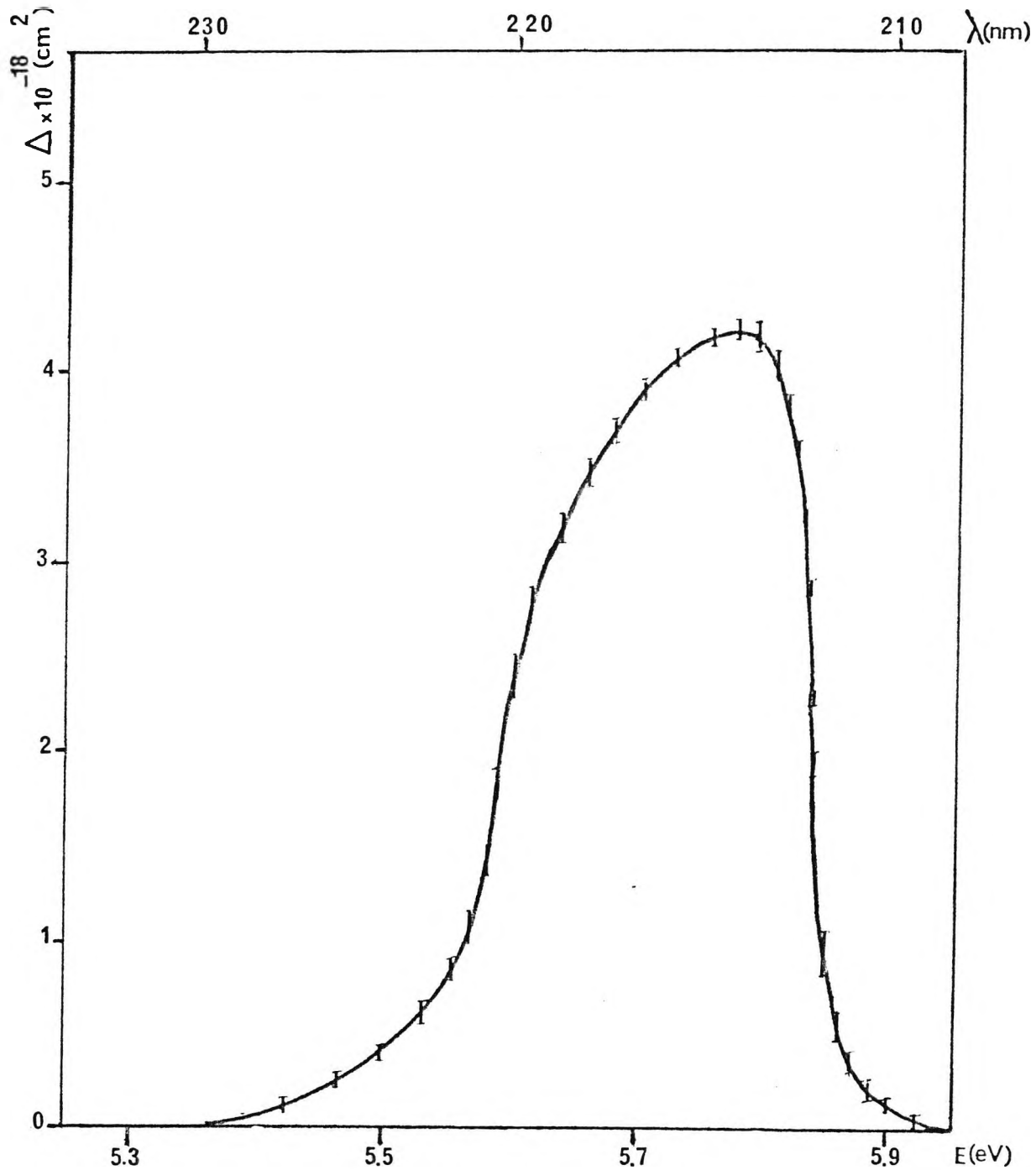

Figure 2.14 Optical determination of constant $\Delta_{max.}$ for the Hg^{2+} absorption band in KF specimen

$$\Delta_{max} = 4.25 \times 10^{-18} \text{ cm}^2 \qquad (2.10)$$

thus

$$N = 2.35 \times 10^{17} \ \mu_{max} \ \text{cm}^{-3} \qquad (2.11)$$

These values are valid for the range $2x10^{16}$ cm^{-3} $\leq N \leq$ $6x10^{18}$ cm^{-3}

Using various mercury -doped alkali halide specimens with different thicknesses and doping levels, similar values were determined for several other alkali halide specimens (see table 2.2).

6. Diffusion of OH^- and alkali metals

6.1 OH^- diffusion

Potassium fluoride specimens were the main material in the OH^- diffusion experiments. They were doped with OH^- ions by water vapour diffusion at 730° C for four days, followed by a rapid quench to room temperature. The resultant absorption spectrum (infrared and ultra-violet) was measured as well as the ionic conductivity. Nominally pure KF specimens as well as mercury-doped and Ca^{2+} -doped specimens were used in the OH^- diffusion experiments. The OH^- -doped specimen was, subsequent to the diffusion experiment, cleaved into two surface specimens and one representing the central part, and coded according to the starting materials and to their OH^- doping level. Then the optical absorption measurements as well as ionic conductivity and electrolytic coloration measurements were performed using these specimens.

Infrared measurements were performed using a Grubb-Parsons spectrophotometer (model MK 2E2) and the Perkin-Elmer 450 spectrophotometer was used for the ultra-violet absorption measurements. All these measurements were made at room temperature. Careful handling, as well as the use of specimens of differing thickness, ensured that the observed spectra were not due to surface contamination. The OH^- concentration was measured using the correlation between the optical spectrum and the concentration of OH^- ions derived by using the method of Anger et al (1963). Other alkali halide specimens were also subjected to this kind of experiment.

6.2 Diffusion of alkali metals

Table 2.2. Divalent mercury concentration $N = \frac{\mu_{max}}{\Delta_{max}}$ measured in cm^{-3} and the range of valid measurement.

	$\Delta_{max}(cm^2)$ (1)	$N\ (cm^{-3})$ (2)	Range	
			$N \geq x\ 10^{16} cm^{-3}$	$N \leq x\ 10^{18} cm^{-3}$
NaCl	4.64	2.16	3	7
KF	4.25	2.35	2	6
KCl	5.21	1.92	4	7
KBr	5.76	1.74	2	5

(1) All the values x 10^{-18}

(2) All the values x 10^{17} μ_{max} . μ_{max} is the absorption coefficient $(cm^{-1}) = \frac{2.3A_{max}}{a}$

The experimental method which was used in this field was similar to that of Jircal et al (1969) with some modification to the furnace and the diffusion ampoule. The alkali metal diffusion (or additive coloration) experiments were carried out in order to obtain results which could be used for comparison with those obtained by electrolytic coloration. Also, additive coloration of alkali fluoride specimens was carried out to investigate the reported difficulty of colouring these specimens using this method (Kikuchi and Ozawa, 1973).

A weighed amount of alkali metal and the specimen were sealed in the stainless steel diffusion ampoule and were held at temperatures near to the melting point of the specimen for 15 to 20 hours under half atmospheric pressure. After the experiment was finished the ampoule was quenched to liquid nitrogen temperature with the minimum delay.

7. Other experimental techniques and measurements

7.1 Sandwich technique

The experiments using this technique were based on the fact that, when two specimens of the same substance are pressed together, the mobile ions are able to pass freely from one specimen into the other. In the same way, if two specimens of two different substances having a mobile ion in common (for example, sodium in NaF and NaCl) are pressed together and a voltage is applied, the mobile ions pass across the boundary in spite of the disparity in the lattice spacing (Mott and Gurney, 1948).

Transference experiments were carried out using a mercury-doped alkali halide specimen placed between two nominally-pure specimens of the same crystal. The specimens were clamped between two flat platinum electrodes and were subjected to electrolysis for extended periods at temperatures near to the melting point. The specimens were cleaved with care so that a good fit was obtained at the interfaces. The experiment was performed in an atmosphere of flowing nitrogen and the specimens were separated after the electrolysis by wedging a razor blade into the junction between them. Generally, they were quite firmly joined and fragments of one specimen often stuck to the other. Before making any optical absorption measurements a thin layer was carefully scrapped from each specimen face. The migration direction of mercury was detected by examining the absorbance of the specimen slices, cut perpendicular to the field direction, after the electrolysis.

The same procedure was used to produce the F_A-centres in alkali halide specimens. F (Na)- and F(Li)- centres were produced by initially preparing the specimen as described above and then subjecting it to electrolytic coloration. This technique has also been used to produce a high concentration of pure F-centres in a thin ($\sim$ 1 mm) specimen. Specimen plates of

various thicknesses were stacked upon one another between the pointed cathode and the flat anode and the usual electrolytic coloration procedure was applied.

7.2 Deformation

The time dependence of the coloration current was studied in specimens containing dislocations in order to verify experimentally the hypothesis that excess anion vacancies are created at dislocations in the bulk of the specimen and also to test the reported correlation between the enhancement of colourability and induced plastic deformation (Mehendru, 1970; Boni et al, 1975).

Specimens (1 to 2 mm thick) which had been annealed at a temperature 50° C below the melting point, were plastically deformed by holding them between two stainless steel plates which were then placed between the jaws of a micrometer screw. Tightening the micrometer screw produced the desired amount of deformation in the specimens.

7.3 Thermal treatment

The method of thermal treatment was used in this work to produce F-aggregate and colloid centres in electrolytically coloured alkali halide specimens containing pure F-centres in high concentration ($\sim 10^{18}$ cm^{-3}). The bleaching of the F-centre and the evolution of the F-aggregate and colloid centres was studied as a function of temperature. The colloid centres were produced at temperatures of a few hundred degrees above room temperature while F-aggregate centres were produced by this method at lower temperatures.

7.4 Ionic conductivity

Specimens of nominally-pure alkali halide as well as electrolytically coloured, mercury-doped, OH^- -doped and calcium-doped alkali halide specimens were subjected to ionic conductivity measurements. These measurements were carried out over the temperature range from 125°C to 800°C. The lower limit was determined by the sensitivity of the apparatus and the upper limit by the failure of the electrodes on the specimen. Thermal annealing was carried out before any ionic conductivity measurement was performed in order to ensure a good specimen-electrode contact. Care was taken to prevent any side effect which this treatment might produce by choosing the proper temperature and time of thermal annealing

The ionic conductivity measurements were made with both increasing and slowly decreasing temperature. Measurements were carried out to ensure that Ohm's law is valid within the range of the experiments. The equipment was the standard arrangement for these measurements. The specimens were heated inside the silica tubes (see section 3.4) using the

same furnace which was usually used in the electrolytic coloration experiments. Two flat sheets of platinum were used as the electrodes. The specimen current was displayed on a chart recorder and careful measurements of the specimen size were carried out to ensure a minimum error of measurement for the ionic conductivity.

8. References

Anger J, Fritz B and Luty F 1963 Z.Phys. 174 240

Boni M, Gamagni P and Giani E 1975 J. Phys. Chem. Solids 36 883

Burstein E,Oberly J J,Henvis B W and Davisson J W 1951 Phys.Rev. 81 459

Dexter D [illegible] 1956 Phys. Rev. 101 48

Flynn C P 1982 Point Defects and Diffusion-Clarendon Press

Garbuny M 1965 Optical Physics-Academic Press

Gilman J J and Johnston W G 1962 Solid St. Phys. 13 147

Gordy W and Thomas W J O 1956 J.Chem. Phys. 24 439

Gorlich P, Karrs H and Kolitz G 1963 Phys St. Solid. 3 1629

Greenwood N N 1984 Ionic Crystals, Lattice Defects and Nonstoichiometry-Butterworths

Gritsenko Yu I 1971 Phys. St. Solid (a) 7 113

Haupt U 1959 Z.Phys. 157 232

Jirgal G H, Shaw M D and Noble G A 1969 Am.J.Phys. 37 963

Kikuchi A and Ozawa K 1973 Phys.St.Solid (a) 18 567

Klick C C, Patterson D A and Knox R S 1964 Phys. Rev. 133 A1717

Kobayashi K and Tomiki T 1960 J. Phys.Soc. Japan 15 1982

1961 J.Phys.Chem. Solids 22 73

Martienssen W 1975 J.Phys, Chem. Solids 2 257

Mehendru P C 1970 J.Phys. C: Solid St. Phys. 3 530

Meistrich M L 1968 J.Phys. Chem. Solids 29 1119

Moser F and Urbach F 1956 Phys. Rev. 102 1519

Mott N F and Gurney R W 1948 Electronic Processes in Ionic Crystals-Dover

Papazian H A 1973 Phys. St.Solid. 59 K 89

Pauling L 1932 J.Am. Chem.Soc. 54 3570

1980 The Nature of the Chem. Bond, Cornell Uni. Press

Pershits Ya N and Ilin A N 1968 Sov. Phys.-Solid St. 10 719

Podini P 1965 Phys. St. Solid 9 737

Schulman J H, Cinther R J and Klick C C 1950 J.Opt.Soc.Am.40 854

Sibley W A, Sonder E and Butler C T 1964 Phys. Rev. 136 A537

Topa T and YusterM 1970 Phys.St. Solid (a) 3 131

Townsend P D and kelly J C 1973 Colour Centres and Imperfections in Insulators and Semiconductors-Sussex Uni.Press

Urbach F 1953 Phys. Rev. 92 1324

Wagner W U 1964 Z. Phys. 181 143

Weast R C 1970 CRC Handbook of Chem. and Phys.-51st ed. The Chem. Rubber Co.

CHAPTER THREE

Mercury-Doped Alkali Halides

1. Optical properties

1.1 Spectra of mercury-doped specimens before coloration

Figure 3. 1 shows typical absorption spectra obtained from quenched and annealed mercury-doped alkali halides. Curve (a) is the.absorption spectrum of a KF specimen doped with 1.3 x $10^{18}cm^{-3}$ of divalent mercury cations. The spectrum was measured immediately after quenching to room temperature from the diffusion temperature (780° C). Three absorption bands peaking at 214 nm, 234 nm and 283 nm were introduced after 1.8 x 10^6 seconds of mercury diffusion. Curve (b), however, shows the spectrum of the same specimen after a thermal anneal at 780° C in nitrogen for 2.4 x 10^5 seconds followed by a slow cooling to room temperature over 1.8 x 10^4 seconds. It is clear from this curve that unquenched mercury-doped KF produces an additional absorption band peaking at 249 nm while the peak at 234 nm declines considerably. The absorption bands peaking at 214 nm and 283 nm decline as well. All the optical measurements were made at room temperature. Optical measurements of the other mercury-doped alkali halides showed that mercury ions introduce identical patterns of spectra; that is three absorption bands if the doped specimens are quenched to room temperature. No absorption bands were observed in the visible and near infrared regions of the spectrophotometer Slow cooling to room temperature, however, produces a fourth band peaking on the long wavelength shoulder of the second absorption band of the quenched mercury-doped specimens.

Mercury-doped KI, NaF and LiF showed different spectra. KI specimens showed only two bands on quenching which peaked at 278 nm and 342 nm. On slow cooling to room temperature these specimens showed a third band peaking at 305 nm. The relation between the 278 nm and the 305 nm bands is identical to that of the 234 nm and 249 nm absorption bands respectively in quenched and unquenched mercury-doped KF.

The spectra of quenched specimens of NaF and LiF containing mercury showed few features compared with the spectra of mercury-doped KF. In both cases a relatively low-amplitude band was observed which extended from about 260 nm to the beginning of the absorption edge at about 195 nm. An additional small peak was observed at 259 nm with mercury-doped NaF. Subsequent annealing at 800° C and cooling slowly over a total time

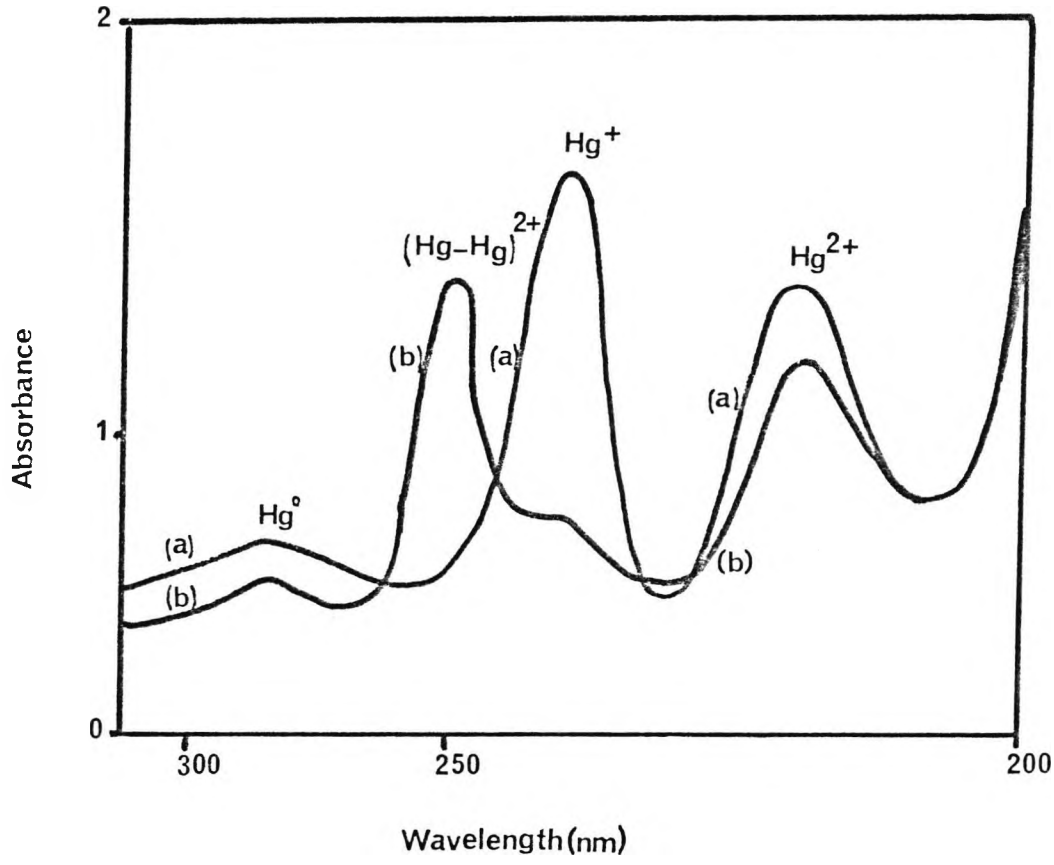

Figure 3.1 Spectra of (a) quenched and (b) unquenched KF:Hg

scale of 1.04 x 10^5 seconds produced a significant increase in the intensity of the broad band in both the mercury-doped NaF and LiF specimens and the disappearance of the 259 nm absorption band in the mercury-doped NaF. The maximum amplitude of the broad band occurred at about 210 nm in both cases. Figure 3.2 (curve (a))shows a typical spectrum obtained from annealed specimens of mercury-doped NaF containing between 1 x 10^{18} and 3 x 10^{18} Hg^{2+} cm^{-3} .The spectrum of annealed mercury-doped LiF shows similar features to curve (a) of figure 3.2. As shown in figure 3.2 the 210 nm band in mercury-doped NaF is a broad and asymmetrical, falling off in intensity more sharply at the shorter wavelength side of its peak position than at the longer wavelength side. This asymmetry indicates an overlapping with another absorption band at the longer wavelength side. This point was justified by recording the spectrum at liquid nitrogen temperature and obtaining a small absorption band at 220 nm.

Figure 3.3 shows the absorption spectra of KBr specimens doped with various concentration of Hg^{2+}. The concentrations of divalent mercury cations in each specimen is indicated on the corresponding spectrum. An analysis of figure 3.3 shows that the 226 nm absorption band increases in intensity proportionally to the divalent mercury cation content. The two absorption bands at the long wavelength side of the 226 nm band appear gradually as the Hg^{2+} concentration increases. The one-band feature at low Hg^{2+} concentration ($\sim 10^{16}$ cm^{-3}) and the evolution of the spectrum to the final characteristic form consisting of three bands at high Hg^{2+} concentration ($\sim 10^{18}$ cm^{-3})are also observed in other mercury-doped alkali halides.

1.2. Spectra of mercury-doped specimens after coloration

Figure 3.4 shows the changes in the ultra-violet absorption spectrum of mercury-doped KF following electrolytic coloration at 700° C. Curve (a) is the spectrum of the quenched specimen immediately after the electrolytic coloration experiment. Comparison between this spectrum and that shown in figure 3.1 (curve (a)) shows that the 214 nm band is slightly suppressed and that there is an enhancement of the 234 nm and 283 nm bands at the expense of the 214 nm band Both spectra (curves (a) in figures 3.1 and 3.4) belong to the same quenched mercury-doped KF specimen. A similar effect was observed when an annealed mercury-doped KF specimen was coloured electrolytically. Electrolytic coloration of mercury-doped KBr, KCl and NaCl produced the same result; that is the suppression of the absorption band nearest to the absorption edge and the enhancement of the bands on the longer wavelength side. This effect can only happen when the higher-valence states of mercury capture electrons and are transformed to lower-valence states. The reduction of valence of Ag^+ and Pb^{2+} ions in silver- and lead-doped alkali halides due to electrolytic coloration is reported in the literature (Kleemann 1968, Topa and Velicesu 1968)

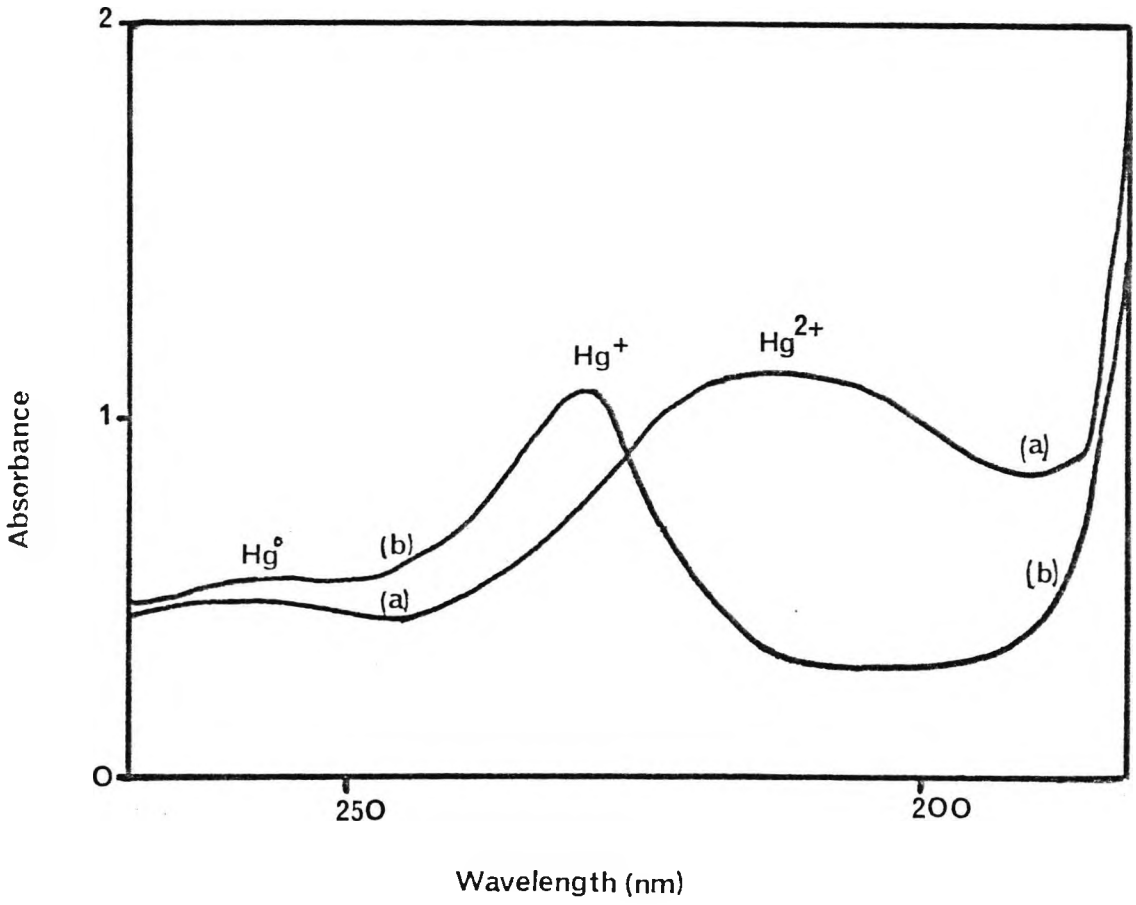

Figure 3.2 Spectra of annealed NaF:Hg (a) before and (b) after coloration / de-coloration

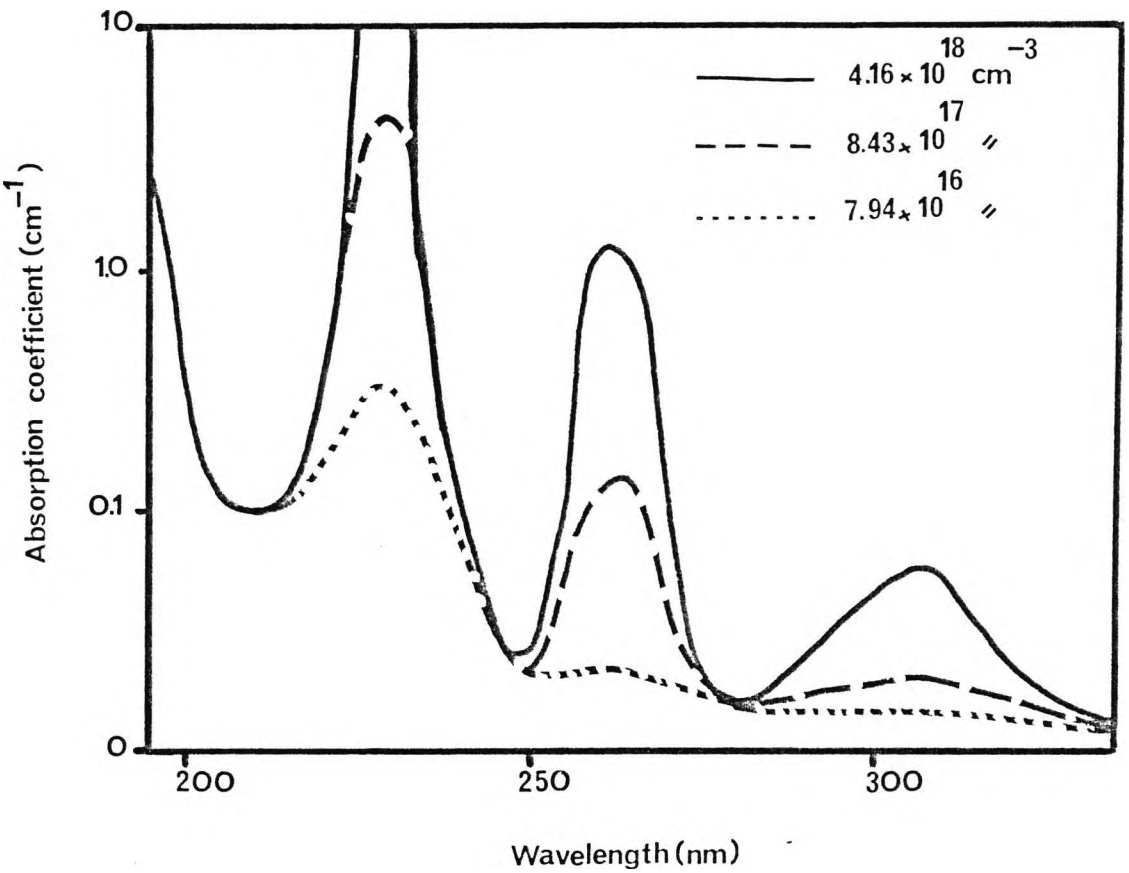

Figure 3.3 Spectra of KBr doped with various concentrations of Hg^{2+}

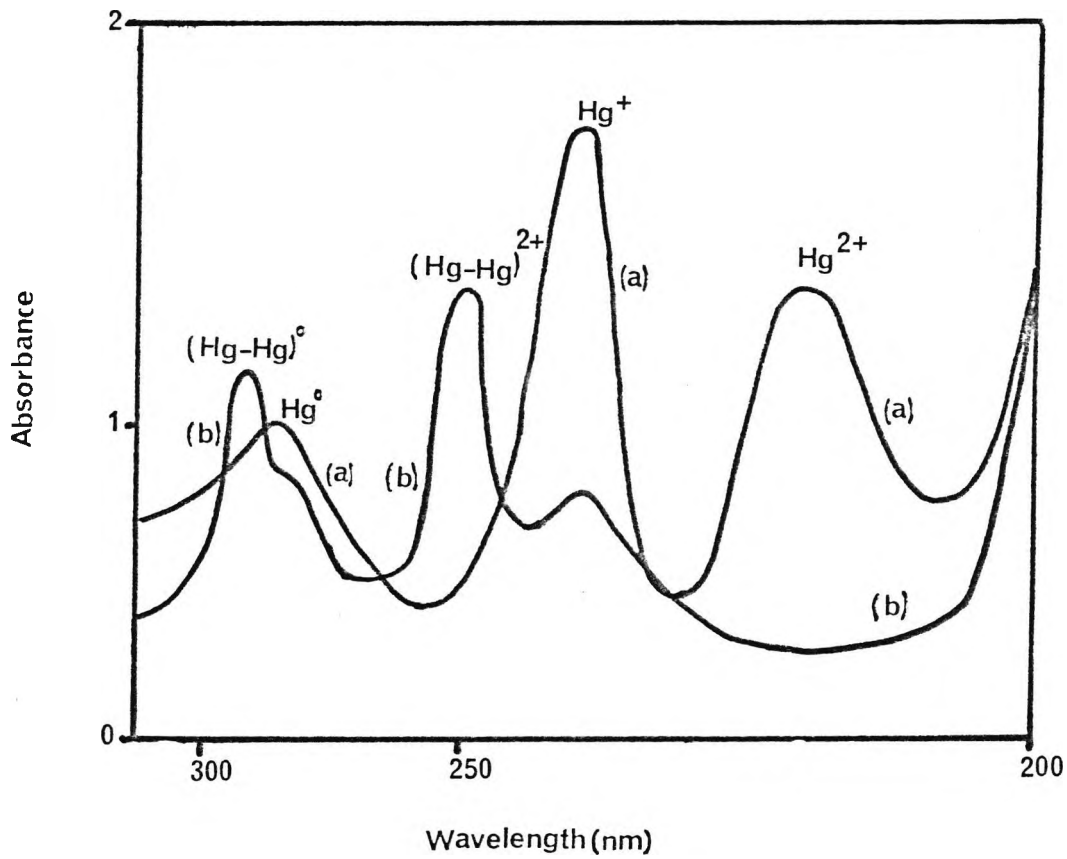

Figure 3.4 Spectra of electrolytically coloured KF:Hg (a) before and (b) after de-coloration

Curve (b) of figure 3.4 was obtained by a two-stage treatment on the annealed mercury-doped KF specimen which gave curve (b) of figure 3.1 before the treatment was carried out. In the first stage the specimen was electrolytically coloured at 700° C. The coloration was then removed electrolytically at the same temperature by reversing the polarity of the electrodes. Apart from an increase in the intensity of the absorption bands on the longer wavelength side of the 214 nm band, two new phenomena were observed. The first is the disappearance of the 214 nm absorption band and the second is the emergence of a new band peaking at 290 nm. Identical results were obtained when quenched mercury-doped KF specimens were treated by the two-stage process.

The two stage electrolytic coloration / de-coloration process was also applied to other mercury-doped alkali halides. The results were similar; a reduction of the absorption bands located nearest to the absorption edge and a simultaneous enhancement of the bands on the longer wavelength side together with the appearance of new bands on the long wavelength shoulder of the third band. Figure 3.2, however, shows the results obtained when a mercury-doped NaF specimen was subjected to the two-stage process. Curve (b) is the spectrum of the annealed mercury-doped NaF after the two-stage process was applied. The 210 nm band was completely removed after the de-coloration process, leaving two bands peaking at 224 nm and 259 nm. The same process produced similar results when applied to mercury-doped LiF specimen. The 210 nm band was completely removed after the de-coloration process with the emergence of two bands at 217 nm and 234-240 nm. The spectra of mercury-doped NaF and LiF specimens after de-coloration support the idea, discussed in the previous section, that the broad and asymmetrical feature of the 210 nm bands in these specimens is caused by an overlapping with another band at the longer wavelength side of the 210 nm band.

The spectrum of a mercury-doped KI specimen after the two-stage treatment showed a different feature from that which was observed in the case of the other mercury-doped alkali halides. The band nearest to the absorption edge (278 nm) did not disappear after de-coloration. A new band peaking at 372 nm appeared after the de-coloration process while the other two bands at 278 nm and 342 nm were enhanced on coloration and de-coloration. The new band at 372 nm could only be obtained with the two-stage treatment.

1.3 Identification of optical absorption bands

The set of three absorption bands introduced in mercury-doped alkali halides by quenching from the diffusion temperature to room temperature are designated as due to isolated Hg^{2+}, Hg^{+} and Hg^{o} centres in order of increasing wavelength. The band obtained on slow cooling is designated as $(Hg\text{-}Hg)^{2+}$, while the new band which appears after the coloration/de-coloration treatment is designated as $(Hg\text{-}Hg)^{0}$. The peak position, halfwidth and oscillator strength of the various absorption bands produced in several alkali halides doped

by mercury diffusion and coloured electrolytically are reported in table 3.1. All the values refer to room temperature except those which are indicated with asterisks which refer to liquid nitrogen temperature.

The absorption bands nearest to the absorption edge are assigned to the divalent mercury cation Hg^{2+}. The peak at 214 nm in mercury-doped KF is located at approximately the same position as that in solutions of $HgCl_2$ (Deacon 1963). This designation is supported by the experimental results of the ionic conductivity measurements on mercury-doped alkali halides. Figure 3.5 shows the ionic conductivity of mercury-doped KCl specimens before the coloration (curve (b)), after electrolytic coloration (curve (c)) and after the de-coloration treatment (curve (d)). It is important to notice the reduction of ionic conductivity following electrolytic coloration and its further reduction after de-coloration. Relating these results to those reported in the previous two sections, it is evident that the ionic conductivity and the Hg^{2+} designated band are reduced simultaneously on electrolytic coloration. Moreover, this band is completely absent and the ionic conductivity is restored to its pre-doping level when the de-coloration treatment is applied. The reduction of the ionic conductivity in these specimens could only happen if the mercury ions are no longer present in the form of divalent cations since it is well known that divalent cation impurities added to an alkali halide occupy substitutional positions in the lattice and produce an equal number of cation vacancies. These results were used as criteria with which to identify the Hg^{2+} absorption bands in various mercury-doped alkali halides. The oscillator strengths of the Hg^{2+} bands were determined using Smakula's equation (equation (2.4)). The concentrations of Hg^{2+} centres were measured optically as described in chapter 2. The values obtained from such calculations are reported in table 3.1.

The peak at 234 nm, which is shown in figures 3.1 and 3.2 for mercury-doped KF, is assigned to isolated Hg^{+} ions on the basis of its relative position compared with the various excited levels of gaseous mercury atoms (Moore 1949, Santaran and Winans 1966) and its method of preparation by quenching. In mercury-doped KCl the nearest band peaks at 244 nm and also appears on the long wavelength side of Hg^{2+} band. The identification of these bands as due to Hg^{+} centres is consistent with the results of the chemical analysis carried out by Ben-Dor et al (1966). A comparison between these results and those reported in the previous two sections supports the designation of the absorption band nearest to the Hg^{2+} band and on its long wavelength side, which is obtained by quenching mercury-doped alkali halides to room temperatures, as due to Hg^{+} centres. Their enhancement after the two-stage treatment at the expense of the Hg^{2+} centres also supports this model.

The low-intensity peak at 283 nm in figures 3.1 and 3.2 may then be identified with the neutral Hg^{o} centre by comparison with the work of Tamai (1961) on Tl-doped KBr specimens. The identification of the 282 nm band in quenched mercury-doped NaCl with the neutral Hg^{o} centre is consistent with the results of Siederdissen and Fischer (1971). They

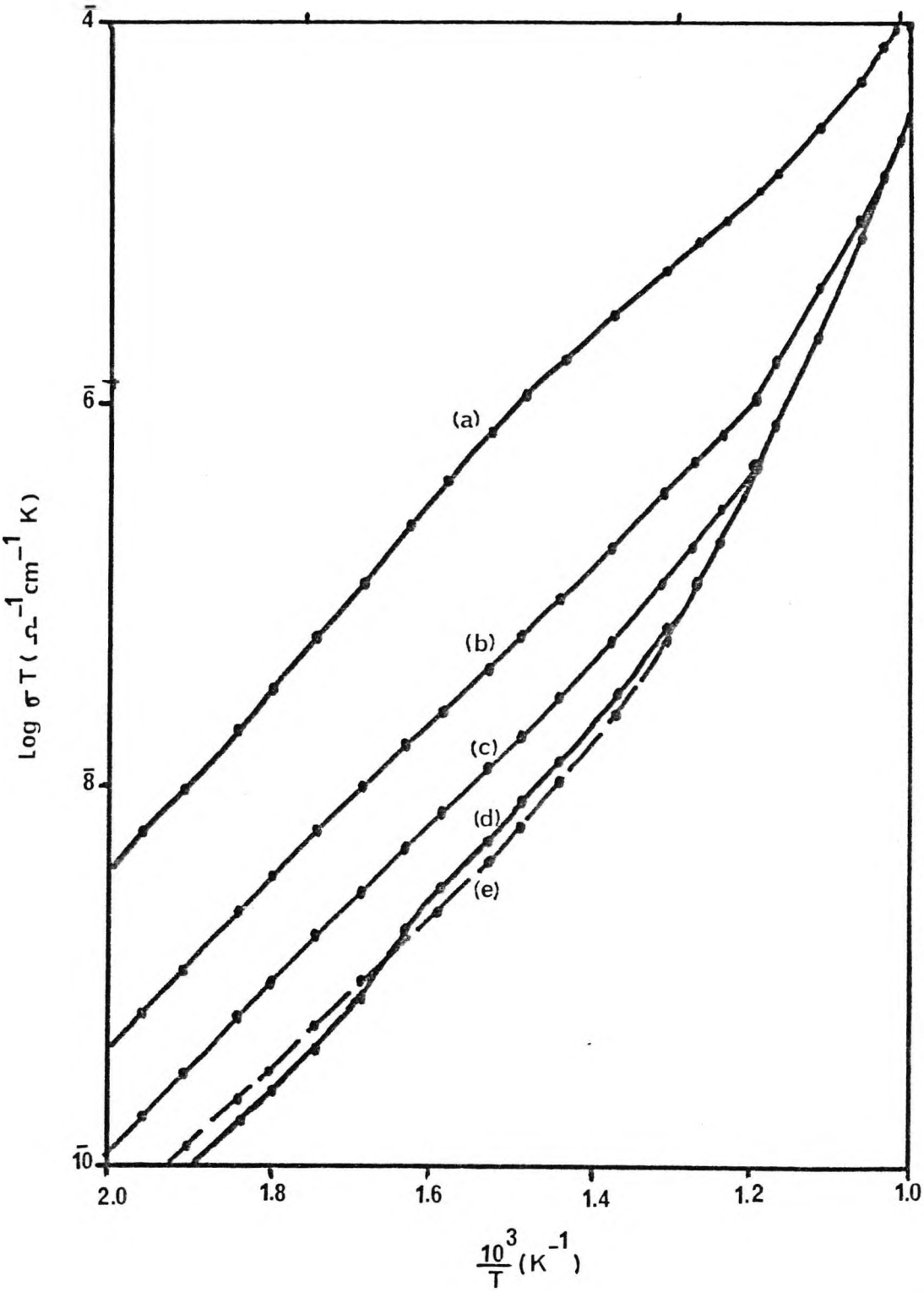

Figure 3.5 Ionic conductivity of KCl:Hg^{2+} specimens (a) doped with 2.86×10^{18} $Hg^{2+} cm^{-3}$, (b) doped with 1.41×10^{17} $Hg^{2+} cm^{-3}$ before coloration, (c) after coloration, (d) after de-coloration and (e) nominally-pure KCl

Table 3.1. Peak position, halfwidth and oscillator strength of the absorption bands due to various mercury ions in mercury-doped alkali halides.

	$(Hg-Hg)^{o}$	Hg^{o}		$(Hg-Hg)^{2+}$	Hg^{+}		Hg^{2+}		
	Peak position (nm)	Peak position (nm)	Half-width (eV)	Peak position (nm)	Peak position (nm)	Half width (eV)	Peak position (nm)	Half-width (eV)	Oscillator strength
LiF	-	234-240	0.74	-	217	.26	210	-	-
		232*			214*	.23	203*	.21	-
NaF	-	259	0.71	-	224	.27	210	-	-
		258*			220*	.24	202*	.22	
NaCl	302	282	0.89	252	236	.22	218	.22	.075
KF	290	283	0.73	249	234	.24	214	.25	.059
KCl	312	290	0.85	265	244	.24	220	.24	.081
KBr	336	315	0.91	287	265	.25	226	.22	.112
KI	372	342	0.86	305	278	.26	-	-	-

Values referred to with asterisks were obtained at liquid nitrogen temperature.
All other values were obtained at room temperature.

studied the optical absorption of Hg^o centres formed on thin layers of alkali halides. The enhancement of this band after the de-coloration treatment also supports this designation. Based on these results, the third absorption band obtained in quenched mercury-doped specimens on the long wavelength side of the Hg^+ band is identified with the Hg^o centre.

The absorption band at 249 nm obtained in mercury-doped KF on slow cooling to room temperature is assigned to the paired aggregate centre $(Hg - Hg)^{2+}$ which is well-known in wet chemistry. The identification of the absorption bands which are located between the peak positions of Hg^+ and Hg^o bands with $(Hg\text{-}Hg)^{2+}$ centres was made by recognising the fact that these bands always appeared on slow cooling and at the expense of the Hg^+ bands. Quenching mercury-doped specimens causes these bands to disappear. Tsuboi (1970, 1976) observed similar bands in thallium-doped KI, KBr and KCl and NaCl specimens. The centres are expected to be formed when paired Hg^+ centres capture electrons released in the mercury-doped specimens to produce aggregates of two Hg^+ centres. The new absorption band peaking at the longer wavelength side of Hg^o is assigned to $(Hg\text{-}Hg)^o$, since this band could only be produced after de-coloration. The capture of further electrons released in the specimen by the bleached F-centres leads to a reduction in the valence of the $(Hg\text{-}Hg)^{2+}$ centres and the formation of $(Hg\text{-}Hg)^o$ centres. Taking into account the interesting results obtained with silver-doped alkali halides where, after electrolytic coloration, Ag^- centres were formed (Kleemann 1968), the $(Hg\text{-}Hg)^o$ designated bands could possibly be due to substitutional Hg^- centres formed on anion sites. Velicescu and Topa (1973) also reported the formation of Pb^-, Sn^- and Ge^- centres in lead, tin and germanium-doped alkali halides after they were subjected to electrolytic coloration.

2. Influence of the divalent mercury cation

2.1. Ionic conductivity

The ionic conductivity measurements were carried out in order to study the relation between the excess cation vacancies introduced by divalent mercury cations and the electrolytic coloration process. These measurements were also used to investigate the nature of the various mercury centres in mercury-doped alkali halides. Accordingly, a nominally-pure KCl specimen together with two mercury-doped KCl specimens were subjected to ionic conductivity measurements. The Hg^{2+} concentration of these two specimens were 2.86×10^{18} cm^{-3} and 1.41×10^{17} cm^{-3}. The measurements were carried out within the temperature range 250° C to 700° C. The ionic conductivity of the KCl specimen doped with 1.41×10^{17} Hg^{2+} cm^{-3} was measured before and after the electrolytic coloration as well as after the de-coloration treatment.

Figure 3.5 shows the results obtained from the above measurements. Curve (a) is the ionic conductivity plot of the KCl specimen doped with 2.86 x 10^{18} Hg^{2+} cm^{-3}. Curve (b) shows the ionic conductivity of KCl specimen doped with 1.41 x 10^{17} Hg^{2+} cm^{-3}. Curve (c) is the ionic conductivity plot of the same KCl specimen used to obtain curve (b) after it was electrolytically coloured at 680° C using a constant current of 1 mA. Curve (d) shows the ionic conductivity of a KCl specimen doped with 1.41 x 10^{17} Hg^{2+} cm^{-3} (taken from the same block as the KCl specimen of curve (b) after it was subjected to electrolytic coloration, using identical coloration conditions as those used with the KCl specimen of curve (c), and to de-coloration treatment at the same coloration temperature. Curve (e) is the ionic conductivity plot of the nominally-pure KCl specimen.

All the curves exhibit a characteristic linear region at which the concentration of cation vacancies remains constant depending on the concentration of divalent mercury cations. The activation energy E_m for the migration of cation vacancies was determined from this extrinsic region. The mean value of the energy obtained from the various curves is 0.69 eV and is in agreement with the value of 0.73 eV reported by Chandra and Rolfe (1970). The Schottky formation energy E_s was determined from the high temperature (intrinsic) region to be 2.44 eV. This value is also in agreement with the value 2.59 eV reported by Chandra and Rolfe (1970). It is clear from the curves that, as the Hg^{2+} concentration increases, the extrinsic region extends to higher temperatures. Figure 3.5 shows that this region extended to about 200°C as the concentration of divalent mercury was increased from practically zero in the nominally pure KCl specimen to 2.86 x 10^{18} cm^{-3} in the KCl specimen of curve (a).

2.2. Colourability of alkali halides

Figure 3.6 (curve (a)) shows the F absorption band of a nominally-pure KCl specimen obtained by electrolytic coloration using the coloration conditions 500° C and 110 μ A. Curve (b) shows the F absorption band of a mercury-doped KCl specimen (1.61 x 10^{18} Hg^{2+} cm^{-3}) obtained by electrolytic coloration using indentical coloration conditions to those used for the specimen in curve (a). Two facts are clearly demonstrated by this figure. The first is the enhancement of the F band absorption due to mercury doping. The second is that the F absorption bands in both cases coincide in most of the central region near to the peak. No shift of peak position of the F band could be observed in other electrolytically coloured alkali halides doped with various concentrations of Hg^{2+}. This observation suggests the formation of F-centres only and the absence of any Z-centres in the close neighbourhood of the F band.

Figure 3.7 shows the influence of Hg^{2+} content on the colourability of KCl and NaCl. Electrolytic coloration experiments were carried out using identical coloration conditions (570°C, 120 μ A). Figure 3.7 demonstrates clearly the fact that F absorption enhancement is proportional to the pre-coloration values of Hg^{2+} concentration in each specimen .This

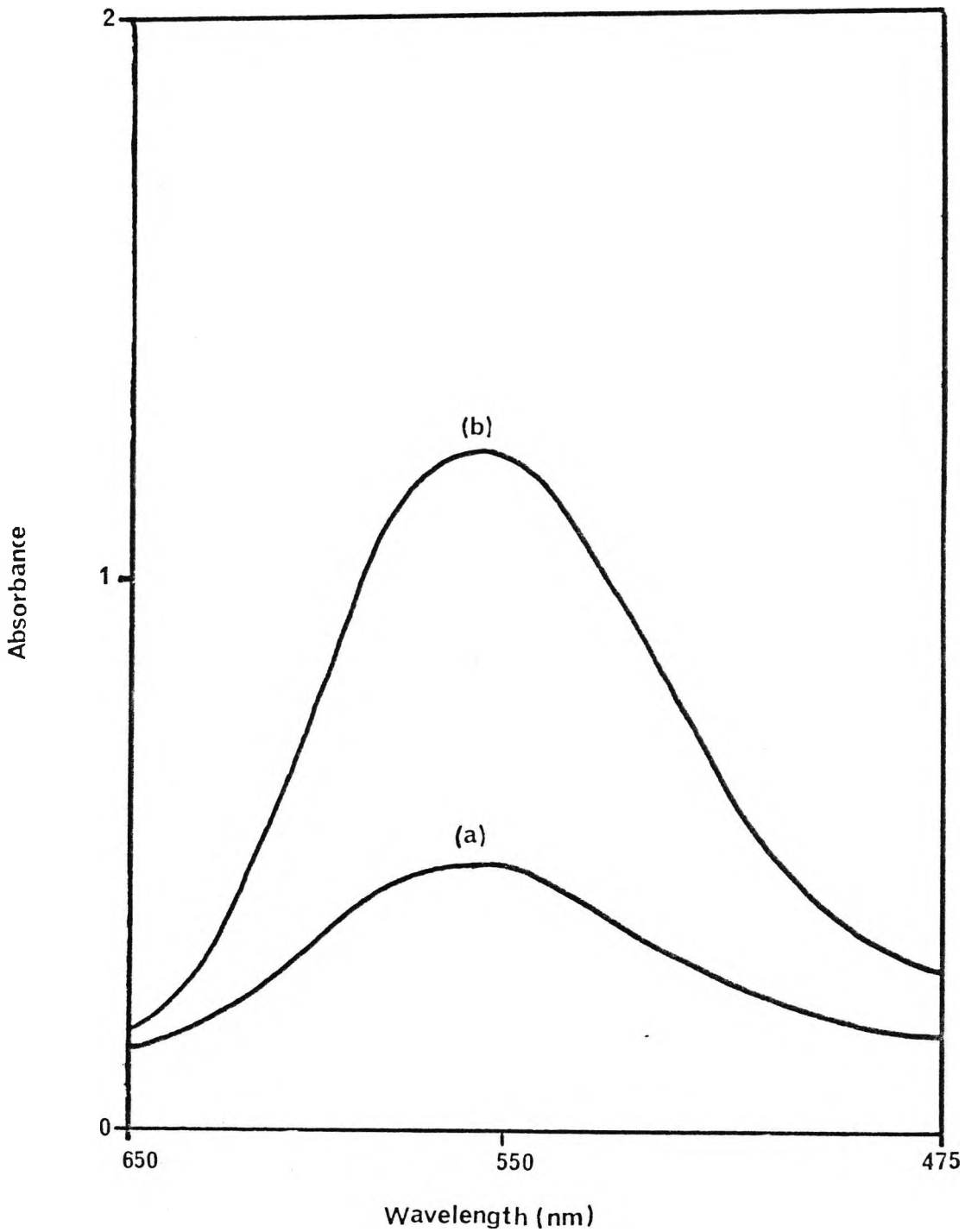

Figure 3.6 F absorption of (a) nominally-pure KCl and (b) mercury-doped KCl containing 1.61×10^{18} Hg^{2+} cm^{-3}

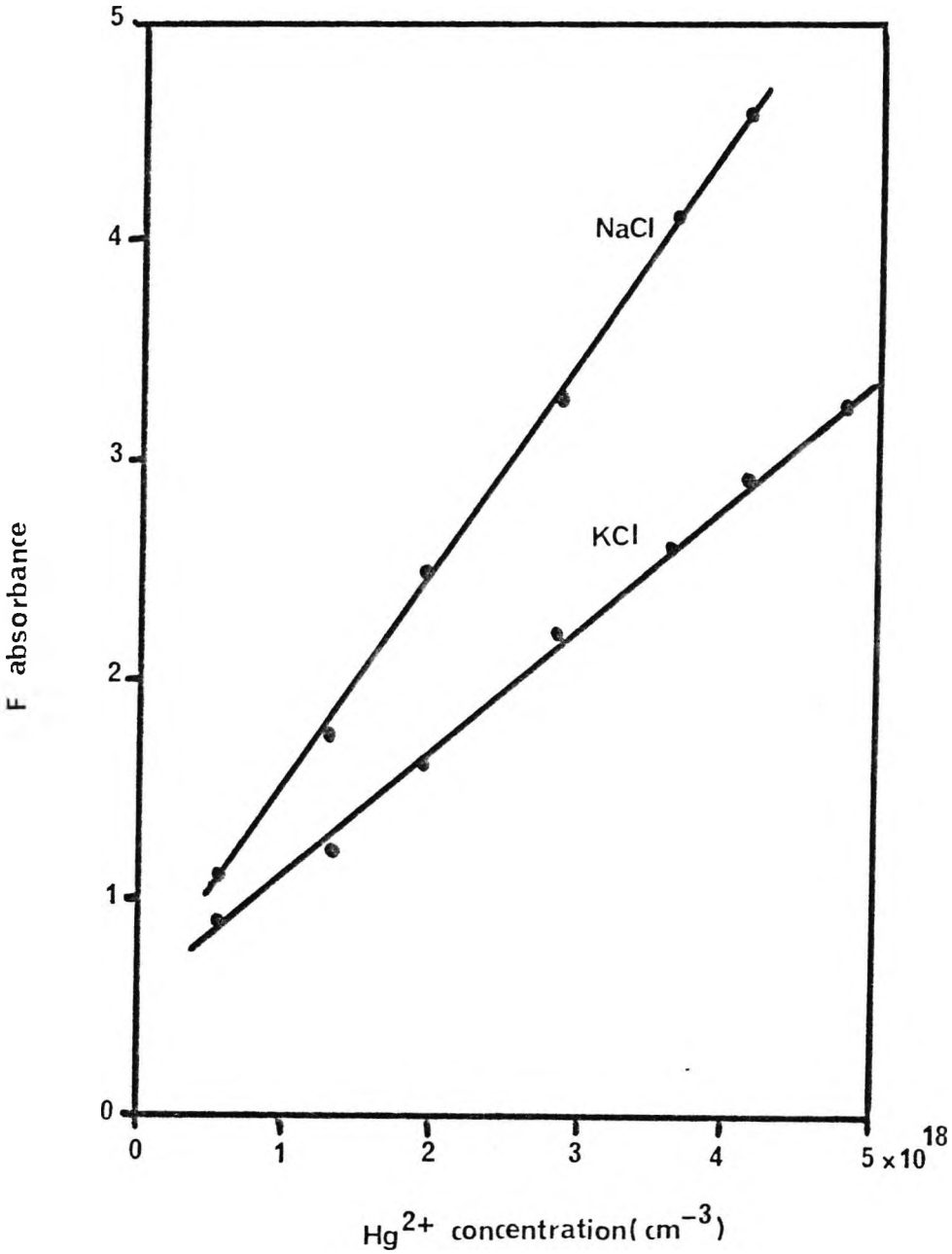

Figure 3.7 The relation between F absorption enhancement and Hg^{2+}content of KCl:Hg and NaCl:Hg

figure also shows that the enhancement of F-centre colourability in mercury-doped NaCl is higher than that of mercury-doped KCl when identical doping levels and coloration conditions are used. Electrolytic coloration carried out at temperatures higher than 620° C using mercury-doped NaCl specimens (.> 6 x 10^{18} Hg^{2+} cm^{-3}) showed the rapid enhancement of the colloid band while the F band growth was saturated. At coloration temperatures higher than 700° C, the F band started to decline while the colloid band became rapidly broader. The coloration temperatures at which the colloid band started to develop were found to decrease with increasing Hg^{2+} concentration.

The current-temperature relationship during the electrolytic coloration process in mercury-doped alkali halides was investigated. Figure 3.8 shows the current-temperature relationship of two mercury-doped NaCl specimens as well as that of a nominally-pure NaCl specimen. Curve (a) obtained from the electrolytic coloration of a NaCl specimen doped with 3.71 x 10^{18} Hg^{2+} cm^{-3} while curve (b) shows the same relationship obtained from the electrolytic coloration of a NaCl specimen doped with 1.26 x 10^{17} Hg^{2+} cm^{-3}. Curve (c), however, is the current - temperature relationship for nominally-pure NaCl. All electrolytic coloration experiments were carried out using the constant-voltage method. It is clear from figure 3.8 that the structure of all three curves are identical to those which are normally obtained for the nominally-pure potassium halides.,as reported in chapter 4 The other important fact to observe is that the coloration starting temperature T_c is lowered continuously from 595°C in nominally-pure NaCl (curve (c)) to 420°C in mercury-doped NaCl (curve (a)) as the concentration of divalent mercury is increased. Comparison of these results with those reported in chapter 4 for nominally-pure alkali halides shows that mercury-doped NaCl (curve (a)) can be electrolytically coloured with almost the same ease as nominally-pure KI specimens.

Figure 3.9 shows the current density – time relationship during the electrolytic coloration of a mercury-doped NaCl specimen compared to the same relationship of nominally -pure NaCl. Curve (a) refers to a NaCl specimen doped with 7.29 x 10^{17} Hg^{2+} cm^{-3}. Curve (b) is obtained from the results reported in chapter 4,figure 4.5 for nominally-pure NaCl. In both cases, electrolytic coloration was carried out at 590°C using the constant-voltage method. It can be seen clearly from figure 3.9 that the first part of the current-time curve is shorter and higher for the mercury-doped specimen than is the case for the nominally-pure specimen. Both of these features are caused by the excess cation vacancies introduced into the specimen of curve (a) by the divalent mercury, since the first part of the current density-time curve is due to an ionic process and is dominated by cation vacancy migration (as reported in chapter 4,section 1.2 ,and discussed in chapter 7). The excess cation vacancies shorten the time needed to form the new alkali metal cathode. In this respect, the behaviour of the first part of curve (a) seems similar to that of the nominally-pure specimen when the coloration experiment is carried out at higher temperatures. Increasing the coloration

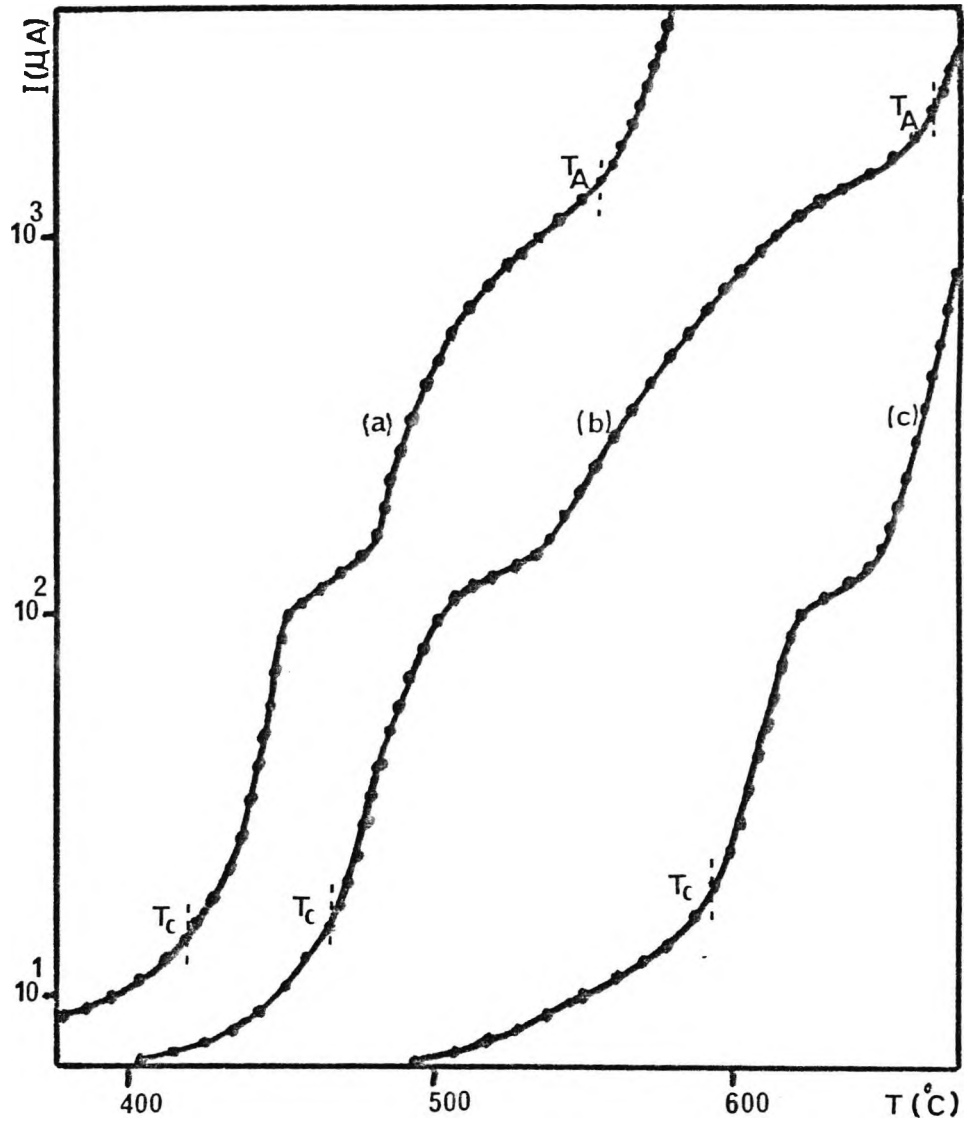

Figure 3.8 Current–temperature relationship of a NaCl specimen doped with (a) 3.71×10^{18} Hg^{2+} cm^{-3}, (b) 1.26×10^{17} Hg^{2+} cm^{-3} and (c) nominally-pure NaCl

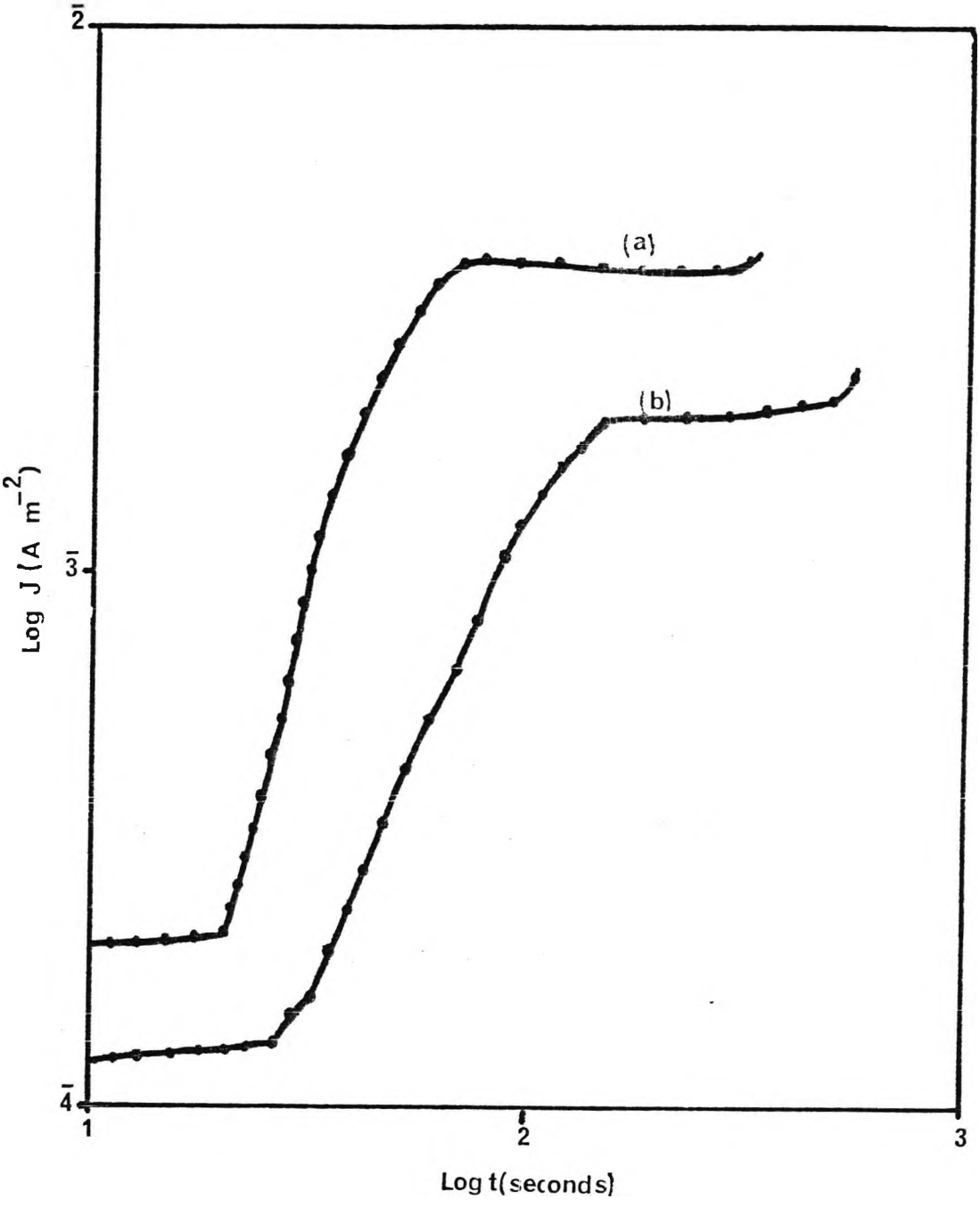

Figure 3.9 Current density–time relationship of (a) mercury–doped NaCl and (b) nominally–pure NaCl

temperature leads to an increase in the anion vacancy concentration as well as in the cation vacancy concentration. Figure 3.9 shows also that the electron injection stage is obtained with a higher coloration rate in the mercury-doped specimen than in the nominally-pure specimen. The steady-current stage seems to be the same in both cases as is to be expected, since this part of the current density-time relationship is dominated by the formation of anion vacancies.

2.3 Other observations

Although LiF specimens when received from Harshaw were difficult to cleave and often broke into small fragments, they became as easy to cleave as any other alkali halides after mercury diffusion. Gilman and Johnston (1958) investigated the same phenomenon in Mg^{2+} - doped LiF and concluded that ionic bonds due to the extra charge of the divalent ions are responsible for the improvement of the cleavage.

Mercury-doped KCl specimens acquired a faint reddish brown colour after annealing in air for long periods whereas mercury-doped KI specimens acquired a yellowish colour. No such colours were observed for the other alkali halides. This phenomenon, however, had no obvious effect on the results since the colours were not bound with any absorption band. No further investigation of the colour effect has been pursued, but it may be related to the diffusion of O^{2-} into the specimens and the formation of certain complexes with mercury ions such as HgO.

3. Diffusions measurements

3.1 Diffusion profiles

Diffusion profiles of divalent mercury cations in alkali halides were measured at six temperatures. After each diffusion experiment thin layers of the exposed specimen surface were repeatedly sectioned in order to measure the concentration gradients of Hg^{2+} . The thickness of each of the sectioned layers was determined by measuring the difference between the thickness of the mercury-doped specimen before and after sectioning. The concentration of Hg^{2+} in each layer was measured optically using the spectrophotometric data and the experimental results of chapter 2, section 5.2. These measurements were made by determining the absorption coefficient of the mercury-doped specimen before and after taking a thin layer from the exposed surface. The mean absorption coefficient of the Hg^{2+} band of the removed thin layers μ_x was then determined by

$$\mu_x = \frac{\mu_i - \mu_j}{\Delta x} \qquad (3.1)$$

where μ_i and μ_j are the absorption coefficients of the mercury-doped specimen before and after sectioning and Δx is the thickness of the thin layer.

This procedure was repeated to various depths x from the original exposed surface at various temperatures and diffusion times. Figure 3.10 shows a typical situation in which the absorption of the Hg^{2+} cations in mercury-doped KF decreases continuously each time a thin layer is removed from the exposed surface. The diffusion conditions of this specimen were 670 °C and 1.44 x 10^6 seconds.

The data obtained for the penetration of Hg^{2+} cations into five KF specimens is shown in figure 3.11. The results obtained in a sixth experiment were neglected because the first slice showed an abnormally high Hg^{2+} concentration. This could have happened because of the condensation of Hg^{2+} vapour on to the KF specimen during the quenching process. The penetration profiles obtained from mercury diffusion experiments carried out at temperatures below 500 °C showed a random scatter of points and less penetration than those which are shown in figure 3.11. The principal reason for such behaviour may be that the solubility of Hg^{2+} cations in alkali halides is lower at low temperatures. The surface concentrations of divalent mercury cations in figure 3.11 were extrapolated from the corresponding plots of log N versus the square of the penetration depth (x^2). Figure 3.12 shows the log N versus x^2 plots for a mercury-doped KF specimen. The diffusion conditions of this specimen were 610 °C and 2.07 x 10^6 seconds. The dashed lines in figure 3.12 are the parts of the curves which are extrapolated and correspond to the dashed lines in figure 3.11.

Figure 3.13 shows the penetration profiles of divalent mercury cations in two KF specimens as a function of diffusion temperature. The data was obtained from two series of mercury diffusion experiments carried out at two different diffusion times. The diffusion time, which was identical for each of the two series of the diffusion experiments, is indicated on each curve in figure 3.13.

3.2 Diffusion coefficient

The diffusion of divalent cations into alkali halides often expressed in the form of what is widely known as Fick's second equation (Jost 1952)

$$\frac{\partial N}{\partial t} = D \frac{\partial^2 N}{\partial x^2} \qquad (3.2)$$

where N is the concentration of the divalent cations at distance x from the diffusion surface. If the diffusion coefficient D is independent of Hg^{2+} concentration, the solution of Fick's

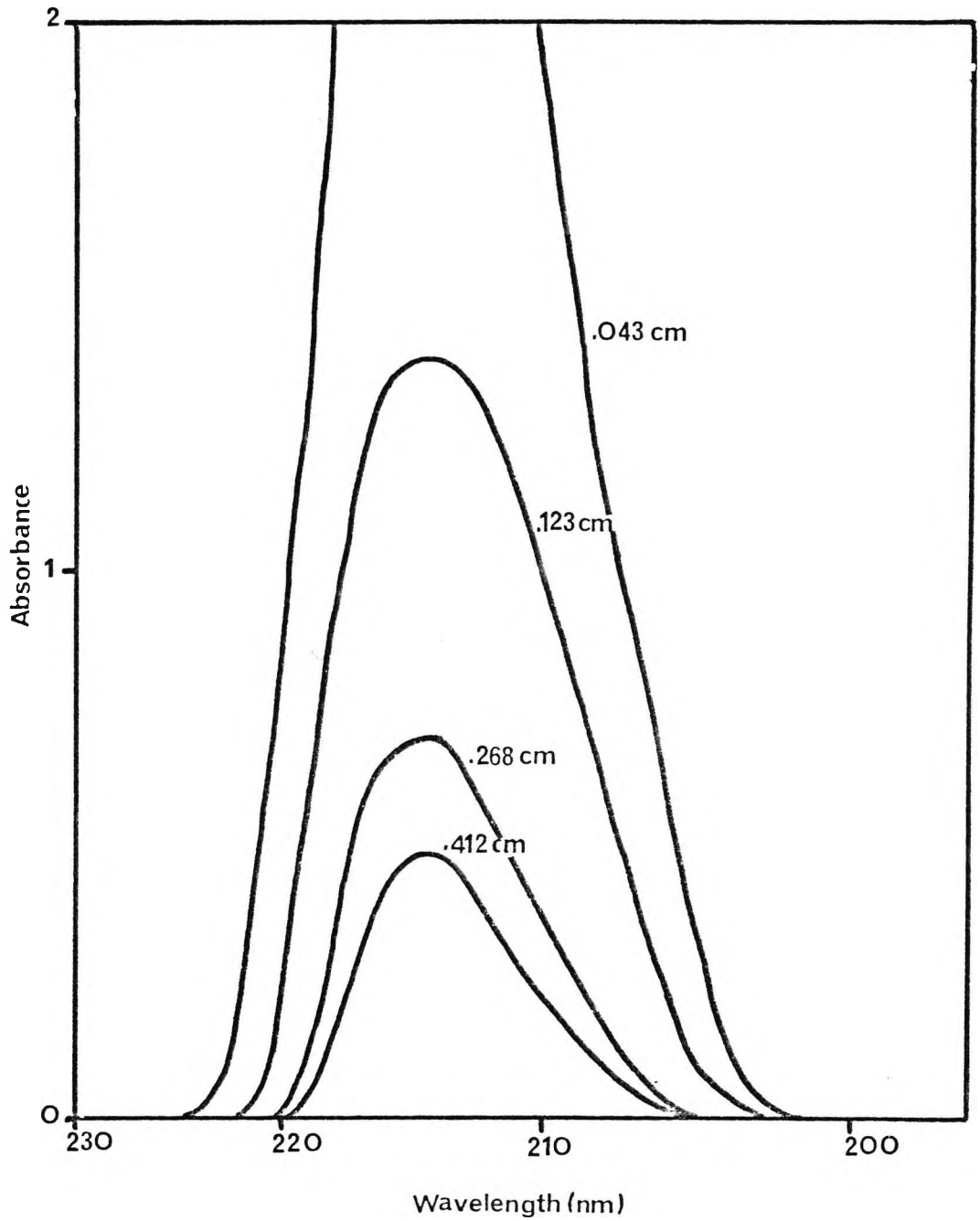

Figure 3.10 The variation of the Hg^{2+} band in $KF:Hg^{2+}$ due to sectioning.The distance x on each curve refers to the total depth removed

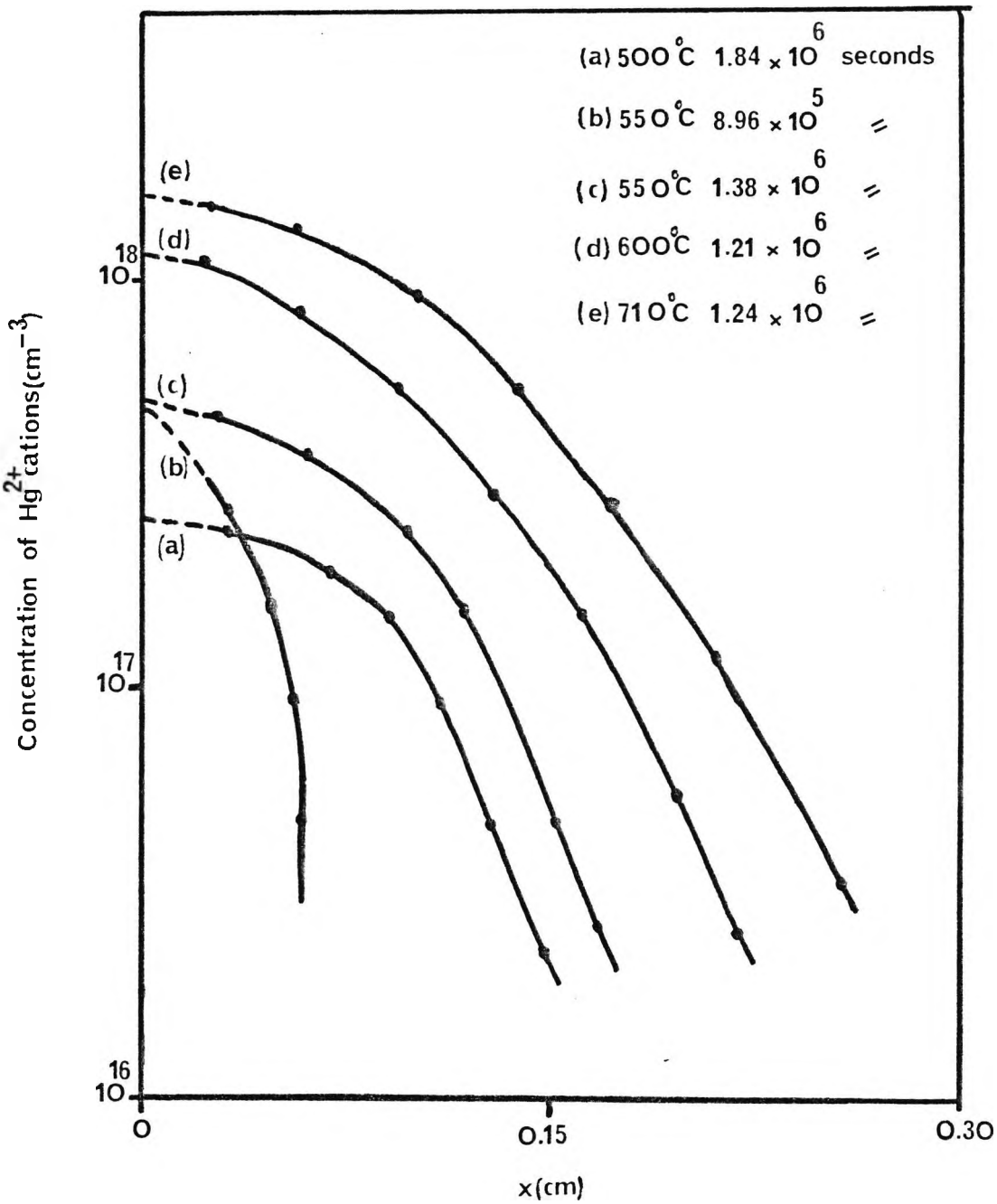

Figure 3.11 Penetration profiles for the diffusion of Hg^{2+} cations in KF

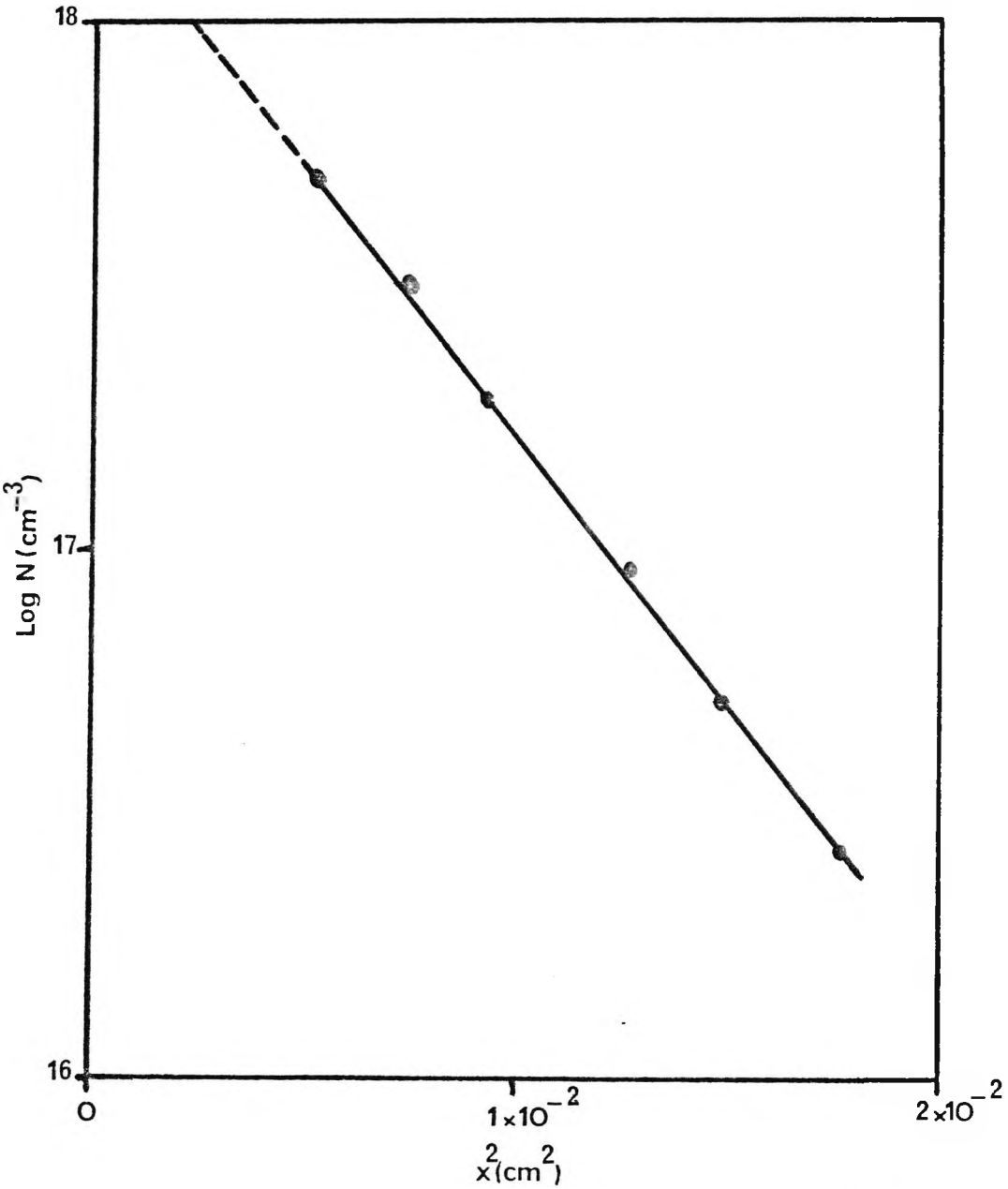

Figure 3.12 Log N versus x^2 plot for KF:Hg^{2+} (600°C, 2.07×10^6 seconds)

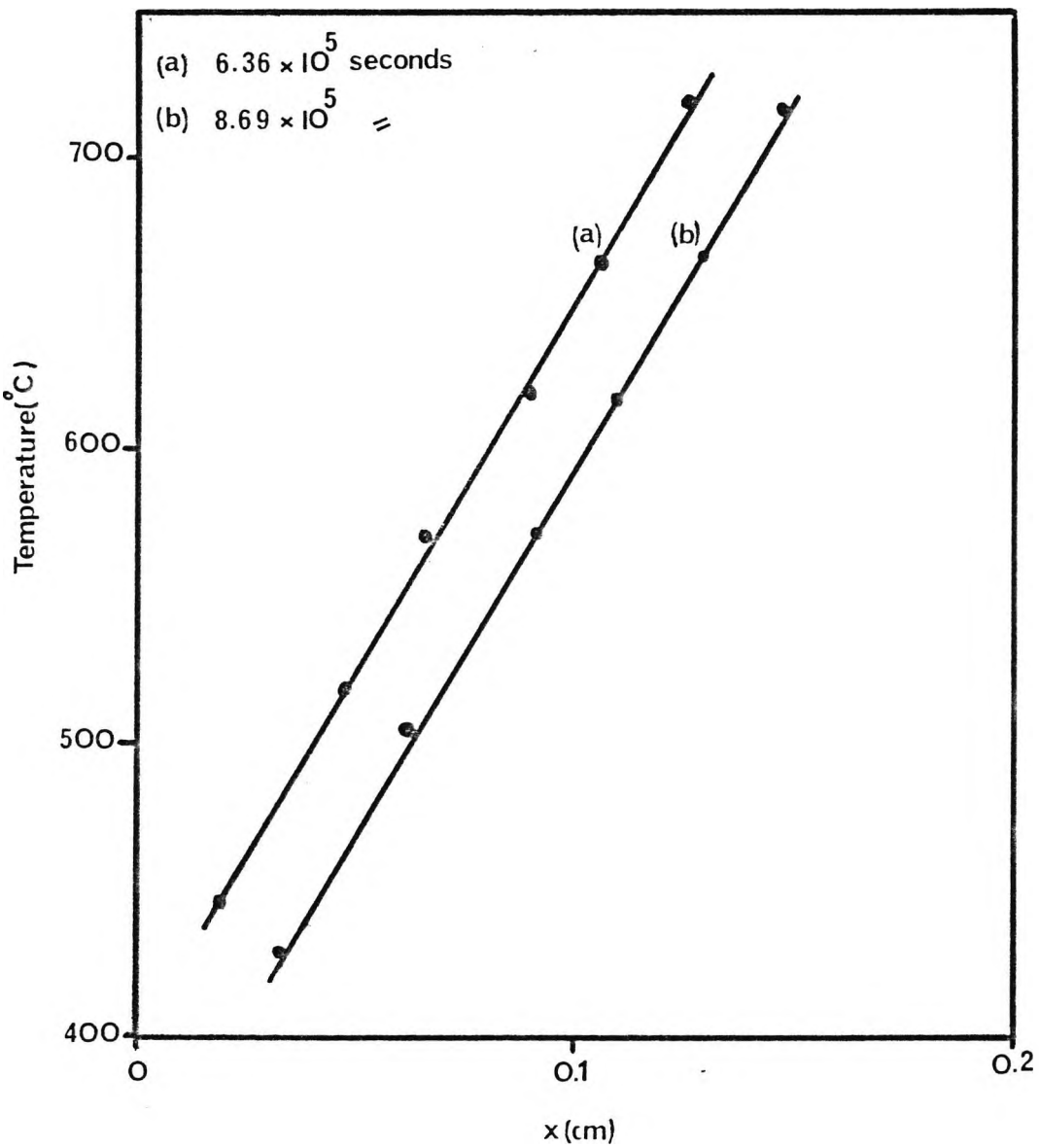

Figure 3.13 Depth of penetration x of Hg^{2+} cations in KF as a function of diffusion temperature for two diffusion times

second equation for one-dimensional diffusion from an infinite reservoir of mercury vapour has the form of a complementary error-function (Tuck 1984).

$$N = N_0 \operatorname{erfc}\left[\frac{x}{(4Dt)^{1/2}}\right] \qquad (3.3)$$

The initial conditions which have been used to obtain equation (3.3.) are

$$N=0 \text{ for } x \geq 0 \text{ at } t=0$$

and the boundary conditions are

$$N = N_0 \text{ for } x = 0 \text{ at } t \geq 0$$

If $y = \dfrac{x}{(4Dt)^{1/2}}$, then

$$\operatorname{erf} y \sim 1 - \frac{e^{-y^2}}{y\sqrt{\pi}}\left[1 - \frac{1}{2y^2} + \frac{1 \times 3}{2^2 y^4} + \cdots\right]$$

$$\sim 1 - \frac{e^{-y^2}}{y\sqrt{\pi}} \text{ for } \frac{1}{2y^2} \ll 1$$

Hence

$$\operatorname{erfc} y = 1 - \operatorname{erf} y$$

$$\sim \frac{e^{-y^2}}{y\sqrt{\pi}} \quad \text{for large } y$$

Equation (3.3) becomes

$$N \sim N_0 \frac{e^{-y^2}}{y\sqrt{\pi}}$$

or

$$\log_e N = \log_e N_0 - y^2 - \log_e y\sqrt{\pi}$$

or

$$\log_e N = \left[\log_e N_0 - \log_e x\left(\frac{\pi}{4Dt}\right)^{1/2}\right] - \frac{x^2}{4Dt} \qquad (3.4)$$

Equation (3.4) is valid for

$$\frac{1}{2y^2} \ll 1; \quad x^2 \gg 2Dt \quad \text{or} \quad t \ll \frac{x^2}{2D} \qquad (3.5)$$

May plot $\log_e N$ versus x^2 to obtain straight line of slope $-\frac{1}{4Dt}$ if $\log_e x \left(\frac{\pi}{4Dt}\right)^{1/2}$ is negligible over the range used and if condition(3.5)holds. The values of D for the diffusion of divalent mercury cations in alkali halides were then evaluated from the plot of $\log_e N$ as a function of x^2. Such plots yield straight lines as is shown in figure 3.12 for the case of mercury-doped KF. Using the sectioning technique, as described in the previous section, the value of D was calculated at various temperatures. The dependence of D on diffusion temperature is given by Jost (1952) as

$$D = D_0 \exp\left(-\frac{E_d}{kT}\right) \qquad (3.6)$$

where E_d is an activation energy for Hg^{2+} cation diffusion and D_o is a constant.

The diffusion coefficients of Hg^{2+} cations in KF specimens were measured in the temperature range 540°C to 800°C. The values of D varied in this range between 1.2×10^{-10} cm^2 sec^{-1} and 2.9×10^{-8} cm^2 sec^{-1}. Figure 3.14 shows a typical plot of log D against $\frac{1}{T}$ for a mercury-doped alkali halide. The diffusion equation which is given by figure 3.14 for KF specimen can be expressed as

$$D = 2.68 \times 10^{-3} \exp\left(-\frac{0.993}{kT}\right) cm^2 sec^{-1} \qquad (3.7)$$

where the value 0.993 eV is the activation energy of Hg^{2+} cation diffusion in KF. Table 3.2 lists the activation energy for the diffusion of Hg^{2+} in KF in comparison with values of E_d for other divalent cations in NaCl and KCl.

4. Other experimental measurements

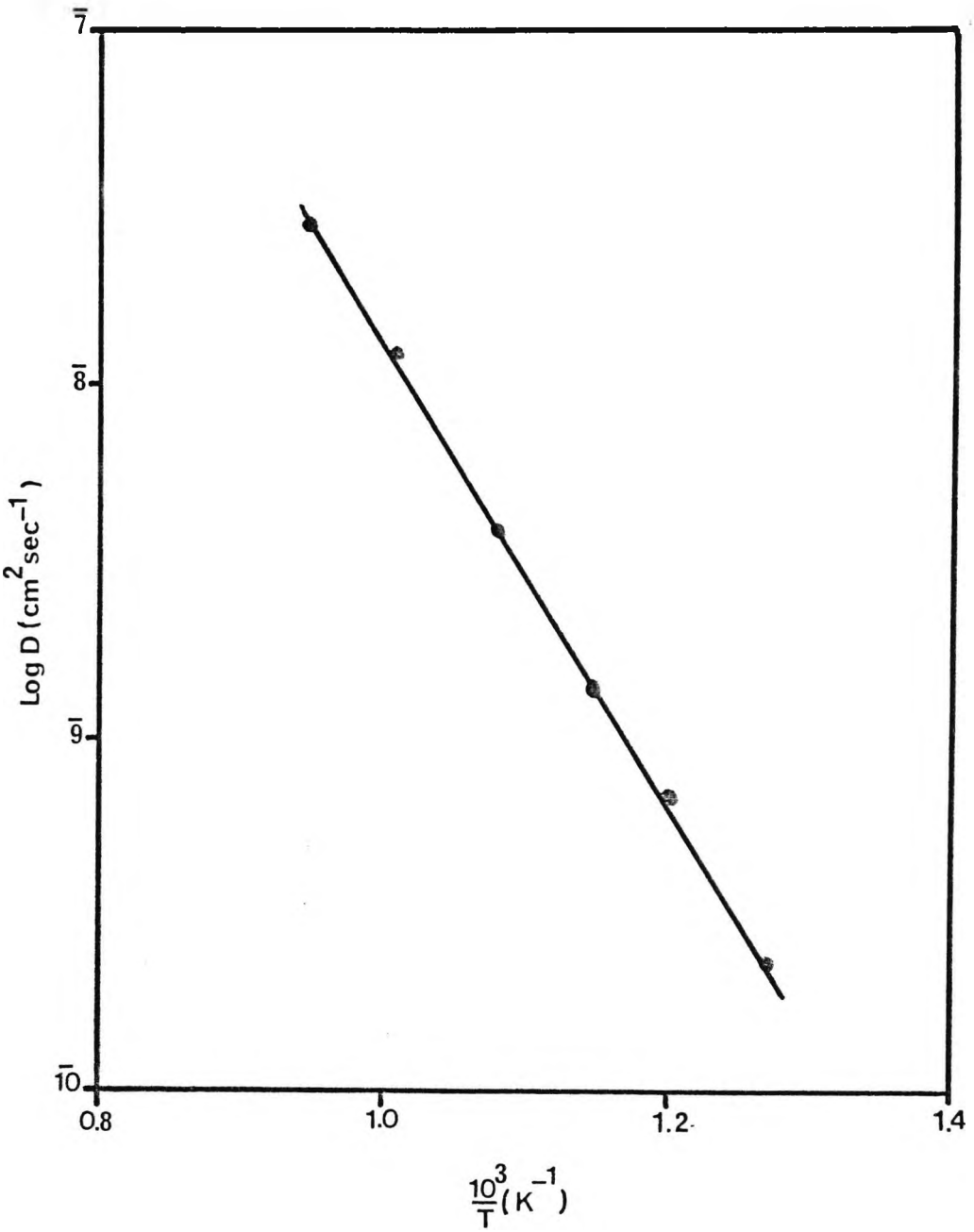

Figure 3.14 Log D as a function of diffusion temperature for the diffusion of Hg^{2+} cations in KF

Table 3.2. The activation energy E_d for diffusion of various divalent cations in KCl , KF and Na Cl. The ionic radii were taken from Pauling (1980).

	Ionic radii (nm)	E_d (eV)	Reference
Zn^{2+}(NaCl)	0.083	0.490	1
Mn^{2+}(NaCl)	0.091	0.710	2
Cd^{2+}(NaCl)	0.097	0.857	3
Ca^{2+}(NaCl)	0.099	0.960	4
Hg^{2+}(KF)	0.110	0.993	This work
Pb^{2+} (KCl)	0.120	1.180	5

(1) Chemla (1956)

(2) Lur'e et al (1963)

(3) Krause and Fredericks (1971)

(4) Murin et al (1962)

(5) Keneshea and Fredericks (1964)

4.1. Transference experiments

Two nominally-pure KCl specimens and one mercury-doped KCl specimen were arranged and treated as described in section 7.1 of chapter 2. Figure 3.15 shows the results obtained from an experiment carried out at 665°C using a $\frac{V}{d}$ value of 30 V cm^{-1}. The electrolytic diffusion time was 1.3 x 10^6 seconds. Curve (a) shows the distribution of Hg^{2+} cations in the mercury-doped specimen. Curve (b) shows the distribution of Hg^{2+} cations in this specimen as well as in the specimen near to the cathode. No Hg^{2+} absorption was observed in the specimen near to the anode. The two dashed vertical lines are used in figure 3.15 to show the arrangement of the three specimens during the experiment. The dashed lines linking curve (b) in the two specimens in the middle and near to the cathode were found by extrapolation as described in section 3.1 of this chapter. It can be seen clearly from figure 3.15 that Hg^{2+} cations diffuse electrolytically towards the cathode. This might indicate that these cations exist at this temperature largely as free positively charged ions.

The sectioning technique was used to determine the distribution of Hg^{2+} cations along the length of each specimen using the spectrophotometric data as described in section 3.1 of this chapter. The diffusion of divalent cations in alkali halide specimens located in a constant electric field E is described by the following equation given by Chemla (1956)

$$\frac{\partial N}{\partial t} = uE\frac{\partial N}{\partial x} + D\frac{\partial^2 N}{\partial x^2} \qquad (3.8)$$

where u is the mobility of the divalent cation and N is the concentration at x and t. The solution of equation (3.8) for an undirectional diffusion similar to the present problem is (Crank 1956, Lidiard 1957)

$$N = \frac{N_0}{(\pi Dt)^{\frac{1}{2}}} \exp\left[-\frac{(x - uEt)^2}{4Dt}\right] \qquad (3.9)$$

where N_0 is the quantity of the divalent cations in unit area of the specimen surface at t = 0. Thus it is possible to determine u by measuring the displacement of the maximum of the diffusion profile x in the direction of the electric field E using the relation

$$u = \frac{x}{Et} \qquad (3.10)$$

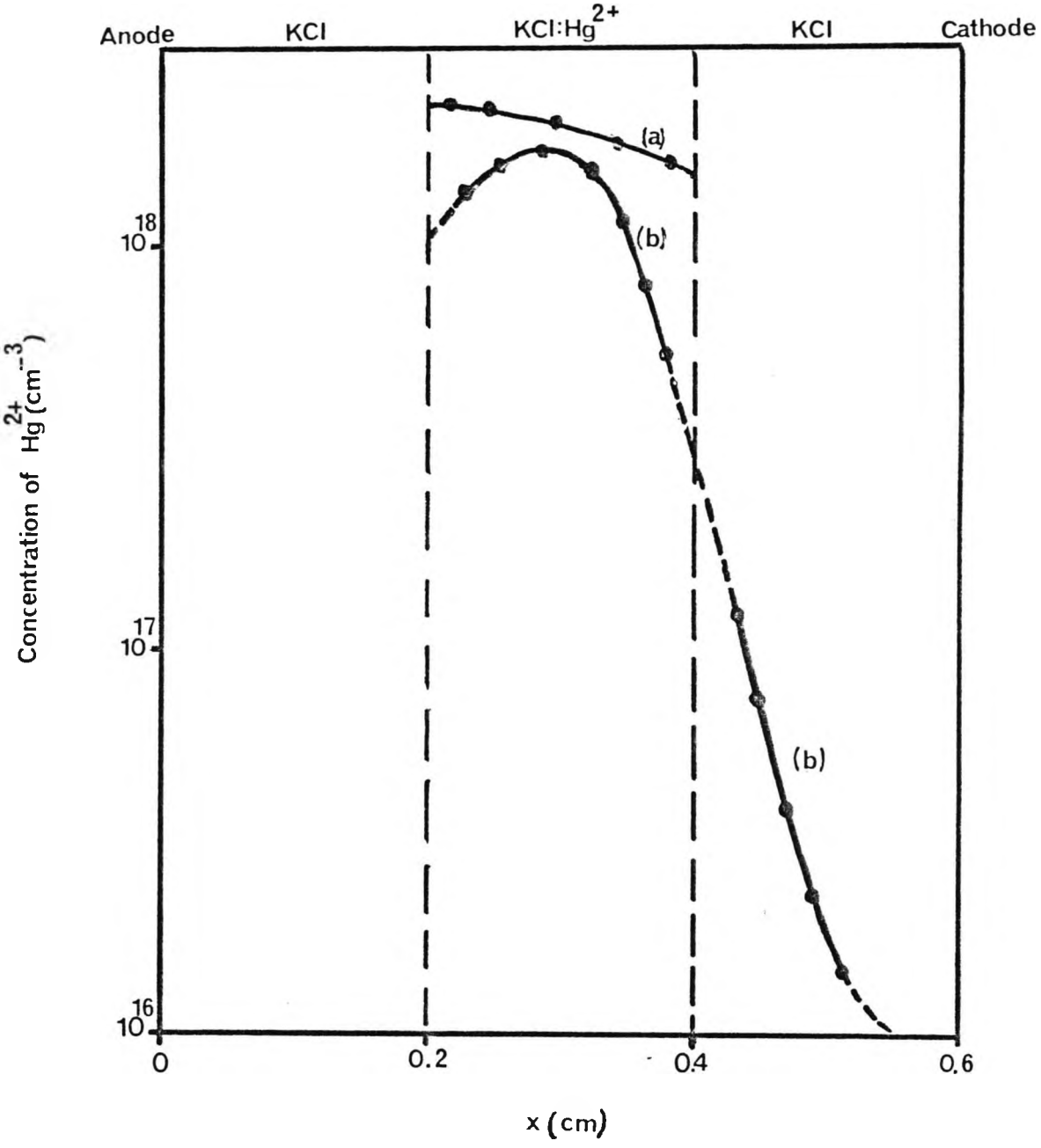

Figure 3.15 Distribution of Hg^{2+} cations (a) before the electrolytic diffusion and (b) after the experiment

where t is the diffusion time. It may be estimated from figure 3.15 that x = 0.1 cm during the electrolytic time t = 1.3 x 10^6 seconds. Assuming that the potential gradient is uniform over the diffusion range, the calculated value of Hg^{2+} cation mobility is then 2.5 x 10^{-9} cm^2 sec^{-1} V^{-1} .

4.2 Thermal measurements

The temperature variation of the absorption spectra of mercury-doped alkali halides was investigated by optical measurements carried out at room and liquid nitrogen temperatures. Figure 3.16 shows the spectra of a mercury-doped LiF specimen. Curve (a) is the spectrum immediately after preparation. Curve (b) is the spectrum of the same specimen after electrolytic coloration and subsequent bleaching of the F-centres by reversing the polarity of the electrodes. These two spectra were measured at room temperature. Curve (c) is the spectrum of a LiF specimen taken from the same mercury-doped block as that of curve (a) but measured at liquid nitrogen temperature. The three bands are identified as Hg^{2+} , Hg^{+} and Hg^{o} in order of increasing wavelength. The peak position of these bands as well as those of mercury-doped NaF are reported in table 3.1. These values are referred to with asterisks. Figure 3.16 shows that the Hg^{2+} and Hg^{+} bands are the most affected by the low temperature measurement. The results also support the assumption that the broad asymmetric feature of the 210 nm band in mercury-doped LiF and NaF is due to overlapping in this region of two bands.

After several weeks at room temperature, the Hg^{2+} band in a KBr specimen doped with more than 4 x 10^{18} cm^{-3} of Hg^{2+} cations weakened and the $(Hg\text{-}Hg)^{2+}$ band appeared to form as a result. Heating a mercury-doped NaCl specimen at 660°C for various durations (up to a total of 10 days) showed that all the absorption bands start to decay. This decay was accompanied by the growth of a new band at 425 nm. The peak position of this band shifts continuously to longer wavelengths on prolonged heating. The 425 nm band reached a maximum, then started to decrease in intensity. Similar measurements were made using a mercury-doped KCl specimen. The results suggest that mercury absorption bands are less stable in sodium halides than in potassium halides. The same 425 nm band was observed in the case of KCl specimen after fourteen days of thermal annealing at 660°C.

5. Conclusions

It has been shown that various mercury centres can be introduced into alkali halides by the vapour diffusion method. Thermal treatment as well as electrolytic coloration is found to produce new mercury centres by changing the valence of these centres. Divalent mercury cations Hg^{2+} , single mercury cations Hg^{+} and neutral mercury atoms Hg^{o} are produced

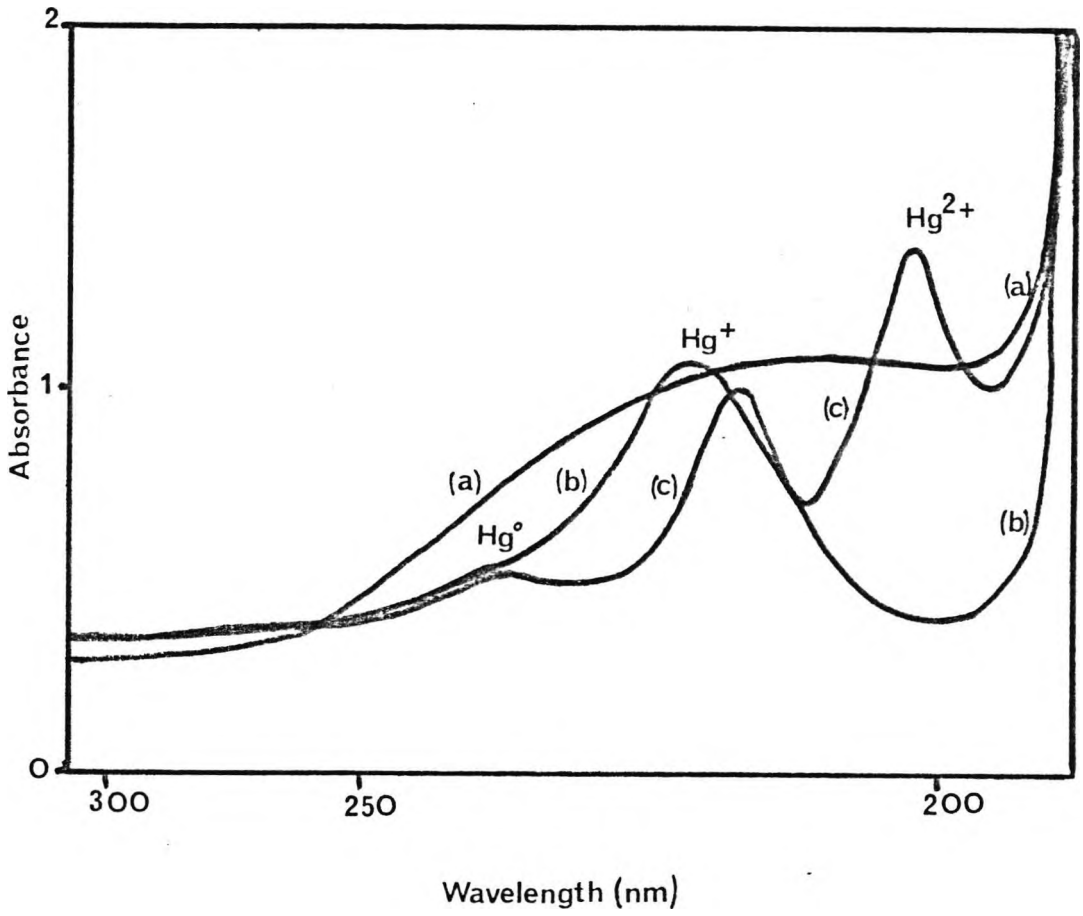

Figure 3.16 Spectra of mercury-doped LiF (a) immediately after preparation, (b) after electrolytic coloration/de-coloration and (c) measured at liquid nitrogen temperature after preparation

initially on quenching the specimen from the diffusion temperature to room temperature. Slow cooling of mercury-doped specimens leads to the formation of aggregates of the single mercury cation to give $(Hg\text{-}Hg)^{2+}$. Electrolytic coloration of mercury doped alkali halides, while bleaching the Hg^{2+} centres, leads to the formation of another new centre which is tentatively designated $(Hg - Hg)^{o}$. The mercury diffusion process differs from the process of additive coloration in so far as no absorption band corresponding to an F band is observed. In all the mercury-doped alkali halides (except KI), mercury centres cause ultra-violet absorption below the fundamental absorption edge of the nominally-pure host specimen. These bands are situated in the spectral range 210 nm to 372 nm.

The experimental results show that mercury is initially present as randomly distributed divalent cations provided that the diffusion temperature is sufficiently high and the diffusion time is sufficiently long. As the concentration of Hg^{2+} centres increases, single_mercury centres and neutral mercury centres are formed in the specimen. It is expected that at higher Hg^{2+} concentrations, stable $(Hg - Hg)^{2+}$ aggregate centres can be formed when two single Hg^{+} centres combine.

The diffusion coefficient of divalent mercury cations within alkali halides has been measured over a wide range of temperature. The activation energy of diffusion is reported for mercury-doped KF. A comparison of the activation energy of diffusion for other divalent cations using the ionic radii as criteria shows that the value obtained in this work for mercury diffusion in KF is within the expected range. No work has been reported in the literature which can provide a value of this kind for mercury diffusion. Also, the mobility of divalent cations in KCl is measured in this work using the electrolytic method of mercury diffusion.

Thermal measurements have shown the tendency to form mercury colloid centres in NaCl more than that in KCl. This might be due to the lattice distortion which such formation introduces. Thus, colloid formation occurs readily in NaCl where the Hg^{2+} ion (ionic radius a = 0.11 nm) is larger than the Na^{+} (a = 0.98 nm)ion, but not in KCl where the Hg^{2+} ion is smaller than K^{+} (a = 0.133 nm) ion.

Ionic conductivity measurements have shown clearly that excess cations are produced as the primarily effect of doping with mercury. Plots of log σ T versus $\frac{1}{T}$ were obtained. They are essentially similar to those obtained for other divalent cations - doped alkali halides (Lidiard 1957). In the temperature range used in the ionic conductivity measurements two regions were observed in the log σ T versus $\frac{1}{T}$ plot. As the Hg^{2+} concentration increases the cation vacancy migration (extrinsic) region extends to temperatures well within the Schottky defect formation region in otherwise nominally-pure alkali halides. The values of the energy of cation vacancy migration obtained from ionic conductivity measurements are in good agreement with those reported in the literature (Chandra and Rolfe 1970)

An experimental investigation of the influence of the Hg^{2+} centre on the colourability of alkali halides using electrolytic coloration has shown that doping with divalent mercury enhances the F absorption as well as promoting the coloration of the alkali fluorides. This effect is linked with the excess cation vacancies produced since the observed lowering of the coloration starting temperature T_c can only happen (according to the results of chapter 4) as a result of an enhanced ionic process involving the migration of cation vacancies. The increase in the coloration rate in the electron injection stage is also seen in this perspective. The fact that mercury-doped specimens show no Hg^{2+} absorption after the two-stage process of electrolytic coloration and de-coloration, and behave like nominally-pure alkali halides, supports the conclusion that excess cation vacancy migration introduced by mercury doping enhances the coloration.

Experimental results obtained from diffusion measurements and the thermal and electrolytic treatment as well as the results of ionic conductivity were used to identify the various mercury centres. However, the absorption bands which are assigned tentatively as $(Hg - Hg)^o$ might also be due to substitutional Hg^- centres, since these centres can only be formed by the electrolytic process of coloration and de-coloration. Electrolytic coloration of alkali halides containing Pb^{2+} ,Sn^{2+} , and Ge^{2+} ,have been found to transform the divalent cation centres to substitutional Pb^- , Sn^- and Ge^- centres (Topa and Velicesucu 1969). The complete absence of the Hg^{2+} absorption bands after de-colouration supports the conclusion that electrolytic coloration reduces the Hg^{2+} centres to Hg^+ , Hg^o and Hg^- centres.

6. References

Ben-Dor L, Zolotov S and Glasner A 1966 Phys.St.Solid 18 593

Burstein E, Oberly J J, Henvis B W 1951 Phys. Rev. 81 459

Chandra S and Rolfe J 1970 Can.J.Phys. 48 397

Chemla M 1956 Ann.Chim.Phys., 959 cited by Lidiard 1957

Crank J 1956, The Mathematics of Diffusion -Clarendon Press

Deacon G B 1963 Rev. Pure Apple. Chem. 13 189

Gilman J J and Johnston W G J 1958 J. Apple. Phys. 29 877

Jost W 1952 Diffusion in Solids, Liquid and Gases-Academic Press

Keneshea F J and Fredericks W J 1964 J. Chem. Phys. 42 3271

Kleeman W 1968 Z.Phys. 214 285

Kfause J L and Federicks W J 1971 J.Phys.Chem.Solids 32 2673

Lidiard A B 1957 Handbuch der Phys. 20 246

Lur'e BG, Murin A N and Brigevich R F 1963 Sov. Phys-Solid St. 4 1432

Moore C E 1949 Atomic Energy Levels (Washington: National Bureau of Standards)

Murin a N , Bonasevich S N and Grushko Yu S 1962 Sov. Phys-Solid St. 3. 1762

Pauling L 1980 The Nature of the Chemical Bond-Cornell University Press

Santaran C and Winans J G 1966 Can.J.Phys.44 1517

Siederdissen J H Z and Fischer F 1971 Phys. St.Solid (b) 48 215

Tamai T 1961 J.Phys.Soc. Japan 16 2463

Topa V and Velicescu B 1968 Inter.Symp. on Colour Centres Rome 1969 Phys.St.Solid 33 K29

Tsuboi T 1970 J.Phys. Soc. Japan 29 1303
1976 Can. J.Phys. 54 1772 and 2418

Tuck T 1984 Introduction to Diffusion in Semiconductors - Peter Peregrinus Ltd.

Velice scu B and Topa V 1973 Phys.St. Solid (b) 55 793

CHAPTER FOUR

Electrolytic Coloration of Nominally-Pure Alkali Halides

1. Production of colour centres

1.1 Temperature

On heating alkali halide specimens from room temperature, the coloration starts at a fixed temperature which is many hundred degrees below the respective melting point. Figure 4.1 shows the variation of electrolytic current as a function of specimen temperature for three potassium halides during a complete electrolytic coloration experiment using the constant-voltage method. The current-temperature behaviour shown in the figure is typical of a specimen undergoing electrolytic coloration using the increasing-temperature method of heating. One obvious feature of the figure is that all curves have a similar structure which indicates that all three specimens are subjected to the same process. Electrolytic coloration of sodium halides gives the same current-temperature structure. Other experiments which will be described show that the thermal and mechanical treatment of alkali halide specimens during their preparation and coloration has no effect on the basic structure of the current-temperature curve. Electrolytic coloration carried out in air, in vacuo (10^{-5} torr) or in a nitrogen atmosphere give the same results. Furthermore, experiments which were carried out by maintaining the alkali halide specimens in a steady electric field under conditions which would exclude coloration showed no such current-temperature curve. Throughout this work V/d is taken as the measure of electric field E.

The main feature of the curves of figure 4.1 is that the current rises at the outset of the electrolytic coloration experiment until it reaches a certain temperature, when there is an abrupt increase in the current. The observed fact is that, at this temperature, which is referred to as T_c in figure 4.1 and elsewhere in this work, the abrupt increase in the current occurs simultaneously with the start of the coloration at the pointed cathode. The migration of the colour through the specimen towards the flat anode takes place between point T_c and point T_A . It was observed that, at T_A , the colour reached the anode and started to intensify. Point T_A is not shown for KCl in Figure 4.1 because it lies beyond the temperature range of the figure. When the electrolytic coloration was carried out using the constant-voltage method, a breakdown took place at point T_A when the field exceeded 120 V cm^{-1} and a channel was created between the two electrodes. The

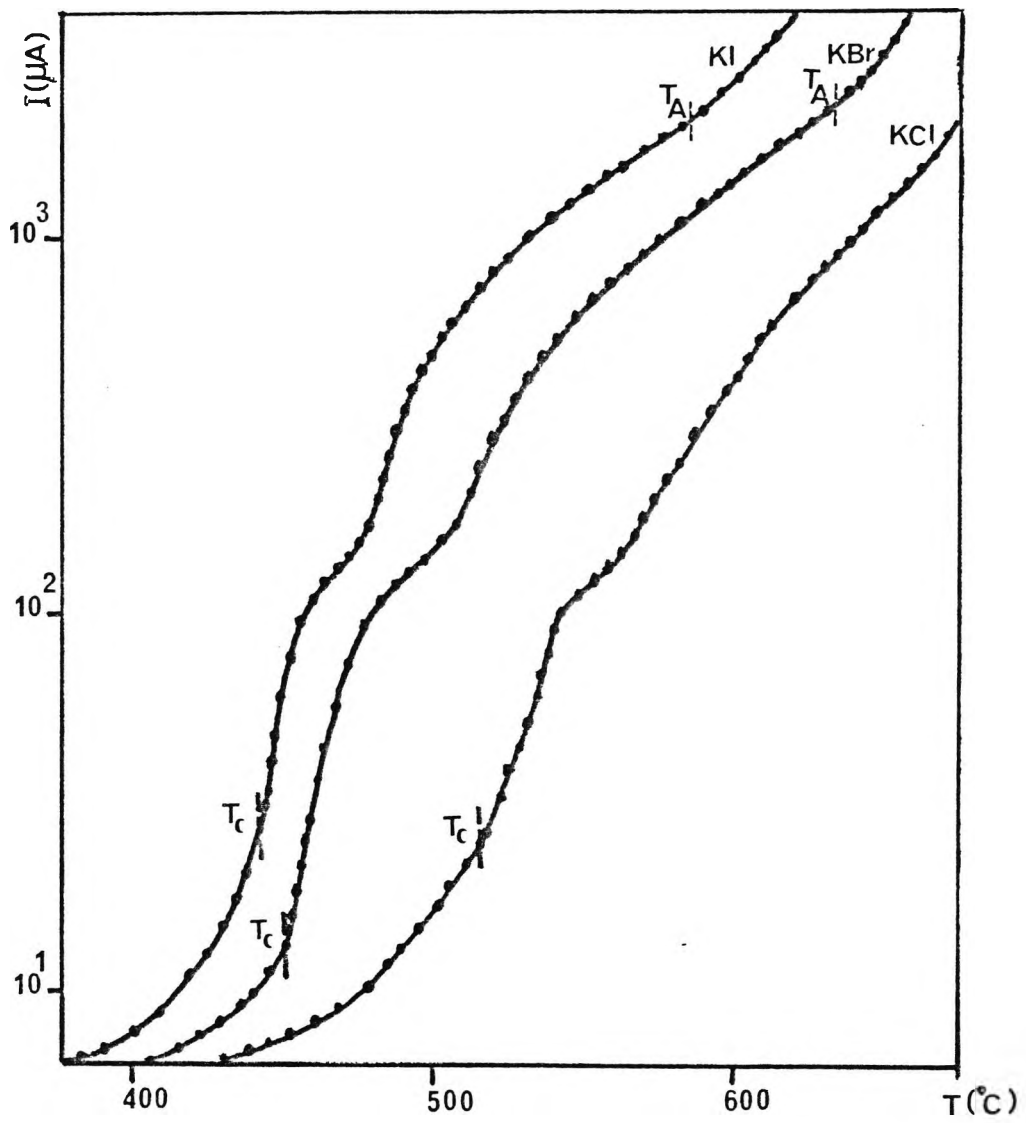

Figure 4.1 Current – temperature relation of a complete electrolytic coloration experiment

same phenomenon was observed when the electrolytic coloration experiments were carried out using the constant-current method with the value of current exceeding 2A.

The bending which is shown by the current-temperature curves of figure 4.1 lasted for a few seconds. This fact may be related to the elimination process (diffusion and evaporation of cations) which plays an important role in the formation of the new alkali metal cathode as has been suggested by Heiland (1950). The formation of this cathode leads to electron injection which causes the simultaneous increase of the current and the start of the coloration at the pointed cathode.

Figure 4.1 also shows that at any temperature, the current is higher for KI than for KBr which is in turn higher than for KCl. It is clear also that the abrupt current increase after point T_c is faster for KI than for KBr and KCl respectively. It was observed from the electrolytic coloration experiments with KI, KCl and NaBr using the constant-voltage method that, as the field increased above 100 V cm^{-1}, the current at T_c declined accordingly. When the field exceeded 1200 V cm^{-1} the resultant absorption spectra showed the formation of colloid centres. At higher fields a discharge took place between the two electrodes and only the surface of the specimen near to the cathode was coloured with colloid of different sizes according to the coloration temperature. The coloration seemed to take place along certain lines on the surface and to penetrate the part of the specimen next to the surface along these lines while leaving the bulk of the specimen clear of any coloration. The colloid centres also seemed to be produced by damage caused by the discharge along the dislocation lines created by this damage. The production of colloidal coloration in this way can take place irrespective of the coloration temperature provided that the field is greater than 1200 V cm^{-1}. The current temperature curve obtained from such an experiment showed no similarity with the curves of figure 4.1. However, it was possible to colour KI, KBr and KCl with fields as low as 30 V cm^{-1}, contrary to the value of 70 V cm^{-1} reported by Paramo and Sanches (1971). This observation may be related to the difference between the material and the geometrical features of the electrode used in their work and those used in the present work. Since Paramo and Sanchez (1971) used Harshaw specimens, the only difference is that they used a pointed cathode made from stainless-steel and not platinum as is the case here.

Figure 4.2 shows the relation between the coloration starting temperatures T_c of various potassium halides and their activation energies E_s. The term $\frac{a}{\alpha}$ is the ratio of the lattice constant to the ionic radius of the anions. It is clear from figure 4.2 that, when the coloration conditions are identical for the various alkali halides, T_c is a characteristic property of the particular salt. The value of T_c increases in the series from

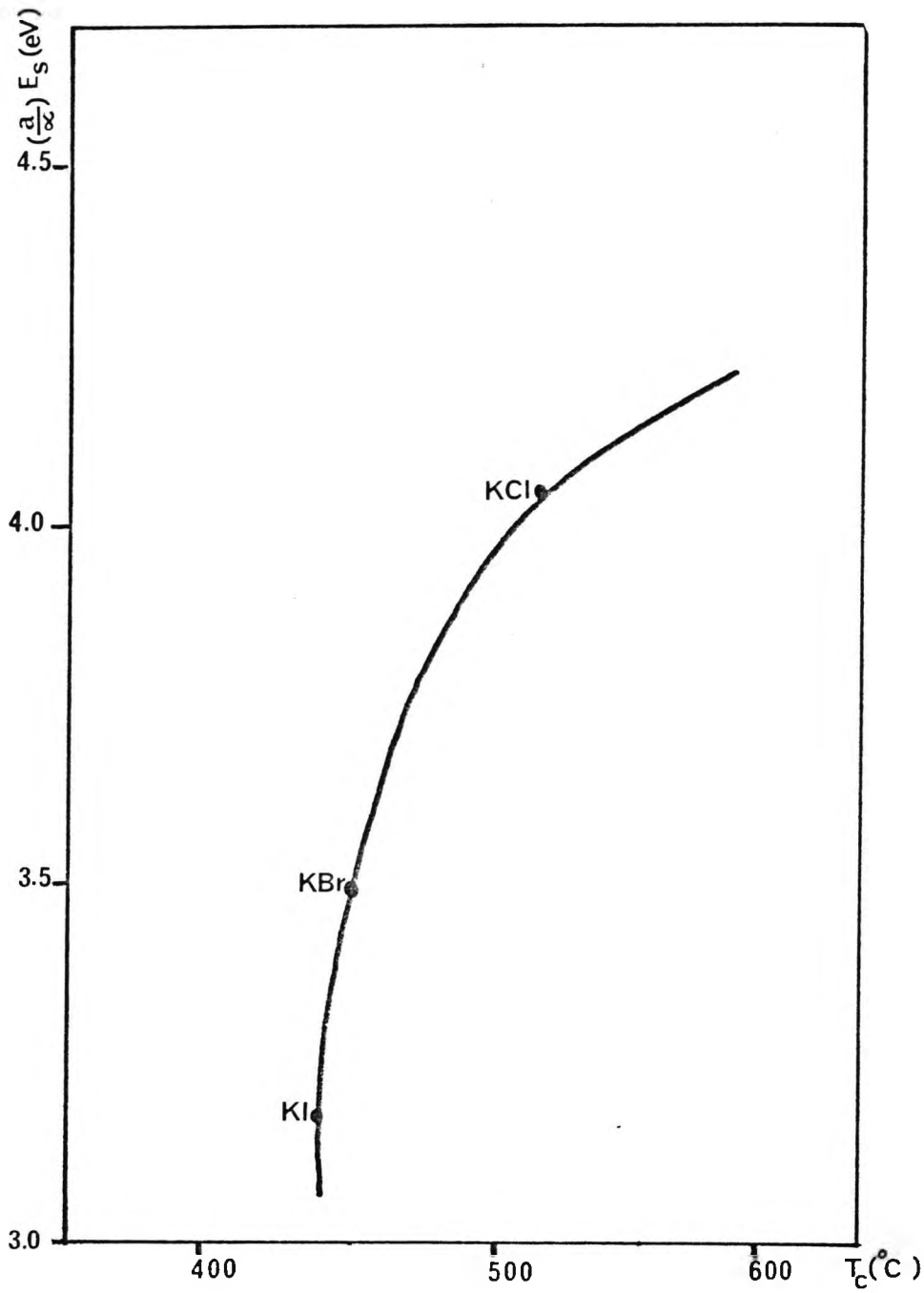

Figure 4.2 The dependence of the coloration starting temperature T_c on the activation energy E_s

the iodide to the chloride. Similar experiments with sodium halides produced similar curves but with higher values of T_c.

Electrolytic coloration experiments performed by heating the specimens to a pre-determined temperature, which is then kept constant whilst a constant current is passed through the specimens, showed that a finite time elapsed before the coloration started. Figure 4.3 shows the variation of this time with the coloration temperature T for KCl specimens. It is evident from the figure that the time which elapses before the start of the coloration becomes shorter as the difference between the coloration temperature T and T_c increases. This is to be expected if a new alkali metal cathode has to be formed by an ionic process involving the accumulation and elimination processes as suggested by Heiland (1950)

Electrolytic coloration experiments were carried out using various values at constant current to show the effect of the current and the coloration temperature on the production of the various colour centres. Figure 4.4 shows that, for each value of constant current, the concentration of F-centres increases with the coloration temperature until it reaches a characteristic temperature when the F-centre concentration becomes saturated. At higher values of the constant current the F-centre concentration increases rapidly as the coloration temperature is increased until it again reaches a saturation level. The experimental results of figure 4.4 are taken from the electrolytic coloration experiments carried out at constant coloration temperature using identical sizes of KCl specimens and coloration time. When the experiments were carried out at a coloration temperature within the intrinsic region of the ionic conductivity of the specimen, M– as well as other F–aggregate centres were produced as the coloration time was increased. The production of these colour centres is also dependent on the magnitude of the current as discussed in the following sections.

1.2 Current flow

Figure 4.5 shows the structure of the current density-time relationship during the complete procedure of a typical electrolytic coloration experiment with NaCl at various coloration temperatures. It is evident from the figure that each curve has a three-part structure while a fourth part appears to be developing as the coloration temperature approaches the melting point.

It is clear from figure 4.5 that the first part of the current-time relationship ends at point T_c which is shown in figure 4 1 for the other alkali halides. This part, however, becomes shorter as the coloration temperature increases, as is shown in figure 4.3.

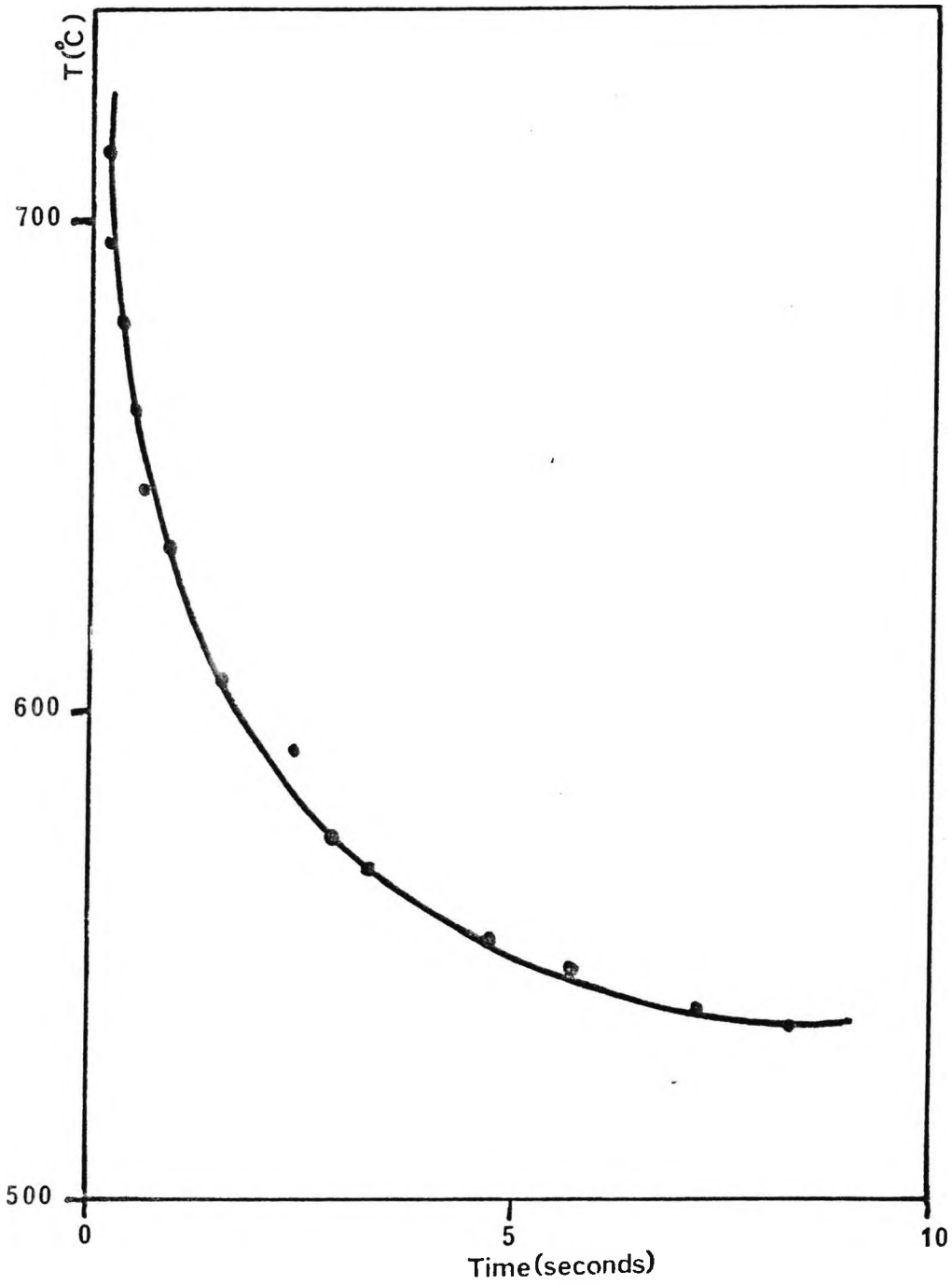

Figure 4.3 The time elapsed before the start of coloration as a function of the coloration temperature of KCl specimens

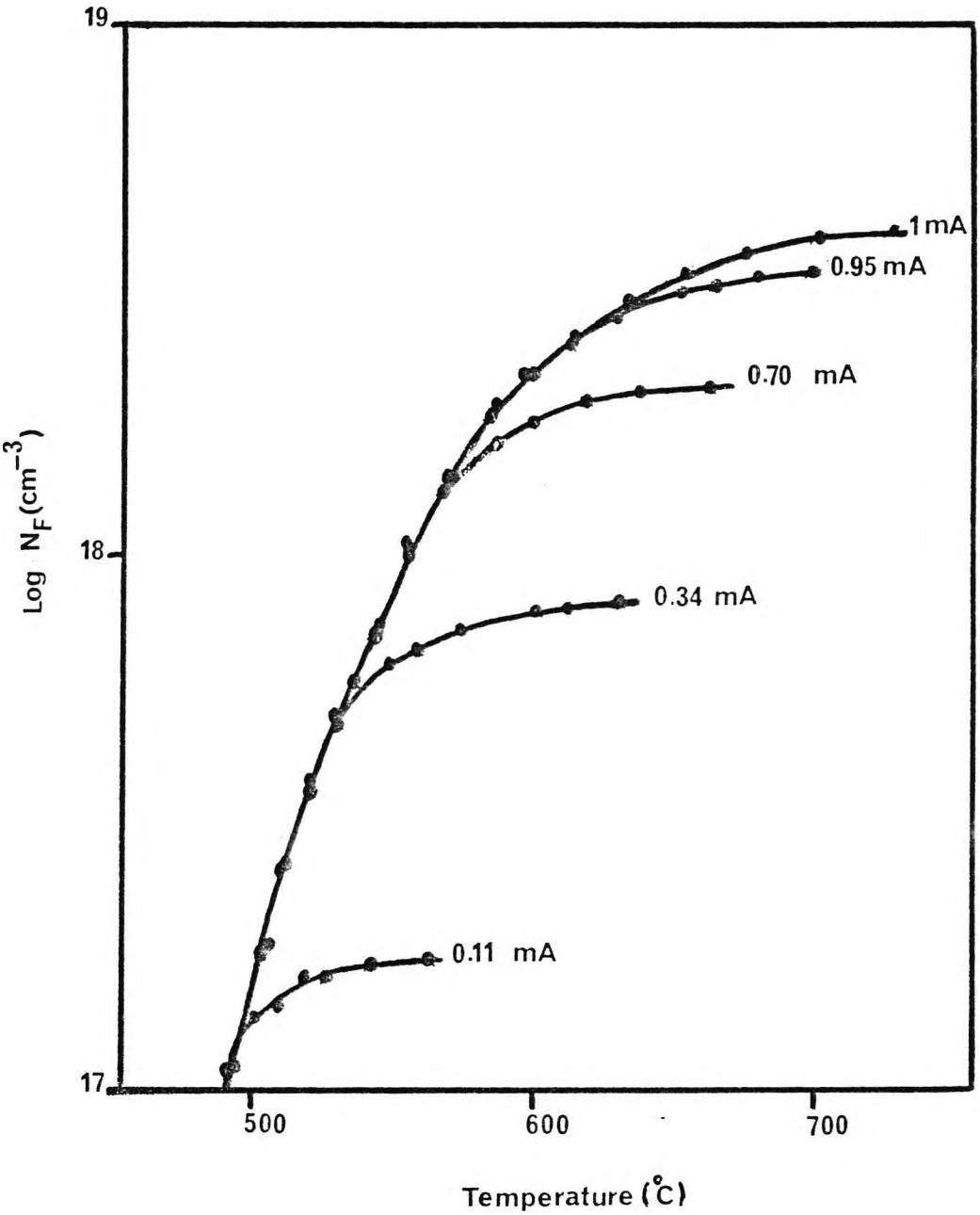

Figure 4.4 Production of the F-centres in KCl as a function of the coloration temperature

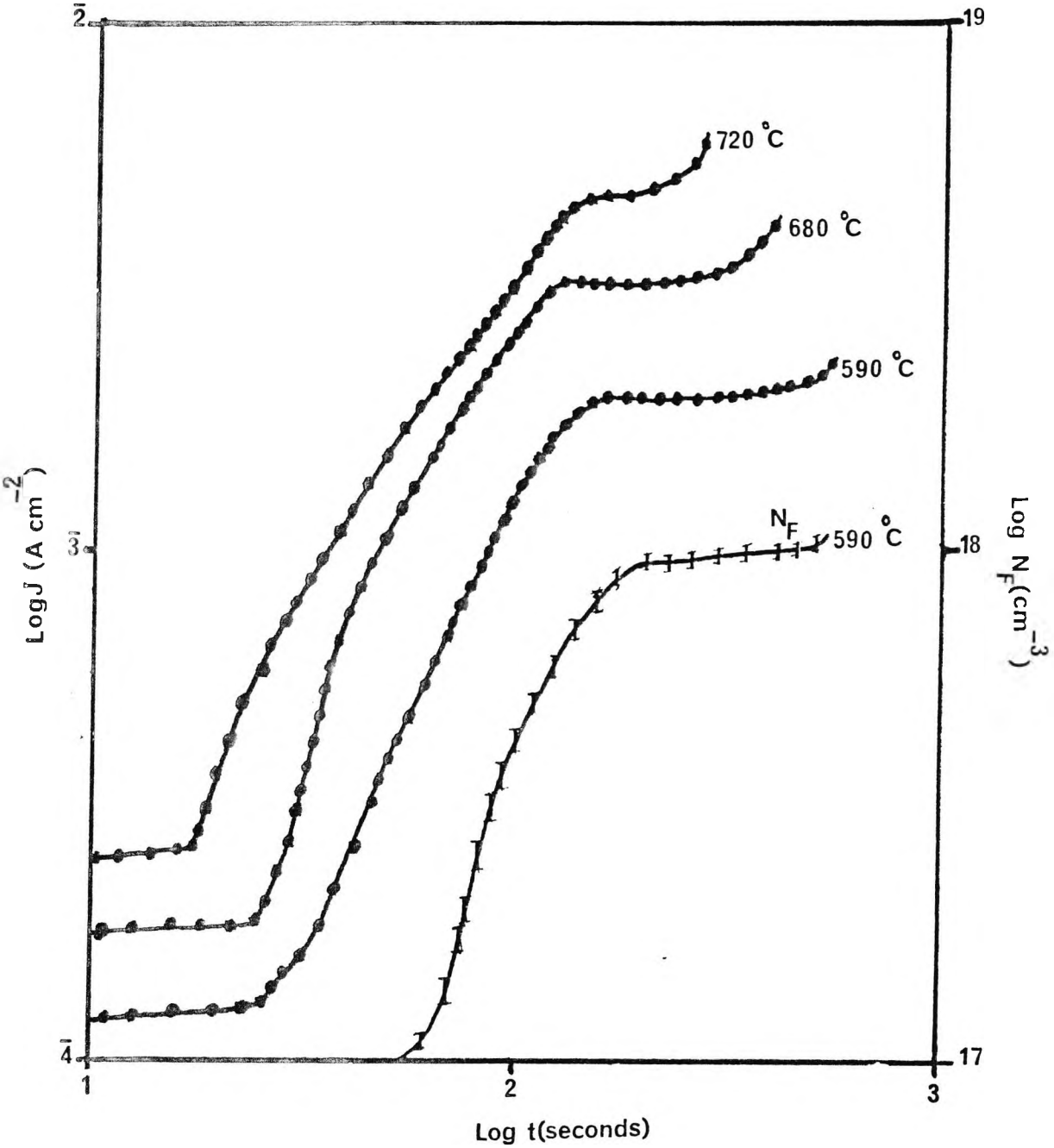

Figure 4.5 The variation of the current density and the concentration of the F– centres with the coloration time of NaCl

Figure 4.3 refers to the electrolytic coloration of KCl. Point T_c is the coloration starting temperature as was observed visually for the electrolytic coloration of all the alkali halides. In order to investigate the nature of this part of the current-temperature relationship the conductivity σ of the alkali halide crystals was measured. Figure 4.6 shows the results of a measurement for NaI which has the typical shape of a $\log (\sigma T)$ versus T^{-1} plot for alkali halides. The experimental points on the conductivity curve were obtained from a continuous record in the region before point T_c where no coloration was observed. The energies which are calculated from this figure are 1.92 eV and 0.54 eV for the Schottky formation energy E_S (the intrinsic region which is referred to as I in figure 4.6) and the cation vacancy migration energy E_m (the extrinsic region which is referred to as II in figure 4.6) respectively. The value of E_s satisfies well the inequality (Hoodless et al 1971)

$$\text{NaI (1.92)} < \text{NaBr (2.16)} < \text{NaCl (2.38)} < \text{NaF (2.72)}$$

which also holds for the potassium halides (Chandra and Rolfe 1970). The value of E_m is in good agreement with that reported by Hoodless et al (1971), which is 0.47 eV. The good agreement of these values with those reported in the literature, which are also determined by ionic conductivity measurements, indicates that there is no space-charge built up in this part of the electrolytic coloration process. The other important fact which is apparent from figure 4.6 is that the current prior to point T_c is due to pure ionic conductivity with the cation vacancy playing the dominant role.

The second part of the current density-time relationship starts at point T_c and is characterised by an abrupt increase of the current and a simultaneous emergence of the colour at the pointed cathode. Figure 4.7 demonstrates the relationship between the electronic conductivity $\Delta\sigma_e$ (curve (b)), which is the extra conductivity superimposed on the original ionic conductivity of the specimen at point T_c and the specimen temperature. The experimental values for $\Delta\sigma_e$ were determined from the difference between the currents in electrolytically-coloured and bleached NaCl. The electrolytic coloration experiments were carried out by using the constant-current method with each point in figure 4.7 obtained from five such experiments which were carried out at five fixed temperatures. The corresponding concentrations of F-centres which were calculated using the spectrophotometric data of the coloured specimens are shown in the figure by curve (a). The good agreement between the values of the F-centre concentration calculated from the optical data and those obtained from $\Delta\sigma_e$ confirms the electronic nature of the extra conductivity which causes the abrupt increase of coloration current at point T_c

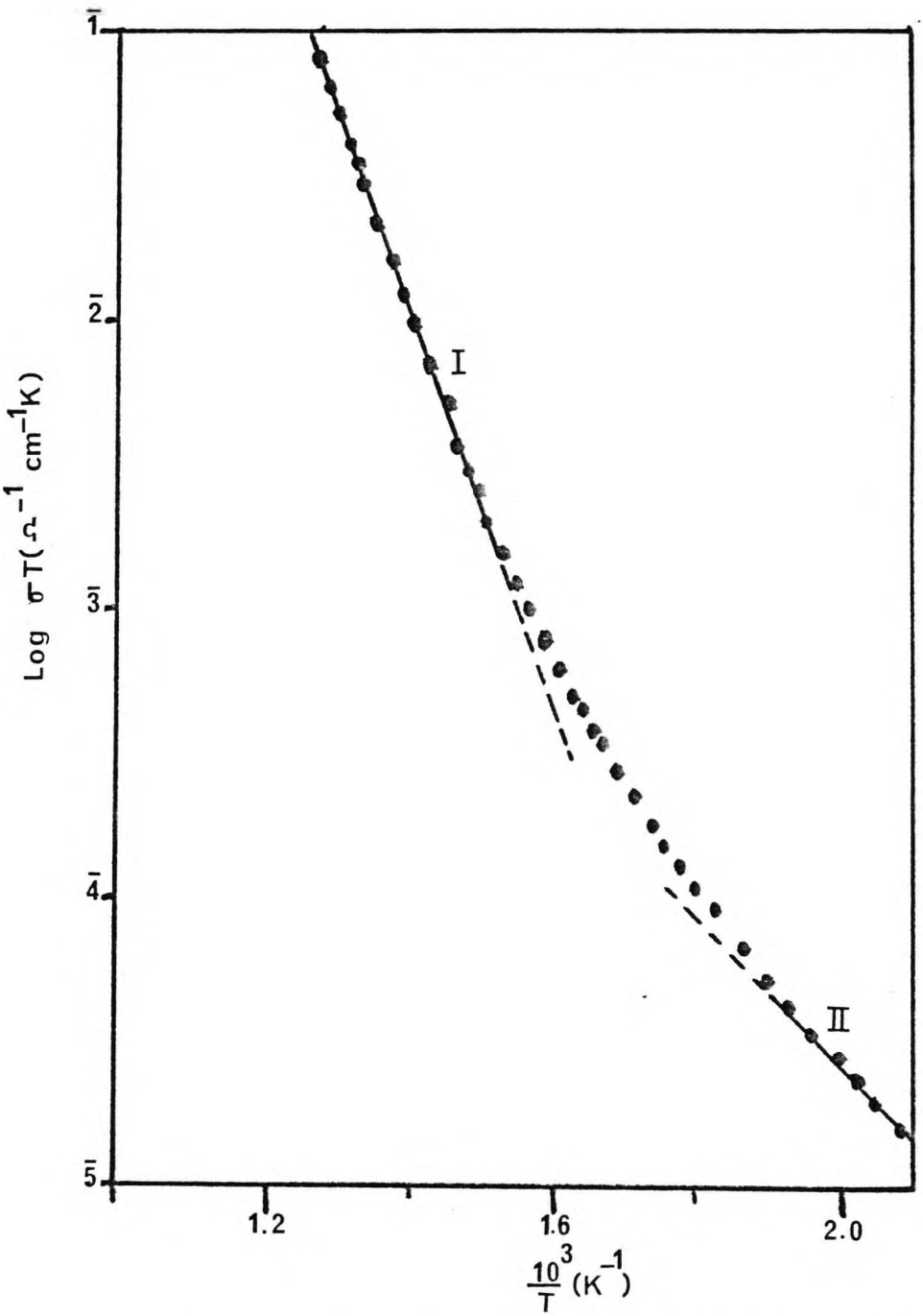

Figure 4.6 The ionic conductivity of NaI before point T_c

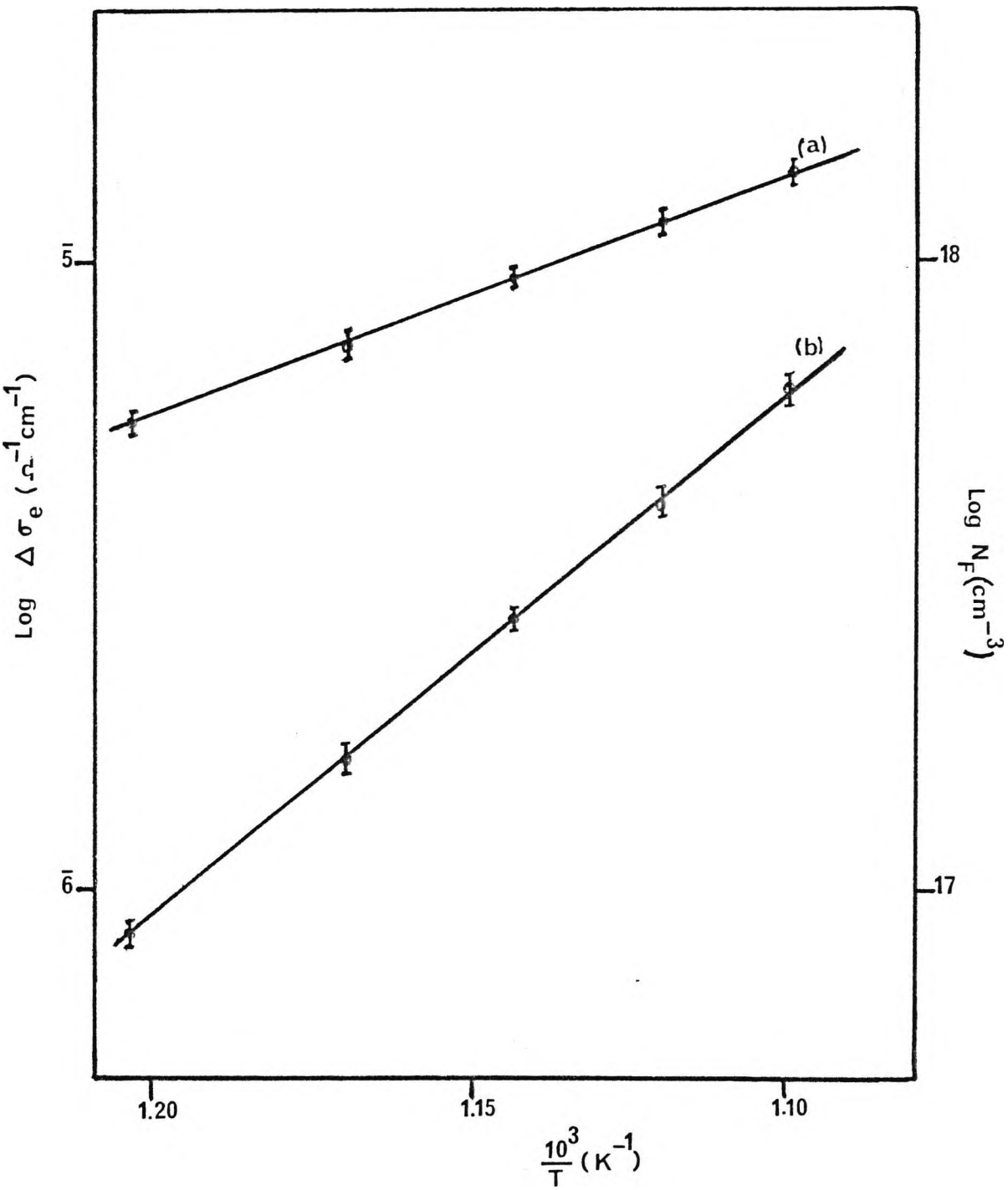

Figure4.7 The concentration of the F-centre, curve(a), and the electronic conductivity $\Delta \sigma_e$, curve(b), as a function of NaCl specimen temperature T

This conductivity is due to electron injection which takes place at point T_c from the new alkali metal cathode formed by the accumulation of this metal on the pointed cathode.

In order to understand the third part of the current density-time relationship, within which the current density J saturates, experiments were carried out to determine the kinetics of this stage of coloration by investigating the relationship between J and the electric field amplitude E at various coloration temperatures T. It was assumed that E is uniform and its magnitude was taken as $\frac{V}{d}$. The values of E in figure 4.8 are average values of three experiments. The relationship was investigated over the temperature range from 500 °C to 690 °C using NaCl specimens. Figure 4.8 shows that J is directly proportional to E at 620 °C. This proportionality was found to characterise the whole range of temperatures investigated. If J_o is the ionic current density, u is the electron mobility and γ is the degree of F - centre dissociation, then, for $J >> J_o$, the following relation is valid (Mott and Gurney 1948)

$$J = eu \gamma N_F E \qquad (4.1)$$

where N_F is the concentration of F-centres. In this relationship, if J is proportional to E, then N_F is constant. This result is in good agreement with the observed spectrophotometric data which are obtained for this stage of coloration. The independence of N_F on E is consistent with the assumption that there is a thermodynamic equilibrium established in the system consisting of the electrodes and the specimen near to the beginning of the steady-state current stage of figure 4.5. At this stage the current density reaches its equilibrium and its value stays constant over a period of time. As the coloration temperature is increased, the current-time relation of figure 4.5 shows that the duration of the steady-state current stage becomes shorter with an apparent tendency to start a build up of current leading to the fourth part of this relationship. This latter part is probably associated with the formation of F-aggregate centres and even the formation of colloid centres as was the case for NaBr and NaCl.

The exact measurement of the coloration time t_c (seconds), the volume of the coloured part of the specimen v (cm^3) and the electronic current I_e (A) provides a useful and accurate means of measuring the concentration of the electron-excess centres. In this way it was possible to calculate the oscillator strength of the F band in various alkali halides using Smakula's equation ,(equation (2.4))and the optical parameters of the F band. The values of N_F were determined by using

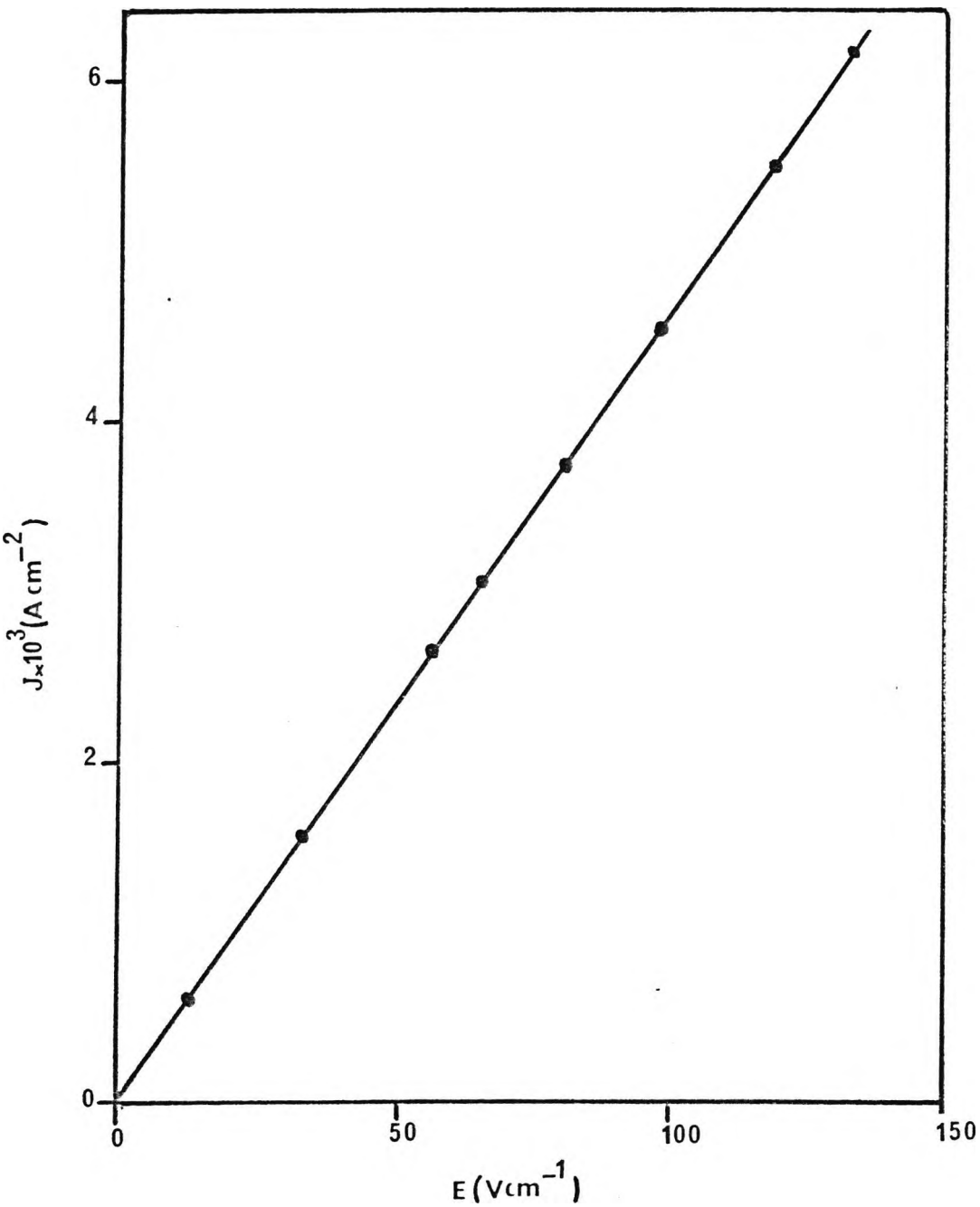

Figure 4.8 The relation between the current density and the electric field intensity at 620°C for NaCl specimens

Table 4.1 Oscillator strength of F-centre in electrolytically coloured alkali halides.

	Oscillator strength	Halfwidth (eV)
KI	0.54	0.502
KBr	0.81	0.693
KCl	0.62	0.449
NaI	0.48	0.761
NaBr	0.64	0.610
NaCl	0.46	0.735

All values refer to room temperature.

$$N_F = \frac{I_c\, t_c}{ev} \qquad (4.2)$$

which is valid only when F-centres are produced by electrolytic coloration. The calculated values of the F band oscillator strength f_F are reported in table 4.1

2. F-centre colourability

2.1 F-band growth curves

A typical growth curve of the concentration of electrolytically produced F-centres is shown in figure 4.5 (curve N_F) for NaCl specimens. This curve was obtained for the electrolytic coloration of NaCl at 590°C using the constant coloration temperature method. The corresponding current density-time relationship is also shown in figure 4.5. The curve demonstrates the formation and growth of the F-centre concentration N_F during the electron-injection stage of the electrolytic coloration process. The saturation of N_F over the period when the coloration process is characterised by a steady-state current is also shown in figure 4.5.

The distribution of F-centres in electrolytically coloured alkali halides was studied by observing the variation in the F band absorbance along the length of the coloured specimens. The F band absorbance in each case represented the value of N_F at the moment when the coloration process was terminated. Figure 4.9 shows typical results for the electron-injection stage and the steady-state current stage of the coloration process. The figure shows the results of two series of electrolytic coloration experiments which were carried out at 680°C (curves (a)) and 590°C (curve (b)). The full lines are the results for the electrolytic coloration development during the electron -injection stage. The two dashed lines are the results of the development during the steady-state current stage. The coloration time is referred to on each line in figure 4.9 by its value in minutes. The length of the specimen is presented as $\frac{x}{d}$, where x is the distance from the pointed cathode and d is the total length of the coloured part of the specimen. Each point on the curves represents the average value of five electrolytic coloration experiments which were carried out under identical coloration conditions.

It is clear from figure 4.9 that, at the outset of electron-injection stage, the maximum concentration of the electrolytically created F-centres occurs near to the pointed

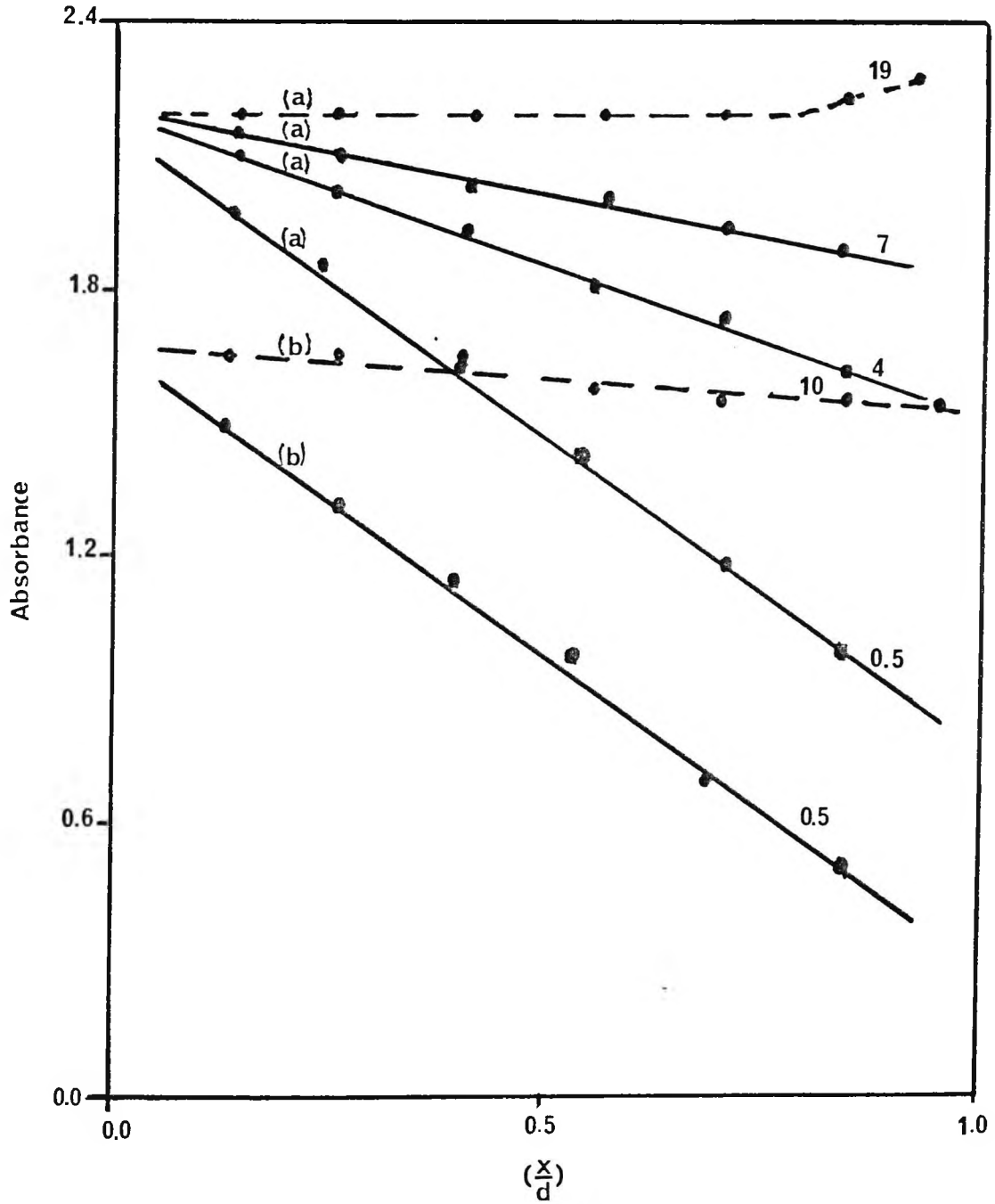

Figure 4.9 The variation of the F band absorbance along the length of NaCl specimen during electrolytic coloration

cathode. This concentration decreases linearly along the length of the coloured specimen from the part near to the cathode towards the part near to the anode. As the coloration time increased towards the end of the electron-injection stage and the beginning of the steady-state current stage of the electrolytic coloration process (see figure 4.5), this process starts a new phase characterised by a homogeneous distribution of F-centres along the length of the coloured specimen. Figure 4.9 shows that this new phase of the electrolytic coloration process takes place apparently by an increase in the concentration of F-centres in the region near to the anode. This observation indicates the formation of anion vacancies in the region near to the anode during the electron-injection stage and the migration of the maximum density of the injected electrons to this region when the electrolytic coloration process proceeds towards the beginning of the steady-state current stage.

A comparison between these results and those of figure 4.5 shows that the establishment of a homogeneous distribution of N_F is due to a dynamic equilibrium between the electron injection and the formation of the anion vacancies during the steady-state current stage. The comparison also shows that, when the coloration current reaches a certain value, this equilibrium no longer holds and a new stage of the current density-time relationship starts by a further increase in the coloration current. This subsequently leads to an increase in the concentration of the F-centres near the anode (see the dashed curve (a) in figure 4.9) which ends the homogeneous distribution stage of the F-centres. The other fact which such a comparison shows clearly is that the homogeneous distribution of the F-centre concentration along the length of an electrolytically coloured specimen lasts for a longer time when the coloration rate (the increase in current during the electron-injection stage) is higher. Electrolytic coloration experiments performed on the other alkali halides showed an identical structure for the F-centre growth curves as shown in figure 4.5 for NaCl specimens and a similar distribution of the F-centre concentration to that which is shown in figure 4.9 for NaCl specimens regardless of the coloration temperature and other conditions.

The growth of the F-centre concentration during the electrolytic coloration process is influenced by several factors. The coloration current and the temperature are the most effective as figures 4.4 to 4.9 clearly show. An additional investigation was carried out to find the correlation between the concentration of the intrinsically produced anion vacancies and the concentration of electrolytically produced F-centres. Electrolytic coloration experiments carried out at 760 °C using NaCl specimens resulted in $N_F \triangleq 3 \times 10^{18}$ cm^{-3}, as expected. The concentration of anion vacancies at thermodynamic equilibrium in NaCl at 800 °C (that is 1 °C below the melting point) is calculated by Greenwood

(1984) to be $\leq 4 \times 10^{17}$ cm^{-3} . A similar value is given by Etzel et al (1950) for the concentration of anion vacancies in NaCl at the same temperature. The same phenomenon has been observed when the measurements were repeated for KBr and KCl. The results were persistent in showing a difference between the concentrations of the anion vacancies and the F-centres by a factor of one order of magnitude. This fact became more apparent when extra concentrations of the other electron-excess colour centres were produced during electrolytic coloration. These results suggest that excess anion vacancies are produced by means other than that of the Schottky formation process. The suggestion that these extra anion vacancies enter the specimen from the anode to compensate for the electron-injection charge (Schulman and Compton 1962) is not consistent with the results shown in figures 4.8 and 4.9 Pick's (1958) suggestion that anion vacancies are formed at the anode due to the migration process is also not valid since no V-centres were observed in the electrolytically coloured specimens when a pointed cathode was used The excess anion vacancies could have been created during the electrolytic coloration process from dislocations produced by compression, which the specimen is subjected to because of the difference in the thermal expansion coefficients of the specimen and the holder (Whiteworth 1975). The production of these vacancies at high temperature seems almost certain to be due to the motion of the dislocations caused by the applied field (Seitz 1950, 1954, Urusovskaya 1969).

2.2. Sandwich technique

Electrolytic coloration experiments were carried out using various combinations of alkali halide specimens instead of the normal single specimen. These combinations have either a mobile ion in common like KBr-KCl-KBr and KCl-NaCl-KCl or no such common mobile ion like KCl-NaBr-KCl. In case (a), which is shown in figure 4.10 , all three specimens in the sandwich were coloured intensively at 700 $^{\circ}$C using a constant current of 750 μA. The spectrophotometric data showed that the concentration of F-centres in the central KCl specimen at the KBr (1)-KCl contact line was strikingly higher than that obtained in electrolytically coloured single specimens of KCl using identical coloration conditions. Other colour centres were also found with higher concentrations than in the standard coloration experiment with a single specimen. The KBr (1) and KBr (2) regions of the sandwich were coloured with the expected concentration of F-centres., under these conditions. When the combination was reversed by putting a KBr specimen between two specimens of KCl, the high concentrations of the various colour centres were equally noticed for the KBr specimen, The concentration of F-centres in KCl (1) in this case was higher than that in KCl (2).

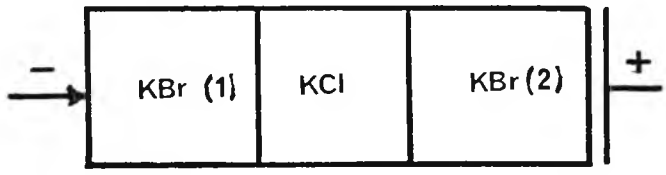

(a)

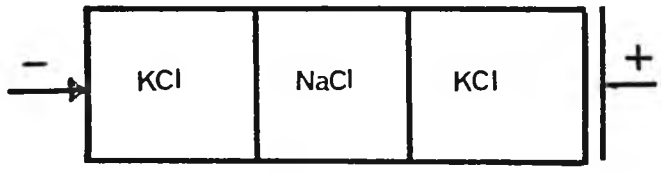

(b)

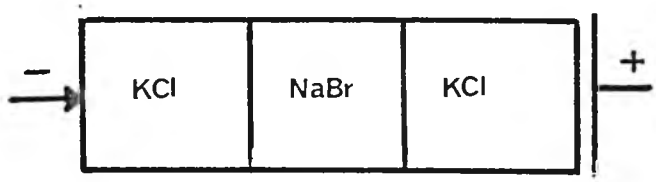

(c)

Figure 4.10 Combinations of spcimens used in the sandwich technique experiments

Returning to case (a), it was noticed that the coloration of KBr (1) started to bleach away beginning from the pointed cathode while the absorption of the F-centres in the central KCl specimen was enhanced beginning from the KBr (1)-KCl contact line when the coloration current was increased to 1 mA. After the coloration experiment was finished, it proved difficult to separate KCl and the KBr (2) regions with part of KBr (2) always being attached firmly to the KCl specimen. The absorption spectrum of this side of the KCl showed an overlap between the F and R_1 , M and R_2 and N_1 and N_2 bands. The peak position of the overlapping pairs were also shifted towards the region between the normal peak positions of the particular absorption bands.

In cases (b) and (c) only it was possible to colour the KCl specimen with a high concentration of F-centres. The NaCl and NaBr specimens stayed uncoloured. The concentration of M-centres was high in both cases.

A principal advantage of this technique in the electrolytic coloration experiments is that it provides alkali halide specimens containing high concentrations of colour centres. The enhancement of the colourability seems to be related to the alkali ion. Electrolytic coloration experiments were also carried out using combination (a) but with a KCl specimen which had been coloured already in a separate experiment. These experiments showed that, simultaneously with the onset of the coloration at the pointed cathode in KBr (1), the bleaching of the coloration in KCl started at the KBr (1) -KCl contact line. At the same time the coloration started to penetrate the KBr (2) specimen from the KCl-KBr (2) contact line, moving towards the anode.

Comparisons between the results obtained using different combinations of alkali halide specimens leads to the conclusion that, whenever these specimens have different alkali ions (cases (b) and (c)), the coloration does not move from the coloured specimen near to the cathode to the next specimen. A similar lack of movement of the coloration is noticed for case (b) when the specimens have the Cl^- ion in common. On the contrary, when the sandwich has the alkali ion in common (case (a)), it is possible to colour all the specimens of the combination regardless of their arrangement.

2.3 Deformation

Figure 4.11 shows the current density-time relationships of two KCl specimens coloured under identical conditions. Curve (a) is the current density-time relationship for a plastically deformed KCl specimen. Curve (b) is the same relationship for an undeformed (control) KCl specimen.

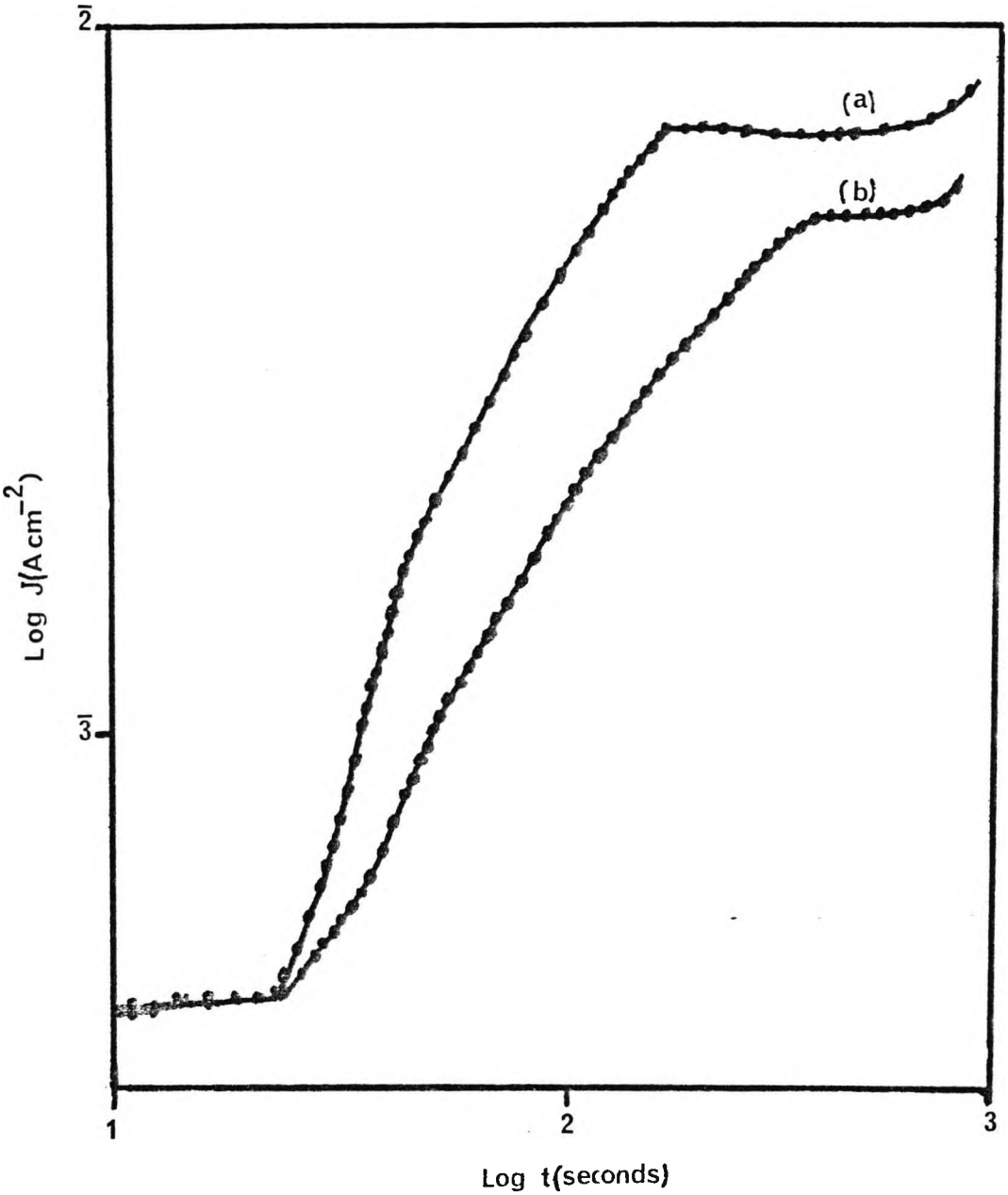

Figure 4.11 Current density–time relationship of(a)a deformed KCl specimen and (b) that of an undeformed specimen under identical coloration conditions

The figure shows clearly that the first part of coloration process, which ends at T_c , is unchanged by deformation. This part is dominated by cation vacancy migration (section 1.2 of this chapter). Hence the formation of the new alkali metal is not affected by the deformation and T_c is the same for both specimens.

Figure 4.11 also shows that, starting at point T_c , the coloration current density increased for the deformed specimen. The enhancement of the coloration rate ended with a longer period of steady-state current. These facts were compared with the observed enhancement of the colour intensity in the deformed KCl specimen. The F absorption depends on the rate of accumulation of excess anion vacancies in the region near to the cathode where the maximum density of electrons exists at the beginning of the electron-injection stage. The increased current in the deformed KCl specimen at this stage may be due to an extra electron injection induced by the dislocations formed as a result of the deformation as was suggested by Tyler (1952). The measurements of the electronic conductivity $\Delta \sigma_e$ show that this is not the case. The other suggestion is that the excess conductivity at T_c could be due either to an additional conduction mechanism such as excess mobility along the dislocation lines (Barr et al ,1960;Kittel,1985) or to a vacancy formation mechanism induced by the dislocations (Whitworth ,1975). The last suggestion is supported by the experimental fact that an increase in N_F is observed in the deformed specimen.

Electrolytic coloration experiments carried out using various deformed alkali halide specimens showed two main facts. The first is that a deformed specimen displays a stimulated growth of F-centres, which is largely in excess (using identical coloration conditions) of that obtained in the control specimen. The second fact is that there is an induced period of homogeneity in the distribution of F-centres during the steady-state current stage of electrolytic coloration. Hence, the equilibrium between the injected electrons and the anion vacancies is established over a longer period in the deformed specimen. Thermodynamic data were used, as in section 2.1 of this chapter, to find a correlation between the concentration of thermally produced anion vacancies and the concentration of the electrolytically produced F- centres. Using a deformed KBr specimen, electrolytic coloration at 640°C produced 3.3×10^{18} cm^{-3} F-centres. At the same temperature Rolfe (1964) measured the equilibrium vacancy concentration to be approximately 2×10^{17} cm^{-3} . This difference strongly suggests an extra source of anion vacancies. Additive coloration of deformed KBr at 640°C (annealing time 10 hours) produced 3.26×10^{17} cm^{-3} F-centres which correlates well with Rolfe's (1964) results.

Measurements were made to relate the excess absorption due to the α -centres in electrolytically coloured and deformed KBr to the suggestion of anion vacancy formation by the induced dislocations. The absorption of the α -centre was obtained by a similar procedure to that described in section 2.3 of chapter 5. The absorbance of the α band was significantly higher than that of the control specimen. Other experiments were carried out by heating the deformed specimens to the same coloration temperature and then annealing them at that temperature for the same coloration time but without passing the ionic current. When quenched these specimens showed no such significant increase in the α band relative to that produced by electrolytic coloration. This fact may indicate that the formation of the anion vacancies in the bulk of a deformed specimen is due to an interaction between the effect of electron injection and the induced dislocation. Since the thermal equilibrium which is established between the core of a dislocation and the point defects in the surrounding lattice leads to a build up of an electric field between the two (Whitworth 1975), the electron injection may unbalance this equilibrium. This can lead to a separation of the anion vacancies and the dislocations through the diffusive motion of the latter (Seitz 1950; 1954). Some of these vacancies will trap the injected electrons to form F-centres and the others will drift in the surrounding electric field.

2.4 Other factors

As described in the previous sections, temperature and current flow are the two principal factors which affect the colourability of alkali halides when using the electrolytic method. The results of the electrolytic coloration experiments using identical coloration conditions showed that this colourability is also a characteristic of the particular alkali halide (Gritsenko 1971). Other factors which affect the colourability of the alkali halides are the divalent impurities which these specimens may contain and the surrounding medium. The first factor is treated in chapters 3 and 6. Heiland (1950) reported that the surrounding medium has an influence on the development of electrolytic coloration. Electrolytic coloration experiments were carried out in air, in vacuo (10^{-5} torr) and in a nitrogen atmosphere using various alkali halide specimens and wide combinations of coloration conditions. However, contrary to Heiland's (1950) observation it was not possible to establish any effect of this factor on colourability. Moisture, however, affects significantly the colourability of KF, NaI and NaBr.

3. Conclusions

The experimental results which are reported in the previous sections show clearly that, as the alkali halides are heated to high temperature, electrolytic coloration starts at a

fixed temperature when the ionic current is applied. This fixed temperature (which is called T_c in this work) is found to be the coloration starting point and is characteristic of the particular alkali halide when these salts are coloured under identical coloration conditions. The experimental results show that, at temperatures below T_c , ionic conductivity is the only process taking place in the specimen. This process is dominated by a cation vacancy migration process, a fact which is supported by the suggestion of Heiland (1950) and Hadley (1968) that the ionic processes taking place below T_c create the necessary conditions for the formation of the new alkali metal cathode at the interface between the pointed cathode and the specimen. This new cathode is formed by the accumulation of alkali metal on to the original pointed cathode. It causes electron injection into the specimen at and above point T_c which was found by Paramo and Schanchez (1971) to be due to thermoionic emission.

The various current-temperature and current-time relationships have been investigated. They show that the electrolytic coloration process consists of two distinct stages. The first or electron injection stage starts at point T_c and is dominated by the formation and migration of the F-centres. The observed results using the sandwich technique (constant-voltage method) show that a cation vacancy migration process is the vital factor which determines the diffusion of the F-centres at T_c is characterised by a sharp increase in the coloration current. The dominating feature of the second stage of the electrolytic coloration process is the steady-state current which passes through the specimens. When the coloration current is increased above the magnitude of the steady-state current, the characteristic features of this stage are cancelled and the coloration process is found to consist of only the first stage; that is the further intensification of the colour. The characteristic feature of the steady-state current is that of a homogeneous distribution of F-centres.

The variation in the distribution of the F-centre concentration has been used to investigate the processes of electrolytic coloration which lead to the various current-temperature and current-time relationships. In the electron-injection stage the concentration of F-centres is a minimum in the region near to the anode and is a maximum in the region near to the cathode. As the coloration continues in this stage, the difference between the maximum and minimum of the F-centre concentration decreases gradually. This finally ends with a levelling out of the F-centre concentration along the length of specimen. The levelling out of the F-centre concentration leads to the homogeneous distribution of F-centres in the specimen which is a characteristic feature of the steady-state current stage. The duration of the homogeneous distribution is found to be longer as the rate of current increase in the electron-injection stage is higher. The higher F-centre concentration in the region near to the cathode and the gradual decrease in

this concentration towards the anode may be related to the fact that the maximum density of injected electrons occurs near to the cathode. But, since the density of alkali halides decreases during electrolytic coloration (Hackskaylo and Groetzinger, 1952), the variation in the distribution of the F-centres along the length of the specimen is related to an equivalent variation of the distribution of the vacancy concentration. The accumulation of anion vacancies takes place in the region near to the cathode due to the migration process in the electron-injection stage. As the coloration moves towards a homogeneous distribution, a dynamic equilibrium takes place between the injected electrons and the anion vacancies as a result of the shift of the maximum density of these electrons from the region near to the cathode to that near to the anode. When this equilibrium is established, the steady-state current stage begins together with the homogeneous distribution of F-centres.

It has been shown that the concentration of excess anion vacancies which is required for the formation of the experimentally observed concentration of F-centres cannot be created only by thermodynamical process of Schottky defect formation or by the compensation process of the electron injection. The experimental results demonstrate that a mechanism of excess anion vacancy formation is involved in the electrolytic coloration process. It is assumed that the excess anion vacancies are formed by the induced dislocations in bulk of the specimen. The formation mechanism is discussed according to the results obtained in this work and to those reported in the literature.

Experimental work has also been carried out to clarify the effect of dislocations induced by deformation on the electrolytic coloration process since Boni et al (1975) found that dislocations modify the X-ray coloration mechanism. The effect of dislocations on electrolytic coloration has been investigated by studying the changes which they induce in the current-time relationship of a deformed specimen. It has been observed that dislocations introduce both an enhancement of the coloration rate during the electron-injection stage and a significant increase in the concentration of the F-centres. It is found that excess anion vacancies are formed by the induced dislocations due to their electrical properties.

A proportion of the excess anion vacancies are formed in the region near to the anode. This is explained by the fact that dislocations accumulate in this region as a result of their motion in the electric field (Urusovskaya ,1969; Whitworth ,1975,Harrison,1982).

It is clear from the results reported in this chapter that it is possible to produce most of the known colour centres in the alkali halides using the electrolytic coloration method together with the appropriate coloration conditions. Alkali halides, however, differ from each other in their colourability with regard to the various colour centres. This colourability is found to be a function of the lattice constant, though other physical

have been produced electrolytically in NaI using the appropriate coloration and optical measurement conditions, though it has been reported that F-centres are very difficult to produce by irradiation and are undetectable when the additive coloration method is used (Fontana and Van Sciver 1970). The coloration of NaBr may also be achieved.

4. References

Barr L.W',Hoodless.I.M.,Morrison J.A.and Rudham R.1960Trans. Faraday Soc 56 697

Boni M, Gamagni P and Giani E 1975 J. Phys. Chem. Solids 36 883

Chandra S and Rolfe J 1970 Can. J. Phys. 48 397

Etzel H W and Maurer R J 1950 J. Chem Phys. 18 1003

Fontana M P and Van Sciver W J 1970 Phys St. Solid 37 375

Greenwood N N 1984 Ionic Crystals, Lattice Defects and Nonstoichiometry - Butterworths

Gritsenko Yu I 1971 Phys. St. Solid (a) 7 K113

Harisson W A 1982 Solid ST. Theory-McGraw-Hill

Heiland G 1950 JZ Phys. 128 144

Hoodless I M, Strange J H and Wylde I E 1971 J. Phys C: Solid St. Phys. 4 2737.

Ivey H F 1947 Phys. Rev. 72 341

Kittel C 1985 Introduction to Solid State Physics-Welley Publisher-New York

Mott N F and Gurney R W 1948 Electronic Process in Ionic Crystal-Dover

Pick H 1958 Nuovo Cimento d. Supple. 7 498

Rolfe J 1964 Can. J. Phys. 42 2195

Schulman J H and Compton W D 1962 Colour Centres in Solids-Pergamon Press

Seitz F 1950 Phys. Rev. 80 239

1954 Rev. Mod. Phys. 26 7

Tyler W W 1952 Phys. Rev. 86 801

Urusovskaya A A 1969 Sov. Phys. -USP 11 631

Whitewoorth R W 1975 Adv. Phys. 24 203

CHAPTER FIVE

Optical Properties of Specimens Containing
F-aggregate Centres

1. Optical spectrum.

1.1. Spectra of coloured specimens

The most accessible alkali halide crystals from the standpoint of electrolytic coloration are KI, KBr and KC1. The optical absorption spectra of electrolytically coloured specimens of these materials are shown in figures 5.1 to 5.3. When an alkali halide specimen has been coloured electrolytically, it acquires a specific colour which is a peculiarity of the particular salt. Figure 5.4 shows the colours of the alkali halide specimens which have been coloured electrolytically in the present work using identical coloration conditions (500 μA and 550°C- except for the alkali flourides, see chapter 6). The specimens contain only F-centres though with different concentrations. The photographs of figure 5.4 were taken at room temperature. At higher temperatures the colours are different when observed under the same laboratory illumination. For example, a coloured KCl specimen appears blue when in the furnace. When it is quenched to room temperature the colour changes to violet. The other factors which affect the colour of the electrolytically coloured alkali halides are the concentration of the F-centres and the presence of other colour centres in the specimen. NaCl, for example, looked yellowish-brown when it contained a low concentration of F-centres (10^{17} cm^{-3}). When the electrolytically coloured NaCl contained 10^{18} F-centres cm^{-3}, the specimen looked brown. This colour started to become blackish when the F-centres were converted to colloid centres

Figure 5.1 shows a typical absorption spectrum of an electrolytically coloured alkali halide specimen measured at room temperature. Curve (a) was obtained for a coloration current of 120 μA. In this case, only F-centres are produced. When the coloration current was increased to 700 μA, curve (b) was obtained and it is clear that M- , R- and N- centres are produced in this case in addition to F-centres. A further increase of the coloration current led to an increase in the concentrations of the F- , M- and R- centres. The absorption spectrum of electrolytically coloured KBr showed similar features (see figure 5.2).

While it has been shown that alkali fluorides cannot be coloured electrolytically unless treated as described in chapter 6, NaI and NaBr specimens needed to be protected firmly from moisture if they were to be coloured successfully. The best conditions for the satisfactory coloration of NaI were a 500 μA coloration current and a coloration temperature

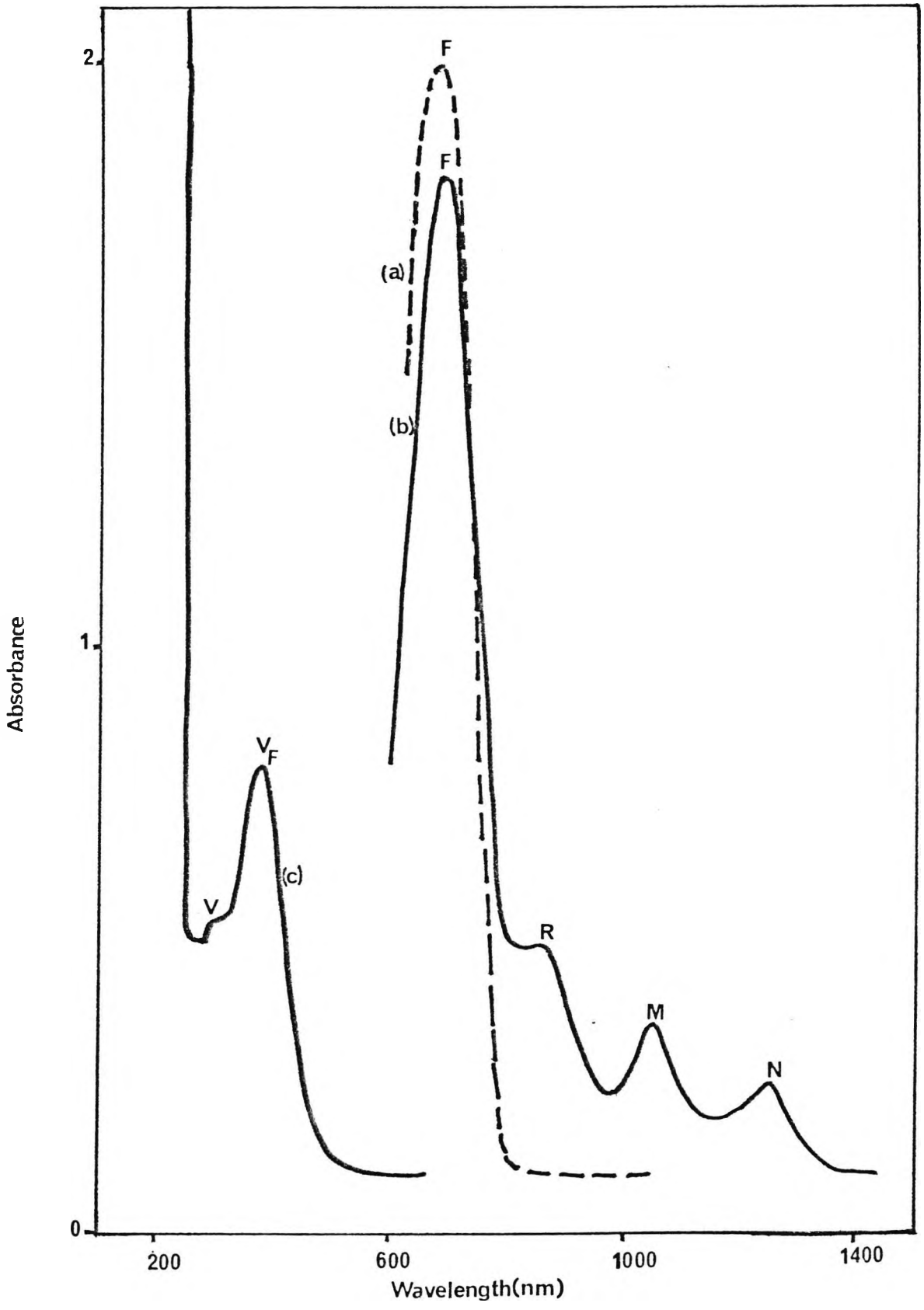

Figure 5.1 Absorption spectra of electrolytically coloured KI. Coloration is carried out using the constant current(a,b) and pointed anode(c) methods

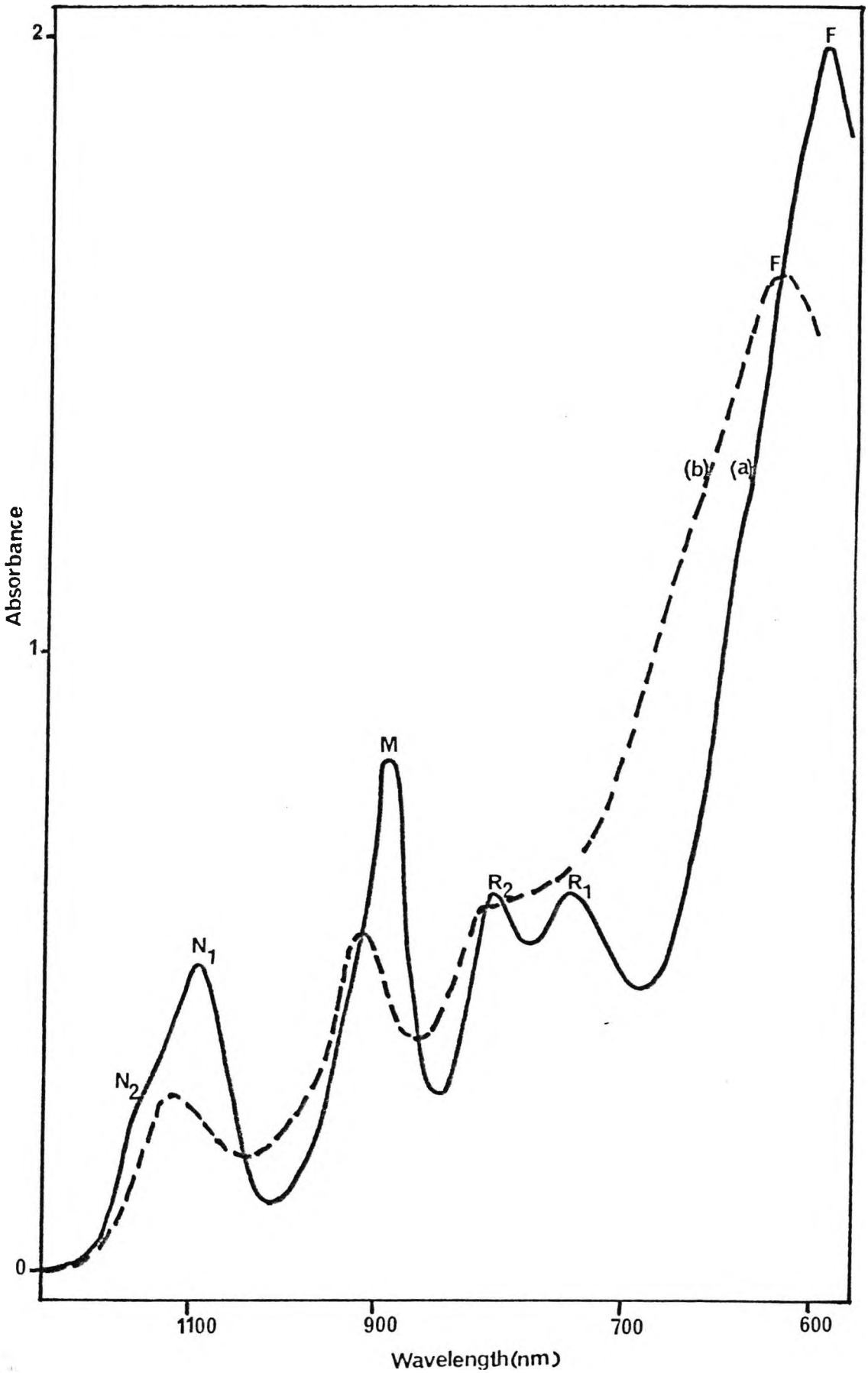

Figure 5.2 Absorption spectra of electrolytically coloured KBr measured at (a) liquid nitrogen temperature and (b) room temperature

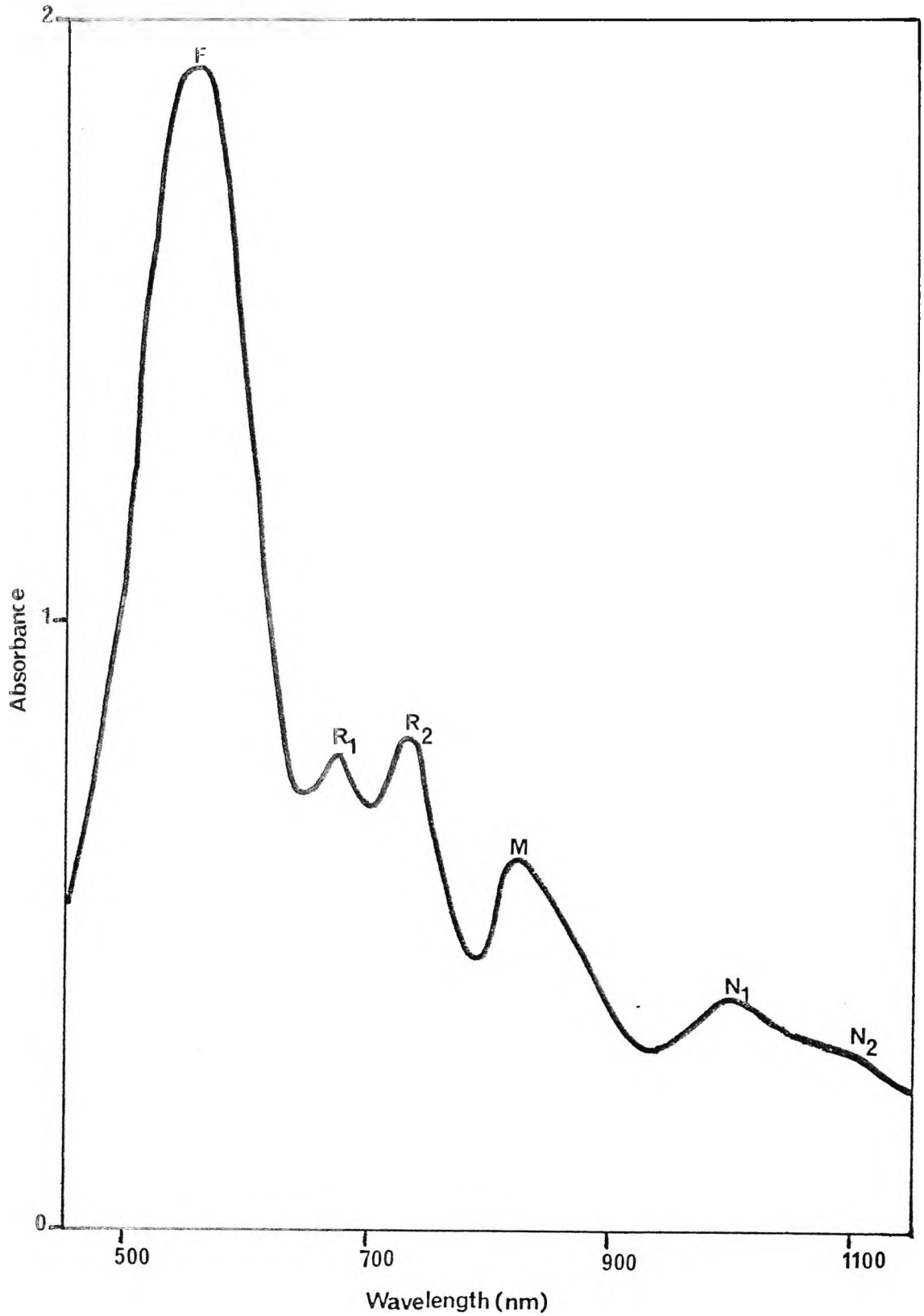

Figure 6.3 Absorption spectrum of electrolytically coloured KCl measured at room temperature

Figure **5.4** Electrolytically coloured alkali halides

of 570°C. For NaBr these conditions were found to be 800 μA and 660°C. These conditions gave the highest possible absorbance of the F-absorption band. Above these temperatures the F band started to decrease in height with the rapid appearance of the colloid band. The coloration current had a similar effect when its value was increased. However, only a small M band was noticed in electrolytically coloured specimens of both NaI and NaBr. When these specimens were coloured in air, the optical absorption spectra showed either a broad absorption band which might be related to colloid centres as was the case with NaBr, or a flat spectrum increasing in height and extending over the three ranges of the spectrophotometer as was the case with NaI.

Curve (a) of figure 5.2 is a typical absorption spectrum of an electrolytically coloured alkali halide specimen measured at liquid nitrogen temperature. Curve (b) shows the same spectrum when the optical measurement was carried out at room temperature. A comparison between the two curves demonstrates the fact that optical measurement at liquid nitrogen temperature enhances the resolution of the R and N bands. The splitting of the R band into well resolved R_1 and R_2 bands and the splitting of the N band into N_1 and N_2 bands are clearly shown in curve (b). In this way all the known absorption bands of the F and F-aggregate centres were obtained when the spectra of electrolytically coloured specimens of the alkali halides were measured at liquid nitrogen temperature. Each band in Figure 5.2 becomes sharper and narrower and shifts to shorter wavelength at the low temperature.

Figure 5.3 shows the absorption spectrum of an electrolytically coloured specimen of KCl measured at room temperature. The obvious difference between this specimen and those which belong to coloured KI and KBr (see figure 5.1 and figure 5.2) is the splitting of the R band into R_1 and R_2 bands. The optical absorption spectrum of coloured NaCl has similar features to that of coloured KCl. F as well as R_1 , R_2, M , N_1 and N_2 bands were obtained when a specimen of NaCl was coloured electrolytically at 750°C using coloration current of 1 mA. On the other hand the spectra of coloured NaI and NaBr, when measured at room temperature, were similar to those of coloured KI and KBr. F as well as R, M and N bands were obtained when a specimen of NaI and NaBr was each coloured electrolytically as described above and then treated optically with F-light (see section 1.2 of this chapter). So it is clear that coloured alkali chlorides have similar absorption spectra and show well-resolved R_1 , R_2 , N_1 and N_2 bands at room temperature, while coloured alkali iodides and alkali bromides have similar absorption spectra with the R and N bands unresolved at room temperature.

However, all the electrolytically coloured alkali halides show a prominent F band, the optical properties of which are given in table 5.1. The table shows that, as the peak position of the F band shifts to shorter wavelength, the halfwidth tends to be broader. The

Table **5.1.** Optical properties of the F band in electrolytically coloured alkali halides

	Peak Position (nm)	Halfwidth (eV)	Oscillator strength
KI	685 (718)	0.502	0.54
	653*	0.493	-
KBr	625 (630)	0.693	0.81
	590 *	0.351	-
KCl	555 (576)	0.449	0.62
	525*	0.397	-
NaI	590 (609)	0.761	0.48
	542 *	0.486	-
NaBr	537 (525)	0.610	0.64
	525 *	0.392	-
NaCl	455 (471)	0.735	0.46
	450*	0.473	-

Values given in parenthesis are calculated from the Ivey relations (1947)

Values referred to with asterisks are for optical measurements carried out at liquid nitrogen temperature. All the other values refer to room temperature.

variation of the peak position (curve (a)) and the halfwidth (curve (b)) with specimen temperature is shown in figure 5.5 for the F band of electrolytically coloured KCl.

Electrolytic coloration of KI using a pointed anode showed a prominent absorption band in the ultra-violet region of the spectrum (see section 2.2 of this chapter) with no absorption bands of any kind appearing in the visible or the near infrared regions of the spectrum (see figure 5.1). Also the spectrum of electrolytically coloured (pointed anode) KBr showed a broad band extending from 205 nm to 250 nm. The absorbance of this band for those samples cleaved from the surface of the coloured specimen are found to be significantly higher than the absorbance of those cleaved from the middle of the single coloured specimen. This band may be due to (non-metallic) colloid centres formed by halogen atoms and ions. This halogen excess may avoid the electron injection through the recombination with alkali metal.

The identification of all the absorption bands which are reported in this section have been made using the Ivey (1947) relations. The peak position and the halfwidth were determined for all the known F-aggregate bands in the alkali halides together with the oscillator strength of these bands in some salts. The optical measurements of these parameters were carried out at room temperature or at liquid nitrogen temperature whenever higher resolution of the R or N bands was required. The results, which are reported in section 1.2, are found to be in good agreement with the Ivey (1947) relations as well as with the results recorded in the literature (Schulman and Compton 1962, Compton and Rabin 1964, Markham 1966, Fowler 1984). It should be noted here that the bulk of the results in the reported literature were obtained using other coloration methods; namely additive and irradiation coloration.

The values of the peak positions of the K band in various electrolytically coloured alkali halides are reported in table 5.2. These results were obtained for F-centre concentration $> 6 \times 10^{18}$ cm^{-3} at liquid nitrogen temperature. The K band appeared as a hump on the shorter wavelength side of the F band at room temperature. The results for KI, KBr and KCl are in good agreement with those reported by Luty (1960).

1.2 Optical bleaching

A typical optical absorption spectrum of an electrolytically coloured alkali halide specimen measured after it had been exposed to F-light bleaching for 16 hours is shown in figure 5.6. Exposure of a coloured NaI specimen containing only F-centres resulted in the formation of M-, R- and N-centres as shown in the figure. M-centres were the first to be formed followed at a slower growth rate by the F- and N- centres. The absorption curves which show the F, M, R and N bands have been re-plotted after applying a correction for

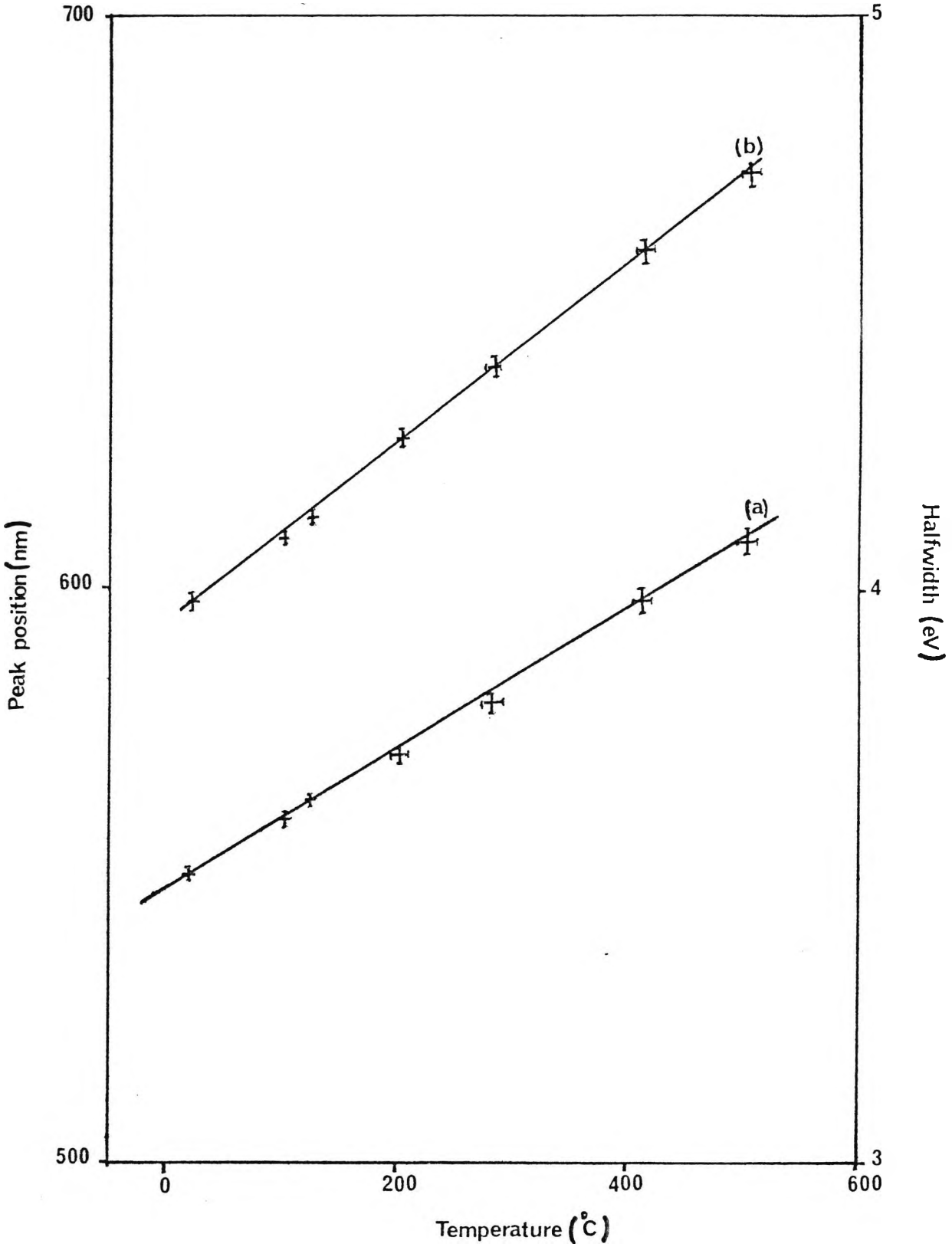

Figure 5.5 The optical properties of the F band as a function of the KCl specimen temperature

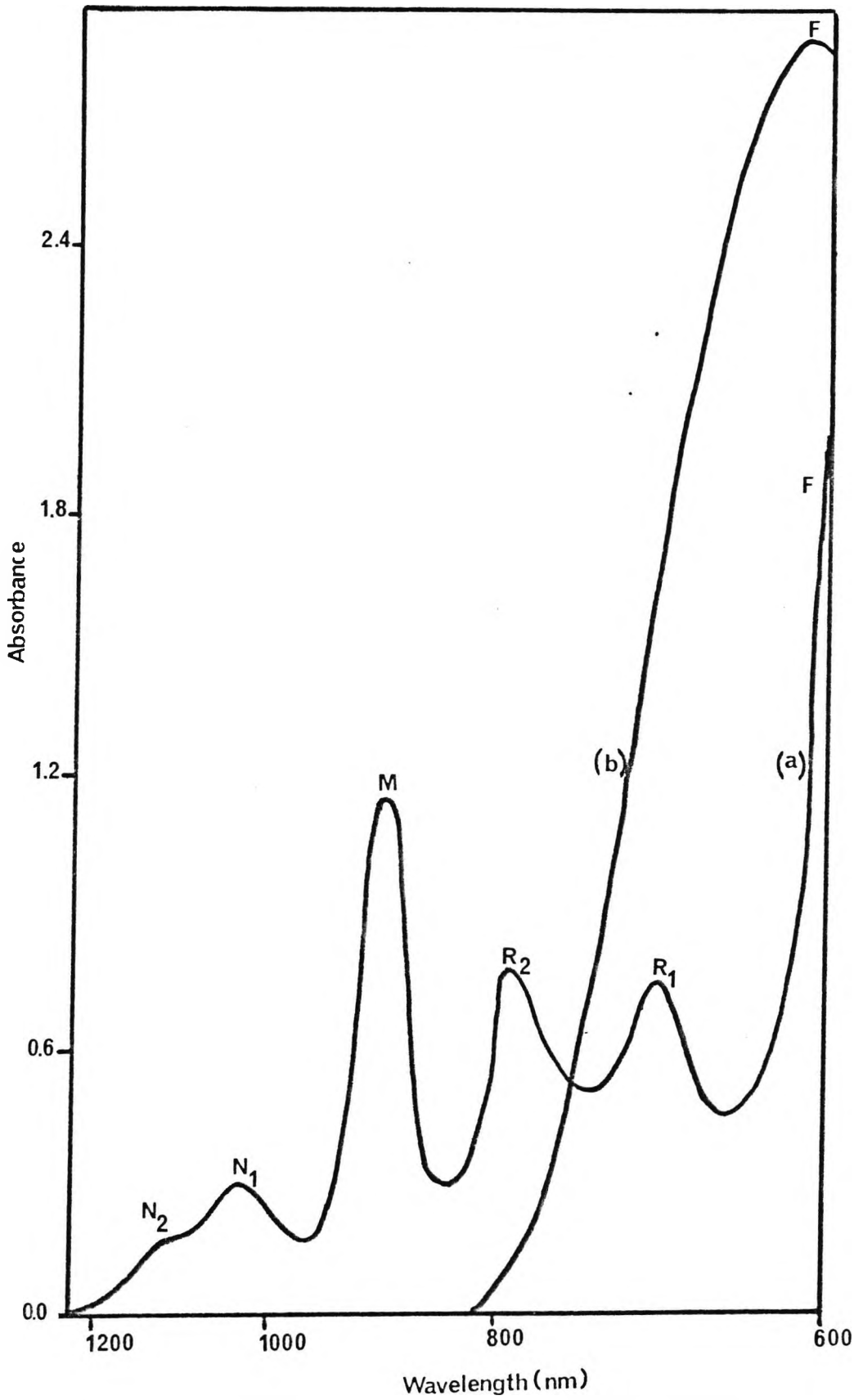

Figure 5.6 (a)F–aggregate bands in NaI produced by F–light treatment measured at liquid nitrogen temperature (b)the F band before the treatment measured at room temperature

Table **5.2.** Peak position of the K band in electrolytically coloured alkali halides

	Peak position (nm)
KI	595
KBr	514
KCl	460 (510)
NaI	472
NaBr	448
NaCl	366

All values refer to liquid nitrogen temperature except that in parenthesis which refers to room temperature.

the background absorption (Konitzer and Markham 1957). The optical measurement of figure 5.6 was carried out at liquid nitrogen

Figure 5.7 shows the variation in the absorbance of the F and M bands with the bleaching time of an electrolytically coloured NaBr specimen exposed to F-light. As the concentration of F-centres decreased steeply and slowly,the concentration of the M-centres increased rapidly during the first 400 minutes of irradiation with F-light. There then followed an intermediate stage of 250 minutes during which a decline in the concentration of M-centres was observed. Subsequently, the concentration of the M-centres started to increase but at a slower rate than previously. The growth curves of the R- and N- centres are also shown in figure 5.7. The identical behaviour of these two curves suggests that they involve a similar mechanism of formation. The relationship between the F and M absorption bands and between the R and N bands is shown in figure 5.8 and its inset respectively for a typical case. The figure shows the linear relation between the R and N bands which was predicted in figure 5.7 . It also shows the contribution of the M-centres to the formation of the R- and N- centres. Both figures 5.7 and 5.8 are taken from the F-light bleaching experiment of an electrolytically coloured NaBr specimen containing only F-centres. The spectrum of the optically treated NaBr is shown in figure 5.9 . The optical measurement of the F-aggregate bands was carried out at liquid nitrogen temperature.

The rate of conversion of F-centres to M-centres and other F-aggregate centres was found to be dependent on the F-centre concentration. Figure 5.10 shows the relationship between the concentration of the F-centres in freshly coloured NaCl specimens and the absorbance at the peak position of the M , R_1 and N_1 bands. All the measurements were carried out after bleaching for 425 minutes with F-light. It is clear from figure 5.10 that the growth rate of the F-aggregate centres increases as the concentration of F-centres in various coloured NaCl specimens increases. By increasing the concentration of the F-centres, the separation between the nearest F-centres has been decreased. This decrease in separation could account for the observed dependence of the F-aggregate growth rate on the concentration of F-centres.

Optical bleaching experiments provided a useful method for producing F-aggregate centres in the sodium halides since, in these specimens, it was difficult to produce all the colour centres directly by using electrolytic coloration. Most of the optical parameters of the absorption bands due to F-aggregate centres, including the oscillator strength, are unknown in the literature (Compton and Rabin 1964, Fowler 1984). In this work all these parameters have been measured in electrolytically coloured alkali halides and are reported in this chapter.

The peak position, the halfwidth and the oscillator strength of the F and F-aggregate bands in all the alkali halides studied were determined in the following manner. The peak position and halfwidth of the F band were accurately determined from the absorption spectrum of coloured specimens which were treated as described in section 1 of chapter 4. so

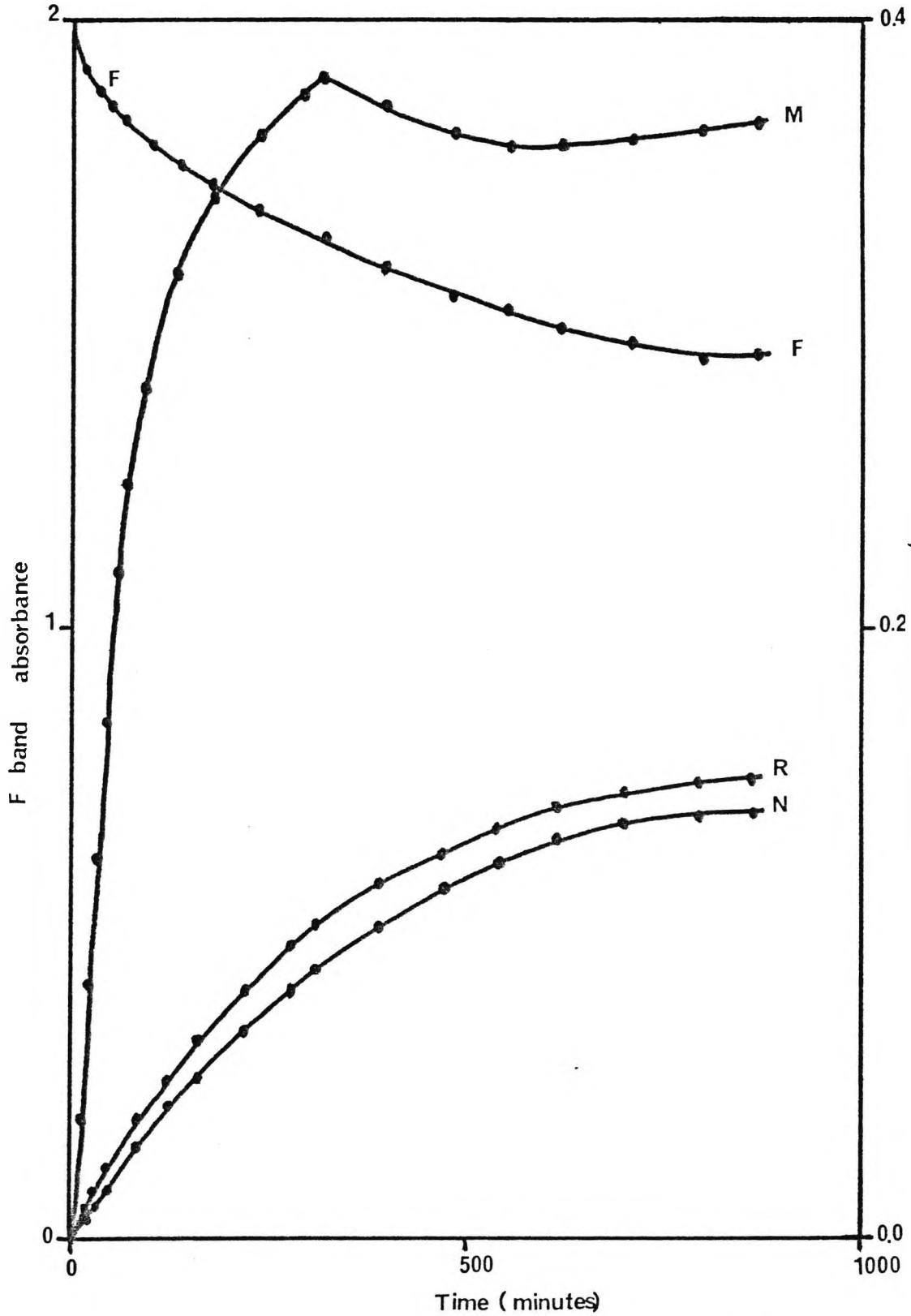

Figure 5.7 The evolution of the F-aggregate bands due to optical bleaching of the F-centres in NaBr as a function of the bleaching time

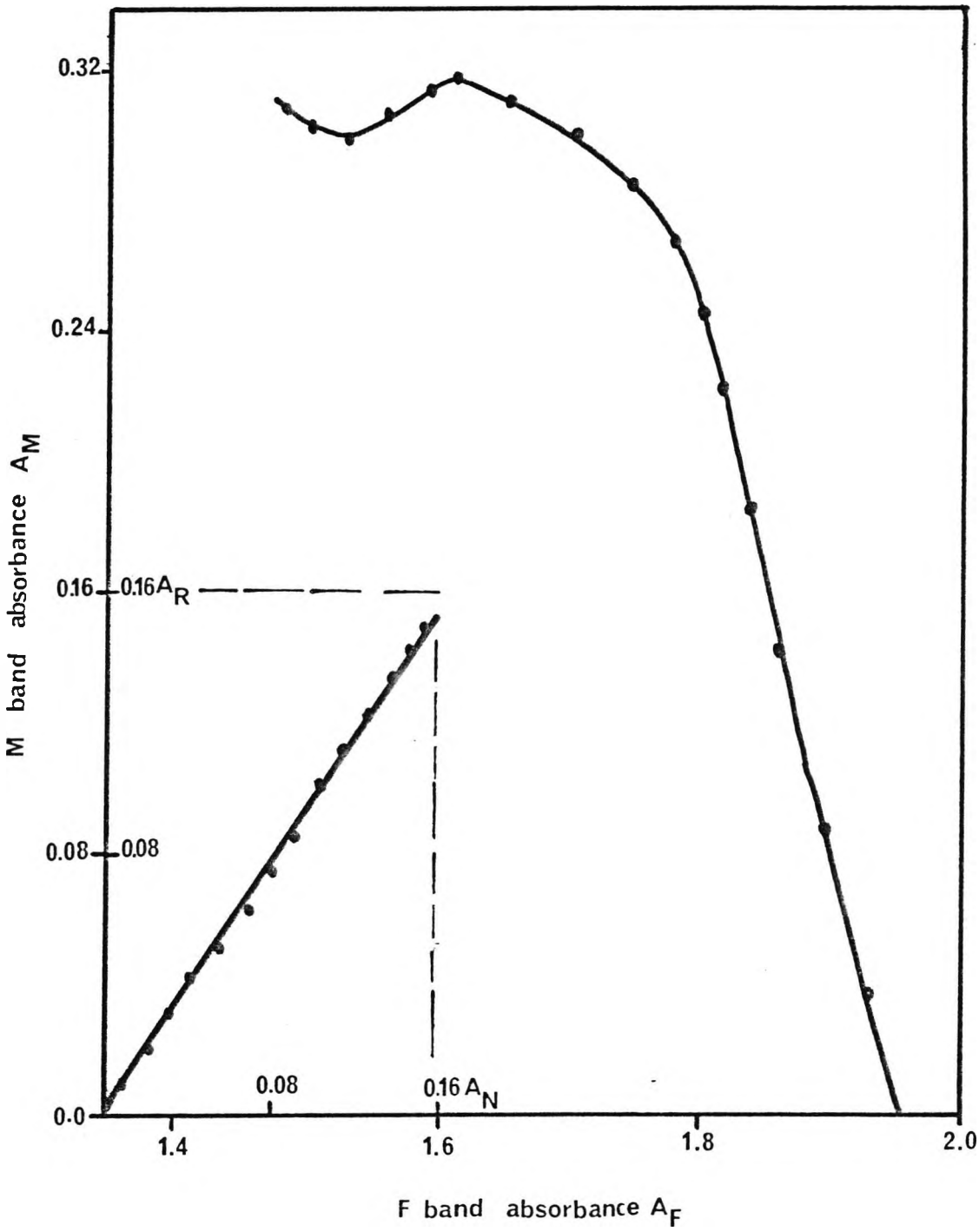

Figure 5.8 The relation between the R and N bands (inset) and between the F and M bands during F-light treatment of coloured NaBr

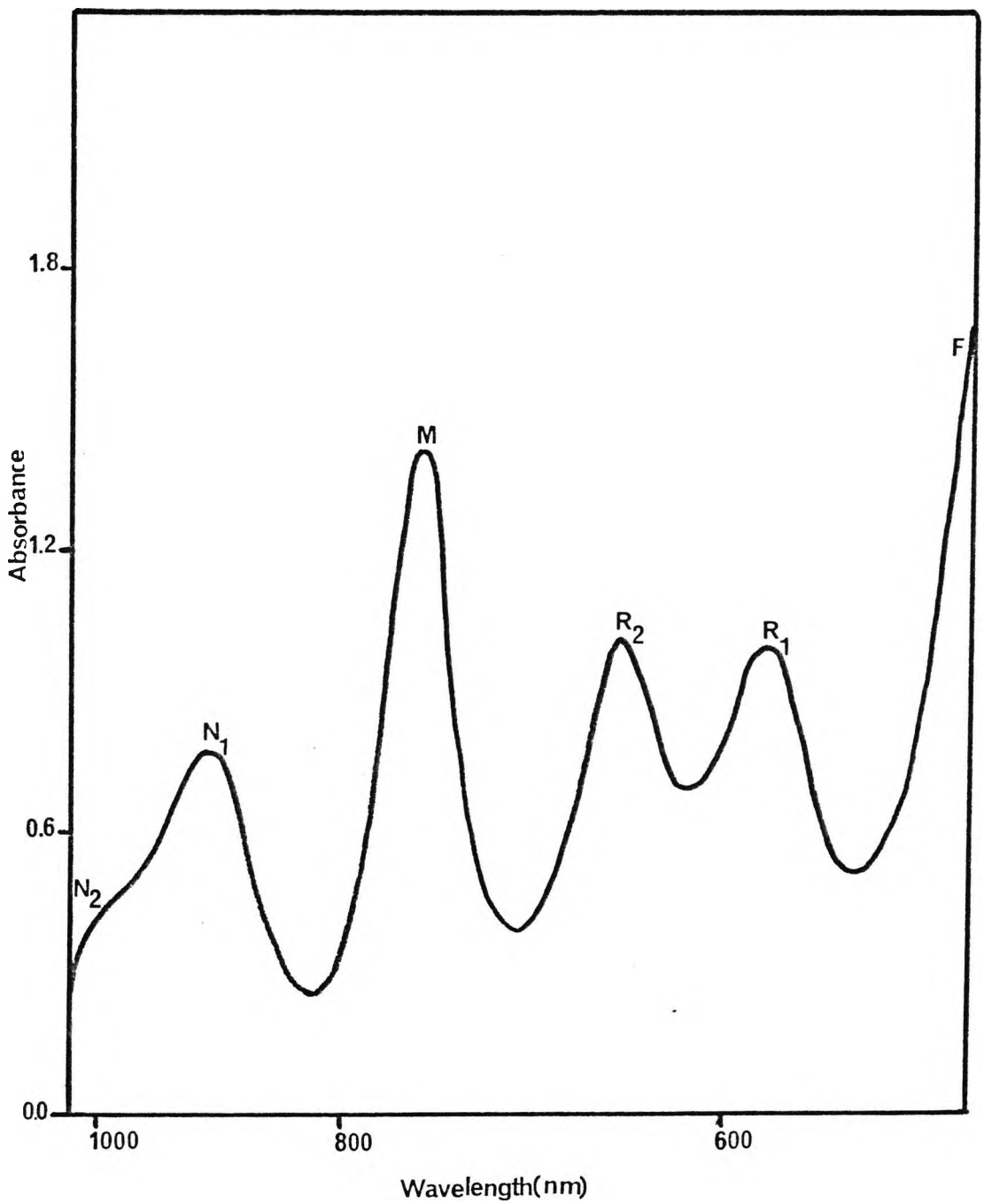

Figure 5.9 Absorption spectrum of the F-aggregate centres in electrolytically coloured NaBr measured at liquid nitrogen temperature

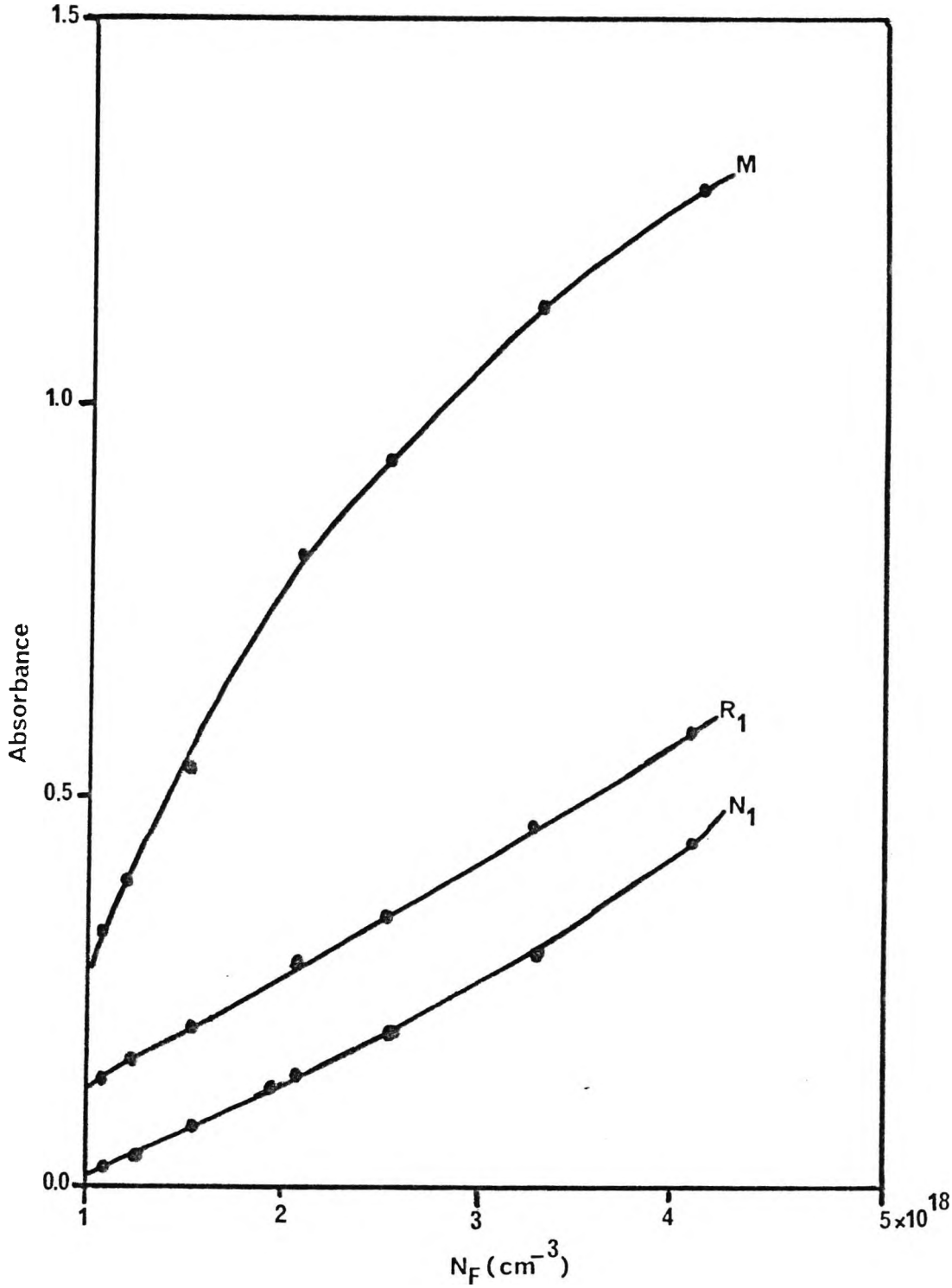

Figure 5.10 The growth of the F – aggregate bands by F – light treatment at room temperature as a function of the F – centre concentration in NaCl

that they contained only F-centres. Since the absorption bands of these centres were isolated, the problems of overlapping and underlying excited states of the F-aggregate bands were avoided. The concentration of F-centres was measured by calculating the number of injected electrons as described in section 1.2 of chapter 4. Inserting these parameter in Smakula's equation (equation (2.4)) it was possible to estimate the oscillator strength of the F band in various electrolytically coloured alkali halides. The results of these measurements are reported in table 5.1.

The peak position and halfwidth of the M band were determined in coloured specimens which contained strong M bands with no other F-aggregate band whatsoever present. This situation was created by bleaching electrolytically coloured specimens containing only F-centres at high concentration ($> 4 \times 10^{18}$ cm^{-3}) with F-light. The bleached specimens were then treated thermally as described in section 1.3 of this chapter to remove the R and N bands if any had been formed during the optical treatment. In this way the M band was well isolated and the results of such measurements are reported in table 5.3.

The long wavelength side of the R bands could easily be separated from the M band when the absorbance of the R bands was sufficiently high. The short wavelength side of the R bands was obtained by subtracting the absorption due to the long wavelength side of the F band from the observed R absorption. The peak position and halfwidth of the R , R_1 and R_2 bands were obtained using this method and the results are reported in table 5.4.

Knowing the peak position and halfwidth of the M band, the short wavelength side of the N band was resolved by subtracting the M absorption from the observed absorption in the N region. The N_1 and N_2 bands were assumed to be symmetrical on the energy scale and the results of such optical measurements are reported in table 5.5.

The results which are reported in the above mentioned tables were all reproducible to within 5% depending on the method of production of the F-aggregate centres. The absorption bands of the F- and F-aggregate centres were particularly reproducible when direct electrolytic coloration or F-light bleaching treatment was used. When produced by F-light bleaching, the R bands showed a tendency to shift their peak positions to shorter wavelengths compared with the peak positions of the same bands which were produced using electrolytic coloration. This effect may be due to the existence of the M_4 band which overlaps the R_1 band (Rolfe and Morrison 1977) caused by optical treatment.

In order to measure the oscillator strengths of the F- and F- aggregate bands, the above optical parameters were required as well as certain corrections to the absorption spectrum. A correction in the observed absorption coefficient of the F band μ_F has to be applied since the contribution of the various excited states of the M band at the wavelength of the peak position of the F band had to be eliminated (Rolfe and Morrison 1977). Neubert and Susman (1965) have shown that the oscillator strengths of the two higher excited states

Table **5.3.** Optical properties of the M band in electrolytically coloured alkali halides. Values given in parenthesis are calculated from Ivey's relation (1947)

	Peak Position (nm)	Halfwidth (eV)	Oscillator strength
KI	1050(1000)	0.213	0.232
	918 *	0.150	-
KBr	920 (897)	0.128	0.234
	880 *	0.079	-
KCl	828 (835)	0.156	0.253
	800 *	0.094	-
NaI	892 (871)	0.251	0.241
	883 *	0.079	-
NaBr	772 (770)	0.175	0.238
	760 *	0.092	-
NaCl	700 (701)	0.182	0.212
	693 *	0.096	-

Values referred to with asterisks were obtained at liquid nitrogen temperature . All other values were obtained at room temperature.

Table **5.4.** Optical properties of the R, R_1 and R_2 bands in electrolytically coloured alkali halides. Values given in parenthesis are calculated from Ivey's relation (1947)

	R band			R_1 band			R_2 band		
	nm	eV	f_R	nm	eV	f_{R_1}	nm	eV	f_{R_2}
KI	900	0.155	0.574	(834)	-	-	(902)	-	-
				841*	0.092	-	895*	0.089	-
KBr	800	0.142	0.526	(732)	-	-	(792)	-	-
				735*	0.088	-	795*	0.077	-
KCl	-	-	-	675(669)	0.096	0.41	735(725)	0.102	0.38
				667*	0.052	-	732*	0.061	-
NaI	780	0.172	0.551	(707)	-	-	(765)	-	-
				689*	0.107	-	780*	0.115	-
NaBr	670	0.165	0.502	(610)	-	-	(660)	-	-
				583*	0.095	-	655*	0.099	-
NaCl	-	-	-	550(547)	0.118	0.44	620(592)	0.127	0.32
				543*	0.084	-	600*	0.095	-

Values referred to with asterisks were obtained at liquid nitrogen temperature. All other values were obtained at room temperature.

Table **5.5.** Optical properties of the N, N_1 and N_2 bands in electrolytically coloured alkali halides.

	N band			N_1 band			N_2 band		
	nm	eV	f_N	nm	eV	f_{N_1}	nm	eV	f_{N_2}
KI	1250	0.162	0.075	-	-	-	-	-	-
				1100*	0.127	-	1154*	0.093	-
KBr	1120	0.186	0.081	-	-	-	-	-	-
				1081*	0.099	-	1148*	0.059	-
KCl	-	-	-	1000	0.108	.086	1100	0.189	0.107
				985*	0.072	-	1062*	0.097	-
NaI	1146	0.240	0.083	-	-	-	-	-	-
				1020*	0.104	-	1114*	0.082	-
NaBr	1000	0.183	0.106	-	-	-	-	-	-
				930*	0.083	-	1006*	0.078	-
NaCl	-	-	-	850	0.146	.068	1030	0.167	0.092
				828*	0.091	-	896*	0.074	-

Values referred to with asterisks were obtained at liquid nitrogen temperature. All other values were obtained at room temperature.

M_2 and M_2' of the M band are the same as those of the M_1 (commonly known as M) band. Utilising this fact together with Smakula's equation (equation (2.4)), the contribution of the excited states to the F absorption was found to lie between $0.6\,\mu_M$ and $0.9\,\mu_M$ for the alkali halides studied.

Assuming that the number of dissociated F-centres is equal to that of the optically created F-aggregate centres, changes in the concentrations of the F- and F- aggregate centres (ΔN_i) during an F-light bleaching experiment have been described by the equation (Compton and Rabin 1964)

$$\Delta N_F + 2\Delta N_M + 3\,\Delta N_R + 4\Delta N_N = 0 \qquad (5.1)$$

This assumption was possible since, in electrolytically coloured specimens, the V band was found to be unaffected by the optical bleaching. However, electrolytic coloration (using the pointed cathode) produced only F-and F-aggregate centres with no absorption bands in the ultra-violet region of the spectrum.

Since the refractive index of a specimen within the wavelength region covered by the F- , M- , R- and N- centres is nearly the same, the following equation is obtained using the Smakula equation and equation (5.1)

$$\frac{W_F}{f_F}\Delta\mu_F + 2\,\frac{W_M}{f_M}\Delta\mu_M + 3\,\frac{W_R}{f_R}\Delta\mu_R + 4\,\frac{W_N}{f_N}\Delta\mu_N = 0 \qquad (5.2)$$

where W_i , $\Delta\mu_i$ and f_i are the halfwidth (eV), the change in the absorption coefficient (cm^{-1}) and the oscillator strength of the particular colour centre respectively. Using the experimental values of f_F (table 5.1) and W_i (table 5.3 to table 5.5) it was possible to measure the values of f_M , f_R and f_N by taking three sets of experimental values of $\Delta\mu_i$ for the F , M, R and N bands produced by bleaching electrolytically coloured alkali halide specimens with F-light. The numerical values of f_M , f_R and f_N obtained by this method are given in tables 5.3, 5.4 and 5.5 respectively.

Irradiation of an electrolytically coloured NaCl specimen with M-light at room temperature produced a decline in the absorbance of the M band and an enhancement of the F, R and N_1 bands. When the same experiment was repeated using an NaCl specimen containing F-aggregate centres formed by F-light irradiation, the N_1 band was enhanced at the expense of the N_2 band. Subsequent bleaching with F-light led to the enhancement of the N_2 band at a greater growth rate than was the case for the standard F-light bleaching experiments under the same conditions.

Upon long periods of irradiation (12 hours) with M-light, electrolytically coloured specimens of NaBr and NaCl which had been treated previously with F-light for 20 hours

showed an enhanced F band with a gradual shift of its peak position towards longer wavelengths. Knowing the optical properties of the F band the shift is interpreted as due to the absorption band which is tentatively identified as the M_2 band (Rolfe and Morrison 1977). The peak position and halfwidth of the M_2 band in NaBr are measured as 532 nm and 0.18 eV respectively, while these parameters in NaCl are 459 nm and 0.17 eV respectively. These measurements were carried out at liquid nitrogen temperature. Before the M-light bleaching experiments were carried out, the R- and N-centres were eliminated thermally as described in section 1.3 of this chapter. In the case of NaCl which contained a high concentration of M-centres (1.26×10^{17} cm^{-3}) bleaching with M-light produced a small absorption band which, when measured at liquid nitrogen temperature, ocurred at a peak position of 527 nm with a halfwidth of 0.12 eV. This band has been tentatively identified as due to the M_4 -centre (Rolfe and Morrison 1977).

R-light bleaching experiments were carried out using specimens of electrolytically coloured KCl, NaI, NaBr and NaCl. Upon irradiation with R-light, all the specimens showed a decrease in the R band and an enhancement of the F and M bands followed by an enhancement of the N_1 band. Further R-light irradiation ($>$ 14 hours) led to the enhancement of the N_2 band. Irradiation with R_1 - and R_2 - light led to the same results.

1.3 Colloid centres

The evolution of the optical absorption spectrum of electrolytically coloured NaBr during the thermal annealing treatment. while exposed to laboratory light is shown in figure 5.11. The aggregation of F-centres into M- , R- and N- centres and the formation of colloid centres (C) were observed when the electrolytically coloured specimens were annealed for equal intervals (15 minutes) at successively increasing temperatures. Similar behaviour was observed when other electrolytically coloured alkali halide specimens were subjected to an identical treatment. The spectrum of the F-aggregate bands in NaCl obtained by thermal treatment is shown in Figure 5.12. Visual observation showed that, after annealing at temperatures higher than 300°C, a bleached layer appeared around the external faces of the specimens. This layer grew in thickness with increasing annealing temperature and, at temperatures higher than 400°C, the specimens were bleached completely. It seems from figure 5.11 that some F-centres were formed when the colloid band started to disappear with rising temperature. It is also apparent from the figure that the F-centres are more stable than the other colour centres, including the colloid centres. The convexity of the decay curves of the F-centre concentration in various electrolytically coloured alkali halides (see figure 5. 13) provides further confirmation of the formation process of F-centres from colloid centres.

When the electrolytically coloured specimens were heated in darkness, the absorption bands of the F-aggregate centres were absent and a pure colloid band was observed

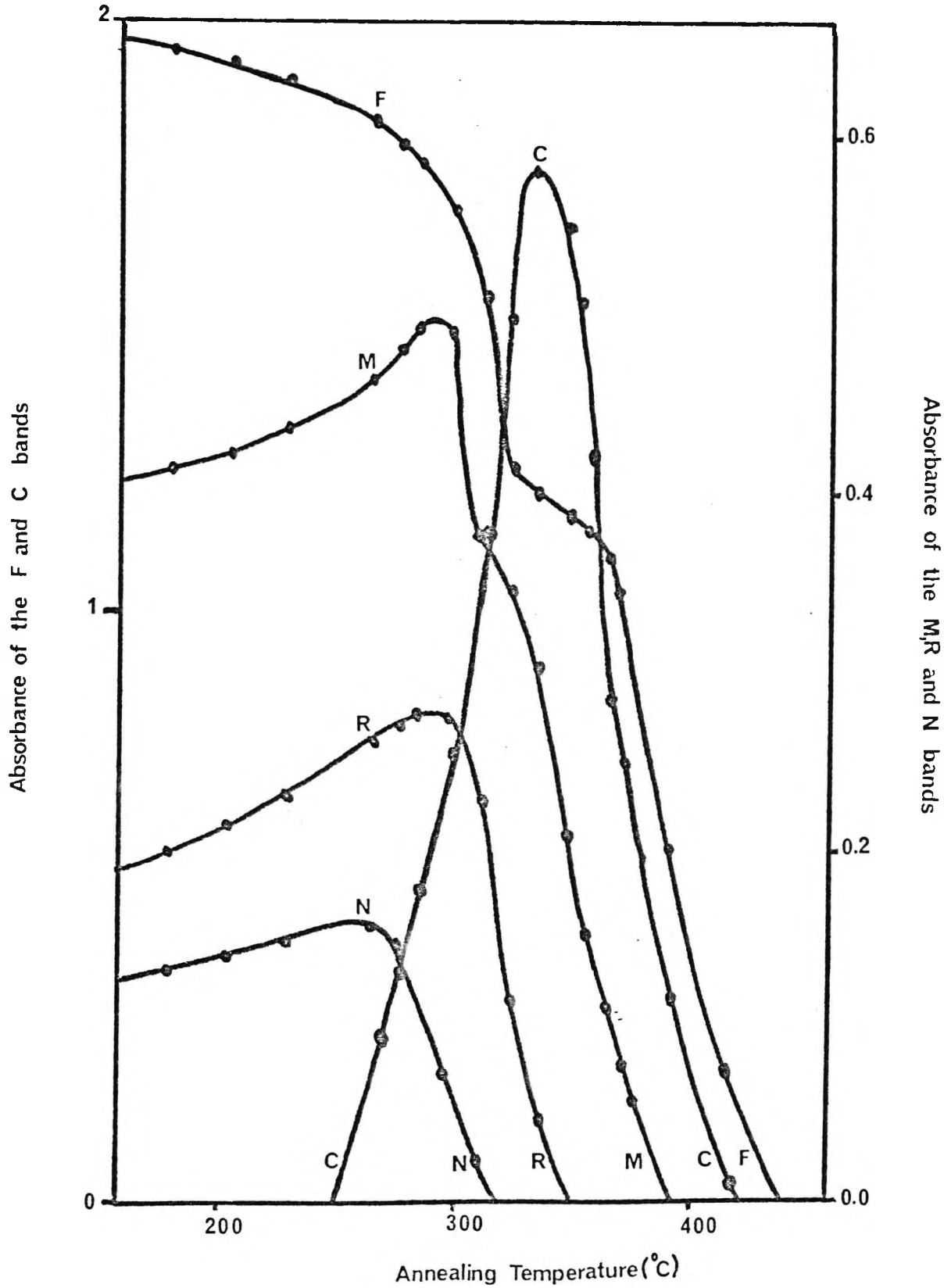

Figure 5.11 Evolution of the colour centres in electrolytically coloured NaBr due to thermal treatment

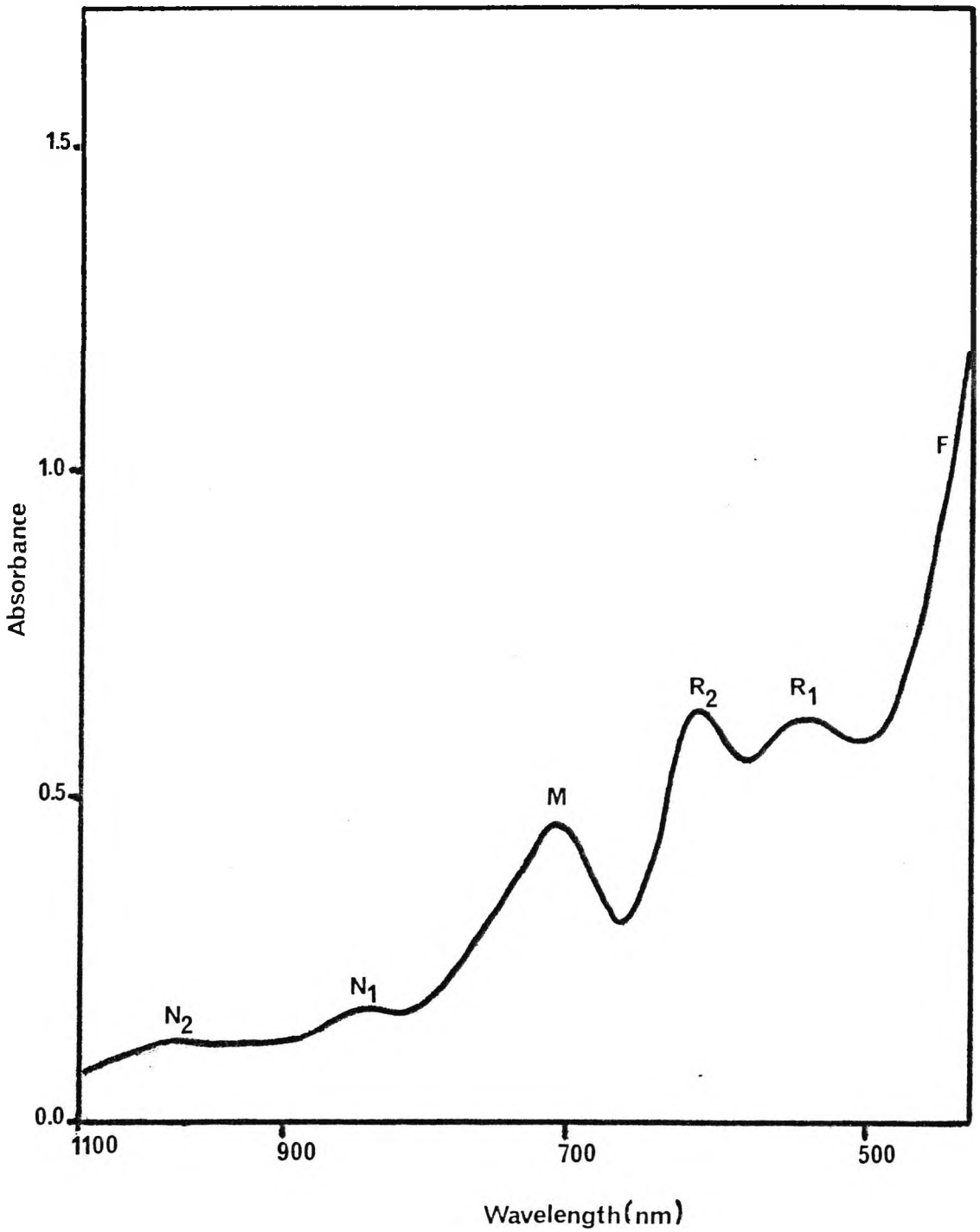

Figure 5.12 F-aggregate absorption bands produced by thermal treatment of NaCl

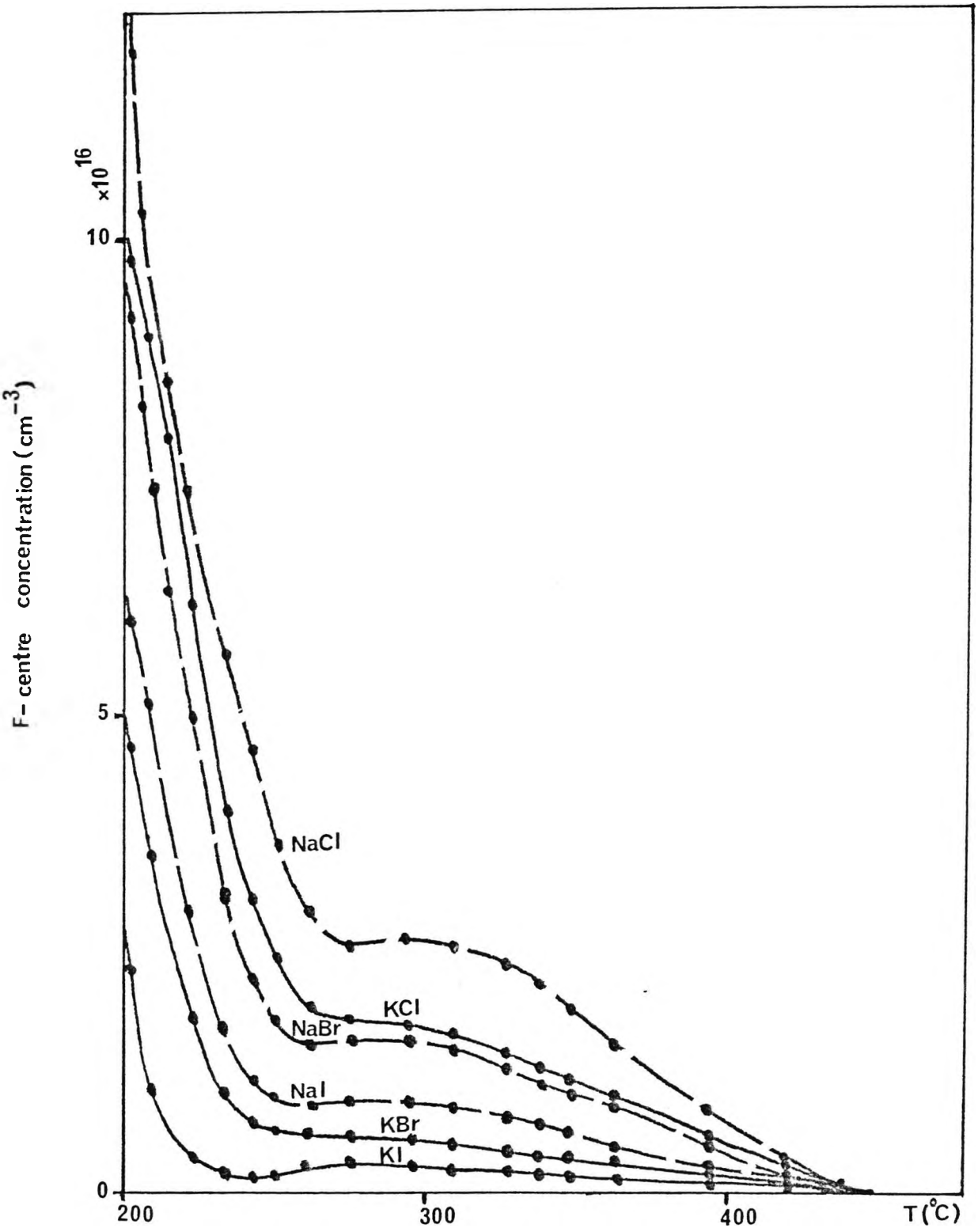

Figure 5.13 Thermal bleaching of F-centres in electrolytically coloured alkali halides as a function of temperature

at temperatures above 400°C. Most of the F-centres were converted into colloid centres at 450°C. As the temperature was raised higher, more and more F-centres were formed at the cost of the colloid centres. At about 550°C, the conversion of colloid centres to F-centres was nearly complete. Figure 5. 14 shows the case for electrolytically coloured NaCl . The temperatures of curves (a) and (b) are 500°C and 450°C respectively.

Prolonged annealing revealed that the colloid centres were stable up to about the same temperature range at which they were formed. Above this range (300°C to 400°) they became unstable. These temperatures are higher than those reported for both additively coloured specimens (250°C -Sastry 1969) and for specimens coloured by irradiation (200°C -Pappu and McCarthy 1970).

Table 5.6 reports the results of a systematic study of colloid centres in electrolytically coloured alkali halides. The calculated values of the peak positions λ (nm) of the colloid absorption bands in alkali halides were obtained using the relation $\lambda = (1 + 2n_0{}^2)^{\frac{1}{2}} \lambda_c$ provided by Doyle (1958) (equation (1.6), chapter 1). λ_c is the critical wavelength (nm) for the onset of ultra violet transparency of the alkali metal. Wood (1933) provided values of λ_c as follows: K (315 nm); Na (210 nm) and Li (205). The exact observed peak positions of the colloid absorption bands depended on the temperature and duration of the anneal. Also the rate of cooling affected the position and the width of the colloid band. Experiments on various alkali halides showed that the peak positions of the colloid absorption bands shifted to longer wavelengths when these specimens were subjected to temperatures higher than 550°C for more than four hours followed by cooling to room temperature over a period of more than five minutes. As the temperature was increased and the cooling time was reduced the colloid band decreased in height and became broader. The extreme cooling time used in this work was less than 30 seconds.

The observed colloid absorption bands were identified as those which are due to small colloids using the criterion that the line shape of the colloid band is insensitive to a change in specimen temperature from room temperature to liquid nitrogen temperature (Schulman and Compton ,1962). The colloid centres were not affected by any form of light bleaching at room temperature whether it was colloid-light, or F- , M- and R- light. Also neither white light nor ultra-violet light had any effect on these centres. These centres did not exhibit any Tyndall scattering which could be observed with a microscope.

2. Other colour centres

2.1 F_A -centres

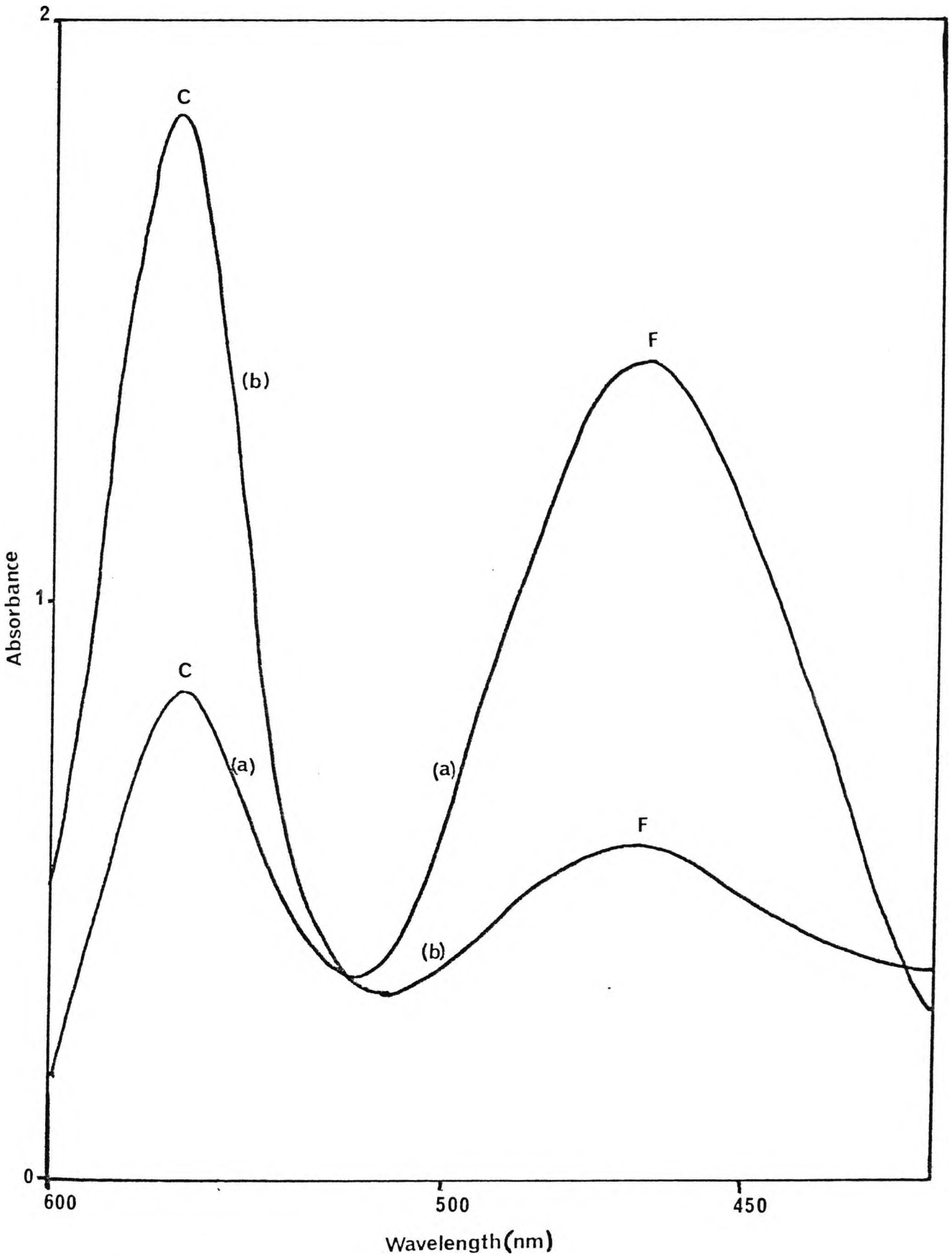

Figure 5.14 Thermal annealing of electrolytically coloured NaCl in darkness

Table **5.6.** Peak position and halfwidth of the colloid bands in electrolytically coloured alkali halides.

	Calculated values (nm)	Experimental values		Literature (nm)
		Peak position (nm)	Halfwidth (eV)	
KI	795.63	815	0.30	800
KBr	749.38	755	0.51	760
KCl	722.42	740	0.43	730
NaI	548.40	610	0.70	-
NaBr	524.56	575	0.64	-
NaCl	492.49	560	0.27	570

The first column contains the peak positions of the colloid absorption bands calculated using equation (1.6) as provided by Doyle (1958). The fourth column contains the reported values of peak positions of the colloid absorption bands in electrolytically coloured alkali halides. The first three values are given by Radchenko and Udod (1971) and the reported value for NaCl is provided by Karlsson and Beckman (1967).

In this work the peak position and the halfwidth of the absorption band of the electrolytically produced F_A - centres in some of the alkali halides are reported (see table 5.7). KI , KBr and KCl specimens were first treated as described in chapter 2 (see section 7.1). Then they were electrolytically coloured in such a way that only F-centres were present in the specimen at a concentration of about 10^{18} cm^{-3} . Some of the specimens showed a small F_A band after the coloration but this was not the case with all the specimens. F_A - centres were produced when the coloured specimens were subjected to irradiation with F-light at room temperature. After 90 minutes exposure to F-light all the F-centres were converted to F_A -centres. Further F-light treatment resulted in the appearance of the M absorption band and the reduction of the F_A band. However, treatment with F-light at liquid nitrogen temperature for a prolonged time (200 minutes) resulted only in the creation of a broad absorption band. The F_A absorption band never appeared even after further exposure to F-light. The broad band disappeared when the specimens were warmed to room temperature and the F_A absorption band was created.

The F_A absorption band usually appeared at the longer wavelength side of the F absorption band with an apparent overlapping between them. The peak position of the F band is shifted by about 10 nm to 20 nm from its usual position. This shift was usually to the longer wavelength side of the normal position in the case of F(Li) and to the shorter wavelength side in the case of F(Na). Using Luty's (1968) notation F_A (I) in table 5.7 refers to the F_A absorption band and F_A (II) refers to the shifted F band. The general feature of the peak positions of the F_A absorption bands is that F(Li) occurs a longer wavelength than F(Na).

The results of F_A - light treatment were not consistent for all the alkali halide specimens. Only in the case of KI (Na) was the conversion of the F_A band to the F absorption band noticeable as a result of F_A -light treatment at room temperature, while KBr (Na) and KCl (Na) had to be heated to 50°C to produce the same observable effect. The F(Li) absorption bands were stable even at temperature in excess of 50°C under F_A - light treatment.

Thermal treatment of alkali halide specimens containing F_A - centres showed that F-centres can be produced again when these specimens are subjected to a thermal anneal for 50 minutes in the dark at temperatures above or equal to 90°C. It took about 70 minutes to bleach the F_A band in the case of a KBr specimen which originally contained 10^{18} F - centres cm^{-3} . Thermal treatment of the other specimens showed also that the F_A absorption band was less stable than the F-aggregate absorption bands.

2.2 V centres

Table 5.7. Peak position and halfwidth of the F_A bands in electrolytically coloured alkali halides.

	F_A (I)		F_A (II)		F
	Peak position (nm)	halfwidth (eV)	Peak position (nm)	Halfwidth (eV)	
KI:Na	740	0.34	660	0.35	685
: Li	775	0.28	690	0.31	
KBr:Na	690	0.32	610	0.37	625
: Li	725	0.27	630	0.32	
KCl:Na	625	0.30	545	0.42	555
: Li	645	0.24	560	0.38	
KCl:Na	585*	0.23*	520*	0.26*	525*

Values referred to with asterisks were obtained at liquid nitrogen temperature. All other values were obtained at room temperature.

In this work attention was paid to the ultra-violet spectrum of the electrolytically coloured alkali halides other than KBr and KI. Table 5.8 gives the values of the peak position of the various V-centres produced using the electrolytic coloration method in KCl, NaI, NaBr and NaCl.

V-centres were produced electrolytically using the pointed anode method. The experimental conditions which were found to give reasonable coloration were 1 mA for the coloration current and a coloration temperature 50° C below the melting point of the particular alkali halide specimen. Under these conditions hole injection occured, and normally a pale yellowish colour migrated from the pointed anode to the flat cathode. When the coloured specimen had cooled to room temperature, this colour either disappeared, as in the case of KCl and NaCl, or changed to a pale brownish-yellow, as in the case of KI, KBr and NaBr. NaI specimens had a milky-yellow appearance at room temperature.

Curve (a) of figure 5.15 shows the optical spectrum of the V_F - designated band produced using the pointed anode method in NaBr. The peak position of this band is designated V_F in table 5.8 since many experiments have shown that V_F -centres produced using this method are the antimorph of the F-centres as has been suggested by Kanzig (1960). Using two pointed electrodes in an electrolytic coloration experiment with KCl showed that both F- and V-centres can be produced simultaneously. The two respective colours were found to emerge from the particular pointed electrode and to advance towards each other. When they met a colourless zone was created in the intermediate part between them. The normal absorption bands of the F- and V-centres were observed when the two coloured parts were investigated optically. The colourless zone showed no such absorption bands, as expected. In the cases when the quenching to room temperature was fast enough (10-15 seconds), other absorption bands appeared. The α band (see table 5.8) was recognised as one of them. The other absorption band is designated tentatively as the V band (the first values in the column labelled V) in table 5.8. This band may be due to the absorption band of the cation vacancy centre. When the KCl specimen was left in darkness, the F band bleached somewhat as the V_F -designated band bleached. This fact suggests that the latter is due to a hole centre. After the holes are released thermally, they are annihilated by combining with F-centres thereby bleaching a band otherwise stable at room temperature.

When the optical measurement were carried out at liquid nitrogen temperature, the width of the V_F band decreased as expected. However, the temperature shift of the peak position was not so large as that of the F band. It was possible to bleach the V_F band optically when an electrolytically coloured (pointed anode) NaI specimen was subjected to irradiation with V_F -light at room temperature. The V_F band bleached with no other V band appearing as was the case in the other alkali halides.

Leaving the V_F -coloured NaBr specimen in darkness at room temperature for four weeks was sufficient to bleach 27% of the V_F absorption band. This phenomenon was

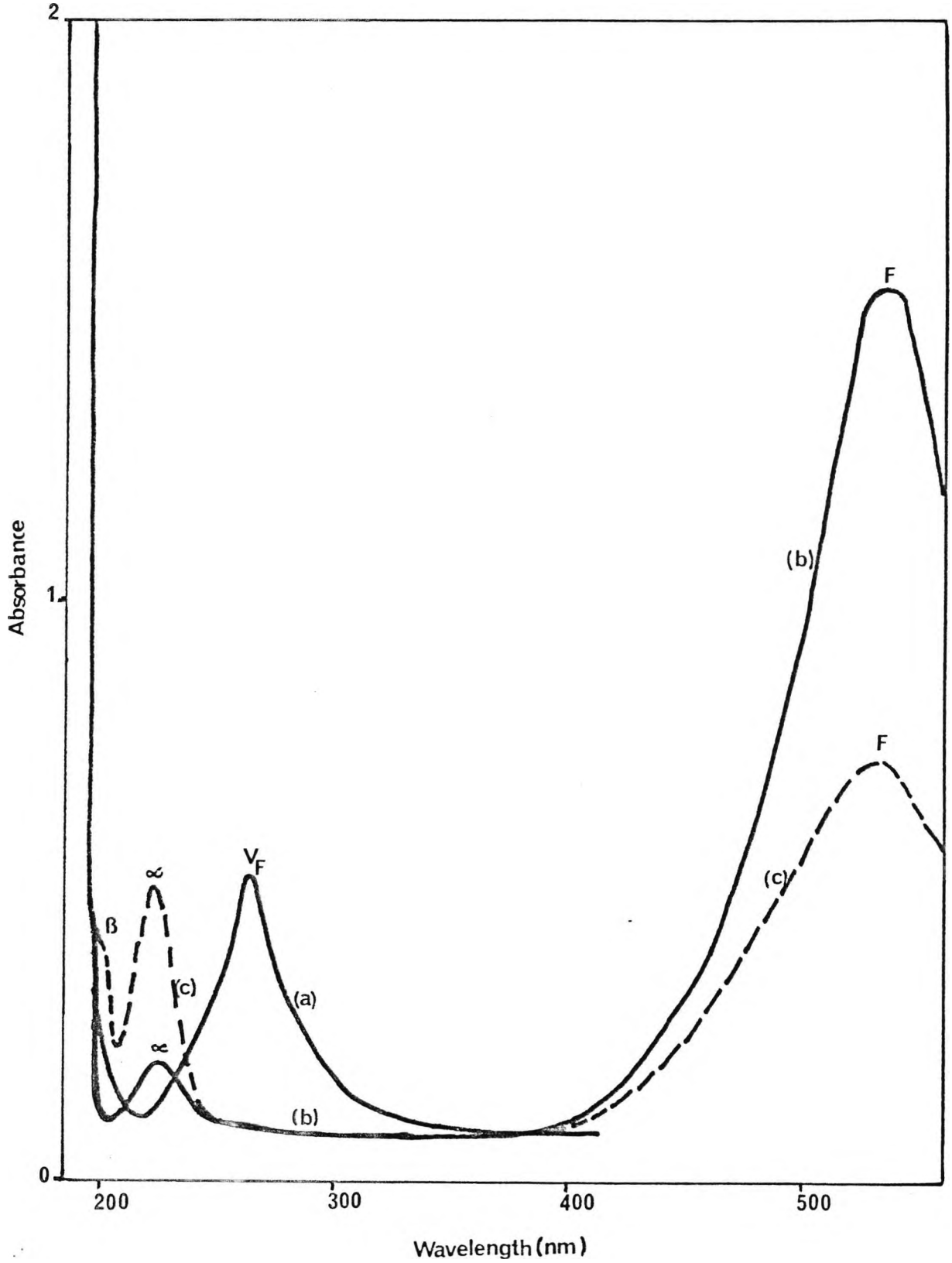

Figure 5.15 Ultra-violet absorption spectra of electrolytically coloured NaBr

Table **5.8** Peak position of the α, β, V_F and V bands in electrolytically coloured alkali halides. The halfwidth and the oscillator strength of the α band is also reported.

	α		β	V_F	V	f_α / f_F
	(nm)	(eV)	(nm)	(nm)	(nm)	
KI	284	.28	250	375	350, 330, 305	1.12
KBr	225	.73	215	265	256 , 235	1.17
KCl	213	.53	-	250	335, 284	1.25
NaI	246	.37	230	370	330	-
	225*	.29	218 *	260*	-	-
NaBr	230	.61	218	278	410, 263	-
	208*	.42	196*	262*	-	-
NaCl	210	.42	-	232	260, 280	1.23

Values referred to with asterisks were obtained at liquid nitrogen temperature. All other values were obtained at room temperature.

accompanied by the appearance of small humps in the ultra-violet spectrum. The peak positions of these new bands are reported in table 5.8 as V bands. The same process of bleaching, but with a considerably increased rate of V_F bleaching, was observed when the specimen was heated at temperatures of several hundred degrees above room temperature. It took only twenty one hours to bleach approximately the same amount of the V_F band when the specimen was heated in darkness at 300°C.

2.3 α -and β -centres

Table 5.8 reports the values of the peak positions of the α and β absorption bands. The values of the halfwidth of the α band are also reported. All the measured values were obtained at room temperature by the optical treatment of electrolytically coloured alkali halide. As in the previous section, additive coloration was used to confirm the results.

The α -centres were produced in this work by reversing the polarity of the electrode after the normal procedure of electrolytic coloration was complete. This process led to the disappearance of the whole coloration. The specimen was then quenched (10 to 15 seconds) to room temperature. The subsequent absorption spectrum showed a prominent α band. The identification of this band was confirmed by optical bleaching experiments at liquid nitrogen temperature. This method is widely reported in the literature as the normal procedure for producing α - centres in alkali halides (Markham 1966). Figure 5.15 shows the relation between the disappearance of the F band and the emergence of the α band in NaBr. Curve (c) shows the absorption spectrum of a partially bleached specimen compared with the absorption of less bleached specimen (Curve (b)).

The reported values of the α band oscillator strength (f_α in table 5.8) were measured using Smakula's equation (equation (2.4)) and the following relation provided by Markham (1966).

$$2F \longrightarrow \alpha + F' \qquad (5.3)$$

The measured values of the f_α were obtained by comparison with the oscillator strength f_F of the F band.

The values of the peak positions of the β absorption bands are also reported in table 5.8. This band has been identified as it normally appears between the α band and the fundamental absorption edge. At room temperature the β band usually appeared as a hump on the fundamental absorption edge but it grew to be a recognisable single band in KI, KBr, NaI and NaBr. In KCl and NaCl the β band overlapped the α band so it is not possible to report the exact peak position of the β band in either of these materials.

3. Conclusion

Upon bleaching F-centres using F-light, the M band grows during the early stage of irradiation and then starts to decline after reaching a maximum. R_1, R_2, N_1 and N_2 bands grow continuously and eventually approach saturations. This behaviour is similar to that of the additively coloured and heavily X-rayed alkali halides. Since no changes have been noticed in the optical parameters of the F band following bleaching with R-light, the suggestion by Compton and Rabin (1964) that the R_3 band exists under the F band is not confirmed. Subsequently, no correction to the F band due to R_3 band has been applied. The results of the M-light irradiation may lead to the conclusion that the $\acute{R}$-centre has been formed, since subsequent bleaching with F-light results in a greater growth rate for the production of the N-centre than by the normal irradiation with F-light. Irradiation of alkali halides at liquid nitrogen temperature with F-light leads to the formation of very broad absorption bands. These bands are identified as F' but it is very difficult to measure their peak positions or their halfwidths.

On annealing the electrolytically coloured alkali halides at high temperatures, the N-centres are the first to be destroyed thermally followed by the R- and M-centres. During thermal annealing colloid centres are produced and on further annealing they start to bleach to the advantage of the F-centres. Thermal treatment experiments show that electrolytically produced colour centres are more stable than those produced by either the irradiation or the additive coloration methods. The thermal conversion of F-centres into colloid centres is faster and occurs at lower temperatures when the thermal annealing is accompanied by irradiation with F-light or is performed in daylight compared with the same process in darkness.

The identification of the absorption bands of the electrolytically (pointed anode) produced V-centres in this work is taken cautiously since only four of these bands are satisfactorily identified. The notation V_1 , V_2 , ... , V_7 has not been used since the same notation has been given in the literature to bands which actually differ in peak position and halfwidth (Seitz 1954, Schulman and Compton 1962). The results of the electrolytic coloration experiments carried out with two pointed electrodes confirm that the V_F - designated band is due to a hole centre, since a recombination process between the F- and V_F - centres takes place in the zone where the two centres meet. Optical measurements on the colourless zone show that both centres are annihilated when their coloration meet.

The reported values of the optical properties of the various colour centres have been confirmed by comparison with the values calculated from the Ivey (1947) relations and by those reported in the literature whenever possible. It is important to note that the values reported in the literature vary from one work to another according to the different methods of coloration and the conditions of the various thermal and optical treatments. A distinct

advantage of the results of this work is that they are produced under similar conditions. The results obtained by additive coloration have not been reported since they are similar to those obtained by electrolytic coloration. Moreover, not all the reported colour centres can be produced using additive coloration. The results are also difficult to reproduce and, in general, the halfwidths of the absorption bands produced using additive coloration have a tendency to be broader compared with those obtained using electrolytic coloration.

4. References.

Barr L W, Hoodless I M , Morrison J A and Rudham R 1960,Trans. Faraday Soc. 56 697

Boni M, Gamagni P and Giani E 1975 J.Phys. Chem. Solids 36 883

Chandra S and Rolfe J 1970 Can.J.Phys.48 397

Compton W D and Rabin H 1964 Solid St.Phys. 16 121

Doyle W T 1958 Phys. Rev. lll 1067

Etzel H W and Maurer F J 1950 J.Chem.Phys.18 1003

Fontana M P and Van Sciver W J 1970 Phys.St.Solid 37 375

Fowler W B 1984 Physics of Color Centers-Academic Press

Greenwood N N 1984 Ionic Crystals, Lattice Defects and Nonstoichiometry - Butterworths

Gritsenko Yu I 1971 Phys.St.Solid (a) 7 K113

Hacskaylo M and Groetzinger G 1952 Phys. Rev.87 789

Hadly W B 1968 Int. Symp. on Colour Centres in Alkali Halides Rome

Heiland G 1950 Z.Phys. 128 144

Hoodless I M , Strange J H and Wylde I E 1971 J.Phys. C: Solid St. Phys. 4 2737

Ivey H F 1947 Phys. Rev. 72 341

Kanzig W 1960 Phys. Rev. Lett. 4 117

Karlson A V and Beckmann O 1967 Solid St. Commun. 5 795

Konitzer J D and Markham JJ 1957 Phys. Rev. 107 685

Luty F 1960 Z.Phys. 160 1

1968 see Fowler 1984 ch.4

Markham JJ 1966 Solid St. Phys. Suppl.8

Mott N F and Gurney R W 1948 Electronic Process in Ionic Crystal-Dover

Neubert T J and Susman S 1965 J.Chem.Phys. 43 2819

Pappu S V and McCarthy K A 1971 J.Phys. Chem.Solids 32 1295

Paramo N and Schanchez C 1971 J>Phys.Soc.Japan 30 1106

Pick H 1958 Nuovo Cimento d.Supple. 7 498

Radchenko i S and Udod V V 1971 Sov.Phys.-Solid St. 12 1186

Rolfe J 1964 Can.J.Phys. 42 2195

Rolfe J and Morrison S.R. 1977 Phys. Rev. B 15 3211

Sastry P V 1969 J.Phys.Soc. Japan 26 73

Schulman J H and Compton W D 1962 Colour Centres in Solids Pergamon Press

Seitz F 1950 Phys. Rev. 80 239

1954 Rev. Mod. Phys. 26 7

Tyler W W 1952 Phys. Rev. 86 801

Urusovskaya A A 1969 Sov. Phys. -USP 11 631

Whitworth R W 1975 Adv. Phys. 24 203

Wood R W 1933 Phys.Rev. 44 353

CHAPTER SIX

Electrolytic Coloration of Mercury-Doped Alkali Halides

1. Electrolytic coloration of alkali fluorides

1.1 The case of nominally-pure specimens

In common with other attempts to colour nominally-pure alkali fluorides electrolytically, electrolytic coloration of nominally-pure KF yields a weak and uneven coloration. Although the magenta colours (at the coloration temperature) associated with the successful experiments on mercury-doped KF was observed in the nominally-pure KF in the high-field region near to the pointed cathode, the coloration failed to move into the bulk of the specimen. Quenching nominally-pure KF to room temperature after the completion of an electrolytic coloration experiment, produced a green colour in the region around the pointed cathode. This colour is related to the F absorption band peaking at 450 nm. It seems that F-centres are produced electrolytically in nominally-pure KF but they are blocked near to the pointed cathode without being able to move towards the flat anode as is the case for the other nominally-pure alkali halides.

Electrolytic coloration of nominally-pure NaF and LiF specimens was also investigated using various coloration conditions. In all cases the single specimens of NaF and LiF showed no coloration whatsoever. Although no coloration could be observed visually or by using the spectrophotometer, the current-temperature relationship of electrolytically coloured NaF showed similar structural features to those given in figures 3.8 and 4.1 (chapters 3 and 4 respectively) for the other nominally-pure alkali halides. This observation suggests that a similar process to that which characterises electrolytic coloration in nominally-pure alkali iodides, bromides and chlorides is taking place in nominally-pure alkali fluorides. The F-centres are produced electrolytically but at very low concentration which the spectrophotometer cannot detect. The coloration temperature had to be kept as high as 760 °C, 840 °C and 820 °C for KF, NaF and LiF respectively in order to observe the above results. In these experiments it was observed that some material was always deposited on the pointed cathode after the electrolytic coloration was completed. A similar observation could only be made after the electrolytic coloration of nominally-pure alkali iodides, bromides and chlorides when the constant voltage method was used with a value of $\frac{V}{d}$ less than 30 V cm^{-1}, where V is the applied inter-electrode potential difference and d is the specimen thickness.

This phenomenon was also observed by Heiland (1950) for KCl specimens and was attributed to the elimination process of the alkali metal on the pointed cathode.

Using the sandwich technique, it was possible to produce F-centres electrolytically in nominally-pure alkali fluorides. The combination NaCl-NaF-NaCl was electrolytically coloured at 780°C with the NaF specimen acquiring a purple colour when it was quenched to room temperature. The spectrophotometric data showed a prominent F absorption band with an estimated 1.06×10^{16} cm^{-3} of F-centres concentrated in the region near to the cathode surface of the specimen. The purple colour faded away in the region near to the anode surface of the specimen while the spectrophotometric data obtained from this part of the specimen showed no absorption band of any kind. When this combination was replaced by one which consisted only of NaF specimens, the purple colour was not observed nor did the optical measurements show any results which differed from those obtained for single specimens of nominally-pure NaF. Using the constant voltage method with a $\frac{V}{d}$ value of 10^4 V cm^{-1}, it was possible to colour the NaF-NaF-NaF combination with various colloid centres. The cathode surfaces of the three specimens were coloured with red laminae. The coloration was partial and was located on certain lines suggested to be dislocation lines by Kubo (1966, 1969). The optical measurements showed the absorption bands of colloid centres of various sizes peaking in the region 485 nm to 515 nm.

1.2. The case of mercury-doped specimens

In marked contrast to the nominally-pure material, specimens of KF containing significant concentrations of Hg^{2+} cations (about 10^{18} cm^{-3}) coloured readily and homogeneously within the approximate temperature range 600°C to 800°C. Specimens of mercury-doped KF coloured electrolytically at 600°C appeared brown-yellow after quenching to room temperature and showed the maximum number of features in the visible. The ultra-violet spectrum of this specimen is shown in chapter 3 (figure 3.4 curve (a)). When the polarity of the pointed cathode was reversed, the de-coloration process started from the new cathode with subsequent optical measurements showing the absence of the F, F-aggregate and Hg^{2+} absorption bands (figure 3.4, curve (b)). a further change in polarity to restore the negative potential to the pointed cathode was unable to induce any coloration and the specimen behaved as if nominally-pure.

Similarly calcium-doped KF specimens were readily and homogeneously coloured within the same approximate temperature range (600°C to 800°C) but, unlike the mercury-doped KF, they could be coloured electrolytically again after the de-coloration process. Since it was not possible to see the changes in the absorption band of divalent calcium, if any, due to electrolytic coloration and de-coloration, and in order to investigate the role of the divalent

cations in both cases, ionic conductivity measurements were carried out using various KF specimens. The ionic conductivity of nominally-pure KF as well as that of mercury-doped KF before coloration and after de-coloration are shown in figure 6.1. The ionic conductivity of calcium-doped KF is also shown in figure 6.1. Curve (a) represents the results obtained for both the calcium-doped specimen before electrolytic coloration and after the de-coloration treatment. This curve shows clearly that electrolytic coloration and subsequent de-coloration does not induce any changes in the ionic conductivity of calcium-doped KF. Curves (b) and (d) show the ionic conductivity of mercury-doped KF before electrolytic coloration and after de-coloration respectively. The results obtained from these three curves and those of the optical measurements as discussed in sections 1.1 and 1.2 of chapter 3 demonstrate clearly, when compared with the above observation of the different effect of de-coloration on the colourability of KF containing mercury and calcium, that the presence of the divalent cations in the specimens is the essential factor in the successful electrolytic coloration of KF.

The presence of divalent calcium and the absence of divalent mercury in KF after de-coloration is the reason why calcium-doped KF may be coloured again, whereas the behaviour of mercury-doped KF is equivalent to that of the nominally-pure material and cannot be subsequently electrolytically coloured.

The energies which are calculated from figure 6.1 are 2.84 eV and 0.81 eV for the Schottky formation energy E_S and the cation vacancy migration energy E_m respectively. The value of E_S satisfies well the inequality (Chandra and Rolfe 1970)

KI (2.21) < KBr (2.53) < KCl (2.59) < KF (2.84)

The value of E_S for KBr was obtained from Rolfe (1964).

Specimens of NaF doped with approximately 10^{18} Hg^{2+} cm^{-3} coloured readily and homogeneously in the temperature range 690°C to 920°C. Only F-and M- centres could be introduced electrolytically into these specimens regardless of the coloration conditions. LiF specimens doped with approximately 10^{18} Hg^{2+} cm^{-3} were also readily coloured in the temperature range 700°C to 810°C. The maximum concentration of F-centres achieved in LiF specimens was 2×10^{17} cm^{-3}, which is an order of magnitude lower than that obtained by using the irradiation method of coloration (Perez et al, 1973). The two-stage electrolytic coloration / de-coloration process was applied to mercury-doped NaF and LiF specimens. In both cases these specimens could not be coloured after the de-coloration treatment. It is also shown here that the removal of the divalent mercury (see the results reported in section 1, chapter 3) by the de-coloration treatment leads to a reduction of the colourability of mercury-doped NaF and LiF to that of the nominally-pure state.

Figure 6.2 shows the current density-time relationship of two mercury-doped NaF specimens containing identical amounts of divalent mercury (10^{18} cm^{-3}) coloured

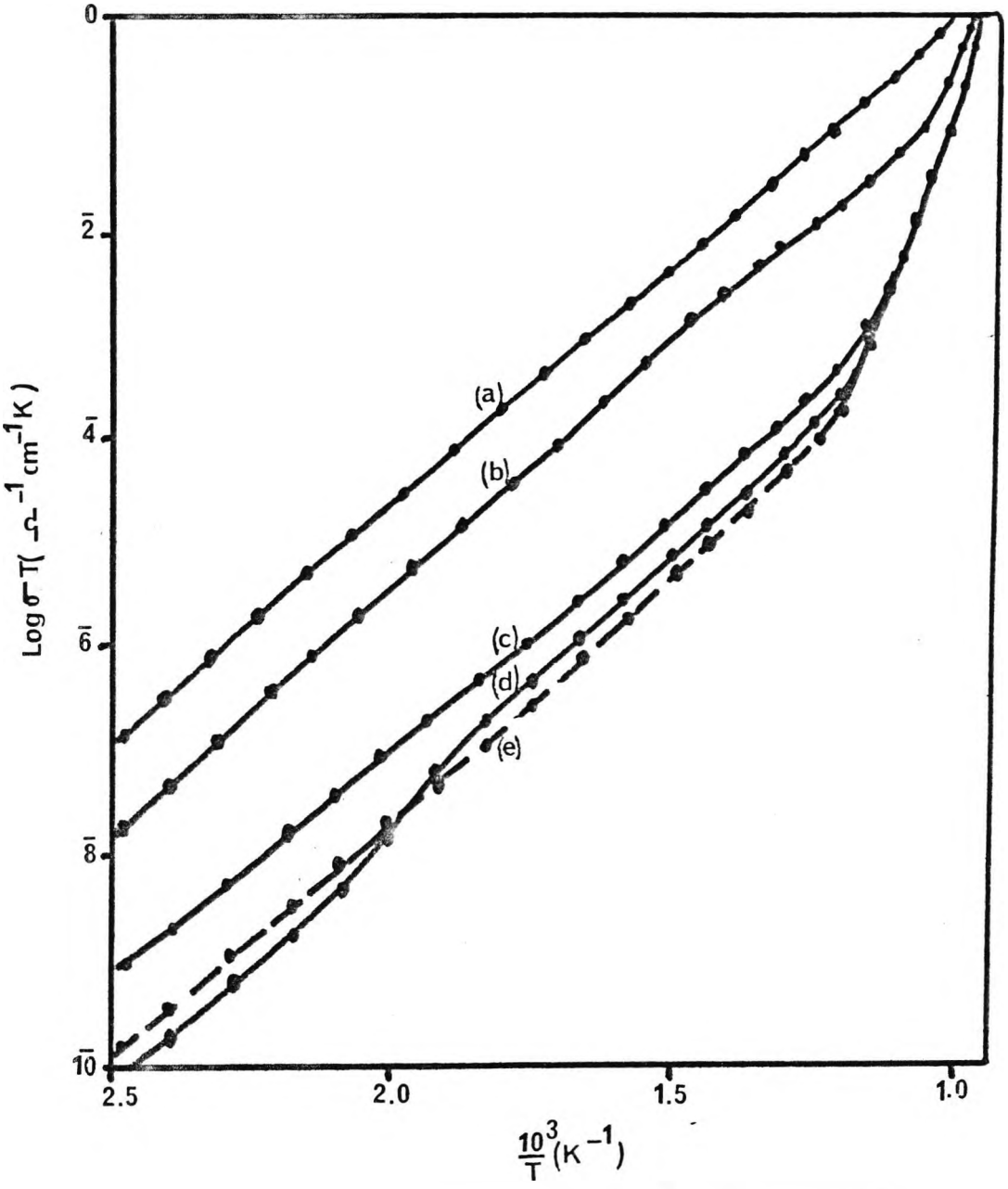

Figure 6.1 Ionic conductivity of KF (a) Ca^{2+}-doped, (b) Hg^{2+}-doped, (c) OH^{-}-doped, (d) Hg^{2+}-doped after de-coloration and (e) nominally-pure

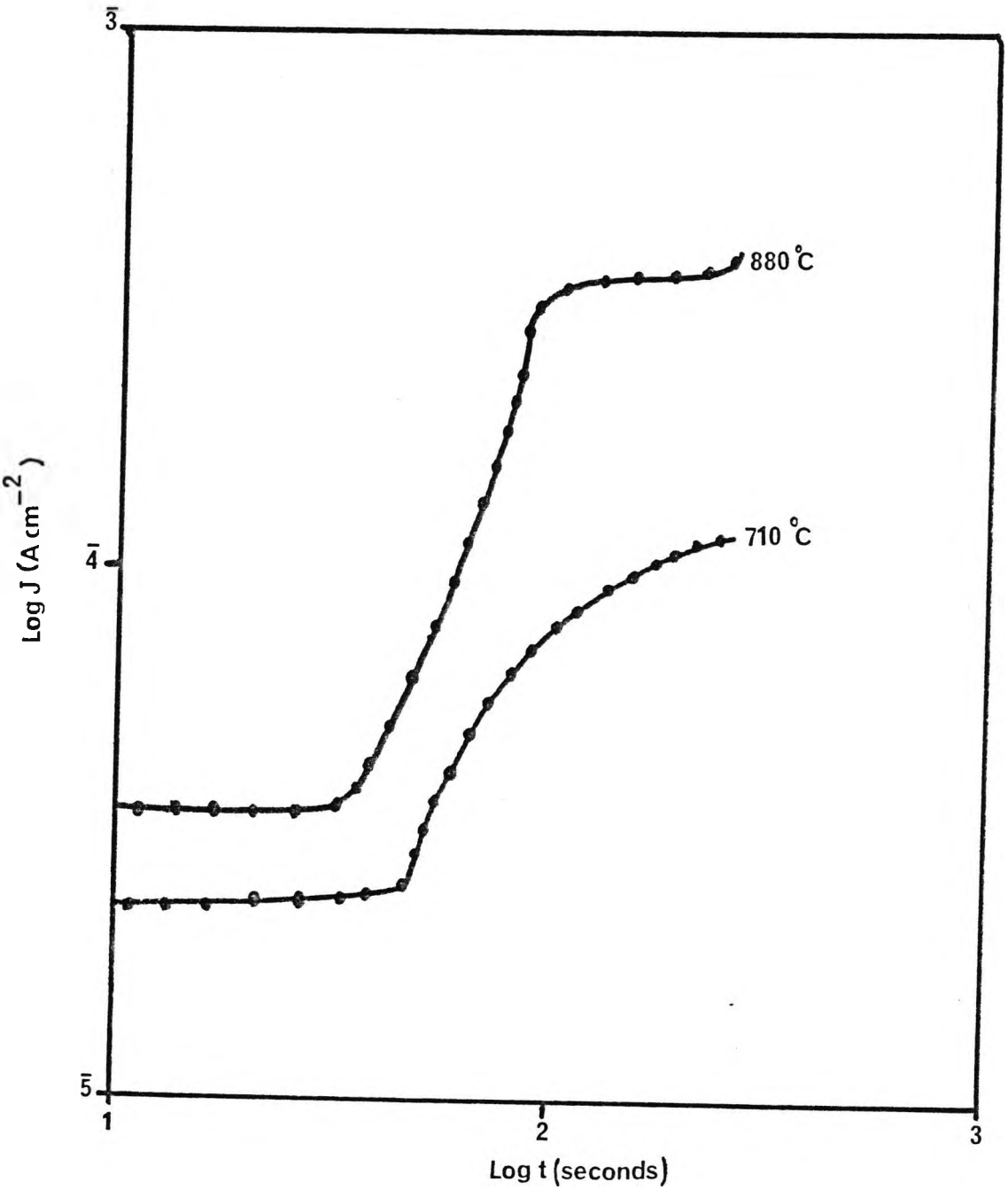

Figure 6.2 Current density–time relationship of NaF:Hg^{2+}

electrolytically at 710°C and 880°C. The first part of this relationship, which characterises the ionic process prior to the coloration starting temperature T_c, is understandably shorter for the experiment carried out at 880°C. But the absence of the steady-state current stage and the low rate of coloration are the most obvious features of the experiments carried out at 710°C. This may indicate the role of the anion vacancy in the formation of F-centres. The concentration of free anion vacancies is determined by the conditions for the thermodynamic equilibrium of ionic defects. Lowering the coloration temperature leads to a reduction in anion vacancy concentration in the temperature range of cation vacancy migration, and so there are less traps for the injected electrons in the experiment carried out at 710°C than in that carried out at 880°C.

1.3 Diffusion of F-centres

Diffusion measurements were carried out in order to investigate the role of the divalent mercury in promoting the coloration rate as was discussed earlier. The diffusion coefficient D of F-centres was measured by using the relation provided by Tyagi et al (1970)

$$D = \frac{(r_2^2 - r_1^2)}{4t}\left[\ln \frac{\left(\frac{\mu_1}{\mu_1 - \mu_2}\right)\ln\left(\frac{r_2}{r_1}\right) + \ln\left(\frac{r_1}{r_0}\right)}{\left(\frac{\mu_2}{\mu_2 - \mu_3}\right)\ln\left(\frac{r_3}{r_2}\right) + \ln\left(\frac{r_2}{r_0}\right)}\right]^{-1} \qquad (6.1)$$

where r_1, r_2 and r_3 are three different points along the length of the electrolytically coloured specimen measured from the pointed cathode, and r_0 is unit distance from the point. μ_1, μ_2, and μ_3 are the absorption coefficients of the specimen at points r_1, r_2 and r_3 and t is the coloration time. Diffusion coefficients of F-centres were also measured using the bleaching method. The average F-centre diffusion coefficients were evaluated from the bleaching rated. Uniformly coloured specimens (coloration was carried out at various values of temperature and time) of thickness 1.0 mm to 3.5 mm were annealed in vacuo in the dark for various intervals of time t and were then quenched to room temperature. Subsequently, the diffusion coefficients were determined from the relation provided by Shavarts et al (1974)

$$\ln \frac{N_0}{N} = \frac{\pi^2}{d^2} Dt \qquad (6.2)$$

where N_0 and N are concentrations of F-centres before and after each annealing treatment respectively and d is the thickness of the specimen. The results obtained from both methods of measurement were identical.

KF specimens containing two different concentrations of divalent mercury cations as well as calcium-doped specimens were used in the measurements of the diffusion of F-centres in electrolytically coloured specimens. The results are shown in figure 6.3. Curve (a) of the figure shows the results of the calcium-doped KF while curves (b) and (c) show the results of the mercury-doped KF specimens. The activation energy E_d for the diffusion of F-centres in these specimens was measured from each line in figure 6.3 using equation (3.6), chapter 3. The three values of E_d are very close and the average value calculated from the three lines is 0.784 eV. This value is very close to 0.810 eV which is the value reported in the previous section for the migration of the cation vacancy in KF. The experimental results of figure 6.3 demonstrate clearly that the diffusion coefficient D increases with the concentration of divalent cations but the migration energy of F-centres is independent of the nature and concentration of the divalent cations.

Figure 6.4 shows the results obtained from diffusion measurements using KCl specimens containing various concentrations of divalent mercury cations. The experimental results of curves (a) and (b) show similar features to those obtained from the diffusion measurements using KF specimens. The average activation energy E_d calculated from these lines is 0.682 eV. It is very close to the value of 0.690 eV for the activation energy for the migration of the cation vacancy E_m obtained from ionic conductivity measurements (see section 2.1 chapter 3) on KCl. The low temperature part of curve (c) in figure 6.4 gives a similar value for E_d. However, as the coloration temperature rises above the range of extrinsic conductivity, the diffusion coefficient increases steeply with temperature as is shown by the upper part of curve (c). The activation energy E_d calculated from this part is 0.87 eV and is very close to the value of 0.90 eV for the self-diffusion of K^+ ions reported by Jain and Parashar (1964) using a radio-tracer technique. Tyagi et al (1970) reported similar results for the diffusion of F-centres in pure KCl. It seems that, at low coloration temperature (extrinsic region of ionic conductivity) and low concentration of divalent cations, the diffusion of F-centres proceeds along cation vacancies. As the coloration temperature rises towards the intrinsic region of ionic conductivity the diffusion of F-centres is mainly governed by the self-diffusion of K^+ ions. By increasing the concentration of divalent cations, the migration mechanism of the diffusion of F-centres along cation vacancies extends to a higher coloration temperature.

2. Optical properties

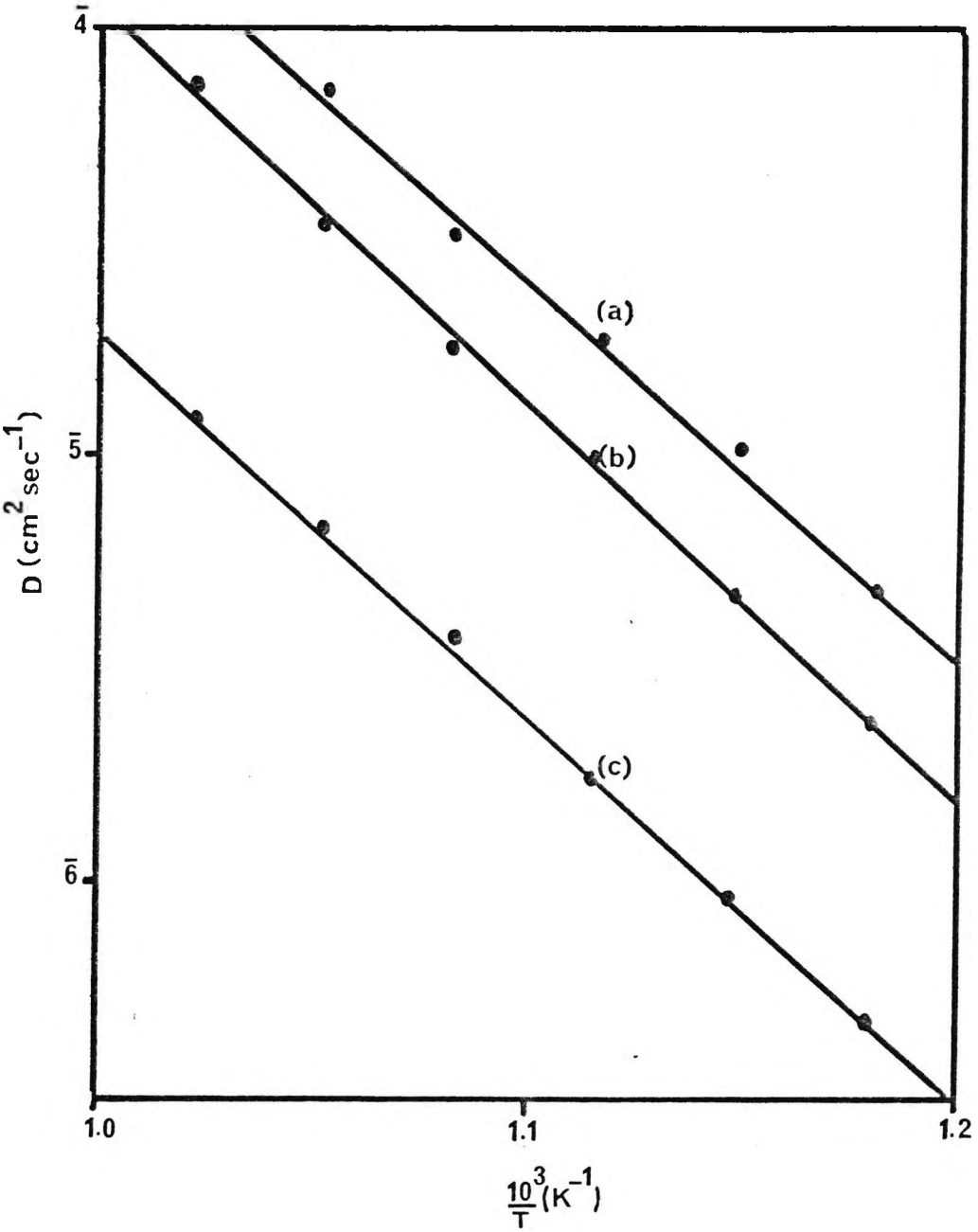

Figure 6.3 Diffusion coefficient of F-centres in (a) KF:Ca^{2+}, (b) KF:Hg containing 1.47×10^{18} Hg^{2+} cm^{-3} and (c) KF:Hg containing 7.18×10^{17} Hg^{2+} cm^{-3}

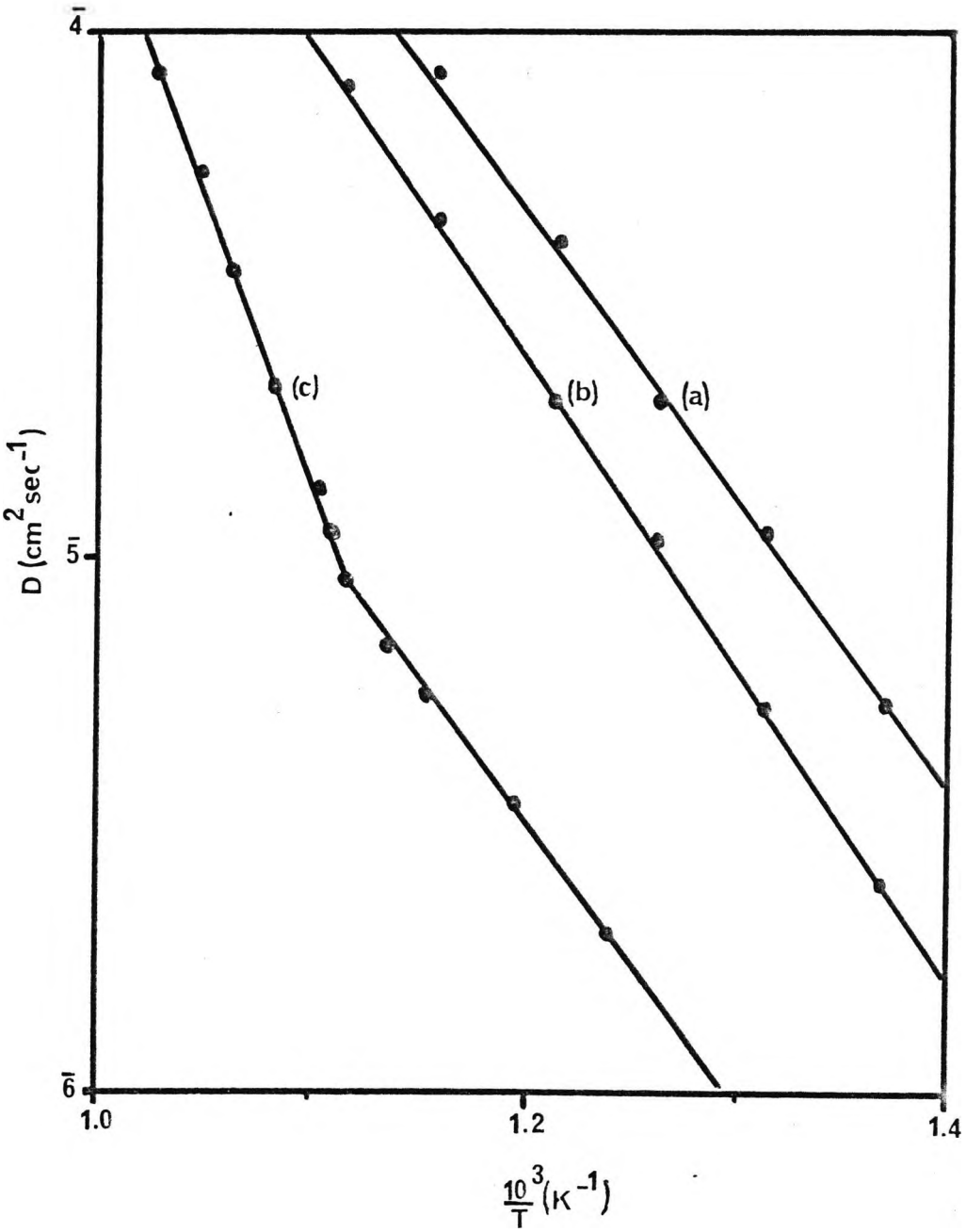

Figure 6.4 Diffusion coefficient of F–centres in KCl:Hg contianing (a) 4.61×10^{18} Hg^{2+} cm^{-3}, (b) 1.97×10^{18} Hg^{2+} cm^{-3} and (c) 4.69×10^{16} Hg^{2+} cm^{-3}

2.1 Spectra of electrolytically coloured alkali fluorides

The coloration starting temperature of a KF specimen containing 1.31×10^{18} Hg^{2+} cm^{-3} is about 570°C using a constant current of 1 mA. As the coloration temperature is increased, the F absorption band increases in height and the F-aggregate absorption bands appear on the long wavelength side of the F band. The M band is the first to appear followed by R_1 and R_2 respectively. At 600°C, the colloid band starts to develop with an increasing tendency to overlap with the M band. As these changes take place in the absorption spectra, the colour of the specimen also changes with the coloration temperature. At room temperature, KF specimens containing only F-centres look pure green while those which contain other colour centres look yellowish-green. Coloured specimens tend to acquire a brown-yellow colour as the colloid band develops at the expense of the F and F-aggregate bands. Figure 6.5 is a typical spectrum recorded at liquid nitrogen temperature in order to resolve the M band and the approximately temperature-independent colloid (C) band. The designations of the absorption bands shown in figure 6.5 are made on the basis of the Ivey (1947) relations. Specimens coloured at 700°C produced a strong F band at 435 nm with a halfwidth of 0.435 eV at liquid nitrogen temperature together with a less intense colloid band at 690 nm. On electrolytic coloration at 800°C, the F band was weak and two intense peaks were produced at the positions of the colloid and R_2 bands. Electrolytic coloration of calcium-doped KF specimens yields similar absorption spectrum when coloured under similar conditions. However, the growth rate of the F-aggregate and colloid centres seems to be suppressed compared with the case of mercury-doped KF using identical coloration conditions. The ultra-violet spectrum of coloured KF in both cases shows different features . While electrolytic coloration of calcium-doped KF shows no absorption whatsoever in the ultra-violet region, the mercury-doped KF shows the familiar spectrum of mercury centres as was discussed in section 1.2 (chapter 3). However, the absorption band designated in chapter 3 as due to the $(Hg - Hg)^0$ centre (see table 3.1) also has a definite relationship with the coloration temperature. Figure 6.6. shows the relation of the absorption of the $(Hg - Hg)^0$ band, which appears usually after the de-coloration treatment, with the coloration temperatures of mercury-doped KF specimens each containing 1.31×10^{18} Hg^{2+} cm^{-3}. Each point in the figure represents the results of four experiments. The figure shows that the absorption of the $(Hg - Hg)^0$ band, which is normalised to the absorption of the F band, increases with decreasing coloration temperature. The other absorption bands in the ultra-violet region were not modified in any way from the results reported in section 1.2 (chapter 3).

Specimens of mercury-doped NaF containing approximately 10^{18} Hg^{2+} cm^{-3} were electrolytically coloured at various temperatures. At 740°C, electrolytic coloration of NaF gives a prominent F band peaking at 340 nm with a halfwidth of 0.577 eV when measured at room temperature. As the coloration temperature was increased to 860°C, a well resolved

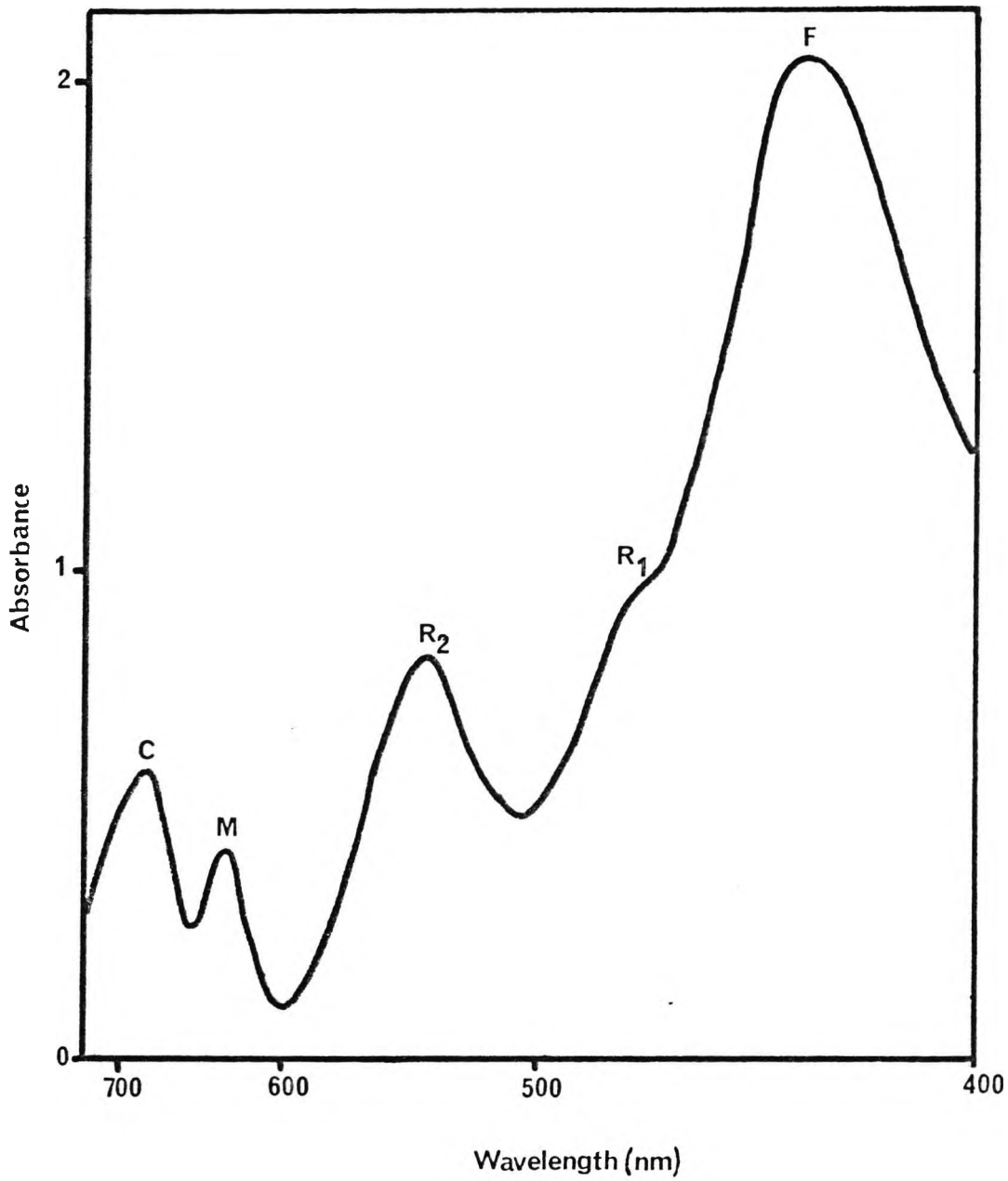

Figure 6.5 Absorption spectrum of electrolytically coloured KF:Hg^{2+} at liquid nitrogen temperature

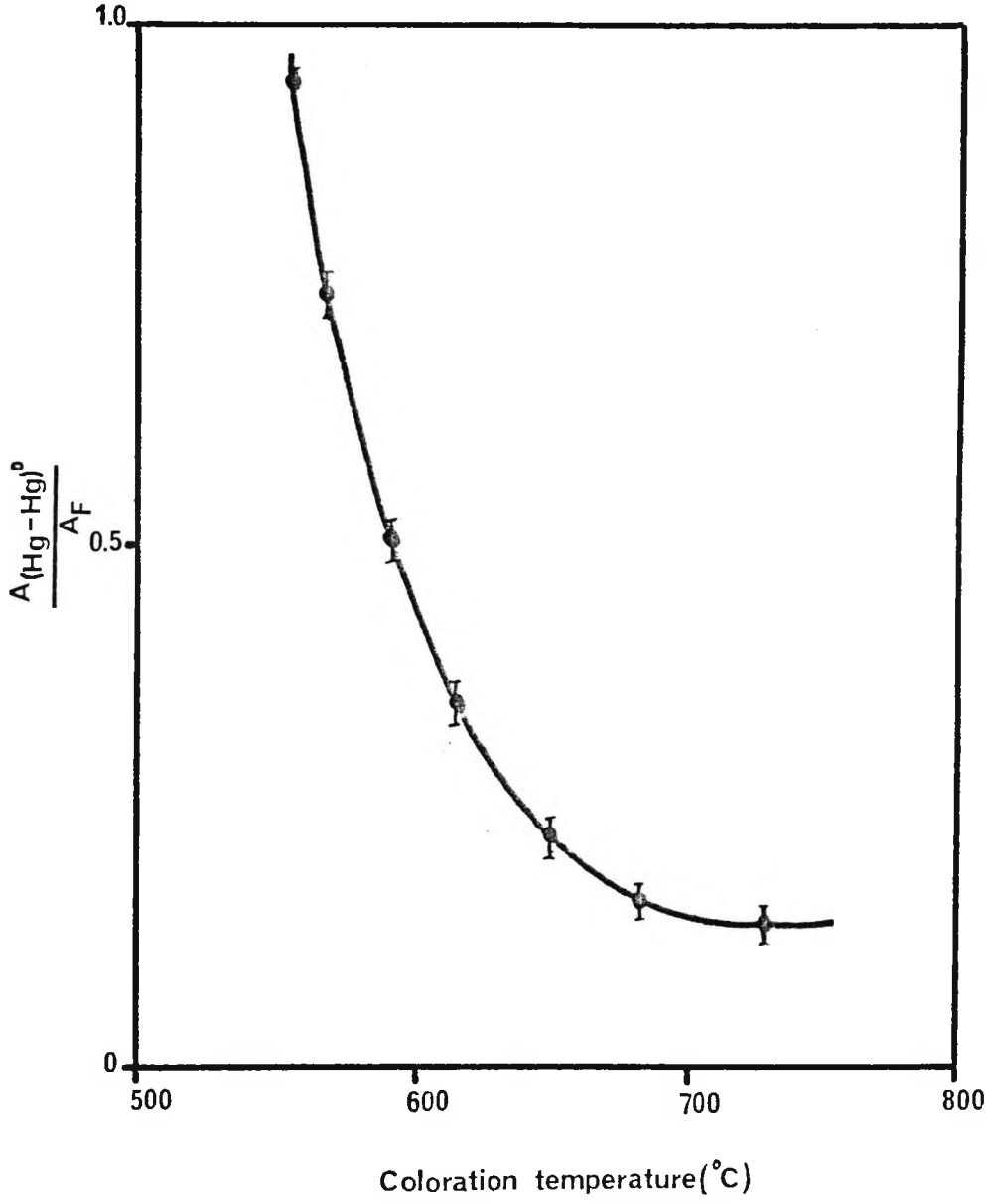

Figure 6.6 The relation of $(Hg-Hg)^0$ centre with the coloration temperature of $KF:Hg^{2+}$

M band peaking at 505 nm with a halfwidth of 0.170 eV appeared, together with a strong F band. At 890° C the colloid band started to develop at 485 nm, while the M band declined and at 910°C this band disappeared completely. Coloured specimens of mercury-doped NaF look yellow while they are in the furnace and purple at room temperature when they contain only F-centres. These specimens acquire an orange colour when other colour centres are present together with the F band.

Specimens of mercury-doped LiF containing approximately 10^{18} Hg^{2+} cm^{-3} produced the expected F band at 259 nm at room temperature with a halfwidth of 0.498 eV when coloured in the temperature range 700°C to 810°C. No other absorption band was produced either in the ultra-violet or visible regions of the spectrum on the long wavelength side of the F band. Figure 6.7 shows a typical spectrum of an electrolytically coloured LiF (810°C, 1 mA) specimen containing 2.6 x 10^{18} Hg^{2+} cm^{-3} measured at room temperature. A similar spectrum was observed for electrolytically coloured NaF (740°C, 1 mA). Coloured LiF specimens look pale yellow when they contain only F-centres and pinkish-yellow when they are in the furnace.

2.2 Production of F-aggregate centres

The aggregation of F-centres into M-, R- and N- centres and the formation of colloid centres (C) occurs with thermal treatment;. Electrolytically coloured NaF containing 3.82 x 10^{18} F-centres cm^{-3} was used in these experiments. The specimen was annealed for equal intervals (5, 10, 20 and 40 minutes) at successively increasing temperatures. The annealing temperatures were increased in steps of 50°C. The spectrum of F and F-aggregate bands in mercury-doped NaF obtained by thermal treatment is shown in figure 6.8. The optical measurements were made at room temperature. The figure shows that initially well resolved R_1 and R_2 bands are produced on thermal treatment, while the N band is still unresolved at room temperature. In the temperature range from room temperature to 150°C the M band developed rapidly. The absorption bands of R_1 and R_2 appeared in the temperature range 50°C to 100°C and started to develop rapidly in the range 100°C to 150°C above which they started to decline. In the temperature range 150°C to 200°C the M band saturated while the N band showed a sharp increase. Annealing in the temperature range 200°C to 250°C showed that the F band decreases while the other F-aggregate bands show a saturation (M and N bands) or a slight decrease as was the case with the R_1 and R_2 bands. On annealing at higher temperature (300°C) all the absorption bands decreased. Visual observation showed that, after annealing at temperatures higher than 300°C, a bleached transparent layer appeared around the external faces of the specimen. With increasing temperature this layer increased in thickness and finally the specimen was bleached at 400°C. The ultra-violet spectrum of the bleached specimen showed the complete bleaching of the Hg^{2+} band as well.

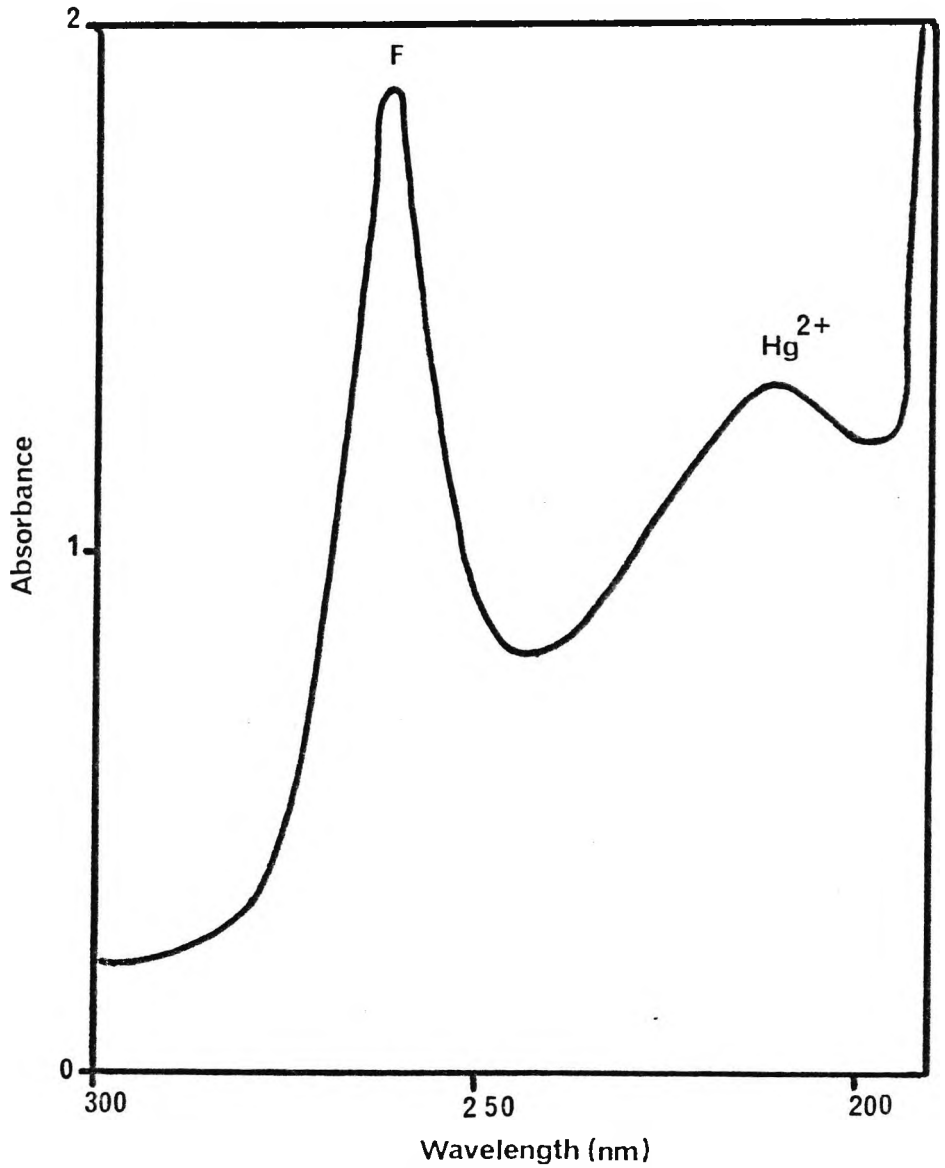

Figure 6.7 Absorption spectrum of electrolytically coloured $NaF:Hg^{2+}$

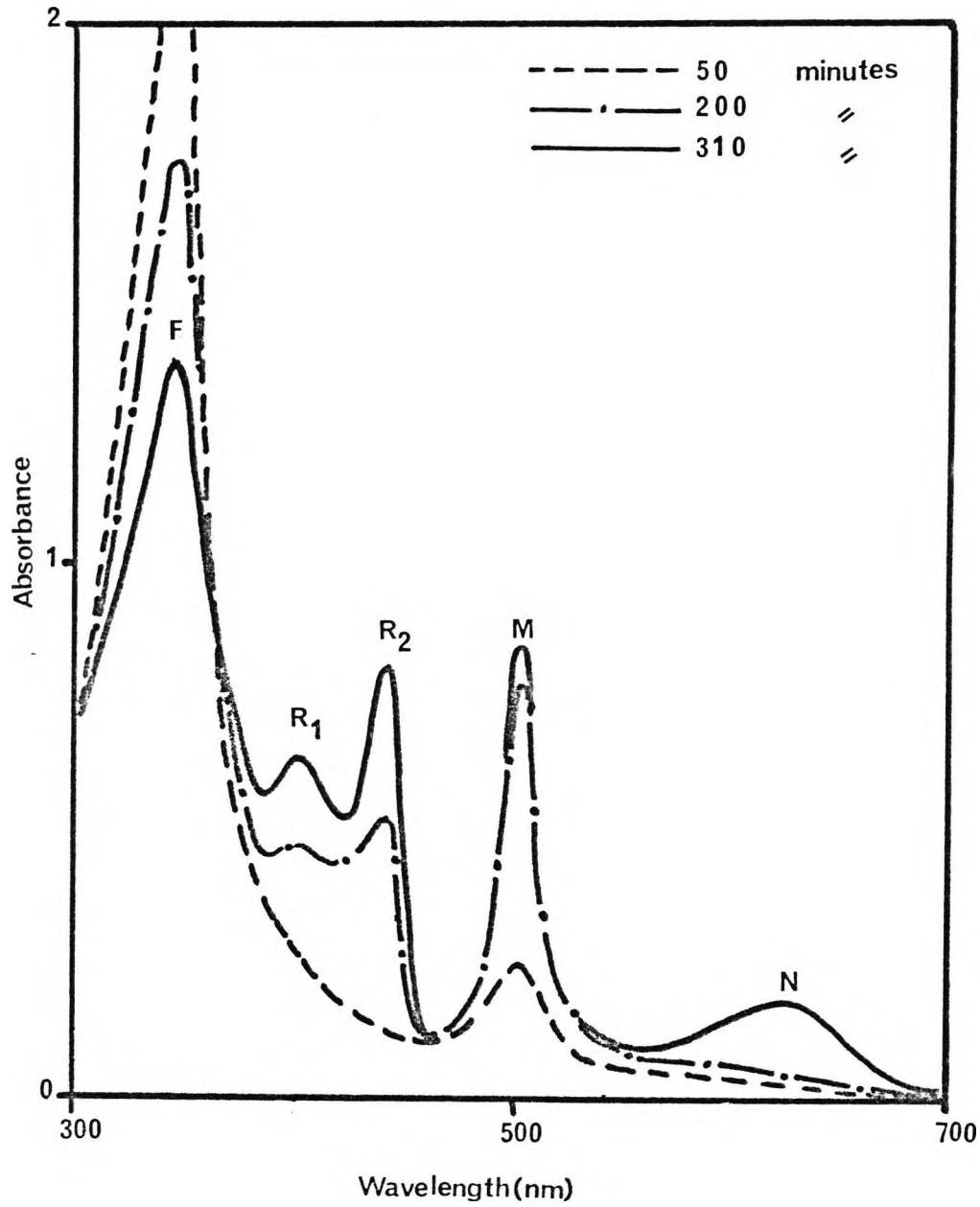

Figure 6.8 Spectra of coloured NaF:Hg^{2+} during thermal treatment

Similar experiments were carried out using electrolytically coloured KF and LiF specimens. Thermal treatment of mercury-doped KF containing 2.82 x 10^{18} F-centres cm^{-3} , in the way described above, produced a similar spectrum as is shown in figure 6.5. The only difference which the spectrum produced by thermal treatment shown is the appearance of an absorption band peaking at 840 nm with a halfwidth of 0.194 eV. Measurements at liquid nitrogen temperature showed that the 840 nm band shifts to shorter wavelength, as do the other F-aggregate bands. This band was assigned to N-centres. The measurements at liquid nitrogen temperature showed no splitting of this band as is the case with N absorption bands in alkali iodides and bromides. Curve (a) of figure 6.9 shows the absorption spectrum of an electrolytically coloured LiF specimen before thermal treatment, and curve (b) of the same figure shows the absorption spectrum after thermal treatment. At liquid nitrogen temperature, all the bands in figure 6.9 shift towards shorter wavelengths and the halfwidths become narrower. The behaviour of the ultra-violet spectrum during thermal treatment of coloured alkali fluorides was similar to that observed during electrolytic coloration. The Hg^{2+} absorption band was reduced in height and then bleached when the colour centres also started to be bleached above 300°C. Table 6.1 reports the results obtained from these measurements. The peak positions and halfwidths of F And F-aggregate bands in alkali fluorides were measured at room temperature as well as liquid nitrogen temperatures. The Ivey (1947) relations were used to identify the peak positions of these bands. The results of table 6.1 are in good agreement with those predicted by the Ivey (1947) relations.

2.3. Colloid centres

F- and F-aggregate centres in electrolytically coloured alkali fluorides were found to be more stable thermally when the thermal annealing treatment was carried out in darkness. Colloid centres were obtained by heating the coloured specimens in darkness above 550°C. Prolonged annealing showed that colloid centres were stable up to about the same temperature range at which they were formed. Above the temperature range 550°C to 650°C they became unstable. Their peak shifted to longer wavelengths, they became broader and were reduced in height. These temperatures are higher than those reported for other electrolytically coloured alkali halides (see section 1.3, chapter 5).

Table 6.2 reports the results obtained for the colloid centres in electrolytically coloured alkali fluorides. The calculated values of the peak positions of the colloid absorption bands were obtained using the relation $\lambda_0 = (1 + 2n_0{}^2)^{\frac{1}{2}}\ \lambda_c$ (equation 1.6, chapter 1) discussed by Doyle (1958). The values of λ_c were obtained from the work of Wood (1933) for the Wood-Zener wavelengths of alkali metals and the values of the refractive index n_0 were obtained from Mott and Gurney (1948). The observed peak positions of the colloid bands reported in table (6.2) are due to the absorption bands of small size particles ($\leq$ 20 nm

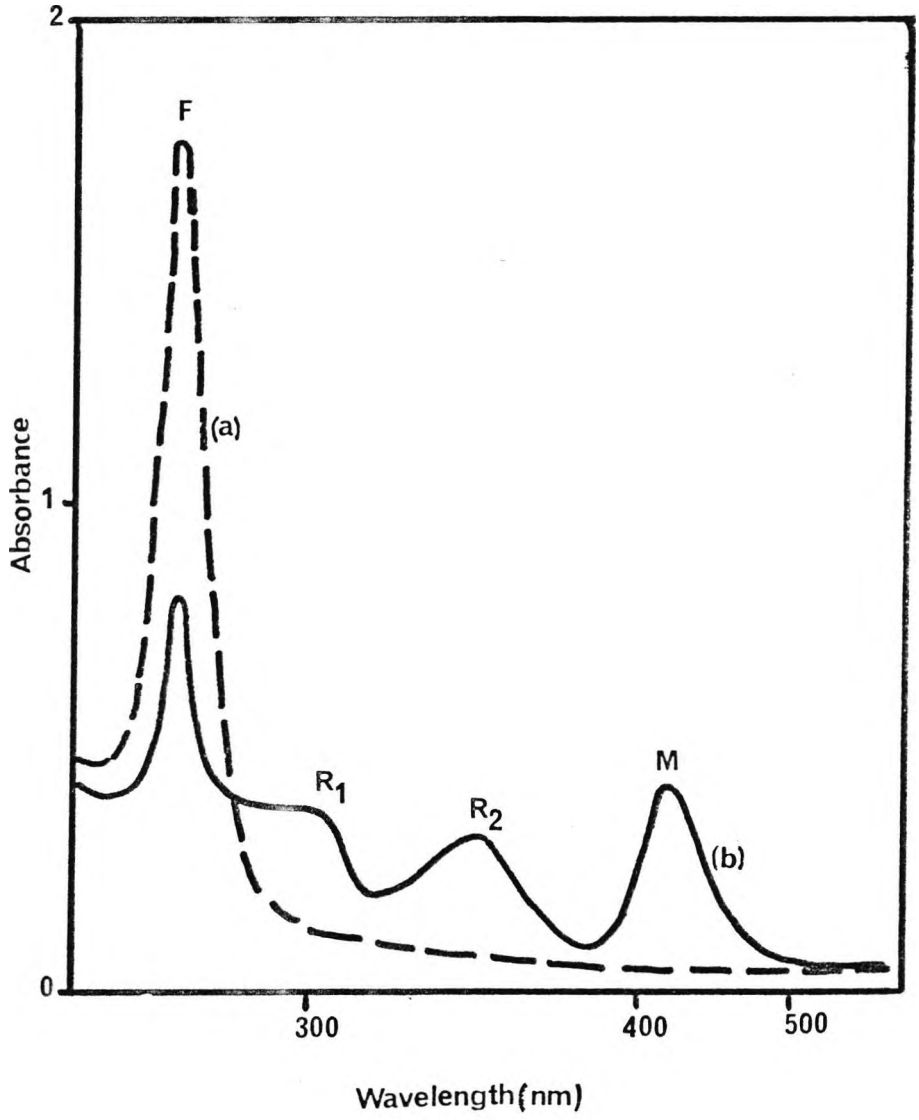

Figure 6.9 Spectra of coloured LiF:Hg^{2+} (a) before and (b) after thermal treatment for 300 minutes

Table 6.1. Peak position and halfwidth of the F and F-aggregate bands in electrolytically coloured alkali fluorides. Values given in parenthesis are calculated from the Ivey relations (1947).

	KF		NaF		LiF	
	Peak position (nm)	Halfwidth (eV)	Peak position (nm)	Halfwidth (eV)	Peak position (nm)	Halfwidth (eV)
F	450 (428)	0.628	340 (328)	0.577	259 (254)	0.498
	435 *	0.435	328 *	0.420	248 *	0.402
R_1	- (497)	-	402 (381)	0.264	305 (295)	0.281
	475 *	0.160	394 *	0.199	295 *	0.203
R_2	555 (538)	0.290	442 (412)	0.279	352 (320)	0.260
	543 *	0.225	430 *	0.152	338 *	0.214
M	645 (648)	0.184	505 (516)	0.170	412 (416)	0.143
	635 *	0.095	500 *	0.110	405 *	0.101
N	840	0.194	627	0.243	-	-
	829 *	0.124	605 *	0.206	-	-

Values referred to with asterisks were obtained at liquid nitrogen temperature. All other values were obtained at room temperature.

Table 6.2. Peak position and halfwidth of the colloid bands in electrolytically coloured alkali fluorides.

	Calculated	Experimental	
	Peak position (nm)	Peak position (nm)	Halfwidth (eV)
KF	683	690	0.34
NaF	445	485	0.47
LiF	451	480	0.32

) as no Tyndall scattering was observed. Also, the identification of these bands as those due to small colloids was made on the basis of the criterion that the line shape of the colloid band is insensitive to a change in the specimen temperature from room temperature to liquid nitrogen temperature (Schulman and Compton 1962).

The colloid band at 485 nm in NaF can be obtained when electrolytically coloured (915°C, 1 mA) NaF is annealed in darkness for long periods (17 hours) together with additional inter-related bands at 525 nm, 505 nm and finally at 575 nm. The band at 505 nm is similar to that assigned to M-centres. The 525 nm and 575 nm bands are thought to be caused by colloids of progressively increasing size. Thermal annealing of electrolytically coloured LiF in darkness at 710°C for long periods (9 hours) produced a brown-yellow appearance to the specimen which coincided with the bleaching of the F band and the generation of temperature independent band peaking at 575 nm. This band is assigned to large-particle colloid.

2.4 Z-centres

F-light treatment of electrolytically coloured KF doped with calcium led to a broadening of the F band. On further irradiation with F - light, the Z-centres manifested themselves in the absorption spectrum obtained at room temperature by the shift in wavelength of the peak position of the F band towards longer wavelengths (470 nm). Optical measurements were carried out at liquid nitrogen temperature for the KF specimen treated for 176 minutes with F-light. At liquid nitrogen temperature the 470 nm band was resolved into F (435 nm) and Z_1 (463 nm) bands.

A thermal anneal of the KF specimen containing F as well as Z_1 - centres for 120 minutes at 150°C resulted in the appearance of a new band peaking at 570 nm. This band is assigned to Z_2 - centres according to the work of Seitz (1954). Further annealing of the specimen at 250°C for 60 minutes led to the disappearance of the Z_2 band and the formation of F-centres on quenching. When this specimen was treated again with F-light, the Z_1 band appeared as discussed above.

On exposing electrolytically coloured KF containing mercury to F-light, no Z-centres could be formed. In two hours the F band could be bleached to 60% of its original height without a corresponding enhancement of the F-aggregate bands. The ultra-violet spectrum of this specimen showed a considerable reduction of the Hg^{2+} bands.

3. Other effects

3.1. Additive coloration

Additive coloration of mercury-doped KCl and KF specimens was carried out. A KCl specimen of volume 1 cm^3 containing 5.32 x 10^{17} Hg^{2+} cm^{-3} could not be coloured uniformly at 550°C, even after 90 hours of diffusion, contrary to the case of nominally-pure KCl. Nominally-pure KCl specimens attained uniform coloration in about 10 hours at 550°C. The results were similar to those obtained by Ben-Dor et al (1966) for cadmium -and mercury-doped specimens and were different from those obtained for specimens doped with alkaline earth impurities (Seitz 1951; Jain and Radhakrishna 1967). Three zones were observed; an outer F-coloured zone followed by a colloidal brown zone and then a transparent mercury-doped zone. The F absorption was found to be a maximum near to the surface and a minimum at the centre of the specimen. The F and Hg^{2+} absorption bands were lower in height by as much as the initial concentration of Hg^{2+} was higher, while the Hg^{+} and Hg^{0} bands were enhanced in the coloured specimens. Even when the specimens contained only a small concentration of divalent mercury cations ($< 3 \times 10^{16}$ Hg^{2+} cm^{-3}), the F-centres were confined to the outer thin layer of the specimen, followed by the brown and the transparent zones.

Additive coloration of a KF specimen containing 1.31 x 10^{18} Hg^{2+} cm^{-3} at 650°C (annealing time 16 hours) showed similar results. The optical absorption spectrum of a slice near to the outer F-coloured zone was identical to that found in electrolytically coloured specimens. The brown zone showed two intense bands in the ultra-violet spectrum (Hg^{+} , Hg^{0}) as well as the colloid band at 690 nm. The transparent zone gave the usual optical absorption bands shown by mercury-doped KF. As the annealing time increased, the brown zone became wider. Additive coloration of KF specimens containing higher concentrations of Hg^{2+} cations showed that the thickness of the F-coloured zone decreased and the absorption bands of Hg^{+} and Hg^{0} centres increased in height in the brown zone with increasing concentration of divalent mercury. Additive coloration of calcium-doped KF (16 hours, 650°C) showed a uniform coloration with a visible spectrum similar to that shown in figure 6.5 .

Additive coloration of a NaF specimen containing approximately 10^{18} Hg^{2+} cm^{-3} at 900° C (annealing time 18 hours) showed similar results to those mentioned earlier. The spectrum of this specimen exhibited an F-band at 485 nm assigned to colloid centres (as discussed in section 2.3 of this chapter) in the orange coloured zone. The third transparent zone showed the usual spectrum of mercury-doped NaF. Mercury-doped LiF, however, did not respond to various attempts to colour it additively.

3.2. OH^- doping

When OH^- ions are diffused into alkali halides they exhibit a strong absorption band in the ultra-violet and another spectrum of various features in the infrared region. The optical

properties of OH^- - doped alkali halides are well documented in the literature (Stoebe 1967, Meistrich 1968). In this work, the relation between OH^- ions and divalent mercury cations, and the influence of the former on the colourability of alkali halides using the electrolytic coloration method, were investigated. The concentration of OH^- ions in the alkali halides were measured using the assumption that the oscillator strength of the OH^- absorption is 1.9. This value is provided by Etzel and Patterson (1958) and widely used in the literature (Kobayashi and Tomiki, 1960,Fowler 1984). However, while the diffusion of OH^- into nominally-pure as well as mercury-doped specimens produced an absorption band in the ultra-violet, calcium-doped KF showed no such absorption but only the infrared spectrum when subjected to identical OH^- -diffusion conditions.

In nominally-pure KF, a broad band was observed peaking at 2680 nm in the infrared region. This band disappeared in mercury-doped specimens on OH^- - diffusions. Instead, two sharp lines were observed ion the 2800 nm region. Figure 6.10 (curve (a)) shows the infrared spectrum of nominally-pure KF containing 2.7×10^{16} OH^- cm^{-3} . Curve (b) shows the appearance of two sharp lines in mercury-doped KF containing an approximately similar amount of OH^- ions. These lines may be ascribed to complexes of divalent mercury cations and OH^- ions, since KF specimens containing only Hg^+ cations (after de-coloration of mercury-doped specimens) showed only the broad band at 2680 nm when subjected to identical OH^- - diffusion conditions.

Electrolytic coloration of KF specimens containing 2.74×10^{18} Hg^{2+} cm^{-3} became more difficult as the coloration starting temperature T_c increased continuously with the concentration of OH^- ions in these specimens. For OH^- concentrations of 10^{20} cm^{-3} and above, the coloration acquired a dendritic form before becoming blocked at the pointed cathode. The later behaviour is similar to that of nominally-pure KF on electrolytic coloration. The effect of OH^- ions on the aggregation of F-centres, and the formation of F-aggregate centres as well as the colloid centres as described in sections 2.2 and 2.3 of this chapter , was to lower the conversion temperatures. It seems from these results that, in mercury-doped KF containing OH^- ions, these ions behave in such a way as to reduce the influence of divalent mercury cations on the electrolytic coloration process. To investigate this effect, ionic conductivity measurements were carried out using mercury-doped KF (1.31×10^{18} Hg^{2+} cm^{-3}) containing 4.6×10^{17} OH^- cm^{-3} . The results are shown by curve (c) in figure 6.1. It is clear that diffusion of OH^- ions into mercury-doped KF tends to reduce the extra cations introduced into the specimen by the divalent mercury cations. Figure 6.11 shows the relationship between the optical spectra of both the Hg^{2+} cations and the OH^- ions. Curve (a) shows the absorption band of Hg^{2+} in mercury-doped KF. Curve (b) shows the 2680 nm band of OH^- ions in the infrared. Curve (c) demonstrates the way OH^- ions reduce the absorption of Hg^{2+} cations. These results, when correlated with those mentioned earlier in this section, support the suggestion that the formation of complexes involving divalent

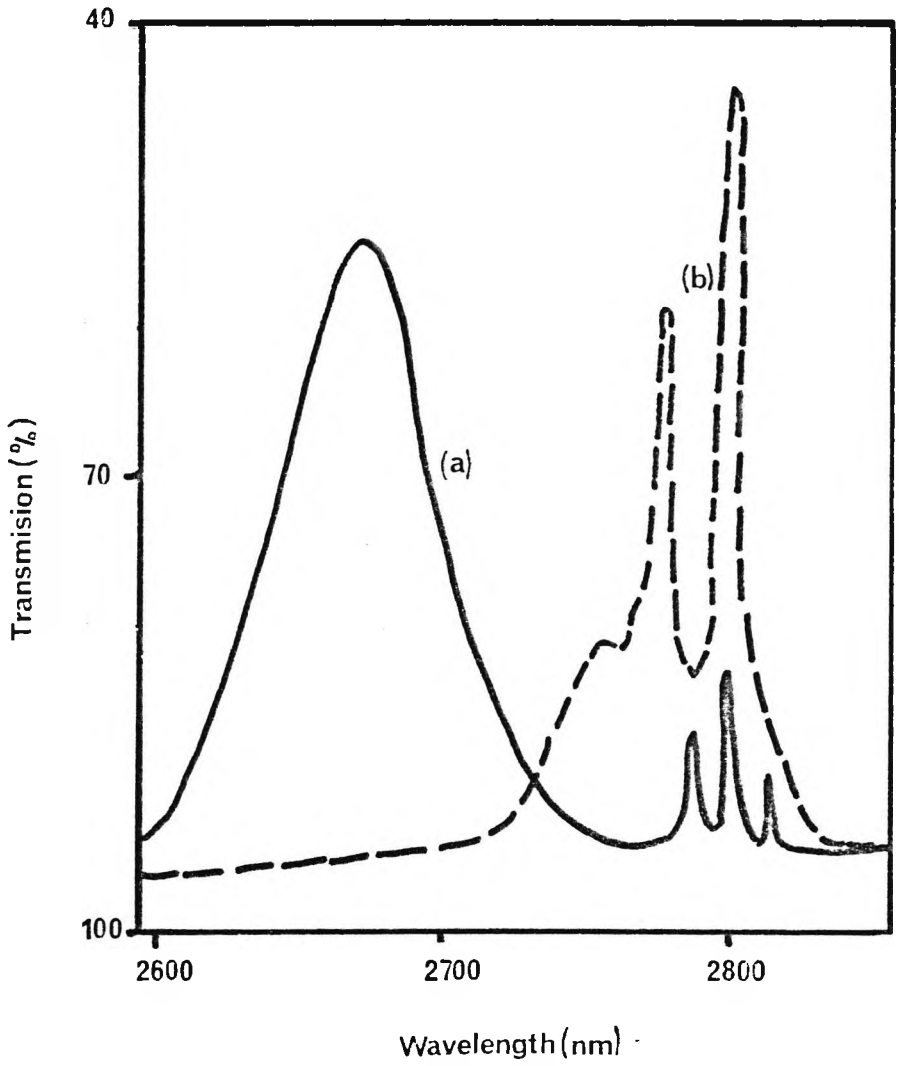

Figure 6.10 Infrared spectra of $KF:OH^-$ (a) nominally -pure and (b) mercury-doped

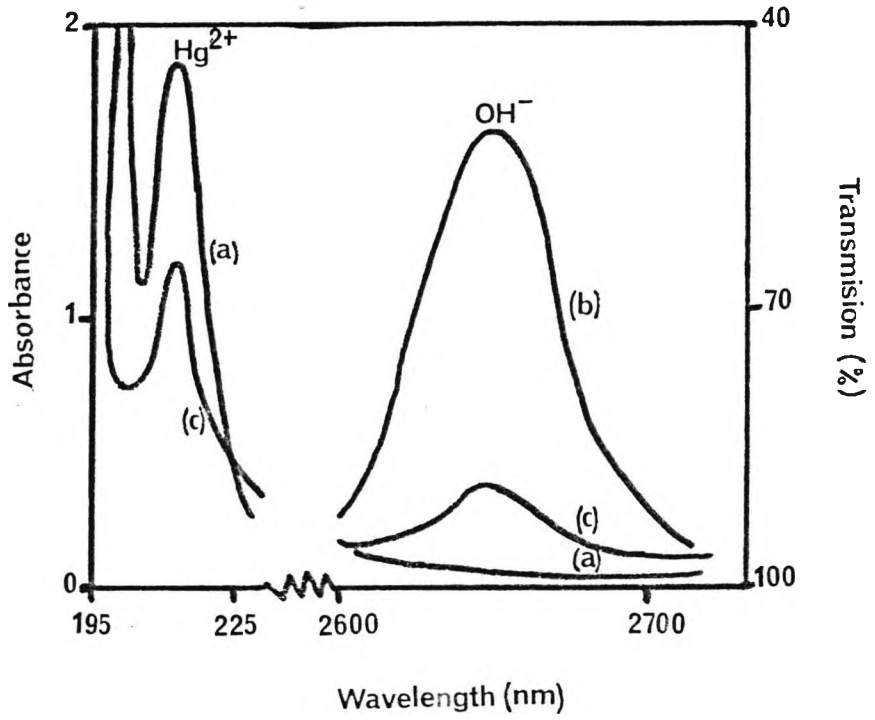

Figure 6.11 Ultra-violet and infrared spectra of KF (a) mercury-doped, (b) OH^--doped and (c) mercury-doped containing OH^- ions

mercury cations and the diffused OH^- ions leads to the removal of the extra cation vacancies which was found to be the reason behind the enhancement of electrolytic coloration of alkali halides containing divalent mercury. These cation vacancies are either involved directly in these complexes or are tightly bound to them (Anger et al, 1963).

The reduction in F band absorption was also observed in nominally-pure KBr, though the coloration starting temperature T_c was slightly changed. For OH^- concentrations above 8×10^{17} OH^- cm^{-3} the coloration acquired a dendritic shape and it seemed to be blocked at the pointed cathode. Nominally-pure NaCl containing 3.6×10^{16} OH^- cm^{-3} was electrolytically coloured and subsequently de-coloured by reversing the polarity of the electrodes. The optical measurement of this specimen showed an increase in the absorption spectrum near to the fundamental edge. When this specimen was optically treated with ultra violet light for 6 hours, a yellowish-brown F coloration was observed in the regions near to the specimen surface. The central region still looked transparent. This effect could only take place if U-centres were present in the specimen after the de-coloration treatment. The process of the formation of F-centres by ultra-violet light treatment of the U-centres was expressed by Delbecq et al (1956) as

$$2U \xrightarrow{h\nu} 2F + H_2$$

The fact that the central region was not coloured on irradiation with ultra-violet light may be due to the absence of OH^- ions in this part of the specimen. Optical treatment with ultra-violet light of OH^- - doped KBr and KCl after the de-coloration treatment also showed a similar effect.

4. Conclusions

F-centres have been produced in mercury-doped alkali fluorides using the method of electrolytic coloration. M- as well as colloid centres were also produced but other F-aggregate centres could only be produced electrolytically in mercury-doped potassium fluoride. These centres, however ,were produced in both electrolytically coloured NaF and LiF using a thermal treatment The results in this field suggest that divalent mercury cations suppress the aggregation rate of F-centres. The temperatures at which the F-centres are converted, by thermal annealing, to colloid centres are higher than those obtained for nominally-pure alkali halides. These centres could not be obtained by bleaching coloured specimens of mercury-

doped alkali halides with F-light. It was observed that optical bleaching of F-centres leads to the same results obtained after de-coloration by reversing the polarity of the electrodes. This might suggest that the F-aggregation mechanism in thermally treated specimens is different from that predominant during the F-light bleaching process.

The results obtained by the electrolytic coloration experiments on nominally-pure alkali fluorides showed that processes which characterise electrolytic coloration in other nominally-pure alkali halides are taking place in these salts as well. F-centres are produced in alkali fluorides but at very low concentrations and they seem to be failing to move towards the flat anode. The experimental work on the diffusion of F-centres showed that there are two mechanisms for the diffusion of F-centres in electrolytically coloured alkali halides. At low temperatures (extrinsic region) and in mercury doped specimens, the diffusion of F-centres was found to be compatible with a predominant diffusion mechanism via cation vacancies. The diffusion coefficient of F-centres increases with increasing concentration of divalent mercury cations and the independence of the activation energy for diffusion of F-centres on the type of divalent cations or their concentration, supports this mechanism. At higher temperatures (intrinsic region) the diffusion of F-centres was found to be dominated by a self-diffusion mechanism via K^+. In the intrinsic region, the anion vacancy concentration increases with temperature. It seems from the results that the F-centre diffusion coefficient is enhanced by as much as the concentration of anion vacancies is suppressed by the extra cation vacancies introduced into the specimen by the divalent cations.

Ionic conductivity measurements have shown that both divalent mercury cations and divalent calcium cations enhance electrolytic coloration through the extra cation vacancies which they supply. Unlike mercury-doped KF and KCl (as reported in section 2.1 of chapter 3), calcium-doped KF did not display any difference in ionic conductivity before coloration or after de-coloration. These results imply that divalent calcium cations are not reduced to a low valence state, as is the case with divalent mercury cations, after de-coloration. Hence the extra cation vacancies supplied by the divalent calcium cations still exist in the specimen after the de-coloration treatment, which explains why calcium-doped KF can be coloured again after de-coloration but mercury-doped KF cannot. These results also support the conclusion that cation vacancies play the essential part in promoting electrolytic coloration in the alkali fluorides.

The fact that Z-centres can be produced in calcium-doped KF but not in mercury-doped KF is related to the fact that divalent mercury cations are reduced to a low valence state after the de-coloration treatment while divalent calcium cations still exist after this treatment (see section 5.4, chapter 1). The change in valence of divalent mercury cations but not of divalent calcium cations is due to their different electronegativity (Topa and Yuste 1970). Divalent mercury cations, unlike those of calcium, have a high value of electronegativity and, therefore, act as direct electron acceptors.

The optical measurements on mercury-doped alkali halides containing OH^- ions have shown that divalent mercury cations form complexes together with OH^- ions. The observed suppression of the ionic conductivity of these specimens support this fact which manifests itself by the replacement of the broad band with a spectrum of sharp lines in the infrared region. The influence of OH^- ions on the colourability of alkali halides using electrolytic coloration can be seen as that of reducing the effect of the extra cation vacancies supplied by divalent cations and has the effect of decreasing the diffusion coefficient of F-centres. The fact that OH^- ions occupy vacant anion sites in nominally-pure alkali halides means a reduction in the probability of an electron-anion vacancy recombination and is responsible for the difficulty of producing F-centres in highly-doped specimens.

5. References

Anger J, Fritz B and Luty F 1963 Z.Phys. 174 240

Chandra S and Rolfe J 1970 CanJ.Phys. 48 397

Delbecq C J , Smaller B and Yuster P H 1956 Phys.Rev. 104 605

Doyle W T 1958 Phys.Rev.111 1067

Etzel H W and Patterson D A 1958 Phys.Rev. 112 1112

Fowler W B 1984 Physics of Color Centers -Ed. W.B.Fowler -Academic Press London

Heiland G 1950 Z.Phys. 128 144

Jain S C and Parashar D C 1946 J.Phys.Chem.Solids 25 1269

Jain S C and Rodhakrishna S 1967 J.Soc.Sci.Indus.Res. 26 324

Kobayashi K and Tomiki T 1960 J.Phys.Soc.Japan 15 1982

Kubo K 1966 J.Phys.Soc.Japan 21 2095

1969 J.Phys.Soc.Japan 26 143

Meistrich M L 1968 J.Phys.Chem. Solids 29 1119

Mott N F and Gurney R W 1948 Electronic Processes in Ionic Crystals-Dover

Perez A, Thevenard P, Davenas J and Duputy C H S 1973 Phys.St.Solid (a) 18 189.

Rolfe J 1964 CaJ.Phys. 42 2195

Schulman J H and Compton W D 1962 Colour Centres in Solids-Pergamon Press

Seitz F 1951 Phys.Rev. 83 134

1954 Rev.Mod.Phys. 26 7

Shavarts K K ,Itskovich Z S, Kalimulin S S and Kalnin Yu Kh 1974 Sov. Phys. -Solid St. 16 1040

Stoebe T G 1967 J.Phys.Chem. Solids 28 1375

Topa V and Yuste M 1970 Phys. St. Solid (a) 3 131

Tyagi R C, Singh R and Gupta A K 1970 J.Phys.C: Solid St.Phys. 3 769

Wood R W 1933 Phys.Rev. 44 353

CHAPTER SEVEN

Electrolytic Coloration: a Proposed Model

1. Introduction

In the previous chapters of this thesis an extensive experimental data was accumulated in order to present a systematic understanding of electrolytic coloration phenomenon in alkali halide crystals. One important characteristic of this phenomenon is the four distinctive zones of the coloration current vs time curves which correspond to the different stages of the coloration processes. Figure 7.1, curve (a), shows a typical case of the current vs time curve in which the four zones are marked.

Experimental results presented in this thesis have already established the nature of each zone. Zone 1 is controlled by purely ionic transport which at the end of it leads to the formation of an ohmic electron injector in the cathodic region. The kinetics and mechanism of formation of this contact is now presented in mathematical expressions. Other experimentally verified expressions are presented in this chapter for the processes controlling zones 2 and 3. Electrons injected from this new cathodic contact give place to both zones and with this injection coloration cloud starts from the pointed cathode towards the flat anode.

Zone 4, however, is shown here to be due to processes occuring in the anode-crystal interface and, thus, it is not intrinsic to the crystal. By suppressing these processes zone 4 is inhibited and only three zones remain in the current vs time curve. Curve (b), figure 7.1 looks similar to a Space-Charge-Limited transient current curve as computed by Many and Rakavy (1962).

According to the kinetic model proposed by Heiland (1950), and since then adapted by electrolytic coloration students, electrical current never saturated and zone 3 should not appear. To overcome this discrepancy with experimental results, many authors introduced several modifications into his equations (Lamb 1986; Kroger 1979;Kucxynski et al 1964). In this work it was found that a space charge controlled process is suitable to understand the experimental results and to derive mathematical expressions that correspond to these results.

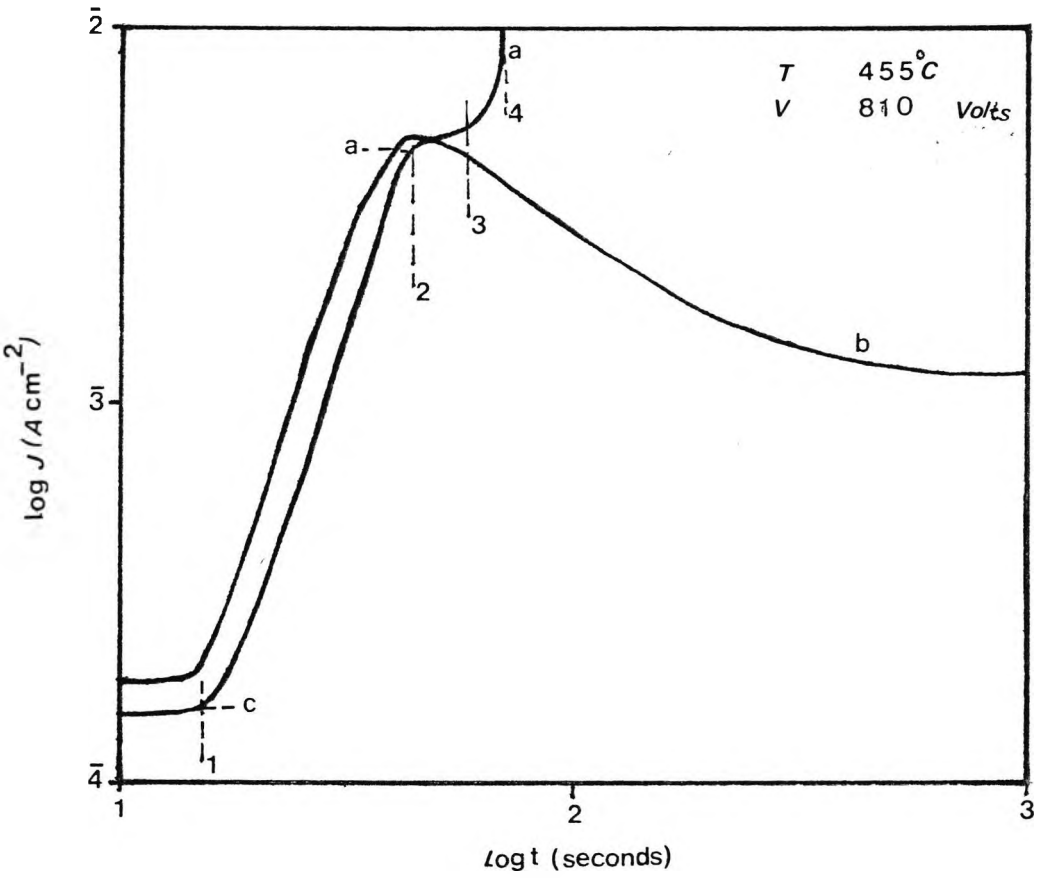

Figure 7.1 Current vs.time curves for *KBr* obtained with (a) *Pt* plate -anode (b) vacuum-evaporated *Al* film as anode

2. Zone 1

2.1. Experimental background

The nature of this zone has already been shown in this work to be ionic transport. The main ionic process in this stage of the electrolytic coloration is that a certain amount of charge is transported and deposited on the pointed cathode for the initiation of electron injection into the crystal. Experimental work made it clear that no electronic current exists during this zone. The ionic current remains nearly constant with the duration time of this zone which starts at t=0, when the temperature reaches its working value and the constant voltage is applied across the electrodes, and ends at $t=t_c$ when an abrupt increase in the current and the simultaneous onset of coloration mark the start of zone 2. The value of t_c depends upon temperature, applied voltage and impurity background of the sample. Consequently no coloration is produced during this stage.

Accumulation of alkali metal around the pointed cathode has been undoubtedly detected by different authors (Dalal et al 1983;Motojo and Sanchez 1974; Heiland 1950). Clear experimental evidence is obtained to show that if the accumulated alkali metal is eliminated, no coloration of the crystal is produced. Possible elimination processes are : oxidation of the alkali metal, chemical reaction with cathode material, diffusion into the cathode, etc.

Alkali ions reach the pointed cathode during this stage, neutralised there by interchanging one electron with the pointed electrode and become neutral alkali atoms. If elimination processes of these atoms are prevented (or, at least, reduced) new cathode is formed. The influence of temperature, applied voltage and impurity has been investigated thoroughly and the results are presented in the previous chapters of this thesis

2.2. Formation of new cathode

For the whole effective area of cathode-crystal contact, the equation for the number of alkali ions , n, reaching the cathode per time is proportional to the ionic current during zone 1:

$$\frac{dn}{dt} \alpha i_c \qquad (7.1)$$

where i_c is the ionic current as measured at the coloration point T_c . To make a realistic approximation about an elimination term, the number of alkali atoms eliminated per time is considered proportional to the number of those deposited around the pointed cathode:

$$(dn)_D \equiv (dn)_E = Mndt \qquad (7.2)$$

where the parameter M is a function of temperature, chemical nature and geometry of the pointed cathode and the atmosphere surrounding the crystal. Using the same electrode and atmosphere, M becomes simply M=M (T). The rate of variation of the number of the deposited alkali atoms can be written as

$$\frac{dn}{dt} = i_c - Mn \qquad (7.3)$$

If the number of atoms necessary to form the new cathode that can produce electron injection is n=0 at t=0 and $n=N_c$ at $t=t_c$, then, equation (7.3) yields:

$$t_c = (-/M)\ 1n\ [1 - (B/i_c)] \qquad (7.4)$$

where B is constant, $B=MN_c$.

The continuous curve in figure 7.2 has been drawn by plotting equation (7.4) with parameters M and B as indicated in the figure. The dashed curve, however, is plotted from the equation which holds if the elimination processes are not taken into account:

$$N_D = i_c\, t_c \qquad (7.5)$$

The duration of zone 1 vs the ionic current at the coloration point, i_c is also shown in the figure. Whenever i_c of equation (7.4) is smaller than $B= MN_c$, the injection process is physically impossible. This means that ionic current must reach a value where a certain minimum amount of charge is to be transported to and deposited on the pointed cathode for the initiation of the electron injection.

Experimental points in figure 7.2 were obtained from a family of curves representing various behaviours of KBr crystal coloured electrolytically at 400^{O} C using different values of constant voltage as indicated in figure 7.3. It is clear that these experimental points fit well the continuous curve in figure 7.2 rather than the dashed curve proving the existence of the elimination processes which were detected by other authors using various experimental means.

From figure 7.2 the number of alkali atoms deposited on the pointed cathode can be calculated by using the relation $B= MN_c$. The value of N_c is found to be 2.57×10^{14} K atom. As the coloration temperature T_c is kept at higher values, N_c is found to increase. This result explains why at very low temperatures no injection of electrons is produced and no colour centres are formed.

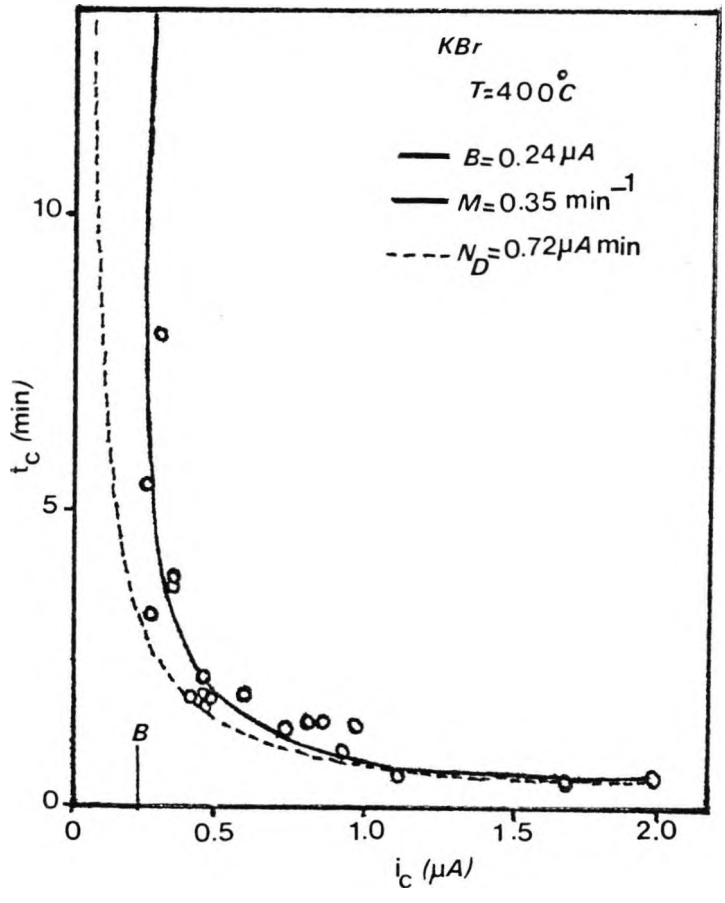

Figure 7.2 The relation between the duration of zone 1, t_c, and the current in the zone, i_c according to equations 7.4 and 7.5

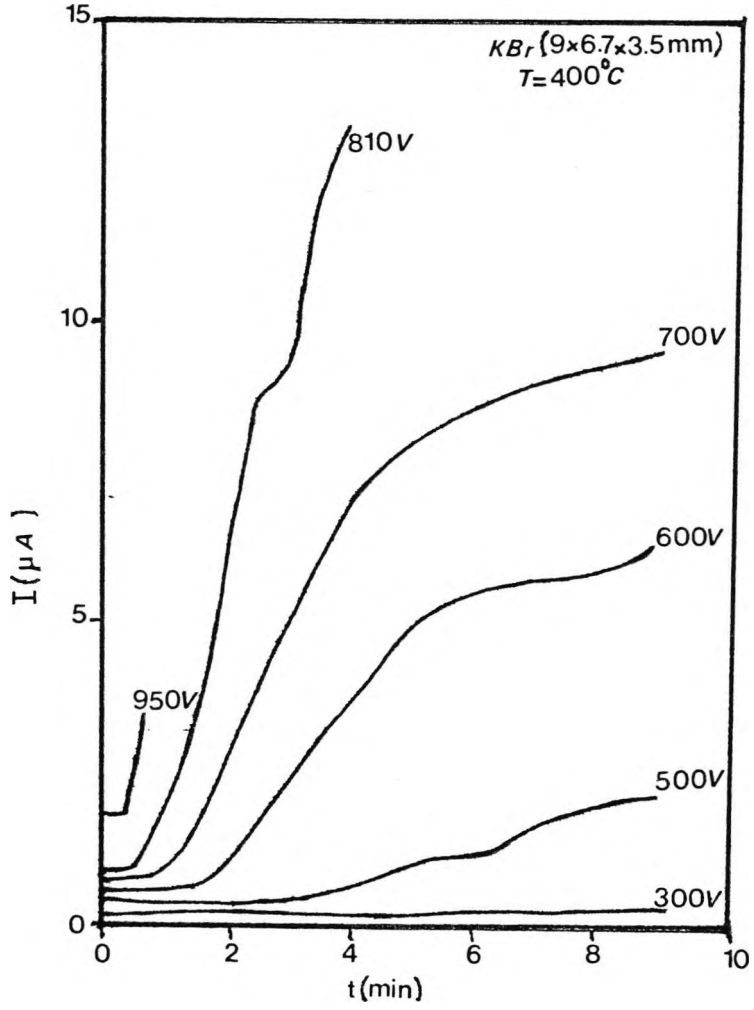

Figure 7.3 Current vs.time curves corresponding to different voltages

3. Zone 2

3.1. Coloration point T_c

Using some assumptions a mathematical relation may be obtained between the coloration point T_c and the applied voltage. By taking a constant heating rate G=dT/dt, and

$$\sigma = AT^{-1} \exp(-U/kT) \qquad (7.5)$$

where σ is the specific ionic conductivity, A is a constant and U is an activation energy as well as considering the fact that the cathodic contact is ohmic under prevailing coloration conditions, then equation (7.1) yields:

$$(dn/dT) \propto ET^{-1} \exp(-U/kT) \qquad (7.6)$$

where E is the electric field through the crystal (E=V/d). If N_c is considered constant and independent of the applied field, then, by using Chen's (1969) approximate interpretation of equation (7.6), with an error of 10%, the integration of both sides between T= R.T. when n=0 and $T=T_c$ when $n = N_c$ yields:

$$N_c \propto E T_c \exp(-U/kT_c) \qquad (7.7)$$

Figure 7.4 shows the relation between applied voltage and coloration temperature T_c obtained from a series of electrolytic coloration experiments carried out by using KBr crystal. Figure 7.5 shows a semi-log plot of ET_c vs T_c^{-1} for the results obtained from figure 7.4. The experimental points define quite well a straight line. The energy calculated from the slop of this line is U = 0.66 eV which stands for the migration of cation vacancy (Chandra and Rolf 1970).

3.2. Thermoionic emission

The extra conductivity superposed at point T_c on the ionic conductivity of the crystal undergoing electrolytic coloration was confirmed to be due to electron injection which takes place by thermoionic emission from the new alkali metal cathode formed by the above described accumulation process. Experimental results obtained in this work strongly support the results presented by other authors (Lampert and Mark 1985; Dalal et al 1983) that the current injected at T_c into the crystal is electronic in nature. If so, this electronic current should obey Richardson's Law of thermoionic emission:

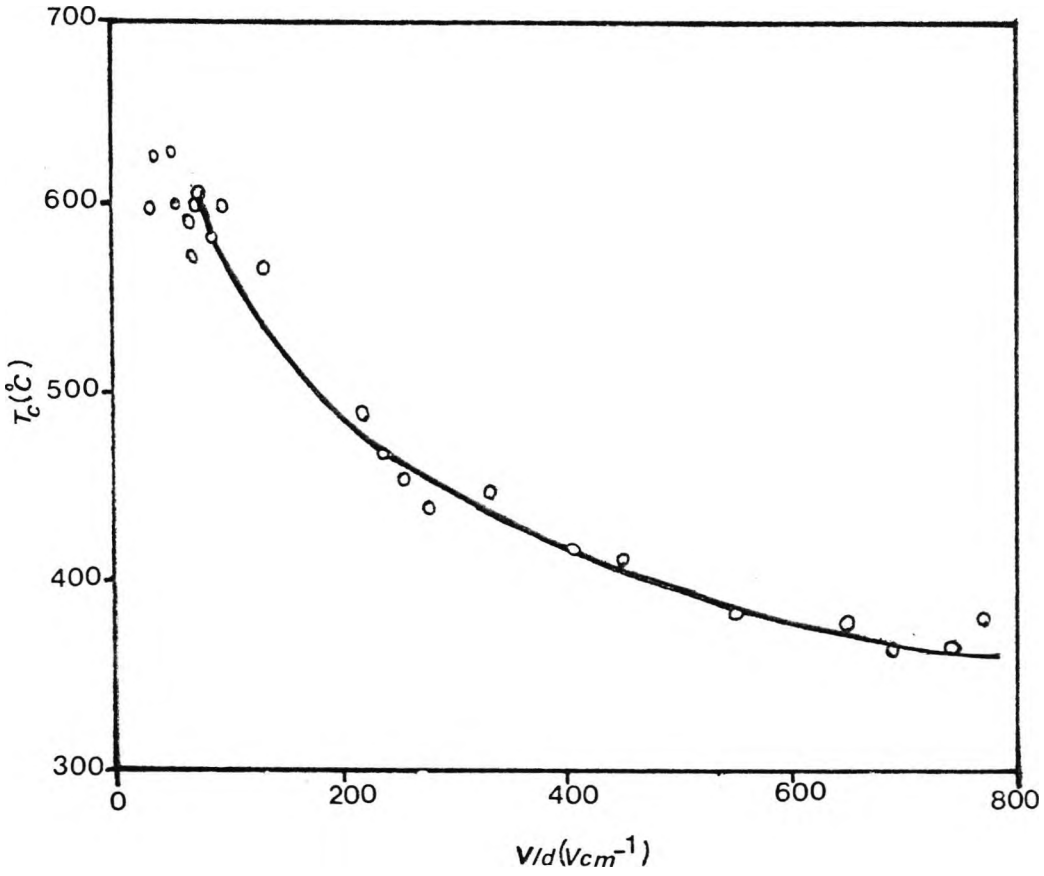

Figure 7.4 Relation between the applied voltage and coloration point, T_c

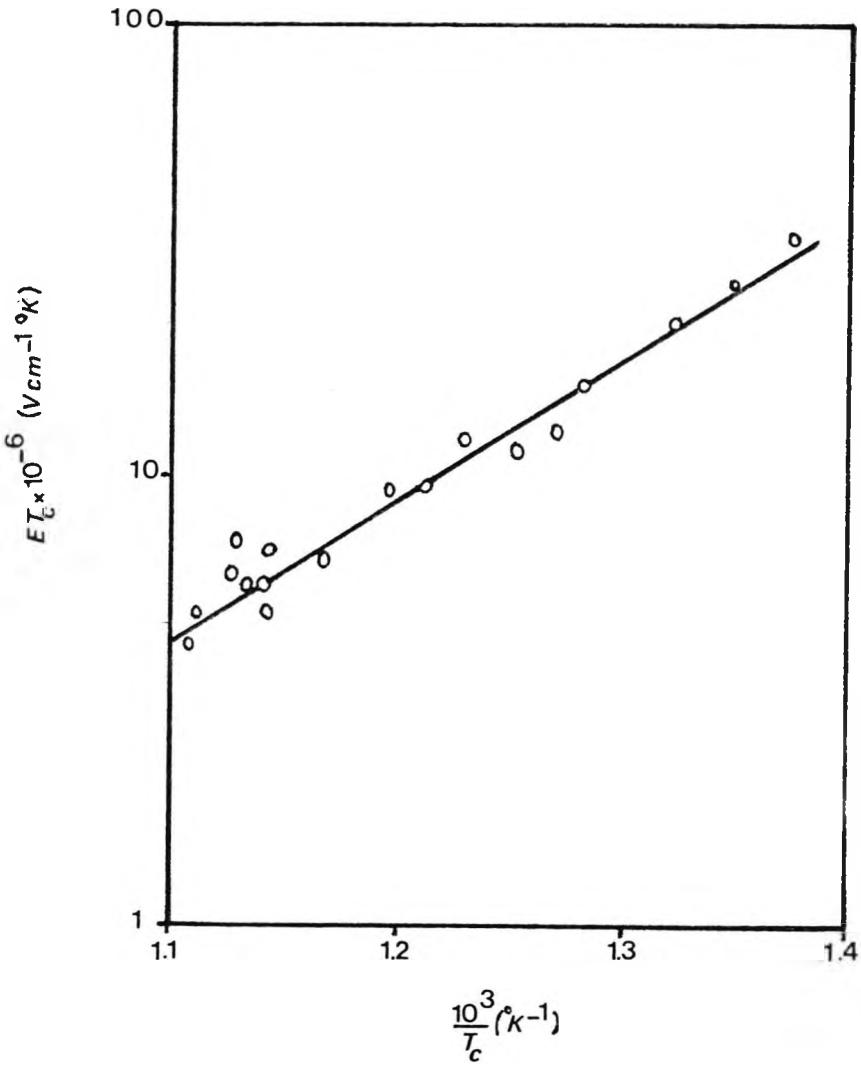

Figure 7.5 The experimental verification of the expression 7.7

$$J_c \cong AT^2 \exp(- \phi / kT) \qquad (7.8)$$

Where A is Richardson's constant and ϕ is the work function for thermoionic emission from alkali metal into alkali halide crystal. Figure 7.6 shows a plot of $\Delta j / T_c^{\,2}$ vs $T_c^{\,-1}$ as a check of Richardson's law. Δ j is the electronic current in zone 2 = the current at point T_A minus that at point T_C (in both cases the ionic current of zone 1 subtracted). The slope of the straight line yields an energy of 1.48 eV which must be compared with the work function for thermoionic emission from potassium into KBr. This value for KBr is in excellent agreement with the measured value: 1.53 eV by Parama and Sanchez (1971) and 1.43 eV by Dalal et al (1983).

3.3. SCL current in zone 2

Space-Charge forces play a prominent role in the electrical properties of insulators due to the fact that these solids normally have relatively low density of free carriers and consequently charge unbalance is easily produced by electrical fields. Very large effects can be produced through the use of ohmic contacts which facilitate the direct injection of excess charge into the insulator. The character and magnitude of these effects are due largely to the presence of localised states which can trap and store charge in an equilibrium with the free, mobile charge. Impurity and defect states in insulators profoundly influence their electrical and optical properties.

SCL currents in solids have previously been discussed by many authors (Rose 1983, Frank and Simmons 1967, Lampert 1956). The exact theory is based on three equations: a current flow equation, Poission's equation and an equation of state relating the free-electron density to the trapped-electron density at the same position. The first equation is

$$j (x , t) = eunE (x , t) - eD \, \partial n (x , t) / \partial x \qquad (7.9)$$

where j is the electronic current density, u and D the electronic mobility and diffusion respectively and n the free electron density. A few simplifying assumptions are introduced in order to obtain a solution of SCLC's equations. Thus, the diffusive contribution to the total coloration current is neglected. Then equation 7.9 is replaced by

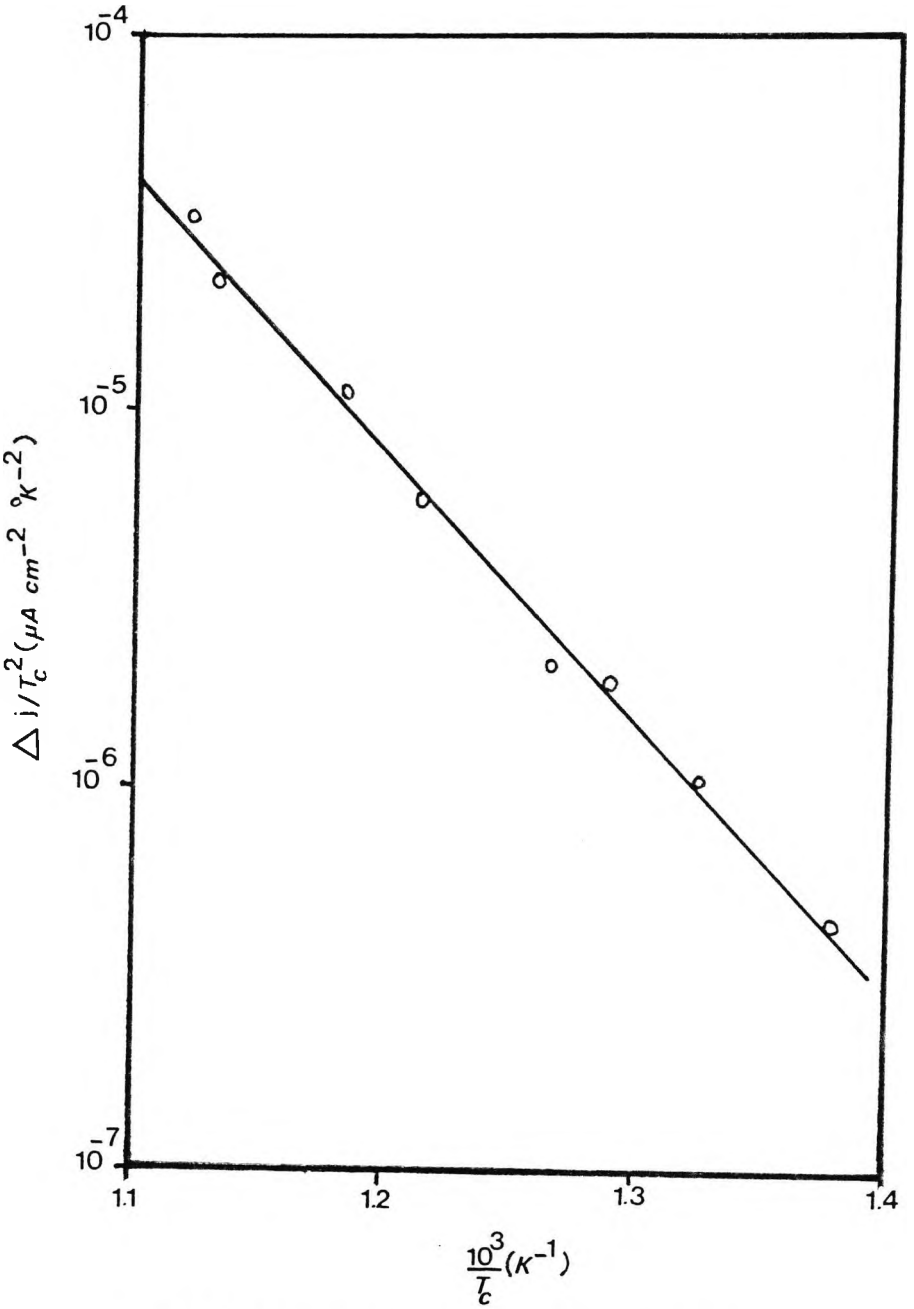

Figure 7.6 Check of equation 7.8 using coloration current and temperature

$$j(x,t) = eun\ E(x,t) \qquad (7.10)$$

At x=0 an ohmic contact is established, near which a large reservoir of electrons is available. Its magnitude is sufficiently large to ensure for any voltage and at all times, the presence of a virtual cathode near the interface where the electric field vanishes. At t=0 no charge redistribution has yet taken place, except very close to the interface (x=0), and hence in the bulk of the sample the field is given by V/d, and the free (n) and trapped (n_t) electron concentrations still retain their values at thermal equilibrium.

However, the appearance of SCLC in wide band gap insulators (i.e. alkali halides) is rare and very few data on their characteristics have been already published. Todheide-Haupt et al (1966) observed both SCL ionic and electron currents in KCl crystalline thin films. Electrolytic coloration experimental techniques make it possible to inject electrons into single crystals of alkali halides from ohmic contact in a way that satisfies the requirements of SCLC theory. By this the results of this thesis enlarge the field of SCLC to wide band gap type materials while offering a new tool to investigate the nature and mechanisms involved in the formation of the four zones of current vs time.

Figure 7.7 shows a SCLC transient as computed by Many and Rakavy (1962) where t_t is the trapping time. The upper curve corresponds to the case of no trapping ($t_t = \infty$). The lower curve in figure 7.7 corresponds to flow under trapping where $t_t = t_s/t_0$; $t_0 = d^2/uV$ is the transit time of a carrier in the absence of space-charge effects and t_s is the trapping time due to all sets of trapping level. The lower curve in figure 7.7 corresponds to flow under trapping with $\emptyset=0$ where $\emptyset$ is the rate of carrier release from traps into the conducting band; $\emptyset = n / n_t$.

At point T_c a certain amount of thrmoionic electrons is allowed to enter the crystal marking the onset of the electronic injection (t=0), giving rise to the initial coloraion current density j(0) in zone 2. Hence, at time t=0 in zone 2 there is a current density

$$j(0) = \frac{KuV^2}{2d^3} \qquad (7.11)$$

where K is the dielectric constant For $t > 0$, more electrons are kept continually injected and the current rises accordingly to:

$$j(t) = \frac{1}{2}\left(1 - \frac{1}{2}t\right)^{-2} \qquad (7.12)$$

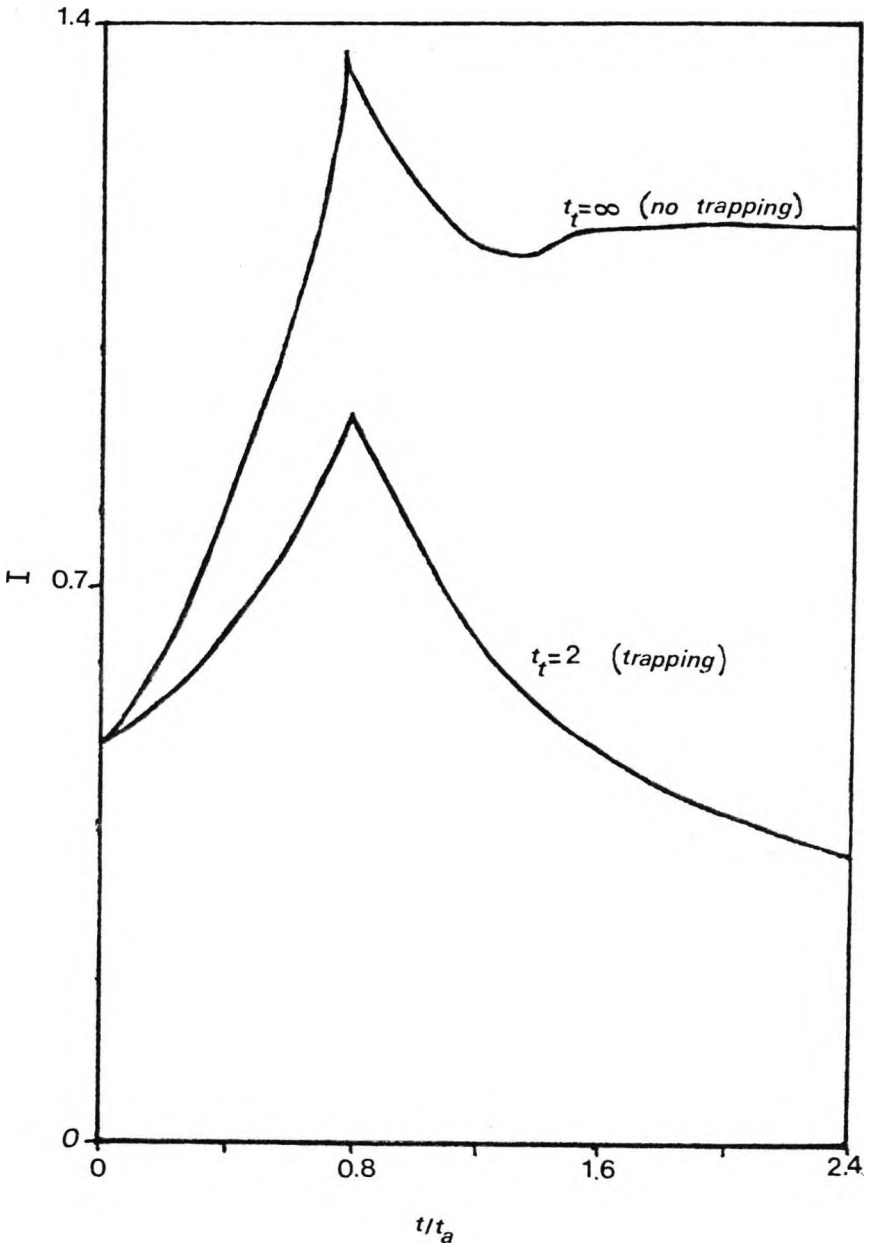

Figure 7.7 Space charge limited transient current as computed by *Many* and *Rakavy* 1962

This process continues up to point T_A ($t = t_a$), when the leading front reaches the opposite electrode. Hence, a maximum of the current is reached at time $t = t_a$ which measures the time of arrival at the anode of the coloration cloud. This time is

$$t_a = 0.786 \frac{d^2}{uV} \simeq 0.786\, t_0 \qquad (7.13)$$

It can be seen in this thesis that the time t_a is of order of minutes, much longer than those observed in semiconductors ($t_a << 1$ S). This clearly implies that the movement of charge is not accomplished by electrons in the conduction band, but ionic processes play an important role, as it should be doing in these ionic crystals where point defects are highly mobile and are present in high concentration at the working coloration conditions.

Experimental results, however, do not show the current cusp so sharply as in the theoretical curves of figure 7.7. Some spreading off is produced since the coloration cloud travels in the crystal with a rounded leading front due to the fact that the injector contact is not a flat one but a pointed cathode. This front does not reach the anode at the same time t_a but progressively. Also, the rounded shape of the maximum in figure 7.8 shows the influence of the ionic processes in the propagation of charge.

In order to show the unique behaviour of the current vs time curve, the results obtained from the electrolytic coloration of KBr crystal; by constant voltage (V=600 volts) and three different values of constant temperatures are plotted in figure 7.8. All the curves are normalised to the time t_a and to the current i_c at point T_c. It is clear that all experimental points describe the same curve, within experimental error. This behaviour is totally parallel to that observed in semiconductor (Lapert and Mark 1985).

4. Zone 3

4.1. The physical nature

Taking into account the results described already, it is possible to elaborate a scheme of the coloration process in zone 3. Electrons injected from the cathode are trapped in anion vacancies existing in the crystal in a concentration determined by the Schottky-pair density in thermal equilibrium. As a consequence the corresponding cation vacancies remain electrically uncompensated. The space-charge created in the crystal modifies the electric field which turns out to be time dependent. The new F-centres created in this zone contribute to the instantaneous current because of its diffusion to the anode under the influence of the applied field.

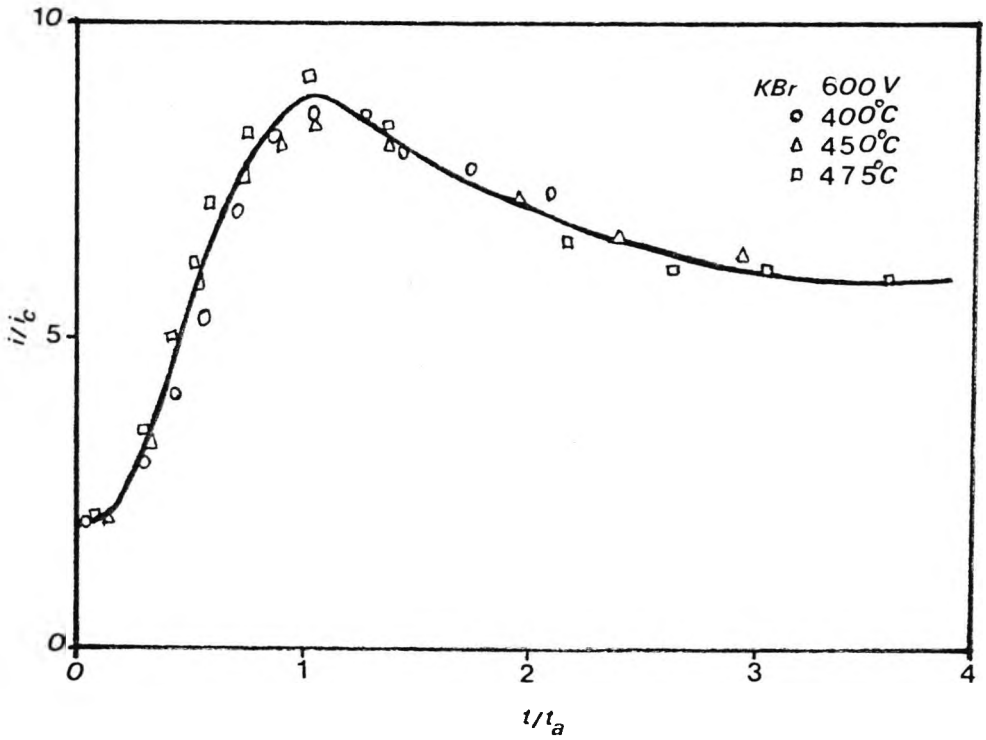

Figure 7.8 Transient currents obtained at different temperatures

At $t \geq t_a$ the final value of current is essentially determined by the charge density which can be injected into the crystal in thermal equilibrium. While the same total charge is injected into the crystal, most of it settles now into traps and thus the rapid decay of coloration current till it subsides to stationary value. The duration and magnitude of this steady-state current depends on the working coloration conditions. The current decays faster the lower t_t is, and the transit time t_a becomes longer. The time required for the transient current to subside is a direct measure of the capture cross section of traps for free electrons. The reduction in current from its peak position is determined by the number and depth of traps as well as the dependence of the ionic current on temperature and applied voltage.

4.2. Mathematical description

The current $j(t)$ in zone 3 settles towards its steady -state value in a time $t \cong 2t_0$. This equilibrium value is then computed according to

$$J(t) = j_c + eu_F N_F(x, t) E(x, t) \qquad (7.14)$$

where u_F is the drift mobility of the colour centres under the action of the electric field and $N_F(x, t)$ is the number of colour centres in a section area of the crystal at a distance x from the cathode at time t where the electric field is $E(x,t)$. The electric field inside the crystal is described by the Poisson equation:

$$(\partial E(x, t) / \partial x) = (e / K) N_F(x, t) \qquad (7.15)$$

The diffusion term is neglected in equation 7.14 because with the electric field used in this work (much higher than KT/e) the diffusion current is small. Taking into account that $j(t)$ in equation 7.14 remains approximately constant and by using

$\bar{E} = -\nabla.V$, $[\partial j_s(t)] / \partial t = 0$ and equation 7.15, a mathematical relation between the steady-state current of zone 3, $j_s = j(t) - j_c$, and V is obtained:

$$j_s = j(\infty) = 9Ku_F V^2 / 8d^3 \qquad (7.16)$$

In order to test this quadratic relation, various current vs time curves were obtained using constant T =400°C and different voltages to colour KBr crystal electrolytically. Zone 1 of these curves is constant and the results are shown in figure 7.3. Ionic current during zone 1 was then subtracted from the values of steady-state current in zone 3 and the results were used

to plot figure 7.9. It is clear that a quadratic relation $j \propto V^2$ is well obeyed in KBr. Similar experiments showed that other alkali halides hold the same relation which is considered as a fundamental property of the SCLC (Rose 1983; Lampert and Mark 1985).

The stationary value of the current is essentially determined by the colour-centre density which represent the charge density injected into the crystal in thermal equilibrium. By combining the two following equations:

$$u_F = D_F e / kT \tag{7.17}$$

and

$$D_F = D_0 \exp(-E_d / kT) \tag{7.18}$$

with equation 7.16, the relation between j and V becomes

$$j_s = \frac{9}{8} \frac{eKD_0}{kT} \frac{V^2}{d^3} \exp(-E_d / kT) \tag{7.19}$$

By plotting $\ln j_s T$ vs T^{-1} the activation energy for F-centre can be obtained. This activation energy is 0.86 eV for KBr as is shown in figure 7.10. Using the same coloration conditions requires longer times to reach j_s, as one moves from KI to KBr to KCl etc and thus a large uncertainty is shown. This result of F-centre diffusion here confirms those obtained and presented in chapter 6.

5. Zone 4

5.1. Analysis of characteristics

In spite of the wide use of electrolytic coloration, many questions left unanswered in so far as the physical nature of zone 4 is concerned. This zone corresponds to a rapid enhancement of the electrical current and F-centre density in the crystal after the steady-state stage of the coloration process. According to authors such as Heiland (1950) and Jaque (1985) this zone should never appear. However, in this work it was noticed that zone 4 appears during the usual procedure of electrolytic coloration when this procedure is left to proceed beyond the steady-state stage. This zone is found to be suppressed whenever a vacuum evaporated metallic anode is used

Figure 7.1, curve (a), shows the current vs time behaviour during the electrolytic coloration of KBr crystal using V=810 volts, T=455^{o} C and Pt plate. Zone 4 is clearly

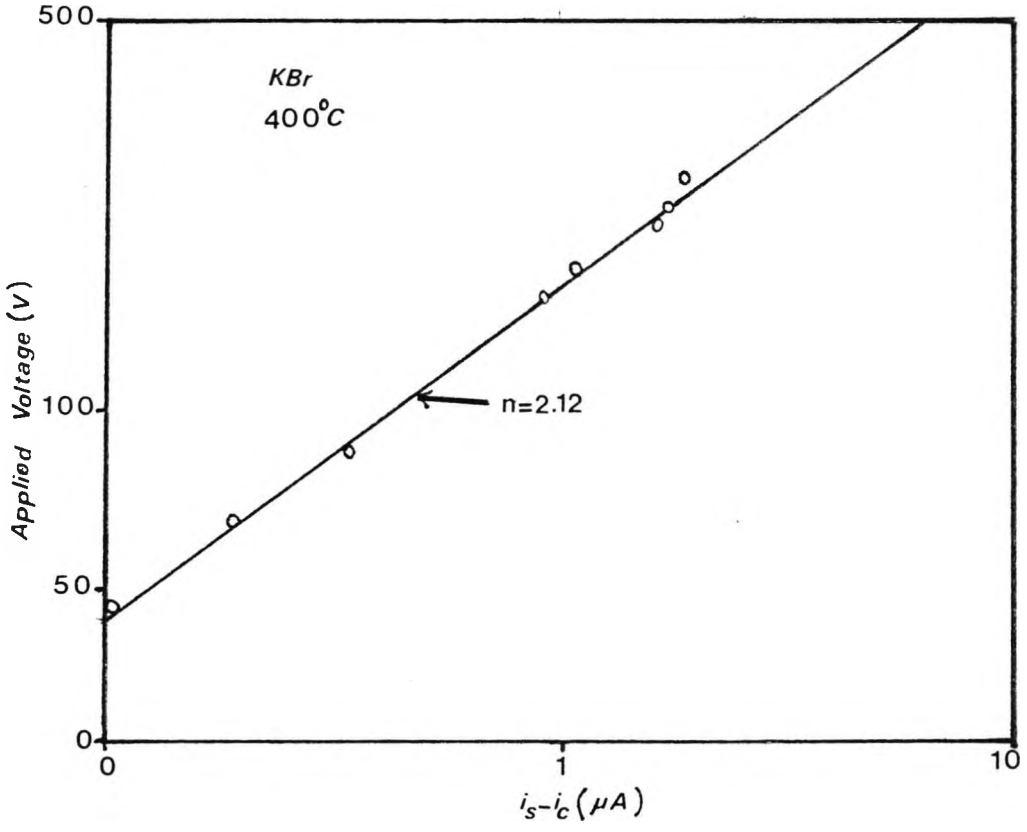

Figure 7.9 A test of the quadratic relation 7.16

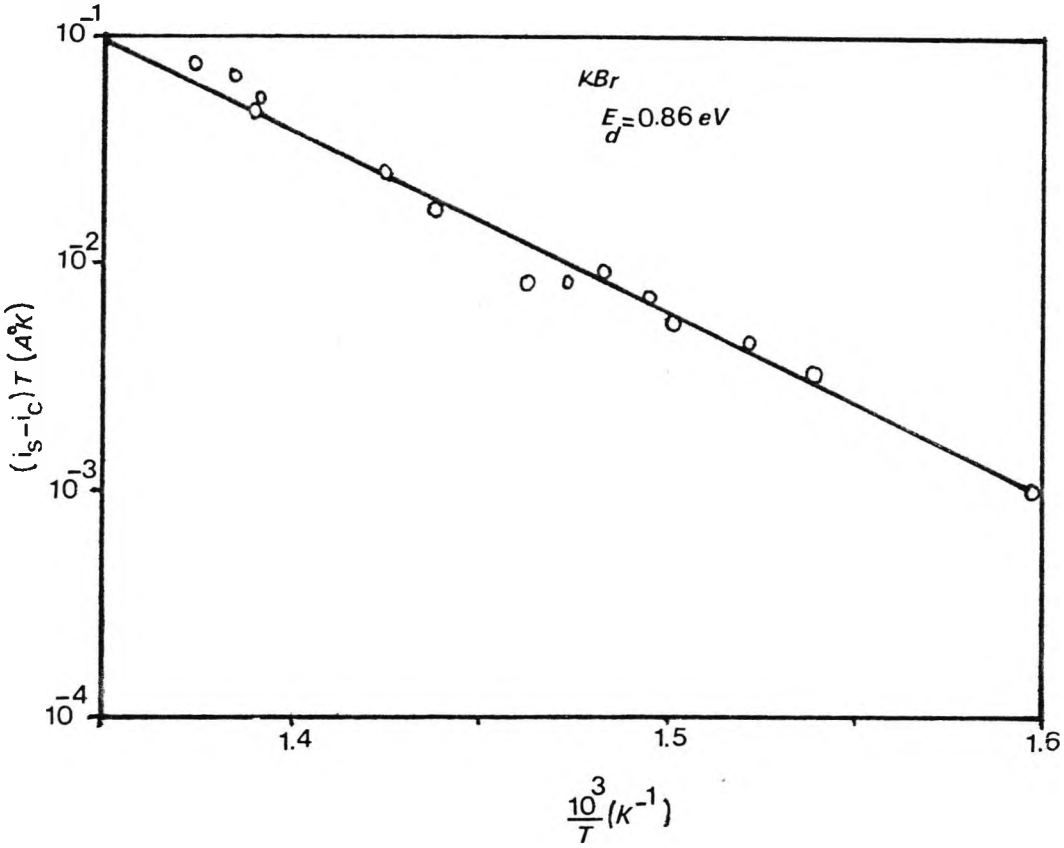

Figure 7.10 Activation energy of *F*-centre diffusion according to formula 7.19

visible here with its characteristic high current and consequently high colour-centre concentration. Furthermore, it was observed that regardless of the atmosphere in which the experiments were performed (air, nitrogen, argon or vacuum) and of the electrodes (tungsten, Pt, stainless steel, aluminum foils), a coloration spot starts building up at the region surrounding the anode during the processes involved in this zone. Also, light emission was observed in the anodic region exclusively during this zone. Thus, the enhancement of the electrical current in this zone is observed to be in parallel to the light emission and both originating from the anode region.

5.2. Light emission

Light emission and high conductivity were also observed when other alkali halide crystals were coloured using various electrodes and atmospheres. The multi-peak spectrum of the emitted light is shown in figure 7.11. Using the same experimental procedure but with different crystals, electrodes and atmospheres, the most relevant parameters from the obtained spectra were found to be the peak positions. Figure 7.11 shows typical results for KBr. The main air component discharge is also quoted for comparison purposes. The intensities of all the lines were considerably improved when the atmosphere was air. No such light emission was detected during other zones of the coloration current vs time curves.

Figure 7.12 shows the relationship between the coloration current during zone 4 and the light intensity measured at λ =3570 $\overset{0}{A}$, using the same coloration conditions as in figure 7.1, curve (a). Both curves rise up proportionally; a behaviour which is repeated in all studied crystals. The slope of the straight line and the value of the electrical current when there is no light intensity are a function of the experimental conditions, but are more affected by the applied voltage and temperature.

5.3. Anodic processes

In order to examine the possible mechanism for the electrolytic coloration process involved in zone 4, the close parallelism exists between the electrical behaviour in this zone and the processes responsible for the light emission was investigated. The anode-crystal contact was accordingly changed. Crystals with vacuum (10^{-6} Torr) evaporated metallic (Al) anodes were prepared while keeping other coloration conditions the same as in figure 7.1, curve (a). The result of such treatment is represented by curve (b), figure 7.1. It is clear that zone 4 is totally inhibited at the same time that no anodic light emission was detected along the whole coloration processes. This simultaneous disappearance of both the light emission and the enhancement of current and colour-centre concentration from the anodic region makes

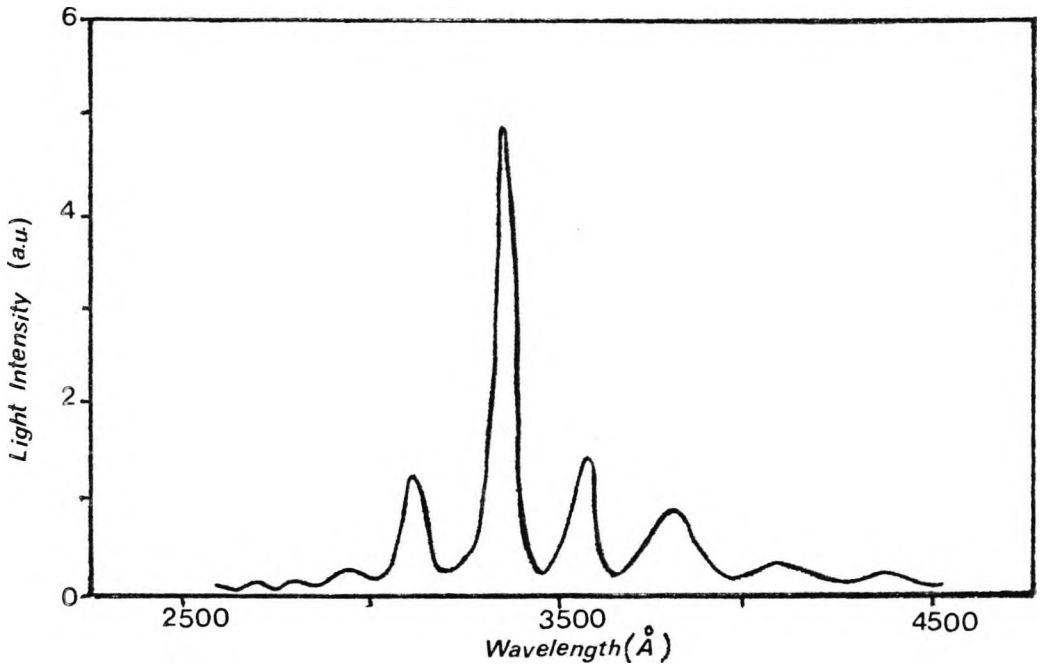

Figure 7.11 Spectrum of light emitted during zone 4.electrolytic coloration of *KBr*

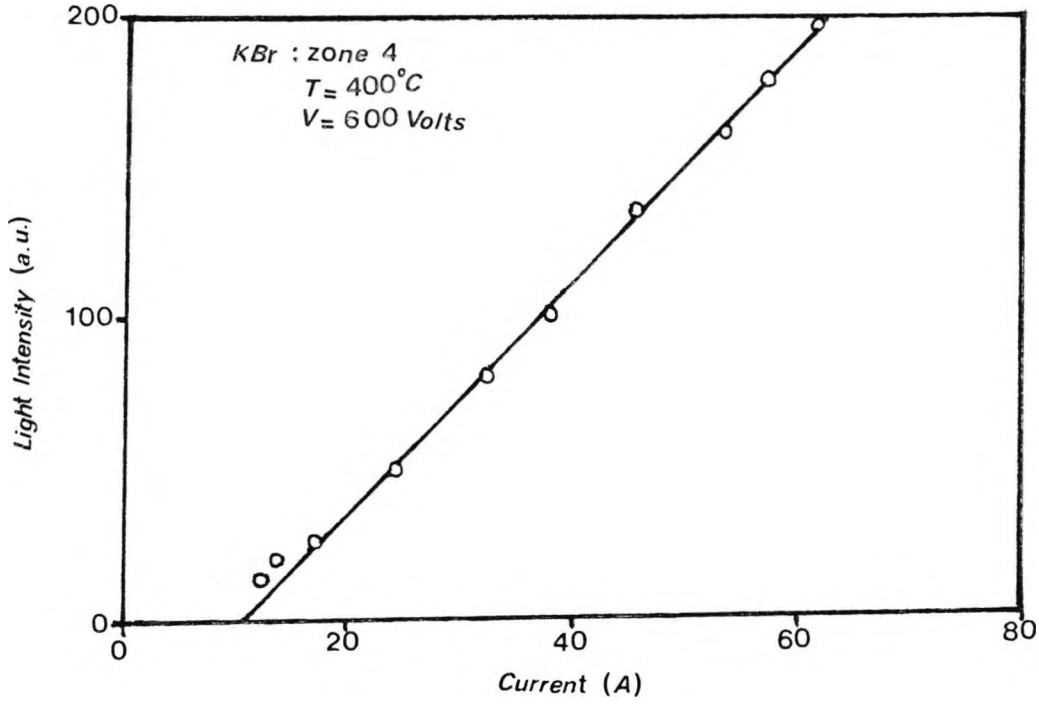

Figure 7.12 Relation between current and light intensity

it clear here that zone 4 is not intrinsic but is due to processes occuring in the crystal-anode interface. When these anodic processes responsible for zone 4 are suppressed the coloration current vs time behaviour follows a curve similar to a SCLC vs time curve for an insulating crystal characterised by various trappings (Lampert and Mark, 1985).

Three facts determine the physical nature of the anodic processes responsible for zone 4. The evidence that using vacuum-evaporated anodes inhibit the light emission, the peak positions of the emission spectra are widely independent of the crystals, electrodes and atmosphere and the fact that a narrow correspondence (within experimental error of $\pm$ 50 A) exists between these values and those related to the air discharge. These facts suggest strongly that air (essentially water vapor) absorbed in the anode-crystal interface plays a major role in the production of zone 4. This water vapor is desorbed during the heating of the sample and retained in the thin and irregular gaps existing in the crystal-anode interface.

Using the same coloration conditions as in figure 7.1, curve (a), alkali halide crystals were heated up to the working temperature in vacuum for more than one hour before applying the electric field to the crystals. In this way curve (b), figure 7.1 was reproduced at the same time that light emission could no longer be detected confirming even further the above argument. Although other factors, such as electrode materials and the gas filling the furnace, may contribute to the production of zone 4 but they should be rather small in comparison with the absorbed water vapour.

It seems that water vapour molecules desorbed from the anodic face of the crystal are decomposed by arcing results in turn from the very high electric field produced through the narrow gaps in the crystal-anode interface due to the accumulation there of a high negative space charge. Oxygen ions react with the metal foils to produce oxides. Furthermore, the principle emission lines correspond to those of the second ionization of oxygen. If M signifies the anodic metal; one possible decomposition reaction could be

$$M + H_2O \rightarrow \quad M + O^{-2} + 2H^{+} \rightarrow MO + 2H^{+} + 2e^{-}$$

This process should be much more complicated but it has been observed in different metallic surfaces under the action of an electric arc (Amsel 1982). Protons liberated in the arc region are injected into the crystal under the electric field existing in the crystal-anode interface. Their high mobility should produce a considerable contribution to the electrical current.

6. References

Amsel G 1982 Physics of Solid Electrolytes, Academic Press, Lndon, pp. 133

Andreev G A, Semuskin G B and Tsikin A N 1968 Sov Phys Sol St 9 2564

Chandra S and Rolf J 1970 Canad J Phys 48 397

Chen R 1969 J Appl Phys 40 570

Critsenko Y I 1971 Phys Status Soldi 7 K113

Dalal M L, Sivaraman S and Murti Y V 1983 J Pure App Phys 21 6

Frank R I and Simmons J G 1967 J App Phys 38 832

Heiland G 1950 Z Phys 128 144

Jaque V 1985 J F Phys 45 97

Kiss K and Jeszenszky B 1962 Int Symp on Colour Centres in Alkali Halides, Stuttgart

Kosman M S and Pisarenko V F 1957 Sov Phys Kokl 2 375

Kroger F A 1979 The Chemistry of Imperfect Crystals, Wiley, new York, pp 800

Kuczynski G C, Hinose H I and Swarrop B 1964 Proc Brit Cream Soc 1 129

Lamb D R 1986 Electrical Conduction Mechanisms in Insulators Methuen Ltd London

Lampert M A 1956 Phys Rev 103 1648

Lampert m A and Mark P 1985 Current Injection in Solids, Academic Press Inc, New York-London

Maiti A K, Goswami K 1983 Solid St. Comm 48 517

Maiti A K, Goswami K, Choudhuri S and Choudhury A 1981 J Electrochem Soc 128 1995

Many a and Rakavy 1962 Phys Rev 126 1980

Markham J J 1966 Solid St Phys Suppl 8

Montojo M I and Sanchez C 1974 J Phys Chem Solid 35 1437

Montojo M I and Sanchez C 1974 Solid State Comm 14 485

Pisarenko V F 1957 Sov Phys Dokl 2 391

Rose S I 1983 Space Charge Effects in Ionic Crystals, University Press, New York, pp.183

Todheide-Haupt U, Gyster A and Rppl W 1966 Phys Status Solidi 15 567